SPECTROSCOPIC, ELECTRICAL AND THERMAL PROPERTIES OF CERTAIN CONDENSED SYSTEMS

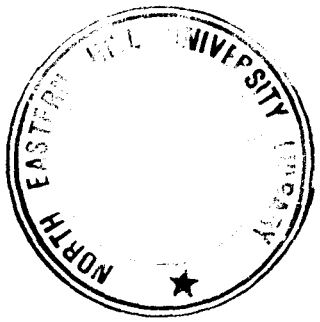

LALMUANAWMA CHHANGTE

DEPARTMENT OF PHYSICS

NORTH-EASTERN HILL UNIVERSITY

SHILLONG, INDIA

SYNOPSIS

Helium-4, a noble gas, liquefied for the first time by Kammerlingh Onnes [1] in 1908, undergoes superfluid transition at 2.17 K. A superfluid (characterised by its unusual properties such as zero viscosity, infinitely high thermal conductivity, existence of quantum vortices, *etc*) represents the manifestation of quantum effects at macroscopic level [2]. As such, the system has been the subject of intense investigations, both theoretically and experimentally for a long time. The wealth of experimental and theoretical studies has been reviewed by several authors [3–5]. Several authors attempted to develop a full microscopic theory of the system, but with little or no success. Most of the microscopic theories developed so far [6–14] start with the basic assumption that the superfluid phase has macroscopic occupation of $p = 0$ state. However, the existence of $p = 0$ condensate has not been confirmed experimentally even after repeated efforts [15]. Since a wholly microscopic theory is not available, liquid helium-4 (LHe-4) continues to be a subject of great interest.

Recently, Jain has used a new approch to develop the microscopic understanding of the phenomena [16–18]; this approach does not assume the existence of either *Cooper pair* type in a fermionic system or BEC state (existence of $p = 0$ condensate) in a bosonic system. This theory (*Macro-orbital Theory*) is consistent with microscopic as well as macroscopic uncertainty, and excluded volume principle. It also provides microscopic foundation for the system to behave as a mixture of two fluid as suggested by Landau [19]. Macro-orbital theory has been succesfully used to explain many of the experimental properties of bulk LHe-4 [20, 21]. The basic objective of the present thesis is to show the agreement of experimentally observed spectroscopic, electrical and thermal properties of LHe-4

and the thermal properties of dilute solution of LHe-3 in LHe-4 with those calculated by using Macro-orbital theory and thereby to conclude that the theory has great potential to explain the properties of similar systems.

This thesis contains seven chapters:

Chapter 1 contains a brief discussion and review on experimental and theoretical studies of LHe-4 and dilute solution of LHe-3 in LHe-4.

Chapter 2 describes the salient features of Macro-orbital theory.

Spectroscopic techniques have been applied in virtually all fields of science and technology. They have become indispensable tools in finding details of structures, symmetry and quantum energy states of atoms, molecules and their larger systems like solids, liquids, polymers, *etc.* They are also widely used in investigations of (i) the phase transformations and order parameter(s) responsible for such changes (ii) changes in electron configurations of the ground as well as the excited states (iii) thermodynamic properties, *etc* [22–25]. Most of our experimental knowledge of electronic structures, internuclear spacings, nature and the strength of inter-atomic bonds and other related properties of molecules are derived from spectral data. Electrical properties (dielectric behavior, electron/ionic conductivity, electrical polarization, *etc.*) of widely different materials are found to be of great significance in relation to their technological application [26–28]. Similarly, from the knowledge of thermal properties, one can often gain valuable information about thermodynamic properties of the system [29–31].

We have studied the spectroscopic properties of LHe-4, namely, the temperature dependence of roton linewidth at saturated vapor

pressure. We include our results in Chapter 3.

Chapter 4 contains our analysis of logarithmic singularity of specific heat of LHe-4 at different pressures.

When small amounts of LHe-3 is added to LHe-4, the resulting dilute solutions have unique properties which found important applications in the fields of both pure science and technology [32, 33]. Mixtures of LHe-3 and LHe-4 are widely used in dilution refrigerators to achieve cooling to temperatures in the millikelvin range [31, 33]. Also, from the theoretical viewpoint, they are excellent examples of interacting Bose and Fermi liquids in nature. A rich array of macroscopic properties can be observed as the ^{3}He concentration is increased [34]. Among these, the natures of the λ transition and of the junction of λ and phase separation curves have been topics of long standing interest [35]. Chapter 5 contains our analysis of transition temperature in dilute solution of LHe-3 in LHe-4 and the phase diagram of LHe-3 and LHe-4 mixtures at various concentrations.

The electrical properties of LHe-4 was not studied in detail for a long time due to the fact that a helium atom is spherically symmetric and hence possesses no permanent dipole moment. However, recent experiments [36] showed that LHe-4 possesses internal electric field. In Chapter 6, we present our explanation of the recent experimental observations.

Chapter 7 contains the conclusion of our investigation.

Bibliography

[1] H. K. Onnes, Leiden Comm. **108**, (1938).

[2] J. F. Annett, *Superconductivity, Superfluidity and Condensates*, Oxford University Press Inc., New York, (2004).

[3] D. R. Tilley and J. Tilley, *Superfluidity and Superconductivity*, Adam Hilger Ltd., Bristol and Boston, (1986).

[4] J. Wilks, *The Properties of Liquid and Solid Helium*, Clarendon Press, Oxford, (1967).

[5] S. J. Putterman, *Superfluid Hydrodynamics*, North Holland/American Elsevier, Amsterdam, (1974).

[6] N. Bogoliubov, J. Phys.(USSR) **11**, 23 (1947).

[7] K. A. Brueckner and K. Sawada, Phys. Rev. **106**, 1117 (1957).

[8] K. A. Brueckner and K. Sawada, Phys. Rev. **106**, 1128 (1957).

[9] K. K. Singh and S. Kumar, Phys. Rev. **162**, 173 (1967).

[10] K. K. Singh and S. Kumar, Phys. Rev. A **1**, 497 (1970).

[11] Y. A. Tserkonikov, Sov. Phys. DOKL, **9**, 1110 (1965).

[12] T. H. Cheung and A. Griffin, Can. J. Phys. **48**, 2135 (1970).

[13] T. H. Cheung and A. Griffin, Phys. Rev. A **4**, 237 (1971).

[14] N. M. Hugenholtz and D. Pines, Phys. Rev. **116**, 489 (1959).

[15] H. R. Glyde and E. C. Svensson in *Methods of Experimental Physics*, (D. L. Price and K. Skold, eds.), Vol. 23, Part-B, Academic Press, London (1987).

[16] Y. S. Jain, J. Sci. Expl. **16**, 67 (2002).

[17] Y. S. Jain, J. Sci. Expl. **16**, 77 (2002);
Am. J. Cond. Mat. Phys **2**, 32 (2012).

[18] Y. S. Jain, J. Sci. Expl. **16**, 117 (2002).

[19] L. D. Landau, J. Phys. (USSR) **5**, 71 (1941).

[20] D. R. Choudhury, *Study of the Dynamical Behaviour of Certain Manybody Systems*, Ph.D. Thesis, Physics Department, North-Eastern Hill University, (1996).

[21] S. Chutia, *A Study of Certain Properties of Superfluid Helium-4 Based on Macro-Orbital Theory*, Ph.D. Thesis, Physics Department,North-Eastern Hill University, (2007).

[22] C. N. Banwell, *Fundamentals of Molecular Spectroscopy*, McGraw Hill, New Delhi, Second Edition, (1972).

[23] R. Chang, *Basic Principles of Spectroscopy* McGraw Hill, Tokyo, (1971).

[24] P. M. A. Sherwood, *Vibrational Spectroscopy of Solids*, Cambridge University Press, Cambridge, (1972).

[25] I. R. Lewis and H. G. M. Edwards, *Handbook of Raman Spectroscopy*, Marcel Dekkar Inc., (2001).

[26] S. Chandra, *Superionic Solids: Principles and Applications*, North Holland, Amsterdam, (1981).

[27] J. C. Burfoot, *Ferroelectrics*, Van Nostrand, London, (1967).

[28] A. R. von Hippel, *Dielectric materials and Applications*, MIT Press, (1995).

[29] S. T. Islander and W. Zimmermann, Jr., Phys. Rev. A **7**, 188 (1973).

[30] R. de Bruyn Ouboter, K. W. Taconis, C. Le Pair and J. J. M. Beenakker, Physica **26**, 853 (1960).

[31] G. Chaudhry and J. G. Brisson, J. Low Temp. Phys. **155**, 235 (2009).

[32] J. C. Wheatley, Am. J. Phys. **36**, 181 (1968).

[33] C. Enns and S. Hunklinger *Low Temperature Physics*, Springer Verlag, Berlin (2005).

[34] S. O. Diallo, J. V. Pearce, R. T. Azuah, F. Albergamo and H. R. Glyde, Phys. Rev. B **74**, 144503 (2006).

[35] T. A. Alvesalo, P. M. Berglund, S. T. Islander, G. R. Pickett and W. Zimmermann, Jr., Phys. Rev. A **4**, 2354 (1971).

[36] A. S. Rybalko, S. P. Rubets, E. Ya. Rudavskii, V. A. Tikhiy, R. Golovachenko, V. N. Derkach and S. I. Tarapov, arXiv: 0807.4810v1.

SPECTROSCOPIC, ELECTRICAL AND THERMAL PROPERTIES OF CERTAIN CONDENSED SYSTEMS

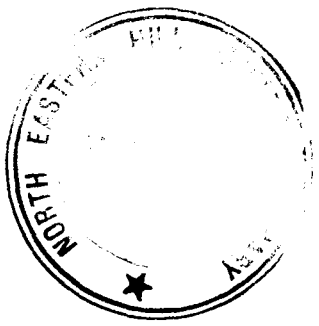

BY

LALMUANAWMA CHHANGTE
DEPARTMENT OF PHYSICS

SUBMITTED
IN PARTIAL FULFILLMENT OF
THE REQUIREMENT OF THE DEGREE OF
DOCTOR OF PHILOSOPHY IN PHYSICS

TO
NORTH-EASTERN HILL UNIVERSITY
SHILLONG, INDIA

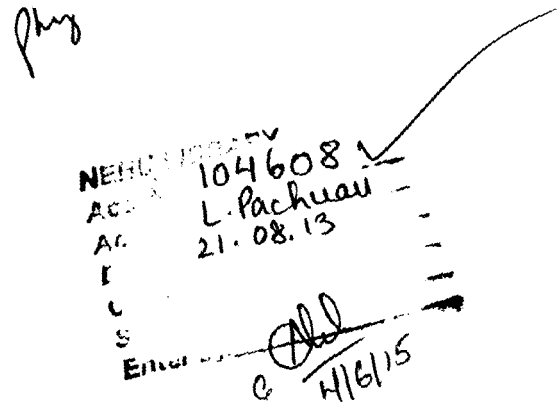
104608
L. Pachuau
21.08.13
6 11/6/15

To the memory of my mother

K. Zaithuami (15.08.1940–19.03.2007)

CERTIFICATE

This is to certify that the research work presented in this thesis entitled " Spectroscopic, Electrical and Thermal Properties of Certain Condensed Systems" is carried out by Shri Lalmuanawma Chhangte under our supervision in the Department of Physics, School of Physical Sciences, North-Eastern Hill University, Shillong. The work embodied in this thesis does not form the basis for the award of any previous degree, diploma, fellowship or any other similar title and it represents entirely an independent work on the part of the candidate.

B'Jyrwa

Prof. B.M. Jyrwa,
Head, Dept. of Physics,
NEHU.

Prof. & Head
Physics Department
N.E.H.U., Shillong-793022

Satish Kumar

Prof. S.Kumar
(Supervisor)

Prof. Y.S.Jain (Retd.)
(Joint Supervisor)

Place : Shillong
Date : 28.6.2012

DECLARATION

I, Lalmuanawma Chhangte, hereby declare that the thesis entitled "Spectroscopic, Electrical and Thermal Properties of Certain Condensed Systems" is the record of the work carried out by me under the supervision of Prof. S. Kumar and Prof. Y. S. Jain (Retd.), Department of Physics, North-Eastern Hill University, Shillong. The contents of this thesis did not form the basis for the award of any previous degree to me or to the best of my knowledge, to anybody else. I also declare that the thesis has not been submitted by me for any research degree in any other University/Institute.

This is being submitted to the North-Eastern Hill University for the degree of Doctor of Philosophy in Physics.

Place : Shillong
Date : 28-6-2012

Lalmuanawma Chhangte,
Department of Physics,
NEHU, Shillong.

ACKNOWLEDGEMENT

I take this opportunity to express my deep sense of gratitude to Prof. Y. S. Jain for his keen interest, invaluable suggestions and inspiring guidance throughout the course of this research. I shall ever remain grateful to him for his affection, his constant motivation and his advice.

I am very grateful to Prof. S. Kumar for his help and understanding.

I wish to convey my gratitude to Prof. B. M. Jyrwa, Head, Department of Physics, NEHU for her encouragement.

I express my heartfelt thanks to the Principal, Lunglei Gov't College, for allowing me to pursue Ph.D program. I am indebted to the Director, Higher and Technical Education, Gov't of Mizoram for granting me study leave.

I shall remain thankful to my friend, Dr. Simanta Chutia, St. Anthony's College, Shillong, who has helped me in every step of this work–be it writing programs, discussion or analysis of the results–he has always been there to help me, right from the beginning till the very end.

I am indebted to my learned colleagues at Lunglei Gov't College– R. Lalrosanga, S. K. Prasad, C. Lalremchhunga and Malsawmtluanga for their understanding, moral support and countless help.

I record my sincere thanks to my friends, Dr. Lalthlamuana Pachuau and Dr. K. Pachhunga for their help and support throughout my research work.

I gladly acknowledge the help of my friends S. Dey, A. K. Jha, J. P. Gewali and N. T. Chanu.

I am grateful to my father, my brothers and my sister for their love and support.

I am very much indebted to my wife and my three kids, for their moral support and patience throughout this work.

Above all, I thank God for making all these happened.

Lalmuanawma Chhangte,
Place: Shillong
Date : 28-6-2012

Contents

List of Tables

List of Figures

SYNOPSIS

Helium-4, a noble gas, liquefied for the first time by Kammerlingh Onnes [1] in 1908, undergoes superfluid transition at 2.17 K. A superfluid (characterised by its unusual properties such as zero viscosity, infinitely high thermal conductivity, existence of quantum vortices, *etc*) represents the manifestation of quantum effects at macroscopic level [2]. As such, the system has been the subject of intense investigations, both theoretically and experimentally for a long time. The wealth of experimental and theoretical studies has been reviewed by several authors [3–5]. Several authors attempted to develop a full microscopic theory of the system, but with little or no success. Most of the microscopic theories developed so far [6–14] start with the basic assumption that the superfluid phase has macroscopic occupation of $p = 0$ state. However, the existence of $p = 0$ condensate has not been confirmed experimentally even after repeated efforts [15]. Since a wholly microscopic theory is not available, liquid helium-4 (LHe-4) continues to be a subject of great interest.

Recently, Jain has used a new approch to develop the microscopic understanding of the phenomena [16–18]; this approach does not assume the existence of either *Cooper pair* type in a fermionic system or BEC state (existence of $p = 0$ condensate) in a bosonic system. This theory (*Macro-orbital Theory*) is consistent with microscopic as well as macroscopic uncertainty, and excluded volume principle. It also provides microscopic foundation for the system to behave as a mixture of two fluid as suggested by Landau [19]. Macro-orbital theory has been succesfully used to explain many of the experimental properties of bulk LHe-4 [20, 21]. The basic objective of the present thesis is to show the agreement of experimentally observed spectroscopic, electrical and thermal properties of LHe-4

and the thermal properties of dilute solution of LHe-3 in LHe-4 with those calculated by using Macro-orbital theory and thereby to conclude that the theory has great potential to explain the properties of similar systems.

This thesis contains seven chapters:

Chapter 1 contains a brief discussion and review on experimental and theoretical studies of LHe-4 and dilute solution of LHe-3 in LHe-4.

Chapter 2 describes the salient features of Macro-orbital theory.

Spectroscopic techniques have been applied in virtually all fields of science and technology. They have become indispensable tools in finding details of structures, symmetry and quantum energy states of atoms, molecules and their larger systems like solids, liquids, polymers, *etc.* They are also widely used in investigations of (i) the phase transformations and order parameter(s) responsible for such changes (ii) changes in electron configurations of the ground as well as the excited states (iii) thermodynamic properties, *etc* [22–25]. Most of our experimental knowledge of electronic structures, internuclear spacings, nature and the strength of inter-atomic bonds and other related properties of molecules are derived from spectral data. Electrical properties (dielectric behavior, electron/ionic conductivity, electrical polarization, *etc.*) of widely different materials are found to be of great significance in relation to their technological application [26–28]. Similarly, from the knowledge of thermal properties, one can often gain valuable information about thermodynamic properties of the system [29–31].

We have studied the spectroscopic properties of LHe-4, namely, the temperature dependence of roton linewidth at saturated vapor

pressure. We include our results in Chapter 3.

Chapter 4 contains our analysis of logarithmic singularity of specific heat of LHe-4 at different pressures.

When small amounts of LHe-3 is added to LHe-4, the resulting dilute solutions have unique properties which found important applications in the fields of both pure science and technology [32, 33]. Mixtures of LHe-3 and LHe-4 are widely used in dilution refrigerators to achieve cooling to temperatures in the millikelvin range [31, 33]. Also, from the theoretical viewpoint, they are excellent examples of interacting Bose and Fermi liquids in nature. A rich array of macroscopic properties can be observed as the ^{3}He concentration is increased [34]. Among these, the natures of the λ transition and of the junction of λ and phase separation curves have been topics of long standing interest [35]. Chapter 5 contains our analysis of transition temperature in dilute solution of LHe-3 in LHe-4 and the phase diagram of LHe-3 and LHe-4 mixtures at various concentrations.

The electrical properties of LHe-4 was not studied in detail for a long time due to the fact that a helium atom is spherically symmetric and hence possesses no permanent dipole moment. However, recent experiments [36] showed that LHe-4 possesses internal electric field. In Chapter 6, we present our explanation of the recent experimental observations.

Chapter 7 contains the conclusion of our investigation.

Bibliography

[1] H. K. Onnes, Leiden Comm. **108**, (1938).

[2] J. F. Annett, *Superconductivity, Superfluidity and Condensates*, Oxford University Press Inc., New York, (2004).

[3] D. R. Tilley and J. Tilley, *Superfluidity and Superconductivity*, Adam Hilger Ltd., Bristol and Boston, (1986).

[4] J. Wilks, *The Properties of Liquid and Solid Helium*, Clarendon Press, Oxford, (1967).

[5] S. J. Putterman, *Superfluid Hydrodynamics*, North Holland/American Elsevier, Amsterdam, (1974).

[6] N. Bogoliubov, J. Phys.(USSR) **11**, 23 (1947).

[7] K. A. Brueckner and K. Sawada, Phys. Rev. **106**, 1117 (1957).

[8] K. A. Brueckner and K. Sawada, Phys. Rev. **106**, 1128 (1957).

[9] K. K. Singh and S. Kumar, Phys. Rev. **162**, 173 (1967).

[10] K. K. Singh and S. Kumar, Phys. Rev. A **1**, 497 (1970).

[11] Y. A. Tserkonikov, Sov. Phys. DOKL, **9**, 1110 (1965).

[12] T. H. Cheung and A. Griffin, Can. J. Phys. **48**, 2135 (1970).

[13] T. H. Cheung and A. Griffin, Phys. Rev. A **4**, 237 (1971).

[14] N. M. Hugenholtz and D. Pines, Phys. Rev. **116**, 489 (1959).

[15] H. R. Glyde and E. C. Svensson in *Methods of Experimental Physics*, (D. L. Price and K. Skold, eds.), Vol. 23, Part-B, Academic Press, London (1987).

[16] Y. S. Jain, J. Sci. Expl. **16**, 67 (2002).

[17] Y. S. Jain, Am. J. Cond. Mat. Phys **2**, 32 (2012);
J. Sci. Expl. **16**, 77 (2002).

[18] Y. S. Jain, J. Sci. Expl. **16**, 117 (2002).

[19] L. D. Landau, J. Phys. (USSR) **5**, 71 (1941).

[20] D. R. Choudhury, *Study of the Dynamical Behaviour of Certain Manybody Systems*, Ph.D. Thesis, Physics Department, North-Eastern Hill University, (1996).

[21] S. Chutia, *A Study of Certain Properties of Superfluid Helium-4 Based on Macro-Orbital Theory*, Ph.D. Thesis, Physics Department,North-Eastern Hill University, (2007).

[22] C. N. Banwell, *Fundamentals of Molecular Spectroscopy*, McGraw Hill, New Delhi, Second Edition, (1972).

[23] R. Chang, *Basic Principles of Spectroscopy* McGraw Hill, Tokyo, (1971).

[24] P. M. A. Sherwood, *Vibrational Spectroscopy of Solids*, Cambridge University Press, Cambridge, (1972).

[25] I. R. Lewis and H. G. M. Edwards, *Handbook of Raman Spectroscopy*, Marcel Dekkar Inc., (2001).

[26] S. Chandra, *Superionic Solids: Principles and Applications*, North Holland, Amsterdam, (1981).

[27] J. C. Burfoot, *Ferroelectrics*, Van Nostrand, London, (1967).

[28] A. R. von Hippel, *Dielectric materials and Applications*, MIT Press, (1995).

[29] S. T. Islander and W. Zimmermann, Jr., Phys. Rev. A **7**, 188 (1973).

[30] R. de Bruyn Ouboter, K. W. Taconis, C. Le Pair and J. J. M. Beenakker, Physica **26**, 853 (1960).

[31] G. Chaudhry and J. G. Brisson, J. Low Temp. Phys. **155**, 235 (2009).

[32] J. C. Wheatley, Am. J. Phys. **36**, 181 (1968).

[33] C. Enns and S. Hunklinger *Low Temperature Physics*, Springer Verlag, Berlin (2005).

[34] S. O. Diallo, J. V. Pearce, R. T. Azuah, F. Albergamo and H. R. Glyde, Phys. Rev. B **74**, 144503 (2006).

[35] T. A. Alvesalo, P. M. Berglund, S. T. Islander, G. R. Pickett and W. Zimmermann, Jr., Phys. Rev. A **4**, 2354 (1971).

[36] A. S. Rybalko, S. P. Rubets, E. Ya. Rudavskii, V. A. Tikhiy, R. Golovachenko, V. N. Derkach and S. I. Tarapov, arXiv: 0807.4810v1.

Chapter 1

Introduction

1.1 Basic facts about Helium

The noble gas helium is the first element of Group VIIIA of the periodic table. It is chemically inert and colorless with a ground state electronic configuration $1s^2$. Evidence for its existence was first obtained by the French astronomer Janssen in the visible spectrum during solar eclipse in India in 1868 [1]. He observed a hitherto unknown yellow line. An English astronomer Lockyer [2] confirmed this observation, and related the new spectral line to a chemical element that had not been discovered on Earth before and suggested the name *helium* for it. On earth helium was discovered in 1895 by the English scientist Ramsay [3] and independently by Swedish chemists, Cleve and Langlet [4] in cleveite, a rocksand mineral. In the same year, Kayser [5] also found helium in gas evolving from a spring in the Black Forest in Germany.

Helium has two stable isotopes, ^{4}He and ^{3}He. ^{4}He makes up about 5.2 ppm of the earth's atmosphere. The lighter isotope ^{3}He was discovered and identified by Oliphant, Kinsey and Rutherford [6] in 1933. ^{3}He atoms are fermions with nuclear spin I=1/2, while ^{4}He atoms are bosons with nuclear spin I=0. In addition to these two stable isotopes, there are two unstable helium isotopes, ^{6}He with a half life of 0.82 s and ^{8}He with a half life of 0.12 s [7]. Since the concentration of ^{3}He in helium from natural gas source is only 0.14 ppm, ^{3}He in quantities for use in experiments must be produced via nuclear reactions. However, Sydoriak, Grilly and Hammel managed to liquefy ^{3}He as early as 1949 and investigated its properties [8].

The combination of the weak binding force and the large zero-point energy renders helium to remain liquid under saturated vapor pressure (SVP) even for $T \rightarrow 0$ K [9, 10]. In its gaseous state, the common isotope ^{4}He survives down to around 4.2 K before it liq-

uefies. Below that temperature, it remains liquid unless subjected to a pressure higher than 25 bar. The boiling point of the isotope ^{3}He is 3.2 K and a pressure of 34 bar is required to produce solid at low temperatures [11].

The liquefaction of helium on July 10, 1908 by Kamerlingh Onnes [12] established the foundation of modern low temperature physics. Since then liquid helium has become the topic of intense research works, both theoretical and experimental. In this chapter, we present a brief review of the work on these fluids—pure liquid ^{4}He (LHe-4) as well as mixtures of LHe-4 and LHe-3.

1.2 Experimental Studies of LHe-4

1.2.1 Density

In 1911, Kamerlingh Onnes found that the density of LHe-4 has a maximum at around 2K [13]. Later investigation showed that there is a sharp kink in the temperature dependence of density at 2.17 K, and that LHe-4 expands again below that temperature [14]. Keesom and Keesom [15] measured the density of LHe-4 as a function of pressure over the temperature range $(1.15 - 4.2)$ K upto 35.5 bar. Kerr and Taylor [16] measured density of LHe-4 under its own vapor pressure over the temperature range $(0.5 - 2.8)$ K with a precision of about 0.006%. A well defined power law behavior of superfluid density near the transition temperature was observed by Chan *et al* [17]. Niemela and Donelly [18] calculated density from dielectric constant in the temperature range $(1.15 - 4.9)$ K and provided formula for absolute density measurement in the range $(0 - 4.9)$ K.

1.2.2 Specific heat

Dana and Kamerlingh Onnes measured the specific heat of LHe-4 in 1923. They found an abnormal rise of the specific heat around 2 K, which they feared might be caused by experimental errors [19]. In 1932 Keesom and Clusius [20] investigated the specific heat of LHe-4 again and observed a sharp jump at 2.17 K, which they attributed to a phase transition.

To distinguish the two phases of LHe-4, the names *helium I* (He I) and *helium II* (He II) were introduced. While He I denotes LHe-4 above the transition, He II refers to the phase below the transition temperature. The shape of the specific heat versus temperature curve resembles the shape of the Greek letter λ and hence, the singular point on this curve is called λ point. One of the most remarkable features of He II is its ability to flow through narrow capillaries without any friction. Just as the frictionless transport of electrons in metals is referred to as the superconducting state, He II is often called *Superfluid* [7]. Keesom and Clusius [20] observed that no latent heat is associated with this transition which concludes it to be a second order phase transition, similar to a superconducting transition. These results were later confirmed by more accurate measurements performed by Fairbank and co-workers [21,22] who were able to measure the specific heat within 10^{-6} of λ point and showed that the changes at this point can be described as logarithmic discontinuity of specific heat. Some other measurements of the specific heat under SVP were reported in [23–30]. Ahlers [31] reported the temperature dependence of specific heat along six different isobars and isochores. Specific heat measurements of pure LHe-4 as well as LHe-4 and LHe-3 mixture were reported by Gasparini and Moldover [32, 33]. Effect of the finite size of the sample was studied by Lipa *et al* [34–36] and Gasparini *et al* [37–39]. Lipa and coworkers [40, 41] reported

measurements of C_p, in and out of the earth's gravitational field.

1.2.3 Dielectric constant

The measurement of the dielectric constant of LHe-4 between its boiling point and 1.9 K by Keesom and Wolfke [42] showed a pronounced maximum in the vicinity of 2.3 K, which was attributed to a liquid to liquid phase transition. The dielectric constant of He I was found to be higher than that of He II. Grebenkemper and Hagen [43] who measured the resonance frequency of helium filled microwave cavity at 9100 MHz obtained similar results. Chase *et al* [44] who measured the dielectric constant in the temperature range 1.4 K–4.2 K showed that polarizability is independent of temperature. Other measurements were reported in [45, 46], the most recent measurement has been made by Niemala and Donelly [47].

1.2.4 Thermal Conductivity

The thermal conductivity of LHe-4 was measured by Keesom and Keesom [15] in 1936. They found that the thermal conductivity of He II attained a maximum value of 810 $\text{cal} \cdot \text{cm}^{-1} \cdot \text{s}^{-1} \cdot \text{K}^{-1}$ below the λ point. Allen *et al* [48] observed that the mechanism of conduction in He II is different from those in other fluids. The so-called *Fountain Effect* (thermo-mechanical effect) was discovered by Allen and Johnes [49] in 1938 in connection with thermal transport measurements. London [50] derived the fountain effect equation which was used to determine entropy and its variation with pressure and temperature. The inverse fountain effect, (mechano-caloric effect) discovered by Daunt and Mendelssohn [51] was confirmed by Brewer and Edwards [52]. The co-efficient of thermal conductivity in thin and bulk LHe-4 was measured as a function of temperature by Um

et al [53]. Kahn and Ahlers [54] measured the thermal conductivity at SVP.

1.2.5 Viscosity

Three different methods are often employed for measuring the viscosity of LHe-4: the damping method, the flow method and the rotary viscometer method. In damping method, viscosity is determined by measuring the damping of the motion of a body immersed in it. In flow method, viscosity is determined by measuring the rate of flow of the fluid through capillary tubes or channels between two parallel plates, while in the third method, viscosity is found by measuring the torque transferred from the rotating inner cylinder to the outer cylinder which is kept stationary. The measurements of viscosity of LHe-4 in 1938 by Kapitza [55] using modified capillary flow method and by Allen and Misener [49] using ordinary flow method showed vanishingly small value of viscosity. The measurements also revealed that the velocity of flow was practically independent of the pressure difference at the ends of the capillary. However, experiments performed by oscillating disc method [56–59], vibrating wires [60] and rotary viscometer method [61–63] showed the existence of a viscous drag, consistent with a viscosity coefficient not much less than that of ^{4}He gas. From the results of these experiments, it appeared that He II was capable of being both viscous and non-viscous at the same time. This apparent contradiction laid the foundation of the two-fluid theory.

1.2.6 Surface Tension

A jump in the surface tension of LHe-4 at the λ point was observed by Urk *et al* [64] in 1926. Many workers have since then measured

the surface tension [65] using different techniques. While the measurements of Allen and Misener [66], Dickson *et al* [67], and King and Wyatt [68] showed good agreement with each other, the data of Atkins and Narahara *et al* [69] and Zinoveva *et al* [70] were found to be slightly larger. Zinoveva *et al* [70] reported a value of 378 mdynes/cm as against Atkins and Narahara [69] who found 371.9 mdynes/cm at absolute zero. Iino *et al* [71] used surface wave resonance and reported 354.4± 0.5 mdynes/cm at $T = 0$ K. Measurements of surface tension near T_λ were also reported by Atkins and Nahara [69], Gasparini *et al* [72], Magerlein and Sanders [73] and Suzuki *et al* [74]. A study of the liquid-solid helium interfacial tension was reported by Gallet *et al* [75]. Later surface tension of LHe-4 was measured by Roche *et al* [76], Nakanishi and Suzuki [77] and Vicente *et al* [78]. Roche *et al* [76] determined surface tension of the liquid by using a complex arrangement of capillaries patterned in chromium on a monocrystalline saphire as substrate. Their results differed from that of Iino *et al* [71] by 6%. The difference was attributed to the meniscus effects which was not considered by Iino *et al* [71]. The measurements by Nakanishi and Suzuki [77] confirmed the findings of Iino *et al* [71] while Vicente *et al* [78] found values in agreement with Roche *et al* [76].

1.2.7 Sound Velocities

Four different sound modes are associated with He II, named as *first, second, third* and *fourth sound*, respectively. *First sound* is the normal longitudinal pressure waves involving fluctuations in the total density at constant temperature, *second sound* is the name given to temperature waves as predicted by Tisza [79] and Landau [80] in their respective two fluid models. While *third sound* is a propagating surface wave on He II films, *fourth sound* represents pressure waves

in He II inside fine pores of small slits where the normal component is immobilized and superfluid is free for motion. Atkins [81] predicted the existence of third and fourth sound. Findlay *et al* [82] determined the velocity of first sound in 1938 using an ultrasonic method for a temperature range 4.22 K – 1.76 K. Using their experimental values they calculated the compressibility of LHe-4; however, their experiments did not show any discontinuity at the λ transition. Chase [83] and Itterbeek *et al* [84] also determined the velocity of first sound using different techniques at different frequencies.

Velocity of second sound was measured by Peshkov [85] by using an electrical heater supplied with alternating current as transmitter and a resistance thermometer as detector. Hall and Vinen [86, 87] studied the second sound in rotating He II. Rudnick *et al* [88] reported generation and detection of third sound. The early experiments on third sound are reviewed by Atkins and Rudnick [89]. Temperature dependence of third sound velocity was studied by Rudnick [90] who observed that third sound disappeared near the transition temperature for steep rise of its dissipation. Ekholm and Hallock [91] measured the third sound velocity on static films. Shapiro and Rudnick [92] studied the temperature variation of fourth sound by setting up standing waves of fourth sound in an acoustic resonator.

1.2.8 Expansion Coefficient

The early measurements of density ρ of LHe-4 by Onnes [13], Onnes and Boks [14] indicated a negative volume expansion coefficient α at about 2.2 K. Atkins and Edwards [93] and Kerr [94] repeated the measurements with improved accuracy. Later, Edwards [95] deduced the value of α from the measurement of refractive index while Chase *et al* [96] obtained it from the measurement of dielectric constant.

These results are reviewed by Kerr and Taylor [97]. Ahlers [31] also studied α at temperatures very close to T_λ on six different isobars.

1.2.9 Compressibility

Keesom and Keesom [15] indicated that the isothermal compressibility of LHe-4 increases with increasing pressure near the λ point. Measurement of compressibility by Grilly and Mills [98] showed that compressibility coefficient (β) of LHe-4 had an anomalous behavior with the temperature near the λ point. Lounasmaa [99] measured the pressure coefficient and β of LHe-4 very close to the λ curve. Boghosian and Meyer [100] measured β as a function of pressure between 0.5 K and 1.4 K using dielectric constant method. The same method was employed by Watson *et al* [101].

1.2.10 Quantum Evaporation

Quantum evaporation in superfluid ^{4}He may be defined as a single quantum process in which one phonon evaporates one helium atom. The phenomenon was studied by Johnston and King [102]. Griffin [103] derived an expression for the evaporation rate by using solid state tunneling theory. The investigation of this phenomenon was done also by Cole [104], Caroli *et al* [105], Balibar *et al* [106], and Baird *et al* [107], using collimated beams of quasiparticles to study the evaporation mechanism. These experiments confirmed the one-to-one transition correspondence between quasiparticles and atom. Recent studies on quantum transition are done by Brown and Wyatt [108], Marris [109], Mulheren and Inkson [110], Dalfovo *et al* [111, 112], Stringari *et al* [113], Sobnack *et al* [114–116] and Williams [117].

1.2.11 Electrical Properties

The interaction between electromagnetic microwaves of frequency in the range $(40 - 200)$ GHz and superfluid helium in a stationary electric field was investigated by Rybalko [118] in 2004. They found that the relative motion of the superfluid and normal components of He II in a second sound wave was accompanied by the appearance of electric induction. In a series of later experiments, Rybalko *et al* [119, 120] observed resonance absorption of microwaves at the frequency corresponding to the roton minimum of the LHe-4 excitation spectrum, and the splitting of the narrow absorption line in the electric field.

1.2.12 Neutron Scattering Experiments

Neutron scattering techniques has been widely used to study the properties of LHe-4. Following the suggestion of Feynman and Cohen [121] that neutron scattering could be used to determine the dispersion relation of the elementary excitations of LHe-4, Goldstein *et al* [122] reported the first neutron scattering study on LHe-4 in 1951, followed by a large number of measurements using a wide range of neutron energies (Henshaw and Hurst [123, 124]). A series of inelastic scattering measurments were performed in the late 1950s [125–129]. These experiments supported the phonon–roton dispersion proposed by Landau [80]. The early neutron scattering experiments up to 1970 were reviewed by Woods and Cowley [130] and Price [131], Glyde and Svenssson [132] summed up results of additional studies performed till early 1980s. The main objective of neutron scattering experiments was to study (i) the nature of the energy dispersion of thermal excitations at low Q, (ii) the temperature dependence of static structure factor $S(Q)$, and dynamic form factor

$S(Q,\omega)$ and (iii) the relation between condensate fraction (macroscopic occupation of $p = 0$ state) and superfluid density if Bose–Einstein Condensation really exists in the liquid. The findings of these experiments provided invaluable information, but the findings about condensate fraction remained inconclusive [132–134].

1.3 Theoretical Studies of LHe-4

Even though most of the peculiar properties of LHe-4 were experimentally observed within the first three decades of its liquefaction in 1908, theoretical investigation of the system was started many years later. In 1937 Frohlich [135] suggested that the λ transition was a special kind of order-disorder transition. London [136] criticized this idea and proposed that the phenomenon was a manifestation of Bose–Einstein Condensation (BEC)—a consequence of Bose–Einstein statistics of non-interacting bosons [137, 138].

In 1938 a phenomenological *Two Fluid Theory* was proposed by Tisza [79, 139, 140] to explain the transport properties of He II. According to this theory, He II behaves as if it were a mixture of two completely interpenetrating fluids, one, the normal fluid, possessing an ordinary viscosity, and the other, the superfluid which is capable of frictionless flow past obstacles and through narrow channels. He considered the motion of He II as some kind of turbulent motion because the velocity–pressure dependence was more similar to turbulent than to laminar motion. The most important achievement of the two fluid theory was the successful prediction of the existence of second sound in He II.

In 1941 Landau [80] published a landmark paper in the history of superfluidity in which he developed quantitatively the two fluid description of He II. Landau's two fluid theory assumed the

existence of two independent motions in He II. These two motions occured without momentum transfer from one to another. To be more specific, He II was considered to be a homogeneous mixture of two fluids: *normal fluid* (N-fluid) and *superfluid* (S-fluid) so that the total density of the fluid ρ is the sum of N-fluid density ρ_n and S-fluid density ρ_s,

$$\rho = \rho_n + \rho_s \tag{1.3.1}$$

In this paper Landau introduced into condensed matter physics the seminal notion of a *quasiparticle*, *i.e*, an excitation of the system from the ground state, which was characterized by a definite energy and momentum, and such that, at least at sufficiently low temperatures, the total energy, momentum, *etc.*, of the system could be regarded as the sum of that carried by the quasiparticles [133]. In this two fluid model there are two kinds of excited molecules—phonons (quanta of longitudinal compressional waves) and rotons. He showed that below a certain critical velocity v_c of the flow of the fluid, creation of phonons or rotons is energetically not favorable and the liquid can behave as superfluid. In case of rotational motion, he proposed that only the N-fluid component is carried along by the walls of the container while the S-fluid component remains stationary. He suggested the following expressions for the excitation spectrum of He II:

$$\epsilon = cp \qquad \text{for phonon} \tag{1.3.2}$$

and

$$\epsilon = \triangle + \frac{(p - p_0)^2}{2\mu} \qquad \text{for roton.} \tag{1.3.3}$$

where μ is the effective mass of the roton, $\triangle$ represents an energy gap for the roton mode and c is the velocity of sound. At 1 K, experimental values of the parameters are $\triangle\ /k_B$= 8.67 K, $p_0\ /\hbar$ = 1.94 Å^{-1}, and μ=0.15m, (m being the mass of a ^{4}He atom) [7]. Although Landau's two fluid model could explain a large fraction of the exotic

behavior of He II without invoking the notion of BEC, it had several shortcomings, inconsistencies and quantitative disagreements with certain experimental results. Putterman [137] gave a review of the shortcomings of Landau's two fluid theory. He remarked that the two fluid model supplemented by the idea of quantized circulation developed by Onsager [141] and Feynman [142] has strong similarities with the old quantum theory where Bohr–Sommerfield quantization was used to select the allowed energy states of an atom. Since the old quantum theory did not take into account the wave particle duality, one naturally expects that Landau's theory plus quantization will have comparable shortcomings. Moreover, Landau's theory is a phenomenological model which cannot be an alternative for a unified microscopic theory.

The next significant contribution to the microscopic theory of LHe-4 came in 1941 from Bogoliubov [143], from his analysis of a system of weakly interacting bosons. He considered LHe-4 as a system of degenerate non-perfect Bose gas and used the method of second quantization to show that in the presence of small interactions between the atoms, the low excited states of the gas could be described as a perfect Bose gas of certain quasiparticles (elementary excitation). On the assumption that the single particle state of lowest energy was macroscopically occupied, this theory showed that the condensate would be depleted by the interactions and derived an excitation spectrum as proposed by Landau. However, the weak point of Bogoliubov's theory was that the inter-atomic interactions between helium atoms to a good approximation are strong, in contradiction to the assumption that LHe-4 was a system of weakly interactiong Bose gas. Thus the problem of justification of the Landau spectrum on the basis of a microscopic theory remained.

In 1953 Feynman [144–146] tried to resolve the problem using

the quantum path integral method. He showed from first principles that LHe-4 should exhibit a transition analogous to the transition of an ideal bose gas regardless of the strong inter-atomic interaction. Also, by considering the symmetry properties of the many boson wave function, he further showed that (i) an excitation spectrum of the Landau type was a natural consequence and (ii) there could not be any low-energy excitation other than phonons in He II. Using variational approach, he obtained the wave function representing an excitation in LHe-4 and showed that the dispersion relation $w(Q)$ for elementary excitations is related to the static structure factor $S(Q)$ by the simple relation

$$\hbar w(Q) = \frac{\hbar^2 Q^2}{2mS(Q)} \tag{1.3.4}$$

Using this approach, the minimum roton energy $\triangle$ calculated was 19.1 K, while thermodynamic data required $\triangle = 9.6$ K. Later in 1956, Feynman and Cohen [147] proposed a more flexible variational wave function that simulated the interaction between phonons. The new wave function suggested that the roton was a kind of quantum mechanical anolog of a microscopic vortex ring, of diameter equal to about the atomic spacing. This yielded a low $\epsilon(Q)$ in good agreement with experiments at SVP, and gave $\triangle = 11.5$ K.

Lee and Mohling [148] in 1959 carefully analyzed the experimental data for the total cross-section for the inelastic scattering of cold neutrons in He II. They found that the projection of the angular momentum on the direction of the momentum p of the roton is equal to zero. In other words, the roton excitations has zero angular momentum indicating that they do not have rotational characters.

Bogoliubov's theory stressed the importance of a degenerate condensate for superfluidity. Later the theory was further developed by Onsager and Penrose [149] and by Bogoliubov [150,151]. Onsager

and Penrose were able to show that BEC took place in LHe-4 at absolute zero. They calculated that almost 8% of the atoms condensed into zero momentum state and further showed that for such state of the system, $< \psi(t,r) > \neq 0$, where $< \psi(t,r) >$ is the mean value of the Bose operator $\psi(t,r)$. This property enabled Bogoliubov [151] and Hohenberg and Martin [152] to obtain the hydrodynamical equation from the microscopic theory which could be used to calculate the spectra of the elementary excitations at small momenta.

Galasiewics [153, 154] and Krasnikov [155] derived the hydrodynamic equation with viscous terms using Bogoliubov's approach. Khalatnikov [156] also derived similar equations using a different approach in which he assumed that the distribution function for elementary excitations in He II satisfied a Boltzmann equation. Existence of the ODLRO (off-diagonal long range order), a criterion for the existence of long-range order [157] was not found in one and two dimensions [158], indicating that the phase transition in 1-D or 2-D systems must differ from that in a 3-D system.

In developing a microscopic theory of He II, the hard core repulsive part of the helium-helium interaction and the macroscopic occupation of a particular state posed serious mathematical complexities. Efforts to overcome these difficulties were initiated by Beliaev [159] and Hugenholtz and Pines [160]. However, exact results were obtained only for long wavelength region.

For small potential the classic work of Bogoliubov on the dilute weakly interacting gas was equivalent to the work of Beliaev [159]. The Bogoliubov approximation may, therefore, be considered as a small potential approximation. However Bogoliubov's theory was inconsistent with experimental results. Nevertheless, its great triumph was that for repulsive potential, it gave a dispersion relation linear with wave vector q.

The Bogoliubov approximation [143] is applicable only in the case of sufficiently weak interaction for which first-order perturbation theory is adequate. Since it is impossible for two He^4 atoms to be at the same point at the same time, the potential is certainly not weak at short distances. To account for the strong repulsive interactions, Brueckner and Sawada [161] developed a theory by assuming that the liquid was dilute. Parry and Ter Harr [162] estimated the error produced by this Bogoliubov approximation to be only about 3%. Goble and Trainer [163] used this theory to show that the condensate fraction varies from $0.37 - 0.79$ as the hard core radius changes from $(3.0 - 1.0)$ Å.

Bycking [164] carried out similar calculation considering all partial waves for Lennard–Jones potential with a hard-core radius of 2.6 Å. The calculated excitation curves agreed qualitatively with the experimental results.

Singh and Kumar [165,166] then included in this theory a weak longer range attractive interaction besides the repulsive core. The attractive interaction was treated by first-order perturbation theory and the repulsive interaction by a T-matrix theory. They showed that at zero temperature, if the parameters of the attractive part of the interaction are suitably restricted, the self-energy part of the Green's function lead to a phonon-like excitation spectrum for small momentum. All these theories gave results which at low frequencies essentially reduced to the Bogoliubov approximation with a modified form of potential.

Another approach approximating the self energy for LHe-4 was that of Tserkonikov [167, 168], Pines [169], Etters [170] and of Cheung and Griffin [171,172] who tried to apply the same approximation as those inherent in the random phasse approximation of an electron gas. But the approach failed to provide improvement in understand-

ing the system.

Several authors tried to exploit the similarity between the λ transition and superconduting transition in metals by suggesting that there was a similar pairing in LHe-4. Valatin anbd Butler [173], Girardeau and Arnowitt [174], Luban [175], Kobe [176] and Brown and Coopersmith [177], assumed a microscopic occupation of the zero momentum state and the Bogoliubov transformation was performed. The remainder of the Hamiltonian was truncated so that it could be diagonalized in a manner similar to that used in the theory of superconductivity. Congilio *et al* [178] and Evans and Imry [179] developed pairing theory in which there was no macroscopic occupation of the zero momentum state, but an effective attractive interaction between the particles to produce a pair condensation.

In a related but somewhat different formalism to that described above, Brandow [180, 181] suggested that instead of using the many-body theory developed by Beliaev [159] and Hugenhotz and Pines [160], one can consider helium as a Fermi system with infinite spin degeneracy. The infinite spin degeneracy permitted the condensation of all the particles into a single spatial state and had the advantage that the techniques developed by Goldstone [182] for Fermi system might be taken over directly to the LHe-4.

A combination of the Transformation method (TM) [143, 161] and the correlated basis-function approach (CBF) [182–187] which had been extensively used to study a strongly interacting N-body system, was also used to express the ground state [187–189]. The U-matrix theory [190] was used by Fung and Lam [191] to study several crucial features of LHe-4 at 1.1 K, based on a model Hamiltonian which includes two particle interaction function.

1.4 Experimental Studies of Liquid ^{3}He and ^{4}He mixtures

Several authors [192] pointed out before any ^{3}He was prepared that the study of the behavior of ^{3}He in LHe-4 would be very important to verify the interpretation of λ point by London as a Bose–Einstein degeneracy. Mixtures of LHe-3 and LHe-4 are also of technical importance for obtaining very low temperature, because the principle of operation of dilution refrigerators, which are widely used for cooling in the milli-kelvin range, are based on the specific properties of dilute liquid helium mixtures [7]. In addition, LHe-3 and LHe-4 mixtures are unique examples of interacting Bose and Fermi liquids in nature, where quantum mechanical exchange effects play a dominant role. As the concentration of ^{3}He in the mixture is increased, a rich array of macroscopic properties are observed.

1.4.1 Separation of ^{3}He

Since ^{3}He is a fermion, only the ^{4}He atoms in the mixture could exhibit superfluid behavior. Daunt *et al* [193] provided the first confirmation of this conclusion. They observed that ^{3}He did not partake in the helium film transfer or superfluid flow through very narrow slits. Their experiments also indicated methods for seperation of mixtures which could be used to enrich the ^{3}He concentration starting from well helium or atmospheric helium which contains ^{3}He in amounts of about $10^{-5}\%$ and $1.4 \times 10^{-4}\%$ as shown by Aldrich and Nier [194]. Thermal diffusion was also used initially to prepare mixtures containing about 1% ^{3}He. Later on in the U.S, pure ^{3}He was produced by nuclear processes. Lane *et al* [195] developed another separation method in the liquid phase below the λ point which was very useful and effective. Using this method the concentration of ^{3}He could be increased by a factor of about 4000. Soller *et al* [196]

improved the efficiency of this method further for separation on a larger scale. Starting with well helium, they could obtain an enrichment factor of 30000.

1.4.2 Specific heat

Important imformation on the behavior of mixtures can be obtained from measurements of the specific heat as a function of concentration and temperature. Above the λ point, the specific heat are not much different from that of pure He I, but the λ point shifts to lower temperatures with increasing concentrations. Ouboter and Taconis [197] measured the specific heat over a complete range of concentrations for the temperature range $(0.4 - 2)$ K. A review of data available upto 1964 was given by Taconis and Ouboter [198]. Unlike the situation in pure ^{4}He, the early specific heat measurements at λ point of the mixtures showed no divergence of C_p at the λ line. Alvesalo *et al* [199] measured the specific heat of the mixtures at SVP for eight different concentrations ranging from 53% to 73% in the temperature range of $(0.6 - 1.4)$ K. They found that the specific heat C_{px} (at constant pressure and constant concentration) at the λ point was finite, continuous and cusped. The estimated experimental error was less than 1%. Gasparini *et al* [200] observed in 1975 that at a fixed concentration, C_{px} was continuous across the λ transition and that C_{px} was singular, reaching a finite value with infinite slope at the λ transition.

1.4.3 The shift of the λ point

The presence of ^{3}He atoms in the mixture causes the shift of the λ point towards the lower temperature. This behavior was first observed by Abraham *et al* [201] for mixtures with ^{3}He concentration

ranging from 2% to 25%. To detect the λ point they made use of superleak made by sealing a platinum wire in a glass capillary. The accuracy of their measurement was about 0.05 K. Eselsohn *et al* [202] performed similar experiments with a ^{3}He concentration of 1.5%, making use of film creep technique to determine the λ point. Due to uncertainty in the concentration of their mixture, the value they obtained was not accurate. Daunt and Heer [203] studied the shift of the λ point of the mixture for concentration ranging from 40% to 90%. For the highest concentrations, the λ point was depressed below 1 K. These temperatures were reached by adiabatic demagnetization of chromium potassium alum. King and Fairbank [204] determined the λ point of the mixture making use of the disappearance of second sound at this temperature. For concentrations below 4%, their results showed that the λ temperature decreased linearly with ^{3}He concentration, with a slope of -1.5 K/mol. Sydoriak and Roberts and [205] determined the λ point from the discontinuity in the slope of the vapor pressure curve, while Doukopil *et al* [206] used the peak in the specific heat to determine the λ point, and Kerr [207] used the discontinuity in the slope of the density.

1.4.4 Finite solubility and molar volume of ^{3}He in ^{4}He

Addition of ^{3}He to ^{4}He increases the molar volume of the mixture, since ^{3}He atoms have lighter mass and greater zero point motion in the solution than ^{4}He atoms [208]. Edwards *et al* [209] determined the solubility curve at SVP in the temperature range $(0.025 - 1.25)$ K with x ranging form 0.392 to 0.1538. They found the limiting solubility at 0 K to be x_0=(6.37$\pm$ 0.05)% ^{3}He. They also found that for small concentration and at 0 K, α_0=0.284$\pm$ 0.005. Boghosian and Mayer [210] gave the value α_0=0.308$\pm$0.010. Abraham *et al* [208] determined α for a mixture concentration of 5.54%.

From this measurement, they found that x_0=6.6% and α_0=0.286. The early measurements on the solubility x of ^{3}He at temperatures in the range $(30 - 150)$ mK could be represented by the empirical expression

$$x(T) = x_0(1 + \beta T^2), \tag{1.4.1}$$

where x_0 is the solubility (6.4–6.6%) at T=0 K and β=$(9 - 11)$ K^{-2}. The coefficient x_0 has a minimum at about 10 bar. Vilches and Wheatley [211] from measurements of the refrigeration capacity of a single cycle of a dilution refrigerator in the region of $(10 - 20)$ mK found that x_0= 6.35%. From the slow neutron experiments, Schermer *et al* [212] gave x_0=6.84%. Watson *et al* [213] studied the pressure dependence of molar volumes of the mixtures in the range $(0 - 22.5)$ atm, within the temperature range $(50 - 500)$ mK for concentrations upto 10%. They reported that x_0 increased from (6.6±0.1)% at 50 mK and 0 atm to (9.5±0.12)% at 10 atm and then dropped back to (8.3±0.14)% at 22.5 atm. Yorozu *et al* [214] reported their results of careful measurements of solubility of ^{3}He in ^{4}He under pressure up to 20 bar in the temperature range $(1 - 250)$ mK. They found that below 60 mK, the solubility varies as T^2 at all pressures. Recently, Hatakeyama *et al* [215] studied the concentration and temperature dependence of BBP parameter for different concentrations. They gave the value of α_0=0.288, within the accuracy of 1%.

1.4.5 Phase diagram

The monotonic decrease of the λ point in helium mixtures continues with increasing ^{3}He concentration, until the tricritical point is reached at 0.87 K. Below 0.87 K, the mixture seperates into two phases, a heavier phase rich in ^{4}He, and a lighter phase rich in ^{3}He. This effect was first detected in the course of magnetic measurements by Fairbank and Walters [216]. The phase separation was

also observed visually [217,218], via the discontinuities in the velocities of ordinary sound [219] and second sound [220], via an inspection of density–temperature curve [221], and via marked anomaly in the specific heat of solutions which coincided with the onset of separation. The phase separation line for solutions under pressure was determined by Zinov'eva [218]. Schermer *et al* [212] studied the phase separation in the temperature interval $(0.04 - 0.85)$ K. In 1993, Kim *et al* [222] reported the phase diagram of liquid helium mixtures kept inside a porous aerogel of 0.98 open volume fraction. They found that the coexistence region of the two phases was detached from the λ line, giving rise to a miscible superfluid mixture at high ^{3}He concentrations and low temperatures. In 1995, Pricaupenkor and Treiner [223] reported their study of phase separation of mixtures kept inside thin channels, in contact with a bulk ^{3}He bath at zero temperature. They found that in thin channels, the ^{3}He-rich phase is richer in ^{3}He and the ^{3}He-rich phase contained a non-zero fraction of ^{4}He.

1.4.6 The influence of ^{3}He on the velocity of second sound

Lynton and Fairbank [224] showed that the velocity of second sound is strongly influenced by the presence of ^{3}He atoms. They measured the velocity of second sound in mixtures with concentration ranging from 0.09% to 0.8%. The velocity of second sound was measured using the pulse method with an error of 1%. They found a significant increase in the velocity of second sound, the increase was more pronounced at lower temperatures.

Weinstock and Pellam [225] used a thermal Rayleigh disk to determine the velocity of second sound. With a 4% mixture they obtained results in good agreeement with those of Lynton and Fairbank. King and Fairbank [226] performed experiments below 1 K

in mixtures with concentrations between 0.0017% and 4.3%. They found that the velocity of second sound was maximum at about 0.9 K, below that temperature it was nearly independent of ^{3}He concentration.

1.4.7 Other Properties

In their experiments on dilute mixtures of ^{3}He and He II, Daunt *et al* [193] found a kind of osmotic effect, while quantitative data were provided by Taconis *et al* [227,228] and by London *et al* [229]. The density under SVP has been measured by Kerr [207] and Ptukha [230]. The phenomenon called *heat flush* first observed by Reynolds *et al* [231] and later by Taconis [232,233] indicated that the heat current carried along the ^{3}He atoms, *i.e.*, ^{3}He solute atoms move only with the normal fluid. This view was confirmed by measurements of density of normal fluid in dilute solutions, using Andronikashvilli's method [234–236]. The propagation of first sound has been investigated in mixtures of ^{3}He and ^{4}He using different methods [237–239]. It was found that the presence of ^{3}He lowers the velocity of first sound. Sommers *et al* [240] measured the integral heat of mixing at constant temperature for 8.6% at 1.02 K. They reported a positive heat of mixing of 1.98 cal/mole of He^3. Seligman *et al* [241] measured the heat evolved when a known amount of ^{3}He was added to LHe-3 and LHe-4 at SVP in the region of 50 mK, for concentration ranging between 0% and 6%. They found that the binding energy for one ^{3}He atom in ^{4}He relative to pure ^{3}He was (0.312 ± 0.007) K. Anderson *et al* [242] studied the thermal and magnetic properties of two dilute solutions of nominal concentrations. Abel *et al* [243] measured the thermal conductivity of two dilute solutions of concentrations 1.3% and 5% in the temperature range of 30 mK down to 5 mK. They found that the thermal conductivity coefficient κ had the same T^{-1}

temperature dependence as a normal Fermi liquid. Abel and Wheatley [244] studied thermal conductivity of dilute solutions of the same concentrations at SVP in the temperature range of $(0.035 - 0.5)$ K. They concluded that in dilute solutions, heat was conducted by ^{4}He phonons at high temperatures, while at low temperatures, the ^{3}He quasiparticles conducted heat, as was previously observed by Abel *et al* [243]

Bertinat *et al* [245] reported measurements of the effective viscosity of dilute solutions between 20 mK and 1 K. Their results differed significantly from the theoretical prediction based on the works of Baym *et al* [246]. Bradley and Oswald [247] measured the viscosity of the mixture using a vibrating wire viscometer placed inside a dilution refrigerator. They found that in the low temperature Fermi liquid regime viscosity is proportional to T^{-2}. Zeegers *et al* [248] reported their results of measurements of the shear viscosity of saturated mixture in the temperature interval of $(7 - 200)$ mK using a vibrating wire viscometer. The extrapolation of their data to Fermi liquid temperature regime yielded a limiting value of ηT^2, in agreement with a more recent measurement of König *et al* [249].

1.4.8 Neutron Scattering Studies

Even though studies of the nature of elementary excitations in pure LHe-4 by inelastic neutron scattering techniques were reported as early as 1958, the application of this technique in liquid helium mixture had been discouraged for many years by the large neutron-absorption cross-section of ^{3}He nuclei. However, with improvements in the accuracy and reliability of neutron techniques, the first neutron scattering measurements at low momentum transfer Q in liquid helium mixtures were reported by Rowe *et al* [250], for a 5% mixture at SVP and a temperature of 1.6 K and by Hilton *et al* [251] for sev-

eral mixtures at SVP for temperature in the range of $(0.6 - 1.5)$ K. Both [250] and [251], which were limited to temperatures close to, or above the Fermi temperature T_F, reported a small shift of the ^{4}He phonon-roton curve but disagreed on the sign of the shift. Fak *et al* [252] investigated the excitations at temperatures below T_F. They found that the line shape of the ^{3}He particle–hole excitation was well described by a nearly-free Fermi gas model at all temperatures, but they found no evidence of a roton-like minimum in the ^{3}He spectrum. Their results confirmed the small shift in the phonon–roton spectrum observed by Rowe *et al* [250] and by Hilton *et al* [251].

Other complementary experimental techniques on helium mixtures include the studies of elementary excitations using Raman scattering by Surko and Slusher [253], and by Woerner *et al* [254]. Suemitsu and Swada [255] reported their study of the static structure factor using x-ray scattering.

In recent years, there are few reported neutron scattering measurements at high Q of liquid helium mixtures. Most of the workers reported values for the single-particle kinetic energies as a function of ^{3}He concentration, in or close to the normal phase [256–258]. Wang and Sokol [259] reported the first neutron scattering measurements of the condensate fraction n_0 in a 10% mixture where they found $n_0 = (18 \pm 3)\%$. Diallo *et al* [260] reported that n_0 increased from $n_0 = (7.25 \pm 0.75)\%$ at x=0 to $n_0 = (11 \pm 3)\%$ at $x = (15-20)\%$. The kinetic energy K_3 per atom of He^3 was found to be the same as it is in pure LHe-3, independent of the concentration, in contradiction to the theoretical prediction [261–264]. However, for ^{4}He, experiments agree qualitatively with theoretical predictions— both Azuah *et al* [257] and Senesi *et al* [258] reporting that the kinetic energy K_4 per atom of ^{4}He decreased with increasing ^{3}He concentration.

1.5 Theoretical Studies of Liquid Helium Mixtures

The behavior of liquid helium mixtures can be described following two different methods: the thermodynamical approach based on the properties of He II extended to mixtures where *ad hoc* assumption about the entropy of mixing was made, and the second approach, based on a more fundamental theory of λ transition in liquid helium. De Boer and Gorter [265], Rice *et al* [266], Stout [267] and Koide and Usui [268] followed the first approach, adopting the assumption of Taconis and Beenakker [269, 270] that ^{3}He formed an ideal mixture with the normal fluid. The second method was followed in the theories of Harasima [271], Heer and Daunt [272, 273], Mikura [274], and Toda and Isihara [275] where the λ transition in LHe-4 was interpreted as a consequence of BEC.

In 1948, Landau and Pomeranchuk [276] predicted that at low temperature, the ^{3}He atoms in very dilute solutions of ^{3}He in ^{4}He constitute an independent excitation system, which existed in the mixture in addition to the phonons and rotons. They proposed the single particle excitation energy spectrum

$$\epsilon = \epsilon_{03} + \frac{\hbar^2 k^2}{2m_3^*} \tag{1.5.1}$$

where ϵ_{03} is the potential energy of a single ^{3}He atom in pure He II and m_3^* is the effective mass of the ^{3}He quasiparticle. In this picture, the ^{3}He $-^4$ He interactions are retained while the ^{3}He $-^3$ He interactions are ignored. At low k, the ^{3}He excitation spectrum observed in neutron scattering experiment [251] agrees well with the Landau–Pomeranchuk (LP) spectrum. For $k \geq 1.5$ Å^{-1}, however, it departs from the theory and falls below the LP curve. Also, experiments performed around 1970 on second sound velocity, fourth sound velocity and normal fluid density revealed that for temperature greater

than a few tenths Kelvin, the normal fluid density and the various thermodynamic quantities could not be treated simply as the sum of the unmodified ^{4}He (that is, phonon–roton) term and the contribution from an ideal ^{3}He-quasiparticle gas [277]. These considerations led Pitaevskii [278] to suggest that the ^{3}He spectrum might exhibit a roton-like minimum. This speculation was supported by calculations by Varma [279] and by Stephen and Mittag [280]. Ruvalds *et al* [281] from first principle calculation concluded that LP form was essentially correct. A recent self-consistent calculation due to Bhatt [282], using the experimentally determined effective mass, yielded an excitation spectrum which deviates gradually, with increasing k, from a purely quadratic form. This spectrum is consistent with the neutron scattering results and also with the other earlier experimental data. Later, Greywall found that a satisfactory fit to his specific heat data [283] and second sound measurements [277] could be obtained with a spectrum which gradually deviated from quadratic form according to

$$\epsilon_q = \frac{q^2}{2m_3}(1 - g(q)) \tag{1.5.2}$$

where

$$g(q) = Dq^2 + Eq^4 + Fq^6 + Gq^8. \tag{1.5.3}$$

The phenomenological spectra of Greywall matched closely with the calculation of Bhatt [282]. The shift of the spectrum from that of pure ^{4}He reported by Rowe *et al* [250] and Hilton *et al* [251] were calculated by Bartley *et al* [284] considering the mode-mode coupling between the phonon–roton and ^{3}He density fluctuations. They concluded that for a ^{3}He-quasiparticle spectrum displaying a roton-like minimum, the shifts of energy near the ^{4}He roton minimum should be positive, increasing with decreasing temperature. However, those calculations failed to explain neutron scattering results of Hilton *et al* [251]. Aldrich and Pines [285] calculated the change in ^{4}He ex-

citation spectrum which arises due to the decrease in the particle density as the concentration of ^{3}He in the mixture increases, an important point not taken into account by Bartley *et al* [284]. With this correction Hilton *et al* [251] estimated the energy shift and obtained results in qualitative agreement with their experimental results. Hsu *et al* [286] showed that the shifts in the phonon–maxon–roton spectrum of ^{4}He observed in liquid helium mixtures results from three distinct physical effects, the change in system density caused by the ^{3}He atoms, the mode–mode coupling between the phono–roton branch and the ^{3}He density fluctuation excitation branch and at temperature above 1 K, scattering of the ^{4}He excitations near the roton minimum against thermally excited ^{3}He-quasiparticles. They also showed that an accurate account of the momentum and concentration dependence found in the experimental results of Hilton *et al* [251] may be obtained at low temperatures T$\leq$0.75 K by considering the combined influence of the density change and mode–mode coupling between the ^{4}He and ^{4}He density fluctuation excitation.

Bardeen *et al* [287] developed a theory of the effective interations between He^3 quasiparticles in dilute solutions. They assumed that the effective interaction between two He^3 quasiparticles depends only on their separation, but not on spin, relative velocity, or concentration. The interaction potential is some function V(q) of the momentum q which is exchanged in the collision between two quasiparticles. V(0) is the average interaction between two quasiparticles. Since ^{3}He and ^{4}He are isotopes, the coordinate space potential between two helium atoms is the same, independent of nuclear mass. The difference between the two isotopes in the liquid is that the He^3 atom, having a smaller mass, occupies a larger volume than a ^{4}He atom. A ^{3}He atom occupies a volume $v_3 = v_4^0(1 + \alpha)$ where v_4^0 is the volume per atom in pure ^{4}He and α is the BBP parameter. The

average interaction is given to be

$$V(0) = -\alpha^2(m_4 s^2/n_4) \tag{1.5.4}$$

where s is the velocity of sound in pure ^{4}He, m_4 is the mass of a ^{4}He atom and n_4 is the ^{4}He atom number density, and

$$V(q) = V(0)\cos(\beta q/\hbar) \tag{1.5.5}$$

with $\beta = 3.16$ Å, and $V(0) = -0.0754 m_4 s^2$. Ebner [288], using the classical gas expression for the diffusion coefficient and experimental value of spin diffusion coefficent, extended the effective interaction between ^{3}He quasiparticles, derived by Bardeen, Baym and Pines to larger values of the momentum. McMillan [289] developed a theory of strongly interacting mixed and pure Fermi gases, based on the theory of strongly interacting Bose gas. Using this theory, he calculated the equilibrium and transport properties of dilute solutions of ^{3}He in ^{4}He at low temperatures. The values for the two quasiparticle scattering amplitudes for small Q were in reasonably good agreement with the low temperature transport coefficients.

Woo *et al* [290] found using the method of correlated basis functions, the value of $m_3^* = 2.37 m_3$ at $P = 0$. Pandharipande and Itoh [291] made a micoroscopic calculations that give a good explanation of the pressure dependence of m_3^*. Boninsegni and Cerperley [263] studied helium mixtures at low temperatures using Path Integral Monte Carlo Simulation. In the limit of low concentrations, they found that $m_3^* = 2.3 m_3$ and a kinetic energy of 17 K was found for the ^{3}He atoms. Microscopic calculation done on the basis of the correlated basis function perturbation theory [292] have been able to give good estimates of chemical potential μ_3 and m_3^* at T = 0 and He^4 equilibrium density $\rho_{eq} = 0.02185$ Å^{-3}.

Very recently, Chaudhry and Brisson [293] determined the

thermodynamic property relations of liquid helium mixtures at SVP based on experimental mesurements of the specific heat. Using those relatons they calculated the thermodynamic properties of liquid helium mixtures at pressures of up to 10 bar and temperature below 1.5 K for all concentration range [294], which are in good agreement with the experimental data at low temperatures (below 0.7 K) and at low pressures.

1.6 Conclusion

From our brief review of the works on LHe-4, one can immediately observe that the untiring efforts of many workers during the last six decades failed to produce either a microscopic or a phenomenological theory that can account for all the unique properties of LHe-4. The two fluid model of Tisza, the two fluid model of Landau and the Ginzburg–Landau Ψ-theory [295] were insufficient to explain the superfluid behavior of LHe-4 (*cf.* section 1.3). Similarly the field theoretical approach followed by Bogoliubov, Beliaev, Hugenholts and Pines, Brueckner and Swada and others, or the variational approach followed by Feynman, Jackson and Feenberg, Jastrow, Penrose and Onsager and others was inadequate to fully account for all the observed properties of He II. In other words, there was no single theoretical formulation which could explain those properties. One often needs one theory to explain one property and another theory to account for another property. However, motivated by those facts, Jain recently developed a microscopic theory of superfluid helium known as *Macro-orbital Theory* [296–298]. This theory neither assumes the existence of $p = 0$ condensate nor applies the variational method. We present the salient features of Jain's Macro-orbital Theory and its significant conclusions and inferences in the next chapter.

Bibliography

[1] P. J. C. Janssen, C. R. Acad. Sci. Paris **67**, 494 (1868).

[2] J. N. Lockyer, C. R. Acad. Sci. Paris **67**, 836 (1868).

[3] W. Ramsay, Nature(London) **51**, 512 (1895) and **52**, 7 (1895).

[4] P. T. Cleve, C. R. Acad. Sci. Paris **120**, 843 (1995).

[5] H. Kayser, Chem. Ztg. **19**, 1549 (1895).

[6] M. L. E. Oliphant, B. B. Kinsey and E. Rutherford, Proc. Roy. Soc. London A**141**, 722 (1933).

[7] C. Enss and S. Hunklinger, *Low Temperature Physics*, Springer-Verlag, Berlin (2005).

[8] S. G. Sydoriak, E. R. Grilly and E. F.Hammel, Phys. Rev. **75**, 303 (1949).

[9] Zygmunt M. Galasiewics, *Helium-4*, Pergamon Press, Oxford (1971).

[10] J. Wilks, *The Properties of Liquid and Solid Helium*, Clarendon Press, Oxford (1967).

[11] Tony Guénault, *Basic Superfluids*, (Taylor and Francis, London 2003).

[12] H. K. Onnes, Proc. Roy. Acad. Sci. Amsterdam **11**, 168 (1908).

[13] H. K. Onnes, Proc. Roy. Acad. Sci. Amsterdam, **13**, 1093 (1911).

[14] H. K. Onnes and J. D. A. Boks, Leiden Comm. **170b**, 18 (1924).

[15] W. H. Keesom and A. P. Keesom, Physica **3**, 359 (1936).

[16] E. C. Kerr and R. D. Taylor, Ann. Phys. **26**, 292 (1964)

[17] M. H. W. Chan, K. I. Blum, S. Q. Murphy, G. K. S. Wong and J. D. Reppy, Phys. Rev. Lett. **61**, 1950 (1988).

[18] J. J. Neimala and R. J. Donelly, J. Low Temp. Phys. **98**, 1 (1995).

[19] L. I. Dana, H. K. Onnes, Proc. Roy. Acad. Sci. Amsterdam **29**, 106 (1926).

[20] W. H. Keesom and K. Clusius, Proc. Roy. Acad. Sci. Amsterdam **35**, 307 (1932).

[21] M. J. Buckingham and W. M. Fairbank in *Progress in Low Temperature Physics*, Vol. VIII, (C. J. Gorter ed.), North Holland, Amsterdam (1961).

[22] W. M. Fairbank, M. J. Buckingham and C. F. Kellers in *Low Temperature Physics and Chemistry*, (J. R. Dillinger ed.) University of Wisconsin Press, Madison, Wisconsin (1958).

[23] H. C. Kramers, J. D. Wasscher and C. J. Gorter, Physica **18**, 329 (1952).

[24] R. W. Hills and O. V. Lounasmaa, Phil. Mag. **2**, 143 (1957).

[25] J. Wiebes, C. G. Niels-Hakkenberg and H. C. Kramers, Physica **23**, 625 (1957).

[26] O. V. Lounasmaa and E. Kojo, Ann. Acad. Sci. Finncae. Ser. A **36** (1959).

[27] G. J. C. Bots and C. J. Gorter, Physica **26**, 337 (1960).

[28] C. J. N. Meijendenberg, K. W. Taconis and R de Bruyn Ouboter, Physica **27**, 197 (1961).

[29] G. Ahlers, Phys. Rev. Lett. **23** 464 (1969).

[30] G. Ahlers, Phys. Rev. A **3**, 696 (1971).

[31] G. Ahlers, Phys. Rev. A **8**, 530 (1973).

[32] F. Gasparini and M. R. Molodover, Phys. Rev. Lett. **23**, 749 (1969).

[33] F. M. Gasparini and M. R. Molodover, Phys. Rev. B **12**, 93 (1975).

[34] J. A. Lipa and T. C. P. Chui, Phys. Rev. Lett. **51**, 2291 (1983).

[35] M. Coleman and J. A. Lipa, Phys. Rev. Lett. **74**, 286 (1995).

[36] J. A. Lipa, D. R. Swansson, J. A. Nissen, Z. K. Geng, P. R. Williamson, D. A. Stricker, T. C. P. Chui, U. E. Israelsson and M. Larson, Phys. Rev. Lett. **84**, 4894 (2000).

[37] T. Chen and F. M. Gasparini, Phys. Rev. Lett. **40**, 331 (1978).

[38] S. Mehta and F. M. Gasparini, Phys. Rev. Lett. **78**, 2596 (1997).

[39] S. Mehta, M. O. Kimball and F. M. Gasparini, J. Low Temp. Phys. **113**, 435 (1998).

[40] J. A. Lipa, D. R. Swanson, J. A. Nissen, T. C. P. Chui and U. E. Israelsson, Phys. Rev. Lett. **76**, 944 (1996).

[41] J. A. Lipa, J. A. Nissen, D. A. Stricker, D. R. Swansson and T. C. P. Chui, Phys. Rev. B **68**, 174518 (2003).

[42] W. H. Keesom and M. Wolfke, Leiden Comm. **190b** (1927).

[43] C. J. Grebenkemper and J. P. Hagen, Phys. Rev. **80**, 89 (1950).

[44] C. E. Chase, E. Maxwell and W. E. Millet, Physica **27**, 1129 (1961).

[45] H. A. Kiersted, J. Low Temp. Phys. **23**, 791 (1976).

[46] M. H. W. Chan, M. Ryschkewitsch and H. Meyer, J. Low Temp. Phys. **26**, 211 (1977).

[47] J. J. Niemela and R. J. Donelly, J. Low Temp. Phys. **98**, 1 (1995).

[48] J. F. Allen, R. Peierls and Z. Uddin, Nature, **140**, 62 (1937).

[49] J. F. Allen and H. Jones, Nature, **141**, 243 (1938).

[50] F. London, Proc.Roy. Soc. A **171**, 484 (1939).

[51] J. G. Daunt and K. Mendelssohn, Nature **147**, 719 (1939).

[52] D. F. Brewer and D. O. Edwards, Proc. Phys. Soc. **71**, 117 (1958).

[53] C. I. Um, S. K. Yoo, S. Y.Lee, S. T. Nam, T. F. George and L. N. Pandey, Physica B **203**, 151 (1994).

[54] A. M. Kahn and G. Ahlers, Phys. Rev. Lett. **74**, 944 (1995).

[55] P. Kapitza, Nature **141**, 74 (1938).

[56] W. H. Keesom and G. E. MacWood, Physica **5**, 737 (1938).

[57] W. H. Keesom and P. H. Keesom, Physica **8**, 65 (1941).

[58] P. L. Smith, Physica **16**, 808 (1950).

[59] A. De Troyer, A. Van Itterbeek and G. J. Van Den Berg, Physica **17**, 50 (1951).

[60] J. T. Tough, W. D. Mc Cormick and J. G. Dash, Phys. Rev. **132**, 2373 (1963).

[61] H. C. Hollis Hallet, Proc. Camb. Phil. Soc. Maths. Phys. Sci. **49**, 717 (1953).

[62] W. J. Heikkila and H. C. Hollis Hallet, Can. J. Phys. **33**, 420 (1955).

[63] A. D. B. Woods and H. C. Hollis Hallet, Can J. Phys. **41**, 596 (1963).

[64] A. T. van Urk, W. H. Keesom and H. K. Onnes, Leiden Comm. **179a**, (1925).

[65] D. O. Edward and W. F. Saam in *Progress in Low Temperature Physics*, Vol.VIIA, (D.F. Brewer ed.), North Holland, Amsterdam (1978).

[66] J. F. Allen and A. D. Misener, Proc. Cambridge Philos. Soc. Math. Phys. Sci. **34**, 299 (1938).

[67] D. P. E. Dickson, D. Caroline and E. Mendoza, Phys. Lett. **33A**, 139 (1970).

[68] I. J. King and A. F. G. Wyatt, Proc. Roy. Soc. London, A **322**, 355 (1971).

[69] K. R. Atkins and Y. Narahara, Phys. Rev. **138**, A437 (1965).

[70] K. N. Zinoveva and S. T. Bolarev, Sov. Phys. JETP **56**, 585 (1969).

[71] M. Iino, M. Suzuki and A. J. Ikushima, J. Low Temp. Phys. **61**, 155 (1985).

[72] F. M. Gasparini, J. Eckardt, D. O. Edwards and S. Y. Shen, J. Low Temp. Phys. **13**, 437 (1973).

[73] J. H. Magerlein and T. M. Sanders Jr., Phys. Rev. Lett. **36**, 258 (1976).

[74] M. Suzuki, M. Iino and A. J. Ikushima, J. Low Temp. Phys. **63**, 129 (1986).

[75] F. Gallet, P. E. Wolf and S. Balibar, Phys. Rev. Lett. **52**, 2253 (1984).

[76] P. Roche, G. Deville, N. J. Appleyard and F. I. B. Williams, J. Low Temp. Phys. **106**, 565 (1997).

[77] K. Nakanishi and M. Suzuki, J. Low Temp. Phys. **113**, 585 (1998).

[78] C. Vicente, W. Yao, H. J. Maris and G. M. Seidel, Phys. Rev. B **66**, 214504 (2002).

[79] L. Tisza, Nature **141**, 913 (1938).

[80] L. D. Landau, J. Phys. USSR, **5**, 71 (1941).

[81] K. R. Atkins, Phys. Rev. **113**, 962 (1959).

[82] J. C. Findlay, A. Pitt, H. G. Smith and J. O. Wilhelm, Phys. Rev **54**, 506 (1938).

[83] C. E. Chase, Proc. Roy. Soc. A **220**, 116 (1953).

[84] A. van Itterbeek, G. Forrez and M. Teirlinek, Physica **23**, 905 (1957).

[85] V. Peshkov, J. Phys. USSR, **10**, 389 (1946).

[86] H. E. Hall and W. F. Vinen, Proc. Roy. Soc. **A 238**, 204 (1956).

[87] H. E. Hall and W. F. Vinen, Proc. Roy. Soc. **A 238**, 215 (1956).

[88] I. Rudnick, R. S. Kagiwida, J. C. Fraser and E. Guyon, Phys. Rev. Lett. **20**, 430 (1968).

[89] K. R. Atkins and I. Rudnick, in *Progress in Low Temperature Physics*, Vol. VI, (C.J. Gorter ed.), North Holland, Amsterdam (1970).

[90] I. Rudnick, Phys. Rev. Lett. **40**, 1454 (1978).

[91] D. T. Ekholm and R. B. Hallock, J. Low Temp. Phys. **42**, 339 (1981).

[92] K. A. Shapiro and I. Rudnick, Phys. Rev. **137**, A1383 (1965).

[93] K. R. Atkins and M. H. Edwards, Phys. Rev. **97**, 1429 (1955).

[94] E. C. Kerr, J. Chem. Phys. **26**, 511 (1957).

[95] M. H. Edwards, Can. J. Phys. **36**, 884 (1958).

[96] C. E. Chase, E. Maxwell and W. E. Millet, Physica **27**, 1129 (1961).

[97] E. C. Kerr and R. D. Taylor, Ann. Phys. **26**, 292 (1964).

[98] E. R. Grilly and R. L. Mills, Ann. Phys **18**, 250, (1962).

[99] O. V. Lounasmaa, Phys. Rev. **130**, 847 (1963).

[100] C. Boghosian and H. Meyer, Phys. Rev. **152**, 200 (1966).

[101] G. E. Watson, J. D. Reppy and R. C. Richardson, Phys. Rev. **188**, 384 (1969).

[102] W. D. Johnston and J. G. King , Phys. Rev. Lett. **16**, 1191 (1966).

[103] A. Griffin, Phys. Lett. **31A**, 222 (1970).

[104] M. W. Cole, Phys. Rev. Lett. **28**, 1622 (1972).

[105] C. Caroli, B. Roulet and D. Saint James, Phys. Rev. B **13**, 3875 (1976).

[106] S. Balibar, J. Buechner, B. Castaing, C. Laroche and A. Libchaber, Phys. Rev. B **18**, 3096 (1978).

[107] M. J. Baird, F. R. Hope and A. F. G. Wyatt, Nature **304**, 325 (1983).

[108] M. Brown and A. F. G. Wyatt, J. Phys. Cond. Matt. **2**, 5025 (1990).

[109] H. J. Maris, J. Low Temp. Phys. **87**, 773 (1992).

[110] P. A. Mulheran and J. C. Inkson, Phys. Rev. B **46**, 5454 (1992).

[111] F. Dalfovo, A. Fracchetti, A. Lastri, L. Pitaevskii and S. Stringari, Phys. Rev. Lett. **75**, 2510 (1995).

[112] F. Dalfovo, A. Fracchetti, A. Lastri, L. Pitaevskii and S. Stringari, J. Low Temp. Phys. **104**, 367 (1996).

[113] S. Stringari, F. Dalfovo, M. Guillemas, A. Lastri and L. Pitaevskii, Czech. J. Phys. **46**, 2973 (1996).

[114] M. B. Sobnack and J. C. Inkson, Phys. Rev. B **56**, R14271 (1997).

[115] M. B. Sobnack and J. C.I nkson, Phys. Rev. Lett. **82**, 3657 (1999).

[116] M. B. Sobnack, J. C. Inkson and J. C. H. Fung, Phys. Rev. B **60**, 3465 (1999).

[117] C. D. H. Williams, J. Low Temp. Phys. **113**, 627 (1998).

[118] A. S. Rybalko, J. Low Temp. Phys. **30**, 994 (2004).

[119] A. Rybalko, S. Rubets, E. Rudavskii, V. Tikhiy, S. Tarapov, R. Golovashchenko and V. Derkach, Phys. Rev. B **76**, 140503 (2007).

[120] A. Rybalko, S. P.Rubets, E. Ya Rudavskii, V. A. Tikhiy, R. Golavashchenko, V. N. Derkach and S. I. Tarapov, arXiv:0807.4810v1.

[121] M. Cohen and R. P. Feynman, Phys. Rev. **107**, 13 (1957).

[122] L. Goldstein, H. S. Sommers Jr., L. D. P. King and C. J. Hoffman, Proc. Int. Conf. Low Temp. Phys.,(R. Bowers ed.), (1951).

[123] D. G. Henshaw and D. G. Hurst, Phys. Rev. **91**, 1222 (1953).

[124] D. G. Henshaw and D. G. Hurst, Phys. Rev. **100**, 994 (1954).

[125] H. Palevsky, K. Otnes, K. E. Larsson, R. Pauli and R. Stedman, Phys. Rev. **108**, 1346 (1957).

[126] H. Palevsky, K. Otnes and K. E. Larsson, Phys. Rev. **112**, 11 (1958).

[127] J. L. Yarnell, G. P. Arnold, P. J. Bendt and E. C. Kerr, Phys. Rev. Lett. **1**, 9 (1958).

[128] J. L. Yarnell, G. P. Arnold, P. J. Bendt and E. C. Kerr, Phys. Rev. **113**, 1379 (1959).

[129] D. G. Henshaw, Phys. Rev. Lett. **1**, 127 (1958).

[130] A. D. B. Woods and R. A. Cowley, Rep. Prog. Phys. **36**, 1135 (1973).

[131] D. L. Price in *The Physics of liquid and Solid Helium*, Part II, (K.H.Bennemann, J.B. Ketterson eds.) Wiley-Interscience, New York (1978).

[132] H. R. Glyde and E. C. Svensson *Methods of Experimental Physics*, Vol. 23, Part B (D. L. Price and K. Skold eds.), Academic Press, London (1987).

[133] A. J. Legget, Rev. Mod. Phys. **71**, S318 (1999).

[134] P. E. Sokol in *Bose Einstein Condensation*, (A. Griffin, D. W. Snoke and S. Stringari eds.) Cambridge University Press, Cambridge (1995).

[135] H. Frohlich, Physica **4**, 639 (1937).

[136] F. London, Nature **141**, 643 (1938).

[137] S. J. Putterman, *Superfluid Hydrodynamics*, North Holland, Amsterdam (1974).

[138] R. K. Pathria, *Statistical Mechanics*, Pergamon, Oxford (1979).

[139] L. Tisza, J. Phys. et Radium. **1**, 350 (1940).

[140] L. Tisza, Phys. Rev. **72**, 838 (1947).

[141] L. Onsager, Nuovo Cimento **6** (Supp.2), 249 (1949).

[142] R. P. Feynman in *Progress in Low Temperature Physics*, Vol.I, (C. J. Gorter ed.) North Holland, Amsterdam (1955).

[143] N. N. Bogoliubov, J.Phys. (USSR) **11**, 23 (1947).

[144] R. P. Feynman, Phys. Rev. **91**, 1291 (1953).

[145] R. P. Feynman, Phys. Rev. **91**, 1301 (1953).

[146] R. P. Feynman, Phys. Rev. **94**, 262 (1954).

[147] R. P. Feynman and M. Cohen, Phys. Rev. **102**, 1189 (1956).

[148] T. D. Lee and F. Mohling, Phys. Rev. Lett. **2**, 284 (1959).

[149] L. Onsager and O. Penrose, Phys. Rev. **104**, 576 (1956).

[150] N. N. Bogoliubov in *Lectures on Quantum Statistics*, Vol.II, Gordon and Breach, New York (1970).

[151] N. N. Bogoliubov in *On the Hydrodynamics of a Superfluid*, Dubna Preprint (1963).

[152] P. C. Hohenberg and P. C. Martin, Ann. Phys. **34**, 291 (1965).

[153] Z. M. Galasiewicz in *Superconductivity and Quantum Fluids* Pergamon Press, Oxford (1970).

[154] Z. M. Galasiewicz, Bull. de l'Acad. de Sci. Polon **15**, 191 (1967).

[155] W. A. Krasnikov, Dissertation, Moscow State Univesity, (1967).

[156] I. M. Khalatnikov, JETP **23**, 21 (1952).

[157] C. N. Yang, Rev. Mod. Phys. **34**, 694 (1962).

[158] J. W. Kane and L. P. Kadanoff, Phys. Rev. **155**, 80 (1967).

[159] S. T. Beliaev, Sov. Phys. JETP **7**, 289 (1958).

[160] N. M. Hugenholtz and D. Pines, Phys. Rev. **116**, 489 (1959).

[161] K. A. Brueckner and K. Sawada, Phys. Rev. **106**, 1117 (1957).

[162] W. E. Parry and D. Ter Haar, Ann. Phys. **19**, 496 (1962).

[163] D. F. Goble and L. E. H. Trainor, Can. J. Phys. **46**, 839 (1968).

[164] E. Bycking, Phys. Rev. **145**, 71 (1966).

[165] K. K. Singh and S. Kumar, Phys. Rev. **162**, 173 (1967).

[166] K. K. Singh and S. Kumar, Phys. Rev. A **1**, 497 (1970).

[167] Y. A. Tserkonikov, Sov. Phys. Dokl. **9**, 1110 (1965).

[168] Y. A. Tserkonikov, Sov. Phys. Dokl. **11**, 723 (1965).

[169] D. Pines in *Many Body Theory* (R. Kubo ed.), New York, Benjamin (1966).

[170] R. E. Etters, Phys. Rev. Lett. **16**, 119 (1966).

[171] T. H. Cheung and A. Griffin, Can. J. Phys. **48**, 2135 (1970).

[172] T. H. Cheung and A. Griffin, Phys. Rev. A **4**, 237 (1971).

[173] J. G. Valatin and D. Butler, Nuovo Cimento **10**, 37 (1958).

[174] M. Girardeau and R. Arnowitt, Phys. Rev. **113**, 755 (1959).

[175] M. Luban, Phys. Rev. **128**, 965 (1962).

[176] D. H. Kobe, Ann. Phys. **47**, 15 (1968).

[177] G. V. Brown and M. H. Coopersmith, Phys. Rev. **178**, 327 (1969).

[178] A. Coniglio, F. Mancini and M. Maturi, Nuovo Cimento B**63**, 227 (1969).

[179] W. A. B. Evans and Y. Imry, Nuovo Cimento B**63**, 155 (1969).

[180] B. H. Brandow, Phys. Rev. Lett. **22**, 173 (1969).

[181] B. H. Brandow, Ann. Phys. **64**, 21 (1971).

[182] J. Goldstone, Proc. Roy. Soc. **A239**, 267 (1957).

[183] E. Feenberg in *Theory of Quantum Fluids*, Academic Press, New York (1969).

[184] A. Bijl, Physica **7**, 869 (1940).

[185] R. B. Dingle, Philos. Mag. **40**, 573 (1949).

[186] R. Jastrow, Phys. Rev. **98**, 1497 (1955).

[187] K. W. Wong and P. C. W. Fung, Nuovo Cimento B **25**, 595 (1975).

[188] P. C. W. Fung, H. K. Tsang and K. W. Wong, Nuovo Cimento B **28**, 313 (1975).

[189] K. W. Wong, P. C. W. Fung and C. C. Lau, Phys. Rev. A **22**, 1272 (1980).

[190] F. J. Dyson, Phys. Rev. **75**, 1736 (1949).

[191] P. C. W. Fung and C. C. Lam, in *3rd Asia Pacific Physics Conference*, Vol. 1, (Y. W. Chen, A. F. Leung, C. N. Yang and K. Young eds.), (1998).

[192] J. Franck, Phys. Rev. **70**, 561 (1946).

[193] J. G. Daunt, R. E.Probst, H. L. Johnston, L. T. Aldrich and A. O. Nier, Phys. Rev. **72**, 502 (1947); J. Chem. Phys. **15**, 759 (1947).

[194] L. T. Aldrich and A. O. Nier, Phys. Rev. **70**, 983 (1946);

[195] C. T. Lane, H. A. Fairbank, L. T. Aldrich and A. O. Nier, Phys. Rev. **73**, 256 (1948); Phys. Rev. **75**, 46 (1949).

[196] T. Soller, W. M. Fairbank and A. D. Crowell, Phys. Rev. **91**, 1058 (1953).

[197] R. de Bruyn Ouboter, K. W. Taconis, C. Le Pair and J. J .M. Beenakker, Physica **26**, 853 (1960).

[198] K. W. Taconis and R. de Bruyn Ouboter in *Progress in Low Temperature Physics*, Vol. IV, (C. J. Gorter ed.), North Holland, Amsterdam (1964).

[199] T. A. Alvesalo, P. M. Berglund, S. T. Islander , G. R. Pickett and W. Zimmerman, Jr., Phys. Rev. A **4**, 2354 (1971).

[200] F. M. Gasparini and M. R. Moldover, Phys. Rev. B **12**, 93 (1975).

[201] B. M. Abraham, B. Weinstock and D. V. Osborne, Phys. Rev. **76**, 864 (1949).

[202] B. N. Eselsohn and B. G. Lazarev, Dok. Acad. Sci. USSR **72**, 265 (1950).

[203] J. G. Daunt and C. V. Heer, Phys. Rev. **79**, 46 (1950).

[204] J. C. King and H. A. Fairbank, Bull. Am. Phys. Soc.(3) **28**, 65 (1953).

[205] S. G. Sydoriak and T. R. Roberts, Phys. Rev. **118**, 901 (1960).

[206] Z. Dokoupil, G. Van Soest, D. H. N.Wansink and D. G. Kapadnis, Physica **20**, 1181 (1954); Z. Dokoupil, D. G. Kapadnis, K. Sreeramamurty and K. W. Taconis, Physica **25**, 1369 (1959).

[207] E. C. Kerr, in *Low Temperature Physics and Chemistry*, (J. R. Dillinger ed.) University of Wisconsin Press, Madison, Wisconsin (1958) .

[208] B. M. Abraham, O. G. Brandt, Y. Eckstein and J. Munarin and G. Baym, Phys. Rev. **188**, 309 (1969).

[209] D. O. Edwards, E. M. Ifft, R. E. Sarwinski, Phys. Rev. **177**, 380 (1969).

[210] C. Boghosian and H. Meyer, Phys. Lett. **25A**, 352 (1967).

[211] O. E. Vilches and J. C. Wheatley, Phys. Lett. **24A**, 440 (1967).

[212] R. I. Schermer, L.Passol and D. C. Rorer, Phys. Rev. **173**, 277 (1968).

[213] G. E. Watson, J. R. Reppy and R. C. Richardson, Phys. Rev. **188**, 384 (1969).

[214] S. Yorozu, M. Hiroi, H. Fukuyama, H. Akimoto, H. Ishimoto and S.Ogawa, Phys. Rev. B **45**, 12942 (1992).

[215] K. Hatakeyama, S. Noma, E. Tanaka, S. N. Burmistrov and T. Satoh, Phys. Rev. B **67**, 094503 (2003).

[216] W. M. Fairbank and G. K. Walters, Nuovo Cimento **9**, Suppl 1, 297 (1958).

[217] K. N. Zinoveva and V. P. Peshkov, Sov. Phys. JETP **10**, 22 (1960).

[218] K. N. Zinoveva, Sov. Phys. JETP **17**, 123 (1963).

[219] T. R. Roberts and S. G. Sydoriak, Phys. Fluids **3**, 895 (1960).

[220] S. D. Elliot and H. A. Fairbank in *Low Temp. Phys. and Chemistry*, (J. R. Dillinger ed.), University of Wisconsin Press, Madison, Wisconsin (1958).

[221] E. C. Kerr, Phys. Rev. Lett. **12**, 185 (1964).

[222] S. B. Kim, J. Ma and M. H. W. Chan, Phys. Rev. Lett. **71**, 2268 (1993).

[223] L. Pricaupenko and J. Treiner, Phys. Rev. Lett. **74**, 430 (1995).

[224] E. A. Lynton and H. A. Fairbank, Phys. Rev. **80**, 1043 (1950).

[225] B. Weinstock and J. R. Pellam, Phys. Rev. **89**, 521 (1953).

[226] J. C. King and H. A. Fairbank, Phys. Rev. **93**, 21 (1953).

[227] K. W. Taconis, J. J. M.Beenakker and Z. Dokoupil, Phys. Rev. **78**, 171 (1950).

[228] D. H. N. Wansick and K. W. Taconis, Physica **23**, 125 (1957).

[229] H. London, G. R. Clarke and E. Mendoza, Phys. Rev. **128**, 1992 (1962).

[230] T. P. Ptukha, Sov. Phys. JETP **7**, 22 (1958).

[231] C. A. Reynolds, H. A. Fairbank, C. T. Lane, B. B. Mcinteer and A. O. Nier, Phys. Rev. **76**, 64 (1949).

[232] K. W. Taconis, Tijdschr Natuurk **16**, 101 (1950).

[233] J. J. M. Beenakker and K. W. Taconis in *Prog. Low Temp. Phys.*, Vol.I, (C. J. Gorter ed.), North Holland, Amsterdam (1955).

[234] J. R. Pellam, Phys. Rev. **99**, 1327 (1955).

[235] N. G. Berezniak and B. N. Eselsohn, Sov. Phys. JETP **4**, 766 (1957).

[236] J. G. Dash and R. D. Taylor, Phys. Rev. **107**, 1228 (1957).

[237] B. M. Abraham, Y. Eckstein, J. B. Ketterson and M. Kuchnir, Phys. Rev. Lett. **20**, 251 (1968).

[238] D. A. Rockwell, R. F. Benjamin and T. J. Greytak, J. Low Temp. Phys. **18**, 389 (1975).

[239] S. A. J. Wiegers, R. Jochemsen, C. C. Kranenburg and G. Frossati, J. Low Temp. Phys. **71**, 69 (1988).

[240] H. J. Sommers, W. E. Keller and J. G. Dash, Phys. Rev. **92**, 1345 (1953).

[241] P. Seligmann, D. O. Edwards, R. E. Sarwinski and J. T. Tough, Phys. Rev. **181**, 415 (1969).

[242] A. C. Anderson, D. O. Edwards, W. R. Roach, R. E. Sarwinski and J. C. Wheatley, Phys. Rev. Lett. **17**, 367 (1966).

[243] W. R. Abel, R. T. Johnson and J. C. Wheatley, Phys. Rev. Lett. **18**, 737, (1967).

[244] W. R. Abel and J. C. Wheatley, Phys. Rev. Lett. **21**, 1231, (1968).

[245] M. P. Bertinat, D. S. Betts, D. F. Brewer and G. J. Butterworth, Phys. Rev. Lett. **28**, 472 (1972).

[246] G. Baym and C. Ebner, Phys. Rev. **164**, 235 (1967).

[247] D. I. Bradley and R. Oswald, J. Low Temp. Phys. **80**, 89 (1990).

[248] J. C. H. Zeegers, A. Th. A. M.Waele and H. M. Gijsman, J. Low Temp. Phys. **84**, 37 (1991).

[249] R. König and F. Pobell, Phys. Rev. Lett. **71**, 2761 (1993).

[250] J. M. Rowe, D. L. Price and G. E. Ostrowski, Phys. Rev. Lett. **31**, 510 (1973).

[251] P. A. Hilton, R. Scherm, and W. G. Stirling, J. Low Temp. Phys. **27**, 851 (1977).

[252] B. Fak, K. Guckelsberger, M. Körfer, R. Scherm and A. J. Dianoux, Phys. Rev. B **41**, 8732 (1990).

[253] C. M. Surko and R. E. Slusher, Phys. Rev. Lett. **30**, 1111 (1973).

[254] R. L. Woerner, D. A. Rockwell and T. J. Greytak, Phys. Rev. Lett. **30**, 1114 (1973).

[255] M. Suemitsu and Y. Sawada, Phys. Rev. B **25**, 4593 (1982).

[256] R. T. Azuah, W. G. Stirling, J. Mayers, I. F. Bailey and P. E. Sokol, Phys. Rev. B **51**, 6780 (1995).

[257] R. T. Azuah, W. G. Stirling, K. Guckelsberger, R. Scherm, S. M. Bennington, M. L. Yates and A. D. Taylor, J. Low Temp. Phys. **101**, 951 (1995).

[258] R. Senesi, C. Andreani, A. L. Fielding, J. Mayers and W. G. Stirling, Phys. Rev. B **68**, 214522 (2003).

[259] Y. Wang and P. E. Sokol, Phys. Rev. Lett. **72**, 1040 (1994).

[260] S. O. Diallo, J. V. Pearce, R. T. Azuah, F. Albergamo and H. R. Glyde, Phys. Rev. B **74**, 144503 (2006).

[261] W. K. Lee and B. Goodman, Phys. Rev. B **24**, 2515 (1981).

[262] J. Boronat, A. Polls and A. Fabrocini, Phys. Rev. B **56**, 11854 (1997).

[263] M. Boninsegni and D. M. Ceperley, Phys. Rev. Lett. **74**, 2288 (1995).

[264] M. Boninsegni and S. Moroni, Phys. Rev. Lett. **78**, 1727 (1997).

[265] J. de Boer and C. J. Gorter, Phys. Rev. **77**, 569 (1950); Physica **16**, 225 (1950).

[266] O. K. Rice, Phys. Rev. **76**, 1701 (1949); O. K. Rice and O. G. Engel, Phys. Rev. **78**, 183 (1950).

[267] J. W. Stout, Phys. Rev. **76**, 864 (1949).

[268] S. Koide and T. Usui, Prog. Theor. Phys. **6**, 622 (1951).

[269] K. W. Taconis, J. J. M. Beenakker, L. T. Aldrich and A. O. C. Nier, Physica **15**, 737 (1949);

[270] K. W. Taconis, J. J. Benakker, L. T. Aldrich and A. O. Nier, Phys. Rev. **75**, 1966 (1949).

[271] A. Harasima, J. Phys. Soc. Japan, **6**, 271 (1951).

[272] C. V. Heer and J. G. Daunt, Phys. Rev. **81**, 447 (1951).

[273] J. G. Daunt, T. P. Seng and C. V. Heer, Phys. Rev. **86**, 911 (1952).

[274] Z. Mikura, Prog. Theor. Phys. **11**, 25 (1954).

[275] M. Toda and A. Isihara, Prog. Theor. Phys. **6**, 480 (1951).

[276] L. D. Landau and I. Pomeranchuk, Dokl. Akad. Nauk. USSR **59**, 669 (1948).

[277] D. S. Greywall, Phys. Rev. B **20**, 2643 (1979).

[278] L. Pitaevskii, Proceedings of the US-Soviet Symposium on Condensed Matter, Berkeley, California, May 1973 (Unpublished).

[279] C. M. Varma, Phys. Lett. **45A**, 301 (1973).

[280] M. J. Stephen and L. Mittag, Phys. Rev. Lett. **31**, 923 (1973).

[281] J. Ruvalds, J. Slinkman, A. K. Rajagopal and A. Bagchi, Phys. Rev. B **16**, 2047 (1977).

[282] R. N. Bhatt, Phys. Rev. B **18**, 2108 (1978).

[283] D. S. Greywall, Phys. Rev. Lett. **41** , 177 (1978).

[284] D. L. Bartley, J.E. Robinson and V. K. Wong, J. Low Temp. Phys. **12**, 71 (1973).

[285] C. H. Aldrich and D. Pines, J. Low Temp. Phys. **25**, 677 (1976).

[286] W. Hsu, D. Pines and C. H.Aldrich, Phys. Rev. B **32**, 7179 (1985).

[287] J. Bardeen, G. Baym and D. Pines, Phys. Rev. **156**, 207 (1967).

[288] C. Ebner, Phys. Rev. **156**, 222 (1967).

[289] W. L. Mc Millan, Phys. Rev. **175**, 266 (1968) and Phys. Rev. **182**, 299 (1969).

[290] C. W. Woo, H. T. Tan and W. E. Massey, Phys. Rev. Lett. **22**, 278 (1969); Phys. Rev. Lett. **185**, 287 (1969).

[291] V. R. Pandharipande and N. Itoh, Phys. Rev. A **8**, 2564 (1973).

[292] A. Fabrocini, S. Fantoni, S. Rosati and A. Polls, Phys. Rev. B **33**, 6057 (1986).

[293] J. G. Brisson, J. Low Temp. Phys. **155**, 235 (2009).

[294] J. G. Brisson, J. Low Temp. Phys. **158**, 806 (2010).

[295] V. L. Ginzburg and L. D. Landau, Zh. Eksperim. i. Teor. Fiz. **20**, 1064 (1950).

[296] Y. S. Jain, *Microscopic Theory of Superfluidity of a system of Interacting Bosons: The liquid* He^4, Technical Report, Physics Dept., NEHU, Shillong, (1995).

[297] Y. S. Jain, J. Sci. Expl. **16**, 67, (2002); J. Sci. Expl. **16**, 77, (2002).

[298] Y. S. Jain, Am. J. Cond. Mat. Phys **2**, 32 (2012).

Chapter 2

Macro-orbital Theory

2.1 Introduction

Liquid helium-4 (LHe-4), a system of interacting bosons (SIB), undergoes superfluid transtion at $T_\lambda = 2.17$ K. The phenomenon has been extensively investigated since it provides an excellent opportunity to study quantum behavior of a system at macroscopic level. Several authors [1–8] reviewed the different aspects of this unique system. Consequently, developing a viable microscopic theory of helium poses a fundamental challenge to many theorists. A wealth of theoretical methods and mathematical models were developed and tested on helium but with little success.

Over the last few years, Jain [9–12] developed, after identifying several weaknesses in the basic assumptions of the conventional approaches, a microscopic theory of LHe-4 called "Macro-orbital Theory" (MO theory). This theory provides a microscopic basis for He II to behave as a homogeneous mixture of two fluids as suggested by Landau [13]. In addition, it establishes some of the important ideas of London [14], Putterman [4] and the Ψ-theory [15]. In formulating his theory, Jain identified the following realities of LHe-4:

1. ^{4}He atoms in LHe-4 move freely within its volume on a surface of constant negative potential $(-V_0)$ unless they collide with each other. One may find that inter-atomic interactions in the liquid can be represented by a two body central potential $V(r_{ij})$ such as Lennard Jones potential,

$$V(r_{ij}) = 4\epsilon \left[\left(\frac{\sigma}{r_{ij}} \right)^{12} - \left(\frac{\sigma}{r_{ij}} \right)^{6} \right] \tag{2.1.1}$$

which could be identified as the sum of:
(i) a short range strong repulsive term $V^R(r_{ij})$ and (ii) a relatively weak long range attractive term $V^A(r_{ij})$. While $V^R(r_{ij})$

can be approximated to hard-core (HC) repulsion $V_{HC}(r_{ij})$ (with $V_{HC}(r_{ij} < \sigma) = \infty$ and $V_{HC}(r_{ij} \geq \sigma) = 0$; σ being the HC diameter of an atom), $V^A(r_{ij})$ is approximated to a constant negative potential $-V_0$. Obviously, $V_{HC}(r_{ij})$ forbids two particle from occupying same point in real space and $-V_0$ keeps particles confined to a fixed volume.

2. Following a systematic analysis of a 3-D case of two HC particles of finite size, Huang [16] established $V_{HC}(r) \equiv A\delta(r)$. The same result has been obtained for 1-D dynamics of two HC particles (*say*, $P1$ and $P2$) by Jain by studying the possible configuration of $P1$ and $P2$ just at the instant of their collision. He finds that while $P1$ and $P2$ keep their centers of gravity at $x = \sigma$ (with $x_2 = \sigma/2$ and $x_1 = -\sigma/2$), they register their physical touch at $x = 0$. Their encounter with $V_{HC}(x)$ in this process is a result of this contact at $x = 0$ beyond which two HC particles can not be pushed in. Naturally, in this process, σ has no importance either as the size of $P1$ or $P2$ or as a distance between their centers of gravity. The process of collision only identifies that particles are hard spheres, (whether of finite σ or of infinitely small σ) and this means $V_{HC}(x) \equiv A\delta(x)$.

3. Analysing the basic nature of the possible dynamics of two particles (say $P1$ and $P2$) in the system, Jain observes that $P1$ and $P2$ encounter δ-potential only when they suffer a collision. While in a two body collision, they simply exchange their momenta, k_1 and k_2, in a many body collision, where they may collide simultaneously with other particle(s), they could be identified to jump from their state of k_1 and k_2 (or their relative momentum $k = k_2 - k_1$ and center of mass (CM) momentum $K = k_1 + k_2$) to that of new momenta k_1' and k_2' (or k' and K'). It is obvious that each of them has free particle motion between two collisions.

Evidently, a state of two particles even in the presence of other particles of the system can be identified characteristically with a state of two HC particles. In other words, a pair of particles forms the basic unit of the system and the wave mechanics of two HC particles serves as an important basis for understanding a many body system.

In this Chapter, we present the salient features of Macro-orbital theory and its important inferences.

2.2 Basic Aspects of an SIB

2.2.1 Hamiltonian

A system of N interacting bosons such as LHe-4 is described [16,17], to a good approximation, by

$$H(N) = \sum_{i}^{N} h_i + \sum_{i<j} V(r_{ij}) \qquad \text{where}$$
$$h_i = -(\hbar^2/2m)\nabla_i^2 \qquad (2.2.1)$$

where m is the mass of a particle and $V(r_{ij}) = V^R(r_{ij}) + V^A(r_{ij})$ is a two body *central force potential*, with (i) $V^R(r_{ij})$ being the short range strong repulsion and (ii) $V^A(r_{ij})$, a weak attraction of slightly longer range. While $V^R(r_{ij})$ can be approximated to hard-core (HC) interaction $V_{HC}(r_{ij})$ [which is defined by $V_{HC}(r_{ij}) \leq \sigma = \infty$ and $V_{HC}(r_{ij} > \sigma) = 0$, with σ being the HC diameter of a particle], $V^A(r_{ij})$ renders a flat surface of constant negative potential (*say*, $-V_0$) for the particles (hard spheres) to remain confined to the volume (V) of the liquid and to move freely, unless they collide with

each other or with the boundaries of the system (*i.e.*, the free surface of the liquid and walls of the container). Foregoing $-V_0$ for its constant value, the effective Hamiltonian of LHe-4 can be written as

$$H_0(N) = \sum_{i}^{N} h_i + \sum_{i>j}^{N} A(r_{ij})\delta(r_{ij}), \tag{2.2.2}$$

using

$$V_{HC}(r_{ij}) \equiv A(r_{ij})\delta(r_{ij}) \tag{2.2.3}$$

with $A(r_{ij})$ being the strength of Dirac delta $\delta(r_{ij})$ repulsion. For impenetrable HC particles, $A(r_{ij}) \rightarrow \infty$, with $r_{ij} \rightarrow 0$.

While the equivalence expressed by eqn (2.2.3) is mathematically shown by Huang [16], its physical basis can be understood by examining the possible configuration of two HC particles (*say*, P1 and P2) right at the instant of their collision. When P1 and P2 during a collision have their individual CM located, respectively, at $\mathrm{r}_{CM}(1) = \sigma/2$ and $\mathrm{r}_{CM}(2) = -\sigma/2$, where r_{CM} (i = 1 or 2) represents the distance of the CM of i^{th} particle from the CM of P1 and P2, they register their physical touch at $r = 0$ and their encounter with $V_{HC}(r_{ij})$ is a result of this touch beyond which the two can not be pushed in. The process of collision only identifies this touch; it does not register how far are the CM points of individual particles at this instant. In other words, the rise and fall of the potential energy of P1 and P2 during their collision at $r = 0$ is independent of their σ and this justifies eqn (2.2.3). However, it may be mentioned that this equivalence would not be justified in relation to certain physical aspects of an SIB (for example, the volume occupied by a given number of particles) where the real size of the particle assumes importance.

2.2.2 Dynamics of a Pair of Particles

Since $V(r_{ij})$ (eqns (2.2.1) and (2.2.3)) is a two body interaction, a pair of particles logically forms the basic unit of an SIB whose dynamics can be described in the CM coordinate system by

$$\begin{aligned} H_0(2)\Psi(r,R) &= \left(-\frac{\hbar^2}{4m}\nabla_R^2 - \frac{\hbar^2}{m}\nabla_r^2 + A(r)\delta(r)\right) \\ &= E(2)\Psi(r,R) \end{aligned} \tag{2.2.4}$$

with

$$\Psi(r,R) = \psi_k(r)\exp(i\mathbf{K}.\mathbf{R}) \tag{2.2.5}$$

where the relative and CM momenta are defined respectively, by

$$\begin{aligned} \mathbf{k} &= \mathbf{p}_2 - \mathbf{p}_1 = 2\mathbf{q} \qquad \text{and} \\ \mathbf{K} &= \mathbf{p}_2 + \mathbf{p}_1 \end{aligned} \tag{2.2.6}$$

and the relative and CM positions by

$$\begin{aligned} \mathbf{r} &= \mathbf{b}_2 - \mathbf{b}_1 \qquad \text{and} \\ \mathbf{R} &= (\mathbf{b}_2 + \mathbf{b}_1)/2 \end{aligned} \tag{2.2.7}$$

with $\mathbf{b}_1$ and $\mathbf{b}_2$ being the positions and $\mathbf{p}_1$ and $\mathbf{p}_2$, the momenta (in *wave number*) of P1 and P2 respectively.

In order to find $\Psi(r,R)$ (eqns (2.2.4) and (2.2.5)), $A(r)\delta(r)$ may be treated as a step potential, since $A(r)\delta(r)$ has infinitely large positive value only at $r = 0$. Consequently, the quantum state of P1 and P2 at all points (excluding $r = 0$) can be represented, to a good approximation, by

$$\Psi(1,2)^{\pm} = \frac{1}{\sqrt{2}}[u_{\mathbf{p}_1}(\mathbf{b}_1)u_{\mathbf{p}_2}(\mathbf{b}_2) \pm u_{\mathbf{p}_2}(\mathbf{b}_1)u_{\mathbf{p}_1}(\mathbf{b}_2)], \tag{2.2.8}$$

where

$$u_{\mathbf{p}_i}(\mathbf{b}_i) = \exp(i\mathbf{p}_i.\mathbf{b}_i) \tag{2.2.9}$$

represents a plane wave with unit normalization. However, for the fact that $A(r)\delta(r) = \infty$ at $r = 0$, the condition that $\Psi(1,2)^{\pm} = 0$ at $r = 0$ is used. Rearranging $\Psi(1,2)^{\pm}$ (eqn (2.2.8)) in terms of CM coordinates, one easily gets

$$\Psi(r,R)^{\pm} = \sqrt{2}\psi_k(r)^{\pm}\exp(i\mathbf{K}.\mathbf{R}), \tag{2.2.10}$$

with

$$\begin{aligned} \psi_k(r)^{-} &= \sin(\mathbf{k}.\mathbf{r}/2) = \sin(\mathbf{q}.\mathbf{r}) \qquad \text{and} \\ \psi_k(r)^{+} &= \cos(\mathbf{k}.\mathbf{r}/2) = \cos(\mathbf{q}.\mathbf{r}) \end{aligned} \tag{2.2.11}$$

Here, $\Psi(r,R)^{-}$ (eqn (2.2.10)), satisfying $\Psi(r,R)|_{r=0} = 0$, has negative symmetry for the exchange of P1 and P2 for which it can be an acceptable wave function for fermions (*not for bosons*), but $\Psi(1,2)^{+}$ (eqn (2.2.10)), having the desired positive symmetry for bosons, does not satisfy $\Psi(r,R)|_{r=0} = 0$. Thus, one needs an alternative of $\Psi(r,R)^{+}$ to describe a pair of HC bosons and Jain found that

$$\begin{aligned} \Phi(r,R)^{+} &= \sqrt{2}\phi_k(r)^{+}\exp(i\mathbf{K}.\mathbf{R}) \qquad \text{with} \\ \phi_q(r)^{+} &= \sin|(\mathbf{q}.\mathbf{r})|, \end{aligned} \tag{2.2.12}$$

not only has positive symmetry but also satisfies the desired condition, $\Phi(r,R)^{+}|_{r=0} = 0$.

Analyzing the wave functions $\Psi(r,R)^{-}$ (from eqn (2.2.10)) and $\Phi(r,R)^{+}$ (from eqn (2.2.12)), and the related relations, he noted the following points:

(i) The fact that eqn (2.2.6) renders

$$\begin{aligned} \mathbf{p}_1 &= -\mathbf{q} + \mathbf{K}/2 \qquad \text{and} \\ \mathbf{p}_2 &= \mathbf{q} + \mathbf{K}/2 \end{aligned} \tag{2.2.13}$$

which, without any loss of generality, reveals that two bosons (or fermions) in $\Phi(r,R)^+$ $[\Psi(r,R)^-]$ state can be identified as particles moving with equal and opposite momenta (**q**, -**q**) with respect to their CM which moves freely as plane wave of momentum **K**. Since this agrees with the fact that $\psi_q(r)^-$ (eqn (2.2.11)) and $\phi_q(r)^+$ (eqn (2.2.12)) represent a standing wave [or what Jain called as *standing matter wave* (SMW)], Jain proposed to call the pair in $\Psi(r,R)^-$ and $\Phi(r,R)^+$ states as $(\mathbf{q},-\mathbf{q})$ pair or SMW pair. In addition, $|\phi_q(r)^+|^2 = |\psi_q(r)^-|^2$ which reveals an important fact that bosonic/fermionic nature does not affect the relative configuration of two HC particles and implies that the laws of bosonic/fermionic distribution of particles should be implemented in relation to the energy levels of allowed **K**. Jain used this inference in constructing N particle wave functions

(ii) As the dynamics of two particles, interacting through a central force, can be described in terms of two independent 1-D motions (relative and CM motions respectively), Jain generalized the result, $< A(x)\delta(x) >= 0$, to conclude that

$$\begin{aligned} &< \Psi(r,R)^-|A(r)\delta(r)|\Psi(r,R)^- > = \\ &< \Phi(r,R)^+|A(r)\delta(r)|\Phi(r,R)^+ > = 0 \end{aligned} \qquad (2.2.14)$$

which renders

$$E(2) =< H(2) >= \frac{\hbar^2 k^2}{4m} + \frac{\hbar^2 K^2}{4m} = \frac{\hbar^2 p_1^2}{2m} + \frac{\hbar^2 p_2^2}{2m} \qquad (2.2.15)$$

as the energy of two HC fermions/bosons. It may be noted that $< H(2) >$ is independent of the use of $\Psi(r,R)^-$ (eqn (2.2.10) for fermions or $\Phi(r,R)^+$ (eqn (2.2.12)) for bosons. This not only simplifies the theoretical derivations, but also underlines the fact that Jain's approach has no problem of energy divergence

due to wave superposition of two HC particles.

(iii) Analyzing the wave mechanics of two HC particles, presumed to have 1-D motion, Jain concluded [10] that the expectation value of their relative separation satisfies $< x > \geq \lambda/2$. Guided by the fact that the relative motion of two particles (interacting through a central force) in 3-D is equivalent to their relative motion in 1-D, this inference is applied to $\phi_k(r)^+$ state (equation (2.2.12)) of P1 and P2 to find that their $< r >$ should satisfy $< r > \geq \lambda/2$, for $\mathbf{k}||\mathbf{r}$ case and $< r > \geq \lambda/2\cos\theta$ (θ being the angle between $\mathbf{k}$ and $\mathbf{r}$), in general. As $|\cos\theta| \leq 1$, two HC particles from an experimental view point can reach the shortest distance of $< r >_0 = \lambda/2$ only and in this situation their individual locations from their CM are given by $< \mathbf{r}_{CM}(1) >_0 = - < \mathbf{r}_{CM}(2) >_0 = \lambda/4$. Using similar result for their shortest possible distance on the ϕ-line ($\phi = kr$), Jain noted that $\Phi(r,R)^+$ state is characterized by

$$\begin{aligned} \lambda/2 \leq < r > \quad &= d \quad \text{or} \\ q \geq q_0 (= \pi/d), \quad & \end{aligned} \tag{2.2.16}$$

with d being the nearest neighbour distance of two particles in an SIB and

$$< \Delta\phi > \geq 2\pi. \tag{2.2.17}$$

2.2.3 Macro-orbital Representation of a Particle

As it is evident from eqn (2.2.15), the wave superposition of P1 and P2, leading to $\Psi(r,R)^-$ (eqn (2.2.10)) or $\Phi(r,R)^+$ (eqn (2.2.12)), does not alter their net energy which is given by the relation $E(2) = \hbar^2 p_1^2/2m + \hbar^2 p_2^2/2m$, in their states represented by two plane waves. This implies that: (i) P1 and P2, in $\Psi(r,R)^-/\Phi(r,R)^+$ states, behave, energetically, like independent particles, (ii) $E(2)$ is shared

equally between P1 and P2, and (iii) the superposition brings P1 and P2 (having different energies, $E_1 = \hbar^2 p_1^2/2m$ and $E_2 = \hbar^2 p_2^2/2m$ respectively) to a single energy state of $(E_1 + E_2)/2$. Each of the two bosons (or fermions) in $\Phi(r,R)^+$ (or $\Psi(r,R)^-$) state, can be identified as an independent particle in a state represented by

$$\xi(i) = \zeta(r_i)\exp(i\mathbf{K}_i.\mathbf{R}_i) \qquad \text{with}$$
$$\zeta(r_i) = \sin(\mathbf{q_i}.\mathbf{r_i}) \qquad (2.2.18)$$

where the subscript i refers to the i^{th} particle ($i = 1$ or 2) of a pair it represents. Since the negative (or positive) sign of $\psi_k(r)^-$ (or $\phi_k(r)^+$) (eqn (2.2.10) or (2.2.12)) loses significance in the light of $|\psi_k(r)^-|^2$ $= |\phi_k(r)^+|^2$, $\xi(i)$ can be used identically to represent a fermion or a boson. $\xi(i)$ is called a *macro-orbital*, because it serves as a basic unit of the macroscopic 3-D network of SMWs and further, it helps in understanding the manifestations of the wave nature of particles at macroscopic level.

The fact that a particle (say, i^{th}) in a *many body quantum systems* (MBQS) naturally assumes a physical state represented by a macro-orbital (eqn (2.2.18)), can also be established by tracking its motion when it collides with another particle (or a set of particles or a boundary of the fluid); it must be noted that the particle, before and after such collision, can have different momenta, say, $\mathbf{p}_i$ and $\mathbf{p}_i^{'}$, indicating that its state ($\psi(i)^{\pm}$), around the point of collision, should be represented by the superposition of $u_{\mathbf{p}_i}(\mathbf{b}_i)$ and $u_{\mathbf{p}_i^{'}}(\mathbf{b}_i^{'})$ which can be expressed by

$$\psi(i)^{\pm} = u_{\mathbf{p}_i}(\mathbf{b}_i)u_{\mathbf{p}_i^{'}}(\mathbf{b}_i^{'}) \pm u_{\mathbf{p}_i^{'}}(\mathbf{b}_i)u_{\mathbf{p}_i}(\mathbf{b}_i^{'}) \qquad (2.2.19)$$

Since $\psi(i)^-$ vanishes at $r = 0$ (the point of collision), it correctly represents the state of the chosen particle (independent of its fermionic or bosonic nature) which, obviously, proves that $\psi(i)^- \equiv \xi(i)$.

Here, it may be noted that the macro-orbital state (eqn (2.2.18)) of a particle has following important aspects:

(i) *MS and SS states* : In what follows from this discussion, equation (2.2.18) virtually represents the superposition of two plane waves which may either be identified with two different particles, P1 and P2, or with two states of the same particle. Obviously, in the former case we have a state of *mutual superposition* (MS) of two particles, while in the latter case we have the *self superposition* (SS) of the same particle. However, there are no means to fix whether P1 and P2 have their MS or each one of them (after the collision) falls back on itself and assumes its SS state. Guided by this fact, it is always possible to identify each of the two particles (in a state of their wave superposition) in its SS state and represent it by a macro-orbital. This makes the macro-orbital representation a tool which greatly simplifies the mathematical formulation of the microscopic theory of a MBQS.

(ii) *Two motions* : Each particle in a macro-orbital state has two motions (q-motion and K- motion) which are respectively, related to the relative and CM motions of the pair it represents. Since only relative motion encounters a potential such as $A(r)\delta(r)$, the possible values of only q are restricted by the interaction. The K-motion is not expected to have any impact of the interaction and K can have any value between 0 and ∞.

2.3 N Particle State

2.3.1 State Function

Using N macro-orbitals for N particles, the state function which represents the j^{th} micro-state of the system is given by

$$\Psi_n^j(N) = (\prod_i^N \zeta(r_i) \sum_P^{N!})[(\pm 1)^P \prod_i^N \exp(iP\mathbf{K}_i.\mathbf{R}_i)] \tag{2.3.1}$$

Here, $\sum_P^{N!}$ refers to the sum of $N!$ product terms, obtained by permuting N particles on different $\mathbf{K}_i$ states. For a state of bosonic or fermionic system, the required symmetric or anti-symmetric nature of $\Psi_n^j(N)$ for an exchange of two particles is taken care of by $(+1)^P$ or $(-1)^P$. Using the fact that the permutation of N particles on different $\mathbf{q}_i$ states also gives $N!$ different $\Psi_n^j(N)$, one can readily obtain

$$\phi_n(N) = \frac{1}{\sqrt{N!}} \sum_{j=1}^{N!} \psi_n^j(N) \tag{2.3.2}$$

as the complete wave function of a possible quantum state of a bosonic or fermionic system.

2.3.2 State Energy

Defining

$$\begin{aligned} h(i) &= \frac{1}{2}[h_i + h_{i+1}] \\ &= -\frac{\hbar^2}{8m}\nabla_{R_i}^2 - \frac{\hbar^2}{2m}\nabla_{r_i}^2 \end{aligned} \tag{2.3.3}$$

with $h_{N+1} = h_1$ and writing eqn (2.2.2) as

$$H_0(N) = \sum_i^N h(i) + \sum_{i>j} A(r_{ij})\delta(r_{ij}) \tag{2.3.4}$$

Jain obtained [10, 12]

$$< \Phi_n(N)| \sum_{i>j}^{N} A\delta(r_{ij})|\Phi_n(N) >= 0 \tag{2.3.5}$$

and

$$\begin{aligned} E_n =& < \Phi_n|H_0|\Phi_n > \\ =& \sum_{i=1}^{N} \left(\frac{\hbar^2 K_i^2}{8m} + \frac{\hbar^2 q_i^2}{2m} \right) \end{aligned} \tag{2.3.6}$$

which concludes that $\phi_n(N)$ is an eigenstate of $H_0(N)$ with $E_n(N)$ as its energy eigenvalue. At first glance, eqn (2.3.6) indicates that $E_n(N)$ is purely kinetic, but the fact that q values are constrained to satisfy $q \geq q_0 = \pi/d$ indicates that HC interaction has an obvious control on $E_n(N)$; and of course this impact comes to surface only at low temperatures at which quantum effects start dominating the behavior of the system.

2.3.3 Ground State

To determine the ground state (G-state) energy of the system, Jain used the inference that $q \geq q_0$ (eqn (2.2.16)) and the fact that K can have any value between 0 and ∞. Putting $q_i = \pi/d_i (\approx q_0)$ and $K_i = 0$ for all particles in eqn (2.3.6) with $d_i = v_i^{1/3}$ where v_i represents the volume of the real space, exclusively occupied by the i^{th} particle, the G-state energy then becomes

$$\begin{aligned} E_{q_i, K=0}(N) &= \sum_{i}^{N} \frac{h^2}{8md_i^2} \\ &= \sum_{i}^{N} \frac{h^2}{8mv_i^{2/3}} \end{aligned} \tag{2.3.7}$$

with

$$\sum_{i}^{N} v_i = V \tag{2.3.8}$$

In writing $\sum_i^N v_i = V$, use has been made of the fact that each particle of the lowest possible $q = q_i$ has the largest possible quantum size $\lambda_i/2$ for which it occupies the largest possible v_i. Even though different particles can occupy, in principle, different volumes, but simple algebra reveals that $E_{q_i,K=0}(N)$ has its minimum value for $v_1 = v_2 = \ldots = v_N = V/N$, so that

$$E_0 = N\frac{h^2}{8md^2} = N\varepsilon_0 \tag{2.3.9}$$

where $\varepsilon_0 = h^2/8md^2$ is the G-state energy of a single particle.

Since all particles in the G-state identically have $q = q_0$ and $K = 0$, equations (2.3.1) and (2.3.2) can be used to write the G-state wave function as

$$\begin{aligned}\Phi_0(N) &= \prod_{i}^{N} \zeta_{q_0}(r_i) \\ &= \prod_{i}^{N} \sin(q_0 r_i)\end{aligned} \tag{2.3.10}$$

From eqns (2.3.9) and (2.3.10), it is clear that each particle in the G-state represents a particle trapped in a box (cavity formed by its neighboring particles) of size d and it rests at the central point of this cavity. Since each $\sin(q_0 r_i)$ in eqn (2.3.10) represents a kind of SMW which joins with other SMWs of neighboring particles at the boundaries between the two cavities they occupy, the G-state wave function seems to be a macroscopically large size 3-D network of SMWs which modulates the *relative positions* of two particles in phase space and extends from one end of the container to another. This network gets energetically stabilized due to some kind

of collective binding and assumes different aspects of macroscopic wave function of the superfluid state, as proposed by London [14]. In view of this inference, eqns (2.2.16) and (2.2.17) imply that the G-state configuration of particles in an SIB satisfies

$$\begin{aligned} &< k > = 0 \\ &< r > = d \qquad\qquad \text{and} \\ &< \Delta\phi > = 2n\pi \qquad\qquad \text{with n=1, 2, 3, ...} \end{aligned} \tag{2.3.11}$$

Although each particle in the G-state of an SIB retains the zero-point energy ε_0, it is evident from $< k >= 0$ that the particles in the G-state cease to have relative motions which is the main cause of inter-particle collisions, scattering and non-zero η. While this explains why the G-state should be a state of $\eta = 0$, it does not forbid the particles from moving in coherence with equal velocity without any change in the order of their locations. Since all particles assume $< r >= d$ (d is the nearest neighbor distance), the G-state represents a close packed arrangement of their wave packets in real space which can sustain phonon-like collective motions.

2.4 λ Transition and Related Aspects

2.4.1 Equation of State

It follows from section 2.3 and eqn (2.2.15) that the energy ϵ of a particle can be written as

$$\epsilon = \frac{E}{2} = \varepsilon(K) + \varepsilon(k) = \frac{\hbar^2 K^2}{8m} + \frac{\hbar^2 k^2}{8m} \tag{2.4.1}$$

which can have any value between ε_0 and ∞. Since this possibility exists even if $\hbar^2 k^2/8m$ is replaced by ε_0 (which is the lowest energy of q-motion) because K can have any value between 0 and ∞, ϵ can be written as

$$\epsilon = \frac{\hbar^2 K^2}{8m} + \varepsilon_0 \tag{2.4.2}$$

Using eqn (2.4.2) in the starting expression of the standard BEC theory [17], the equation of state of the system is given by

$$\frac{PV}{k_B T} = -\sum_{\varepsilon(K)} \ln[1 - z\exp(-\beta[\varepsilon(K) + \varepsilon_0])] \tag{2.4.3}$$

and

$$N = \sum_{\varepsilon(K)} \frac{1}{z^{-1}\exp(\beta[\varepsilon(K) + \varepsilon_0]) - 1} \tag{2.4.4}$$

with $\beta = 1/(k_B T)$ and fugacity $z = \exp(\beta\mu)$, (μ being the chemical potential. Redefining the fugacity as

$$\begin{aligned} z^{'} &= z\exp(-\beta\varepsilon_0) \\ &= \exp[\beta(\mu - \varepsilon_0)] \\ &= \exp(\beta\mu^{'}) \end{aligned} \tag{2.4.5}$$

where

$$\mu^{'} = \mu - \varepsilon_0 \tag{2.4.6}$$

and following the procedure of standard BEC [17], MO theory gives

$$\frac{P}{k_B T} = -\frac{2\pi(8mk_B T)^{3/2}}{h^3}\int_0^\infty x^{1/2}\ln(1 - z^{'}e^{-x})dx = \frac{1}{\lambda^3}g_{5/2}(z^{'}) \tag{2.4.7}$$

and

$$\frac{N - N_0}{V} = \frac{2\pi(8mk_B T)^{3/2}}{h^3}\int_0^\infty \frac{x^{1/2}dx}{z^{'-1}\exp^x - 1} = \frac{1}{\lambda^3}g_{3/2}(z^{'}) \tag{2.4.8}$$

where $x = \beta\varepsilon(K)$, $\lambda = h/(2\pi(4m)k_B T)^{1/2}$ and $g_n(z^{'})$ has its usual expression. This reduces an SIB to a system of non-interacting bosons (SNIB) but with a difference. Firstly, m is replaced by $4m$ and z by $z^{'}$. Secondly, the theory of an SNIB gives $z = 1$ (or $\mu = 0$) for $T \leq T_\lambda$ and $z < 1$ (or $\mu < 0$) for $T > T_\lambda$. However, MO theory fixes $z^{'} = 1$

(or $\mu^{'} = 0$, rendering $\mu = \varepsilon$ (equation (2.4.6))) for $T \leq T_\lambda$ and $z^{'} < 1$ (or $\mu^{'} < 0$ which requires $\mu < \varepsilon_0$ for $T > T_\lambda$). Eqns (2.4.3), (2.4.4) and (2.4.7), (2.4.8) can be used to evaluate different thermodynamic properties. For example, using eqns (2.4.7) and (2.4.8), the internal energy of the system is found to be

$$\begin{aligned} U &= \frac{3}{2} k_B T \frac{V}{\lambda^3} g_{5/2}(z^{'}) + N\varepsilon_0 \\ &= U^{'} + N\varepsilon_0 \end{aligned} \tag{2.4.9}$$

where $U^{'} = -\frac{\partial}{\partial\beta}\left(\frac{PV}{k_B T}\right)|_{z',V}$ represents the internal energy of K-motion, while $N\varepsilon_0$ comes from k-motion. Similarly, the Hemholtz free energy of the system can be expressed as

$$\begin{aligned} F &= N\mu - PV \\ &= N\varepsilon_0 + (N\mu^{'} - PV) \\ &= F(q = q_0) + F(K) \end{aligned} \tag{2.4.10}$$

2.4.2 Onset of $K = 0$ Condensate and T_λ

In what follows from eqns (2.4.7) and (2.4.8), applying the theory of an SNIB [17], Jain concluded that an SIB should exhibit a transition at

$$T_b = \frac{1}{4} T_{\text{BEC}} = \frac{h^2}{8\pi m k_B}\left(\frac{N}{2.61\text{V}}\right)^{2/3} \tag{2.4.11}$$

representing the onset of $K = 0$ condensate in a gas of non-interacting quasi-particles which could be attributed to K-motions. Here, T_{BEC} represents the usual temperature of BEC [17] in an SNIB and the factor (1/4) signifies that each boson, for its K-motion, behaves like a particle of mass $4m$. However, as the derivation of equation (2.4.11) does not take into account the q-motions of the particles, to get T_λ

(*the real transition temperature*), T_b should be added to

$$T_0 = \frac{h^2}{8\pi m k_B} \frac{1}{d^2} \tag{2.4.12}$$

which represents the T equivalent of ε_0, because $N\varepsilon_0$ component of U (eqn (2.4.9)) and F (eqn (2.4.10)), too, comes from the thermal energy of the system. This renders

$$T_\lambda = \frac{h^2}{8\pi m k_B} \left[\frac{1}{d^2} + \left(\frac{N}{2.61\mathrm{V}} \right)^{2/3} \right], \tag{2.4.13}$$

which clearly differs from that of a system of non-interacting bosons. While $K = 0$ condensation of particles in an SIB occurs in its G-state characterized by non-zero energy (ε_0), the $p = 0$ condensation in an SNIB occurs in the G-state of zero energy. In addition, while particles in an SIB are representatives of (**q**, -**q**) pairs, those in an SNIB are simply independent particles which have no mechanism to identify the presence of each other.

2.4.3 Nature of Transition

When the system is cooled through T_λ, it transform from a state of random distribution of its particles in ϕ-space to that of orderly distribution with $\Delta\phi = 2n\pi, (n = 1, 2, 3, \dots)$ (*cf.* section 2.3.3). This means that λ transition represents an onset of order–disorder of particles in ϕ-space followed by BEC of the particles in the state of $K = 0$ and $q = \pi/d$. Since BEC of the particles in $K = 0$ state is not different from the BEC of non-interacting bosons (which is a well known second order transition [17]) and the order–disorder of particles in ϕ-space is accomplished simply by a reshuffle of their momenta (kinetic energy) without any change in inter-particle distance and potential energy. This implies that there is no change in the total energy of the system at λ point which concludes it to be a

second order transition.

2.4.4 Free Energy and Order Parameter of T_λ

The free energy F of the system has two components which can be written as (*cf.* section 2.4.1)

$$F = F(q) + F(K) \approx N\varepsilon_0 + F(K) \tag{2.4.14}$$

where

$$\begin{aligned} F(K) &= k_B T \frac{2\pi(8mk_BT)^{3/2}}{h^3} \int_0^\infty x^{1/2} \ln(1 - z' e^{-x})\, dx \\ &= k_B T \frac{1}{\lambda^3} g_{5/2}(z') \end{aligned} \tag{2.4.15}$$

Eqn (2.4.14) is valid, to a good approximation, even for $T = T_\lambda^+$ (*i.e.*, just above T_λ) since almost 95% particles in the system at T_λ are estimated to have ε_0 energy. Guided by this fact and the expected occurence of λ transition (*cf.* section 2.4.2), F can be expanded as a function Ω, (an order parameter of the transition):

$$F(T, \Omega) = F_0 + \frac{1}{2}A\Omega^2 + \frac{1}{4}B\Omega^4 + \frac{1}{6}C\Omega^6 + \ldots \tag{2.4.16}$$

where F_0 is the constant component of F and A, B, C, *etc.*, are the coefficients of expansion which may depend on the physical conditions of the system such as temperature and pressure. It may be noted that it is $F(q)$ (but not $F(K)$) which is responsible for the unique properties of an SIB below T_λ since a gas of non-interacting bosons is not expected to exhibit superfluidity and its related properties despite its BEC into zero momentum state. Defining $A = \alpha(T - T_\lambda)/T_\lambda$, and taking B as positive and independent of T and taking terms containing Ω^6, Ω^8, *etc.*, as zero, Jain obtained

$$\Omega_R(T) = \frac{\Omega(T)}{\Omega(0)} = \sqrt{\frac{T_\lambda - T}{T_\lambda}} \tag{2.4.17}$$

Since almost all particles occupy their G-state at $T = T_0$, the system hardly retains any energy with its excitations. That is, the system at $T = T_0$ is effectively in the $T = 0$ state for which $\Omega(T_0) \approx \Omega(0)$. Renormalizing the T-scale by replacing T in eqn (2.4.17) by $T^* = T - T_0$, the expression for $\Omega_R(T)$ can be written as

$$\begin{aligned} \Omega_R(T^*) &= \sqrt{\frac{T_\lambda^* - T^*}{T_\lambda^*}} \\ &= \sqrt{\frac{T_\lambda - T}{T_\lambda - T_0}} \end{aligned} \tag{2.4.18}$$

which correctly has its maximum value of 1.0 at $T = T_0$.

As observed for LHe-4, a number of physical properties of an SIB can be expected to exhibit notable dependence on T around T_λ. Those properties are:

(i) The fraction of the number of bosons, $n_{K=0}(T) = N_{K=0}(T)/N$ which condensed into $q = q_0$ and $K = 0$ state.

(ii) The fractional number of particles $n^*(T \leq T_\lambda)$, which is defined as $n^*(T \leq T_\lambda) = [N^*(T_\lambda) - N^*(T)]/N^*(T_\lambda)$, which increases smoothly from $n^*(T_\lambda) = 0$ to $n^*(0) = 1$, in a manner $\Omega(T)$ is expected to increase with fall in T. Here $N^*(T)$ is defined as the number of particles in the excited states of energy, ε $[\varepsilon \geq \varepsilon_c (= \hbar^2 Q_c^2/2m$, with $Q_c = 2\pi/\sigma)]$ so that

$$N^*(T) = \frac{\mathrm{V}}{4\pi^2}\left[\frac{2m}{\hbar^2}\right]^{3/2} \int_{\varepsilon_c}^{\infty} \left[\exp\left(\frac{\varepsilon - \varepsilon_0}{k_B T}\right) - 1\right]^{-1} \sqrt{\varepsilon} d\varepsilon \tag{2.4.19}$$

To a good approximation, these states correspond to a single particle motion, since the excitation wave length $\Lambda^* \leq \sigma (< d)$ which implies that the impact of the excitation is localized to a space shorter than the inter-particle distance, indicating that

the energy and momentum of the excitation is carried basically by a single particle.

(iii) The *volume expansion of the system*, forced by zero-point force, on cooling through T_λ, which can be viewed as strain in inter-particle bonds, is defined by $\delta(T) = \Delta d/d_\lambda = (d_T - d_\lambda)/d_\lambda$, *etc.*

Since particles in an SIB for their K-motions behave like non-interacting bosons, $n_{K=0}(T)$ (identified as (i) above) can be evaluated by using $n_{K=0}(T) = [1-(T/T_\lambda)^{3/2}]$, obtained from the standard theory of BEC of an SNIB [17]. Recasting $n_{K=0}(T)$ on the T^*-scale, Jain obtained its equivalent for an SIB given by

$$n_{K=0}(T^*) = \frac{N_{K=0}(T^*)}{N} = \left[1 - \left(\frac{T^*}{T^*_\lambda}\right)^{3/2}\right] = \left[1 - \left(\frac{T - T_0}{T_\lambda - T_0}\right)^{3/2}\right]. \quad (2.4.20)$$

2.4.5 Single Particle Density Matrix and ODLRO

The single particle density matrix, $\rho_1(\mathbf{R}' - \mathbf{R})$, which is a measure of the probability of spontaneous motion of a particle from $\mathbf{R}$ to $\mathbf{R}'$ or *vice versa*, becomes significant at $T \leq T_\lambda$. $\rho_1(\mathbf{R}' - \mathbf{R})$ is also known as the measure of *off diagonal long range order* (ODLRO). To obtain $\rho_1(\mathbf{R}' - \mathbf{R})$, Jain noted that:

(i) to a good approximation, almost all particles in an SIB [in its low temperature (LT) phase as well as at T_λ^+ (just above T_λ) in the high temperature (HT) phase] have $(\mathbf{q}, -\mathbf{q})$ pair state with $q = q_0$ and

(ii) such a particle, when made to move with momentum $\Delta\mathbf{q}$, assumes a state of $(\mathbf{q}+\Delta\mathbf{q}, -\mathbf{q}+\Delta\mathbf{q})$ which not only implies that

its state changes from

$$\sin(\mathbf{q}.\mathbf{r}) \rightarrow \sin(\mathbf{q}.\mathbf{r}) \exp i(\mathbf{K}.\mathbf{R}) \qquad (2.4.21)$$

(with $\mathbf{K} = 2\Delta\mathbf{q}$), but also concludes that particles with $K = 0$ [*i.e.*, whose states are defined simply by $\sin(\mathbf{q}.\mathbf{r})$], are basically localized particles with their wave packets spreading over a $\lambda/2 = \pi/q_0 = d$ space; the number of such particles ($N_{K=0}(T^*)$), grows from its zero value (in the HT phase) to a macroscopically large fraction in LT phase.

Using these observations, Jain obtained the single particle density matrix:

$$\rho_1(\mathbf{R}' - \mathbf{R}) = \left[\frac{N_{K=0}(T^*)}{V} + \frac{N - N_{K=0}(T^*)}{V} \exp\left(-\pi \frac{(R^* - R)^2}{\lambda_T'^2}\right)\right] \times (\sin^2 \frac{\pi}{d} r) \qquad (2.4.22)$$

by separating particles having $K = 0$ from those with $K \neq 0$ and evaluating the second term on the right by following the standard procedure for non-interacting bosons [17] which is justified by the fact that K-motions encounter no interactions. The $(\sin^2 \pi r/d)$ term in eqn (2.4.22) shows the variation of the probability density around the center of a particle wave packet in the cavity (of size d) formed by the neighboring particles.

Using the value of $N_{K=0}(T^*)$, it is clear that $\rho_1(\mathbf{R}^* - \mathbf{R})$ (under the limit $|\mathbf{R}^* - \mathbf{R}| \rightarrow \infty$) has non-zero value for the LT phase and zero value for the HT phase of an SIB. This firmly proves that MO theory is consistent with (a) the criterion of Penrose and Onsager [18] for the occurence of BEC in the G-state of the system defined by $K = 0$ and $q = \pi/d$ and (b) the idea of ODLRO, spontaneous

symmetry breaking and phase coherence suggested respectively by Yang [19], Goldstone [20] and Anderson [21].

2.4.6 Evolution of the System on Cooling

For a constant particle density, the interparticle seperation d remains constant while thermal de Broglie wavelength λ_T increases with decreasing temperature. As a result $(d-\lambda/2)$ decreases with decreasing T and at a certain $T = T_\lambda$, $(d-\lambda/2)$ vanishes. Consequently, the system at T_λ has $q = q_0 = \pi/d$ for all particles and its state (eqn (2.3.2)) is now expressed by

$$\Phi_n^S(N) = \Phi_0(N)\Psi_K(N) \qquad \text{with}$$
$$\Psi_K(N) = \sum_P^{N!}[\prod_i^N \exp i(P\mathbf{K}_i \cdot \mathbf{R}_i)] \qquad (2.4.23)$$

The superscript S in $\phi_n^S(N)$ refers to the fact that the system becomes superfluid at $T \leq T_\lambda$. Eqn (2.4.23) implies that all the $N!$ micro-states of the system appearing in $\phi_n(N)$ (eqn (2.3.2)) merge into one and the entire system at T_λ attains a kind of oneness as suggested by Taubes [22].

2.4.7 Volume Expansion on Cooling

In what follows from section 2.4.6, the q-motion energy of almost all particles gets frozen at ε_0, when an SIB is cooled to $T = T_\lambda$. ε_0 would tend to fall further because a particle (trapped in a cavity formed by its nearest neighbors) in its G-state exerts zero-point force ($f_0 = -\partial_d \varepsilon_0 = h^2/4md^3$) and tries to expand the cavity against a force f_a (originating from inter-particle attraction); it may be noted that f_0 comes into play only at $T \leq T_\lambda$ where $\lambda/2$ tends to have a value d_λ^+ (slightly larger than d_λ decided by $V(r_{ij})$). The equilibrium of f_0 and

f_a leaves an increase in the cavity size from d_λ to $d_T = d_\lambda + \Delta d$ and this happens to all particles. Consequently, the system on its cooling is expected to have volume expansion around T_λ. The fact that this prediction of MO theory is confirmed by experimentally observed negative thermal expansion co-efficient of LHe-4 at $T \leq T_\lambda$ [1] clearly reveals the accuracy of MO theory. Obviously ε_0 of each particle decreases by

$$\begin{aligned}\Delta\epsilon(T) &= [\varepsilon_0(T_\lambda) - \varepsilon_0(T)] \\ &\approx \frac{h^2}{4md_\lambda^2}\frac{d_T - d_\lambda}{d_\lambda} = 2\varepsilon_0\frac{d_T - d_\lambda}{d_\lambda}\end{aligned} \tag{2.4.24}$$

Analysis of the equilibrium between f_0 and f_a reveals that the net fall in energy is only $(1/2)\Delta\epsilon(T)$ because $(1/2)\Delta\epsilon(T)$ is retained as per particle strain energy for the expansion in interparticle bonds by $\Delta d = d_T - d_\lambda$.

2.4.8 Quantum Correlation And Their Importance

Quantum correlations between particles, originating from their wave nature, play an important role in relation to the behavior of an SIB. These correlations can be expressed in terms of what is known as quantum correlation potential (QCP) [17, 23, 24] which can be obtained by comparing the partition function (under the quantum limits of the system)

$$Z_q = \sum_n \exp(-E_n/k_BT)|\phi_n^S(N)|^2 \tag{2.4.25}$$

with its classical equivalent,

$$Z_c = \sum_n \exp(-E_n/k_BT)\exp(-U_n/k_BT) \tag{2.4.26}$$

Here, $\Phi_n^S(N)$ is given by eqn (2.4.23). Jain found that quantum correlation potential has two components:

1. U_{ij}^s, which pertains to k motion, controls the $\phi = kr$ position of a particle. This potential is given by

$$U_{ij}^s = -k_B T_0 \ln[2\sin^2(\phi/2)] = -k_B T_0 \ln[2\sin^2(2\pi r/\lambda)] \quad (2.4.27)$$

where T has been replaced by T_0 because the temperature equivalent of k-motion energy at all $T \leq T_\lambda$ is T_0. It has the minimum value $-k_B T_0 \ln 2$ at $\phi = (2n+1)\pi$ (with n=0,1,2,3,...) and the maximum value ∞ at $\phi = 2n\pi$ (with n=0,1,2,3,...). U_{ij}^s always increases for any small change $\delta\phi$ at its minimum, as

$$\frac{1}{2}C(\delta\phi)^2 = \frac{1}{4}k_B T_0(\delta\phi)^2 \quad (2.4.28)$$

with force constant C defined by

$$C = \frac{1}{2}k_B T_0. \quad (2.4.29)$$

Therefore, the particles experience a $force = -C\delta\phi$ which tries to maintain $\delta\phi = 0$ and sustain the order of particles in ϕ-space.

2. The second component pertaining to K-motion is given by

$$U_{ij} \simeq -k_B T \ln\left[1 + \exp\left(\frac{-2\pi|R' - R''|^2}{\lambda_T'^2}\right)\right] \quad (2.4.30)$$

with $\lambda_T' = h/(2\pi(4m)k_B T)^{1/2}$ which is identical to the expression obtained for non interacting bosons [17]. This potential is the origin of the force that drives the particles of the system in K-space towards $K = 0$, (BEC state of K motion) where it has its minimum value $-k_B T \ln 2$.

2.4.9 Logarithmic Singularity of Specific Heat

MO theory predicts simultaneous occurence of two separate phenomena at T_λ: (i) BEC of SMW pairs and (ii) ordering of particles in phase space. It predicts that when the particles move from their un-

correlated state ($\phi = 2n\pi \pm \delta\phi_\lambda$) at T_λ^+ (just above T_λ) to correlated state ($\phi = (2n+1)\pi$) at T_λ^- (just below T_λ), the system releases energy $\Delta\varepsilon$ which is responsible for the singularity of specific heat at λ transition. If N_λ particles move from their uncorrelated state to correlated state, $\Delta\varepsilon$ is given by

$$\Delta\varepsilon = -N_\lambda k_B T_0 \left[\ln 2 \sin^2\left(\frac{2n\pi \pm \delta\phi_\lambda}{2}\right) - \ln 2\right] \tag{2.4.31}$$

Following the theories of critical phenomena [25]

$$\delta\phi_\lambda = \delta\phi_\lambda(0)|\zeta|^\nu[1 + a_2|\zeta|^2 + a_3|\zeta|^3] \tag{2.4.32}$$

with $\zeta = \frac{T-T_\lambda}{T_\lambda}$. To a good approximation

$$\Delta\varepsilon = -N\frac{T - T_\lambda}{T_\lambda} k_B T_0 \ln\left(\frac{\delta\phi_\lambda(0)|\zeta|^2}{2}\right) \tag{2.4.33}$$

where

$$\delta\phi_\lambda = \delta\phi_\lambda(0)|\zeta|^\nu \qquad \text{and}$$
$$N_\lambda = \frac{N(T - T_\lambda)}{T_\lambda} \tag{2.4.34}$$

Using LHe-4 parameters and choosing $\nu = 0.55$ and $\delta\phi_\lambda(0) = \pi$, eqn (2.4.33) gives

$$C_p(\text{ J mol}^{-1}\text{ K}^{-1}) = -5.71 \ln|\zeta| - 10.35 = -A \ln|\zeta| + B \tag{2.4.35}$$

However, experimental results reveal that $A = 5.355$ and $B = -7.77$ for $T > T_\lambda$ and $A = 5.1$ and $B = 15.52$ for $T < T_\lambda$ [26]

2.4.10 Thermal Excitation

A system like LHe-4 is expected to exhibit (i) no transverse mode because the shear forces between its particles are negligibly small, and (ii) only one branch of longitudinal mode because the system is isotropic. Also since the particles in the G-state of an SIB form a

kind of close packed arrangement with $\Delta\phi = 2n\pi$ (*cf.* section 2.3.3), one can visualize waves of ϕ-oscillations. Using a linear chain of atoms with nearest neighbor interactions, the frequency dispersion of ϕ-oscillations can be written as

$$\omega_\phi(Q) = \sqrt{\frac{4C}{\beta}} |\sin(Qd/2)| \tag{2.4.36}$$

where Q is the wave vector and β is the measure of inertia for ϕ motion. ϕ oscillations can appear as the oscillations of both r and q since $\delta\phi = 2q(\delta r) + 2r(\delta q)$. While r-oscillations could be identified as phonon modes when all particles retain $q = q_0$, the q-oscillation at which r remains fixed at d is represented by *omons*, a new kind of quantum quasi-particle which represents a phonon-like waves of momentum oscillation.

Evidently, $\omega_r(Q)$ of phonons can be represented, to a good approximation, by the dispersion of the elastic waves in a chain of identical atoms and it can be obtained from eqn (2.4.36) by replacing β and C by m and C^*, respectively. From eqn (2.4.29)

$$C^* = 4\pi^2 C/d^2 = 2\pi^2 k_B T_0/d^2 = \pi h^2/4md^4 \tag{2.4.37}$$

it may be mentioned that d and C^* are descending and ascending functions of Q because an increase in energy of the particles by an excitation reduces wave packet size of the particles which decreases d and increases C^*. As such the phonon energy, $E_{ph}(Q)$, is expressed more accurately by

$$E_{ph}(Q) = \hbar\omega_r(Q) = \hbar\sqrt{\frac{4C(Q)}{m}} |\sin(Qd(Q)/2)| \tag{2.4.38}$$

The use of $C^*(Q)$ and $d(Q)$ not only explains the experimentally observed $E_{ph}(Q)$ of He II but also accounts for its anomalous nature at low Q [9]. This aspect has been studied in detail in [27].

However, since $d(Q)$ can not be smaller than σ, $d(Q)$ and $C(Q)$ are bound to become Q independent for $Q > \pi/\sigma$ and the maximum in $E_{ph}(Q)$ (*i.e.*, the position of the so-called *maxons*) should fall at maxon $Q = Q_{max} = \pi/\sigma$ and $E_{ph}(Q)$ over the range $Q > \pi/\sigma$ and $< 2\pi/d$ should follow

$$E_{ph}(Q) = \hbar\omega_r(Q) = \hbar\sqrt{\frac{4C(Q_{max})}{m}}|\sin(Q\sigma/2)| \tag{2.4.39}$$

The phonon-like dispersion is expected till the excitation wavelength $\Lambda > d$ remains larger than d (*i.e.*, $Q < 2\pi/d$). However, the momentum and energy of the excitation would be carried by only a single particle, if $Q < 2\pi/d$ (*i.e.*, $\Lambda < \sigma$) and this implies that $E(Q)$ for $Q > 2\pi/d$ would follow

$$E_{sp}(Q) = \frac{\hbar^2 Q^2}{2m_F} \tag{2.4.40}$$

which represents a kind of *single particle* dispersion. Here m_F represents a kind of effective mass that measures the effect of quantum correlation in the $(\mathbf{q}, -\mathbf{q})$ pair configuration. It is expected to be around $4m$ near $Q = 2\pi/d$ and then decrease slowly with increasing Q beyond this point. The transition of $E(Q)$ from $E_{ph}(Q)$ to $E_{sp}(Q)$ takes place over the range $2\pi/d < Q < 2\pi/\sigma$ before $E_{ph}(Q)$ reaches its zero value at $Q = 2\pi/\sigma$. MO theory predicts a minimum value of $E(Q)$ (identified as the *roton minimum* for He II) at $Q = Q_{min}$ near the mid-point of $Q = 2\pi/d$ and $Q = 2\pi/\sigma$,*i.e.*,

$$Q_{min} \cong [\frac{\pi}{d} + \frac{\pi}{\sigma}] \tag{2.4.41}$$

Evidently eqns (2.4.38), (2.4.39), (2.4.40), (2.4.41) represent a Landau type spectrum and using eqn (2.4.37) in (2.4.36), one finds

$$v_p = v_g = \sqrt{\pi}h/2md \tag{2.4.42}$$

where v_p and v_g respectively represent the phase and group velocities of phonons at $Q \approx 0$.

2.5 Superfluidity And Related Aspects

2.5.1 Energy Gap and Bound Pairs

Following section 2.4.4 the following points may be noted: (i) cooling an SIB through T_λ decreases $F(K)$ (eqn (2.4.15)) to its zero value at $T = 0$ and keeps $F(q)$ (eqn (2.4.14)) at nearly constant value $F(q_0)(= N\varepsilon_0)$ and (ii) the order parameter Ω (eqn (2.4.17)) assumes maximum value at $T = 0$ where K-motions cease to exist. Evidently, $F(q)$ and the atomic arrangement which does not differ significantly from that in the G-state (eqn (2.3.11) over the entire temperature range $T = 0$ to $T = T_\lambda$ are the most relevant factors for superfluidity and related properties of an SIB at $T < T_\lambda$; thermal excitations, accounting for $F(K)$, have counter effect on these properties. In finding $F(q) \approx F(q_0)(= N\varepsilon_0)$, Jain used $A(r)\delta(r)$ as an approximation for $V^R(r_{ij})$ repulsion and $-V_0$ as a major contribution of $V^A(r_{ij})$ attraction. However, since V_0 does not represent the net impact of $V^A(r_{ij})$ on $F(q)$, Jain used it as a perturbation on the states of HC particles and determined its role for superfluidity and related aspects.

Jain first used $V^A(r_{ij})$ perturbation on the states of a pair of particles and diagonalized the (2x2) energy matrix, defined by $E_{11} = E_{22} = \varepsilon_0$ and $E_{12} = E_{21} = \beta_0$, with $\beta_0 =< V^A(r_{ij}) >$, since two particles in their wave mechanical superposition have identically equal energy ε_0. This renders two states of energy $\varepsilon_0 \pm |\beta_0|$ for the pair; however, $|\beta_0|$ may be better replaced by $|\beta_0(T)|$ since the overlap of macro-orbitals of two particles may depend on T. The states of energy $(\varepsilon_0 - |\beta_0(T)|)$ and $(\varepsilon_0 + |\beta_0(T)|)$ can respectively

be identified as bonding (or paired) and anti-bonding (or unpaired) states. This follows the established approach of Molecular Orbital Theory [28] applied to a similar case in which two identical atomic orbitals form two molecular orbitals of bonding and anti-bonding nature. The pair is expected to be in bonding state provided the two particles remain locked in the relative configuration characterized by equations (2.3.11). The fact that this situation arises for almost all particles (excluding a small fraction of particles in the states of $q \geq 2q_0$) at $T \leq T_\lambda$ only, distinguishes the state of particles in the LT phase from that in the HT phase.

Applying the same approach to the state of all the N particles, one can construct an $N \times N$ matrix for $H_r(N) = -(\hbar^2/2m) + \sum_i \nabla^2_{r_i} + \sum_{i<j}[A(r_{ij}\delta(r_{ij}) + V^A(r_{ij})]$ (Using eqn (2.3.3) and retaining terms related to q-motions of particles) with $[H_r(N)]_{mn} = \varepsilon_0$ for $m = n$ and $[H_r(N)]_{mn} = [V(r)]_{mn}$ for $m \neq n$ with $[V(r)]_{mn}$ having non-zero value only if m and n refer to two *neighboring particles.* This requires, in principle, the knowledge of the number of neighbors of a particle which depends on the symmetry of the spatial arrangement assumed by the particles), however, such details are unimportant for finding a quantitative relation for the energy gap $E_g(T)$. The diagonalization of this matrix renders $N/2$ energy levels with energy $> N\varepsilon_0(T_\lambda)$ (the anti-bonding states) and $N/2$ energy levels with energy $< N\varepsilon_0(T_\lambda)$ (the bonding states). Obviously, particles prefer to occupy bonding states causing the net energy of the system to fall below $N\varepsilon_0(T_\lambda)$ by $E_g(T)$.

Although the binding ($|\beta_0(T)|$) of a pair of particles may have very small value, the collective binding $E_g(T)$, resulting from it for a system of macroscopically large N can be too large to allow thermal excitations in the system to compensate for it [29]. Since with the onset of λ transtion, the q- motions get delinked from K-motions,

$F(q)$ and $F(K)$ assume their separate identities and the perturbative effect of $V^A(r_{ij})$ lowers $F(q)$ from $N\varepsilon_0(T_\lambda)$ to $N\varepsilon_0(T < T_\lambda)$. Since this happens to all the particles identically, the net fall in energy $E_g(T)$ can be easily obtained by using eqn (2.4.24). This gives

$$\begin{aligned} E_g(T) &= \frac{1}{2}N\Delta\epsilon \\ &= N\varepsilon_0\frac{d_T - d_\lambda}{d_\lambda} \\ &\approx Nk_BT_0\frac{d_T - d_\lambda}{d_\lambda} \end{aligned} \tag{2.5.1}$$

which can be identified as an energy gap between superfluid and normal fluid states of the system. This implies that the entire system at $T < T_\lambda$ behaves like a macroscopically large single molecule as visualized by Foot and Steane [30] for the BEC state of trapped dilute gases and it is obvious that the stability of this state can not be disturbed by any perturbation of energy $< E_g(T)$.

$E_g(T)/N$ in its magnitude equals per particle strain energy, $\epsilon_s(T) = \Delta\epsilon(T)/2$ (proposed to be known as *self energy* of a particle), which is stored in expanded inter-particle bonds of the system (*cf.* section 2.4.7). This implies that particles in LT phase of the system are pushed to higher potential energy in comparison to those in HT phase and this increase depends on the wave packet size $\lambda/2(= \pi/q)$ of the particles. The net strain energy, $\Delta V_s(T) = N\epsilon_s(T)$, is, therefore, a function of q values of particles, *i.e.*, $\Delta V_s = \Delta V_s(q_1, q_2, \ldots q_N)$ which prepares the system to sustain phonon-like waves of collective oscillations of momentum q around q_0 which manifest as a quantum quasi-particle proposed to be known as *Omon*. The existence of these waves is predicted for the first time from the present theory. Identifying $\Delta V_s(T)(q_1, q_2, q_3, \ldots)$ as the energy of omon field and using the fact that $\Delta V_s(T)$ increases with decreasing T which implies that omon field intensity increases when phonon field intensity decreases

and *vice versa*, one may find that an omon is an *anti-phonon* quantum quasi-particle. Evidently, collective motions, such as phonons, can be seen in Jain's system even at $T = 0$ at the cost of omon field energy $\Delta V_s(T)$ which assumes maximum value at $T = 0$.

Since each particle in Jain's system represents a $(\mathbf{q}, -\mathbf{q})$ pair and assumes a binding with other particles with binding energy $E_g(T)/N$ in the LT phase, it represents a $(\mathbf{q}, -\mathbf{q})$ bound pair and an unbound $(\mathbf{q}, -\mathbf{q})$ pair in HT phase which underlines the basic difference of the two phases. In what follows from eqn (2.3.11), this inference implies that particles in each pair are locked at $< k >= 0, < r >= d$ and $< \phi >= 2n\phi$ with $E_g(T)/N$ binding energy per particle in all the three (k-, r- and ϕ-) spaces. It must be clear, however, that, the bound pair of MO theory differs from the $(\mathbf{q}, -\mathbf{q})$ bound pair of electrons (known as *Cooper pair* used in the BCS theory of metallic superconductors [31, 32]). While the binding of electrons in a Cooper pair originates from electrical strain (polarization) of the lattice, binding of atoms in an SIB originates from the strain in inter-atomic bonds (a kind of mechanical strain). In addition, unlike the pair binding of electrons in a superconductor which includes only those electrons that occupy energy levels around the Fermi-level of the system, binding of particles in an SIB arrests all of the N atoms.

2.5.2 Energy Gap and Its Consequences

In what follows from section 2.4.4, an SIB has two components, fluid F1 and fluid F2 with free energies represented respectively by $F(K)$ and $F(q)$. Evidently $F(K)$ and $F(q)$ get delinked from each other at T_λ with the freezing of q-motion at $q = q_0$. Hence the fact that $F(K)$ represents quasi-particle excitations originating from K-motions (unaffected by interactions), implies that $E_g(T)$ modifies only $F(q)$ to $F(q) = N\epsilon_0(T_\lambda) - E_g(T)$ which obviously means that the

origin of different LT properties (including superfluidity and related aspects) of an SIB lies with $E_g(T)$. This inference can be used to analyze the following aspects of an SIB at $T \leq T_\lambda$.

Superfluidity and related properties

If two heads X and Y in the system have small T (temperature) and P (pressure) differences, the equation of state can be expressed as $E_g(X) = E_g(Y) + S\Delta T - V\Delta P$. Using $E_g(X) = E_g(Y)$ for equilibrium, we get

$$S\Delta T = V\Delta P \tag{2.5.2}$$

This shows that: (1) the system should exhibit thermo-mechanical and mechano-caloric effects and (2) while the measurements of η by capillary flow method performed under the condition $\Delta T = 0$ should find $\eta = 0$, measurement of thermal conductivity Θ under $\Delta P = 0$ should find $\Theta \approx \infty$.

Several important aspects of the system can also be followed qualitatively from the configuration of F2 defined by eqn (2.3.11). For example, (i) a close packed arrangement of particles in a fluid-like system can have no vacant site, particularly, because two neighboring particles experience zero point repulsion which, naturally, means that the system should have very large Θ which further means that the system cannot have temperature gradient and convection currents and this explains why He II does not boil like He I, (ii) since particles in F2 cease to have relative motion and they can move only in the order of their locations, the system is bound to exhibit vanishingly small η, particularly for their linear flow in narrow capillary, *etc.* However, the rotating fluid may exhibit normal viscous nature since particles moving on the neighboring concentric circular paths of quantized vortices have relative velocity which explains both viscosity and rotation paradoxes [4]. In what follows from these

observations the loss of viscosity in linear flow is not due to any loss of viscous forces among the particles, rather it is the property of the LT phase configuration in which particles cease to have relative or collisional motion.

Critical velocities and stability of LT phase

Following eqn (2.4.21) and the basic arguments behind it, it is easy to see that the G-state wave function $\phi_0(N)$ changes to

$$\phi_0^*(N) = \phi_0(N) \exp(i\mathbf{K}.\sum_i^N \mathbf{R_i} \exp[-i[N(\varepsilon_0 + \varepsilon(K)) - E_g(T)]t/\hbar] \tag{2.5.3}$$

when the system is made to flow with velocity $v_f = \hbar\Delta\mathbf{q}/m$. This shows that $\phi_0(N)$ remains stable against the flow unless its energy $Nmv_f^2/2 = N\varepsilon(K)$ overtakes the collective binding $E_g(T)$ and this fact should explain critical velocity v_c for which the system loses its superfluidity totally. Equating $E_g(T)$ and $Nmv_f^2/2$ with $v_f = v_c$, one easily gets

$$v_c(T) = \sqrt{[2E_g(T)/Nm]} \tag{2.5.4}$$

which represents its upper bound. A $v_c < v_c(T)$, at which a superfluid may show signs of viscous behavior, can be expected due to creation of quantized vortices. However, this cause would not destroy superfluidity unless energy of all vortices produced in the system exceeds $E_g(T)$.

Coherence Length

Since the main factor responsible for the coherence of F2 is its configuration which locks the particles at $\Delta\phi = 2n\pi$ (*cf.* eqn (2.3.11)) with collective binding $E_g(T)$, the *coherence length* (not to be confused

with *healing length* [4]) can be obtained from

$$\xi(T) = 1/mv_c(T) = h\sqrt{[N/2mE_g(T)]} \tag{2.5.5}$$

Superfluid density

Correlating the superfluid density, ρ_s, as the order parameter of the transition, with $E_g(T)$, one has

$$\rho_s(T) = \frac{E_g(T)}{E_g(0)}\rho(T) = \frac{d_T - d_\lambda}{d_0 - d_\lambda}\rho(T) \tag{2.5.6}$$

to determine $\rho_s(T)$, and normal density $\rho_n(T) = \rho(T) - \rho_s(T)$. It is evident that $v_c(T), \xi(T)$ and $\rho_s(T)$ can be obtained if $E_g(T)$ is known (eqn (2.5.1)). Also, since the superfluid state wave function (eqn (2.4.23)) is expected to vanish at the boundaries of the system, it is natural that $E_g(T)$ and $\rho_s(T)$ also vanish there.

Superfluid Velocity

Concentrating only on the time independent part of ϕ_0^* (eqn (2.5.3), one can write

$$\phi_0^*(N) = \phi_0(N)\exp(iS(R)) \tag{2.5.7}$$

by using

$$S(R) = \mathbf{K}.(\sum_i^N \mathbf{R_i}) \tag{2.5.8}$$

as the phase of the superfluid state. This renders

$$\mathbf{v_s} = \frac{\hbar}{2m}\nabla_{R_j} S(R) = \frac{\hbar\Delta\mathbf{q}}{m} \tag{2.5.9}$$

as a relation for the superfluid velocity; here the fact that $\nabla_{R_j} S(R)$ renders the momentum of the pair (*not of a single particle*) has been used. One may find that eqn (2.5.9) does not differ from the superfluid wave function presumed in the ψ-theory of superfluidity [33];

of course for the well defined phenomenological reasons, the ϕ-theory assumes $S(R)$ to be a complex quantity.

Quantized Vortices

Using the symmetry property of a state of bosonic system, Feynman [34, 35] showed that κ (the circulation of the velocity field) should be quantized and be given by $\kappa = nh/m$ with $n = 1, 2, 3, \ldots$ However, Wilks [1] rightly pointed out that this account does not explain the fact that He I to which Feynman's argument applies equally well, does not exhibit quantized vortices. Using eqn (2.5.8), one finds that

$$\kappa = \sum_i \mathbf{v}_s(i).\Delta\mathbf{r}_i = \frac{\hbar}{m}\sum_i \Delta\mathbf{q}_i.\Delta\mathbf{r}_i = \frac{nh}{m} \tag{2.5.10}$$

with the condition that $\sum_i \Delta\mathbf{q}_i.\Delta\mathbf{r}_i = 2n\pi$, which presumes that the particles moving on a closed path maintain phase correlation. To this effect, MO theory reveals that particles have their ϕ-positions locked at $\Delta\phi = 2n\pi$ only in the LT phase for which only this phase can exhibit quantized vortices. Since particles in HT phase have random distribution ($\Delta\phi \geq 2n\pi$) in ϕ-space, they can not sustain ϕ-correlation and quantized vortices.

2.6 Corroborating Facts

In this section, we compare the G-state of an SIB (*cf.* section 2.3.3) with that is concluded from Bogoliubov model (*cf.* section 2.6.1), discuss how MO theory is compatible with experimentally founded *two fluid theory* and Ψ-theory (*cf.* section 2.6.2) and establish that a macro-orbital state and the arrangement of particles in the superfluid state of an SIB (*cf.* sections 2.2.3, and 2.3.3) find strong experimental support from certain plain facts unearthed from: (i)

the experimental existence of an electron bubble and (ii) the observation of very sharp lines in the ro-vibrational spectra of several embedded molecules in ^{4}He nanodroplets which conclude that such a molecule rotates like a free rotor. We do not dwell into a comparison of experimental and theoretical values of thermodynamic and hydrodynamic properties of any particular SIB, because the excitation spectrum of an SIB ($E(Q) = \hbar^2 Q^2/4mS(Q)$, with $S(Q)$ being the structure factor of the fluid at wave vector Q), as concluded by MO theory [36], not only agrees well with Landau spectrum [37] at qualitative level, but also matches closely with the experimentally observed spectrum [3,6] for LHe-4 at quantitative level which ensures that our theory can accurately explain the thermodynamic properties of LHe-4. Similarly, the fact that v_c, ρ_s and ρ_n, calculated by using relevant relations (*cf.* section 2.5.2), agree closely [38] with experimental values for LHe-4 [4], demonstrates that MO theory has great potential to accurately account for the unique hydrodynamic properties of the superfluid phase of an SIB.

2.6.1 Bogoliubov Picture

In what follows from the theory of BEC [17], 100% of particles in an SNIB at $T = 0$ occupy $p = 0$ state of a single particle. However, Bogoliubov's theory [39] of weakly interacting Bosons reveals that this does not hold exactly for an SIB; the number of particles having $p = 0$ gets depleted by $\Delta N^* = N - N_0$ particles which move to the states of $p \neq 0$, because the G-state energy of the system increases by certain value (*say*, ΔE_0), due to inter-particle repulsion $V^R(r_{ij})$. It is obvious that ΔE_0 and ΔN^* increase with increase in the strength of $V^R(r_{ij})$. Calculations based on widely different mathematical tools reveal that condensate gets depleted to a value, as low as, 10% [6,40] in LHe-4 and $\approx$ 60% in trapped dilute gases [41].

However, MO theory finds that ΔE_0 is equal to $N\varepsilon_0$ and it is shared equally among all the N particles. Each particle in an SIB, at $T = 0$, occupies single state of energy $\epsilon(K) = 0$ and $\epsilon(q) = \varepsilon_0$ (or, momentum $K = 0$ and $q_0 = \pi/d$).

2.6.2 Phenomenological Pictures

Two fluid theory

As concluded from sections 2.4.4 and 2.5.2, an SIB at $T \leq T_\lambda$ gets separated into two fluids F1 and F2. While F2 has all the characteristic properties of a superfluid *viz.*, zero entropy, zero viscosity, *etc.*, since it comprises particles in their G-state, with their positions locked at $< k >= 0$, $< r >= \lambda/2 = d$ and $\Delta\phi = 2n\pi$ (eqn (2.3.11)), for which they cease to have relative motion (or *collisional motion*), F1, identified with a gas of non-interacting quasi-particle excitations, has all properties (such as non-zero entropy, non-zero viscosity, *etc.*) of a normal fluid. This not only concludes that an SIB, below T_λ, should, undoubtedly, behave as a homogeneous mixture of two fluids that have all the properties suggested by Landau [37], but also provides microscopic foundation to *two fluid phenomenology.* It also concludes that each particle with its q-motion participates in F2 and with K-motion in F1. It does not support the perception that certain atoms participate in F1 and rest in F2.

Ψ-theory

According to MO theory, superfluidity of an SIB is basically a property of its F2 component (or the G-state), represented by $\Phi_0(N)$ (eqn (2.3.10)), which can also be written as

$$\Phi_0(N) = \sqrt{n} \tag{2.6.1}$$

with $n = N/V$. However, when F2 is made to flow, its state is given by $\Phi_0^*(N)$ (eqn (2.5.7)). For the phenomenological reason that $\rho_s(T) = n_s m$ at $0 < T < T_\lambda$ is $< \rho = nm$, one also assumes that the phase $S(R)$ (eqn (2.5.8)) is a complex quantity

$$S(R) = \xi_r(R) + i\xi_i(R) \tag{2.6.2}$$

which renders $n_s = n \exp(-2\xi_i(R))$. As such $\Phi_0^*(N)$ has the standard structure of Ψ-function that forms the basis of the well established Ψ-theory of superfluidity [15] and this shows that MO theory also renders microscopic foundation to this phenomenology.

Quantum Phase Transition

As discussed in section 2.4.8, MO theory finds that λ transition and superfluidity are the results of quantum nature of particles. When this observation is clubbed with the fact that superfluidity is basically a property of F2 component (comprising particles in their $T = 0$ state) of an SIB which, however, exists even at non-zero $T < T_\lambda$ due to its proximity with F1, representing a gas of quasi-particle excitations, whose energy measures the T of the system, we find that λ transition could be identified as a quantum transition [42]. While particles in excited states attributed to their q-motions (*viz.*, with $q = 2q_0, 3q_0, ...,$ *etc.*) could be, naturally, identified with F2, their number is found to have maximum of only $\approx 5\%$ at T_λ and it decreases exponentially to 0 value at $T = 0$.

2.7 Experimental Support

An excess electron in LHe-4 exclusively occupies a self-created spherical cavity (known as electron bubble) of certain radius, when it assumes its *lowest possible energy* in the cavity. To create the said cav-

ity, it exerts its zero-point force on the surrounding atoms, against the forces originating from inter-atomic interactions and external pressure on the liquid [43, 44]. It is evident that the bubble formation is a consequence of the facts that: (i) an excess electron experiences a strong short range repulsion with ^{4}He atoms which forbids its binding with them and (ii) the electron, for its quantum nature, manifests as a wave packet whose size increases with the decrease in its energy. This implies that any quantum particle that experiences similar repulsion with ^{4}He atoms should have similar state in LHe-4 and this is found to be true with positron [45] and other particles (ions, atoms, molecules, *etc.* [46]). Guided by these observations, it is natural to believe that each ^{4}He atom in LHe-4 should assume similar state when it occupies its lowest possible energy, because it, too, is a quantum particle and experiences strong short range repulsion with other ^{4}He atoms. Here, we also find that the electron in a drifting bubble has two motions: one, representing its zero-point motion as a trapped particle and the other, representing its drift with the bubble. This not only helps in having a better understanding of the two motions of a single quantum particle in an SIB like LHe-4, but also proves that the state of the electron in electron bubble is not different from a macro-orbital state. In other words, the existence of an electron bubble not only renders a clear experimental proof for the macro-orbital state of a HC boson in an SIB like LHe-4, but also provides strong foundation to MO theory.

Experimental study of high resolution ro-vibrational spectra of embedded molecules (*e.g.*, OCS /N_2O molecules in ^{4}He droplets and $^4He_y - OCS$ or $^4He_y - N_2O$ clusters [47, 48] where y = number of ^{4}He atoms) provides another foundation to MO theory because these studies conclude that superfluidity exists even in systems having few ^{4}He atoms (*viz.*, about 6 or more) which implies that the phenomenon has no relation with $p = 0$ condensate since ^{4}He atoms

in these systems are confined to a space of size, $s \approx 5$ Å for which each atom is expected to have reasonably high momentum $\approx \pi/s$ rather than zero. Further, since each cluster is expected to have certain stable structure (which of course would depend on inter-particle interactions and may change with change in y), the embedded molecule sees a time independent potential which implies that ^{4}He atoms around the rotor cease to have collisional motions. In other words, ^{4}He atoms in these droplets and clusters are localized with position uncertainty decided by their least possible momentum of their confinement which agrees closely with MO theory. In addition, as inferred in section 2.3.3, particles in superfluid state of an SIB can move with equal velocity on a closed path without any change in the order of their locations which implies that particles on two such nearest possible paths (*viz.*, two concentric circular paths) can have different velocities consistent with the theory of experimentally observed quantized circulation in superfluid ^{4}He [4]. Evidently, it is not surprising that a molecule (or its cluster with a few close by atoms which bind with it to follow its rotation) is observed to have free rotation within a 3-D shell or a ring (formed by ^{4}He atoms in its surrounding) that does not participate in the rotation. It also finds that OCS or N_2O molecule embedded in superfluid state of ^{4}He droplets shows sharp rotational lines because ^{4}He atoms cease to have collisional motion but not in normal liquid state of ^{3}He [47] where particles are known to have mutual collisions. In other words, rotational lines do not have collisional broadening in superfluid ^{4}He which they have in liquid ^{3}He. As such experimental observations related to the ro-vibrational spectra of embedded molecules support MO theory.

2.8 Conclusions

This approach to the microscopic understanding of a SIB concludes that each particle in the system has two motions (q- and K-), because it represents a pair of particles moving with equal and opposite momenta (**q**, -**q**) with respect to their CM which moves with momentum **K** and its state is described by a *macro-orbital* (eqn (2.2.18)) The onset of λ transition is an order–disorder of particles in ϕ-space, followed, simultaneously, by their BEC in the state of $q = q_0$ and $K = 0$. The condensate fraction, $n_{K=0}(T^*)$, rises smoothly from $n_{K=0}(T_\lambda) = 0$ to $n_{K=0}(0) = 1.0$; in what follows from eqn (2.4.17), it is expected to assume unit value at $T = T_0$. The origin of λ transition lies with the wave nature of particles, leading to their quantum correlations, which drive their q and K, respectively, towards $q = q_0$ and $K = 0$. It can also be identified as a consequence of zero-point force, f_0 (resulting from the wave nature of particles), exerted by each particle on its neighbours, to push them away against the inter-particle attraction; when the two forces reach a state of equilibrium, each particle has a small fall in its energy (eqn (2.5.1)) and an increase in d by $d_T - d_\lambda$ (*cf.* section 2.4.7) which represents a kind of mechanical strain in inter-particle bonds whose energy $\Delta V_s(T) = N\epsilon_s(T)$ (*cf.* section 2.5.1) depends on the q values (fluctuating around q_0) of particles for which the system sustains a new quantum quasi-particle *omon*, similar to a phonon (*cf.* section 2.5.1); it may be noted that oscillations of relative momentum $k = 2q$ (leading to an omon) are as likely as the oscillations of relative position r (leading to a phonon), since k and r for two nearest neighbour particles in the LT phase of the system are inter-related through $kr = 2\pi$. For the above said expansion in inter-particle bonds, the system is expected to exhibit negative thermal expansion coefficient around T_λ and this prediction is confirmed by the experimental observation on LHe-4 [1].

The approach does not find any reason for a fraction of particles to have zero momentum in the superfluid state of an SIB. Instead, it discovers that the state is characterized by a fraction of particles $[n_{K=0}(T^*)]$ condensed into a state represented by $q = q_0$ and $K = 0$ as (**q**,-**q**) bound pairs (*cf.* section 2.5.1). This explains why existence of $p = 0$ condensate in LT phase of LHe-4 could not be confirmed through any experiment *beyond a point of doubt* [49]. The state is also consistent with excluded volume condition, envisaged by Kleban [50], because each particle in an SIB is revealed to exclusively occupy identically equal volume, with identically equal zero-point energy ε_0 or momentum $q = q_0$.

One may find that MO theory not only explains why LT phase of an SIB should behave like a homogeneous mixture of two fluids F1 and F2 (found to, respectively, have different properties of normal fluid and superfluid of Landau [37]) and thereby, renders microscopic basis to two fluid theory, but also provides similar foundation to Ψ-theory. Superfluidity and related properties are, basically, the properties of $T = 0$ state of the system (represented by F2) which implies that λ transition is a kind of quantum transition which occurs at a non-zero T, for the proximity of F2 with F1. Particles in F2 represent (**q**, -**q**) bound pairs, not only in q-space, but also in r- and ϕ-spaces. They assume a kind of close packed arrangement of their representative wave packets, with *collective binding*, which leads the entire system to behave like a macroscopically large single molecule. The collective binding represents an energy gap between the superfluid and normal fluid states. The superfluid state is consistent with microscopic uncertainty, as evident from $q \geq \pi/d$, as well as, macroscopic uncertainty, since the 3-D network of SMWs represented by $\Phi_0(N)$ (eqn (2.3.10)) vanishes at the boundaries of the system.

The merit of this approach lies in the fact that it finds the origin of λ transition, the nature of BEC, superfluidity, *etc.*, of an SIB simply by analyzing the solutions of its N-particle Schrödinger equation. It makes no assumption, such as, the existence of $p = 0$ condensate or pair condensate, *etc.*, in the superfluid phase of the system, as made by conventional approaches. It not only renders a mathematically simple theory, but also provides unique results with no scope for their change, since no adjustable parameter is used in its formulation. It beautifully demonstrates that the wave nature has amazing capacity to organize particles in phase space at $\phi = 2n\pi$, with $< r >= \lambda/2 = d$ and helps in clarifying the difference between superfluid and normal fluid states, even to a layman, as these states can be identified, respectively, with: (i) the ordered positions and motions of soldiers in an organized army platoon and (ii) random positions and motions of people in a crowd. While the people in the former have coherent motion with no chance of mutual collision, those in the latter have incoherent motion with very high probability of such collisions.

In what follows from this approach, an SIB can have an onset of superfluidity, provided it keeps its fluidity up to a T at which its $\lambda_T > d$ and the zero-point force of its particles dominates its state which is indicated by its volume expansion on cooling and this T falls slightly higher than its T_λ. As evident from eqn (2.4.13), T_λ depends on microscopic d, rather than the net V or net N of the sample and as per MO theory, λ of no particle at $T < T_\lambda^+$ assumes a value higher than $2d$ and thus, it is natural that superfluidity and related properties can be exhibited by nanodroplets and clusters of few atoms, as observed recently [46–48]

In this context, it may also be noted that MO theory is also applied to study the quantum behaviour of some other many body

systems and as discussed briefly in [51], it is found to have great potential to unify the physics of widely different many body systems of interacting bosons and fermions including low dimensional systems, newly discovered BEC states of trapped dilute gases, *etc.* It is evident from the analysis of N HC particles in 1-D box [12] and microscopic theory of superconductivity [52] that a fermionic system differs from a bosonic system for its particle distribution on its allowed states of K-motion which is constrained to follow Fermi–Dirac statistics, rather than Bose–Einstein statistics. It is interesting to find that MO theory [52] can account for the highest T_c of a high T superconductor that we know today. Similarly, it also explains [53] why superfluid transition in LHe-3 occurs around a few mK, in close agreement with experiments. It may be noted that the zero-point force of a particle, emphasized in these studies as the origin of a strain in the structure of the neighbouring particles (*viz.*, the lattice in case of superconductors or inter-atomic bonds/distance in LHe-3), is a natural consequence of wave nature of particles, for which a particle behaves as a wave packet and exclusively occupies a space of size $\lambda/2$ and this aspect is experimentally observed for an electron trapped in an electron bubble and the volume expansion of LHe-3 on its cooling below about 0.6 K [1]. Like an electron in electron bubble, it is natural that an electron conducting through a lattice of a superconductor, too, occupies as much more space as possible when it is cooled through a T equivalent of its ground state energy; this is particularly supported by the study of a particle trapped in 1-D box of slightly flexible size [54].

In summary, this non-conventional approach works well in developing the microscopic theory of a bosonic system like LHe-4, and a fermionic system, like, electron fluid in superconductors, discussed in [52] (which is also valid for LHe-3 type systems).

Bibliography

[1] J. Wilks, *The Properties of Liquid and Solid Helium*, Clarendon Press, Oxford, (1967).

[2] Z. M. Galasiewics , *Helium 4*, Pergamon, Oxford, (1971).

[3] A. D. B. Woods and R. A. Cowley, Rep. Prog. Phys. **36**, 1135 (1973).

[4] S. J. Putterman, *Superfluid Hydrodynamics*, North Holland, Amsterdam, (1974).

[5] K. H. Benneman and J. B. Ketterson, eds., *The Physics of Liquid and Solid Helium*, Part I, Wiley, New York, (1976).

[6] H. R. Glyde and E. C. Svensson in *Methods of Experimental Physics*, (D. L. Price and K. Skold eds.) Neutron Scattering, Vol. **23**, Part B, Academic, San Diego, (1987).

[7] A. Griffin *Bose Einstein Condensation*, (D. W. Snoke and A. Stringari, eds.) Cambridge University Press, Cambridge, (1995).

[8] J. G. M. Armitage and I. E. Ferquhar, eds., *The Helium Liquids*, Academic Press, London, (1975).

[9] Y. S. Jain, J. Sci. Explor. **16**, 67 (2002); J. Sci. Expl. **16**, 77 (2002).

[10] Y. S. Jain, Cent. Euro. J. Phys. **2**, 709 (2004).

[11] Y. S. Jain, Am. J. Cond. Mat. Phys **2**, 32 (2012).

[12] Y. S. Jain, cond-mat/0606409, e-print, www.arXiv.org, (2006).

[13] L. D. Landau, J.Phys. USSR **5**, 71 (1941).

[14] F. London, Nature **141**, 644 (1938).

[15] V. L. Ginzburg and L. D. Landau, Zh. Eksperim. i. Teor. Fiz. **20**, 1064 (1950).

[16] K. Huang, *Statistical Mechanics.*, McGraw Hill, New Delhi, (1991).

[17] R. K. Pathria, *Statistical Mechanics*, Pergamon Press, Oxford, (1976).

[18] O. Penrose and L. Onsager, Phys. Rev. **104**, 576 (1956).

[19] C. N. Yang, Rev. Mod. Phys. **34**, 4 (1962).

[20] J. Goldstone, Nuovo Cim. **19**, 154 (1961);

[21] P. W. Anderson, Rev. Mod. Phys. **38**, 298 (1966).

[22] G. Taubes, Science **269**, 152 (1995)

[23] B. G. Levich, *Theoretical Physics* Vol. 4, North Holland, Amsterdam (1973).

[24] G. E. Uhlenbeck and L. Gropper, Phys. Rev. **41**, 79 (1932)

[25] M. E. Fisher, Rep. Prog. Phys., **30**, 615 (1967).

[26] G. Ahlers in *The Physics of Liquid and Solid helium*, (K.H. Benneman and J. B. Ketterson, eds.), Wiley, New York, (1976).

[27] D. R. Chowdhury, Ph.D Thesis, Department of Physics, North Eastern Hill University, Shillong, India (1996).

[28] M. Karplus and R. N. Porter, *Atoms and Molecules*, Benjamin/Cummins, Menlo Park, (1970).

[29] Y. S. Jain, arXiv:cond-mat/0606571.

[30] C. J. Foot and A. M. Steane, Nature **376**, 213 (1995).

[31] J. Bardeen, L. N. Cooper and J. R. Schrieffer, Phys. Rev. **108**, 1175 (1957).

[32] D. R. Tilley and J. Tilley, *Superfluidity and Superconductivity*, Adam Hilger Ltd., Bristol, (1986).

[33] V. L. Ginzburg, Rev. Mod. Phys. **76**, 981 (2004).

[34] R. P. Feynman in *Prog. Low Temp. Phys.*, Vol. I, (C. J. Gorter, ed.), North Holland, Amsterdam, (1955).

[35] R. P. Feynman *Statistical Mechanics*, MA: W. A., Benjamin, (1976).

[36] Y. S. Jain, arXiv: cond-mat/0609418v1.

[37] L. D. Landau, J. Phys. U.S.S.R **11**, 91 (1947).

[38] S. Chutia, Ph.D. Thesis, Physics Dept., North Eastern Hill University, Shillong, India (2007).

[39] N. Bogoliubov, J. Phys. (U.S.S.R) **11** 23 (1947).

[40] R. N. Silver, Los Alamos Science **19**, 158 (1990).

[41] F. Dalfovo, S. Giorgini, L. P. Pitaevskii and S. Stringari, Rev. Mod. Phys. **71**, 463 (1999).

[42] S. Sachdev, Rev. Mod. Phys. **75**, 913 (2003).

[43] M. Rosenblit, J. Jortner, Phys. Rev. Lett. **75**, 4079 (1995); M. Farnik, U. Henne, B. Samelin and J. P. Toennies, Phys. Rev. Lett. **81**, 3892 (1998).

[44] H. Marris, S. Balibar, Phys. Today **53**, 29 (2000).

[45] P. Hautojärvi, M. T. Loponen and K. Rytsölä, J. Phys. B: At. Mol. Phys. **9**, 411 (1976).

[46] J. P. Toennies and A. F. Vilesov, Ann. Rev. Phys. Chem. **49**, 1 (1998).

[47] S. Grebner, J. P. Toennies and A. F. Vilesov, Science **279**, 2083 (1998).

[48] A. R. W. Mckellar, Y. Xu and W. Jager, Phys. Rev. Lett. **97**, 183401 (2006); K. Nauta and R. E. Miller, J. Chem. Phys. **115**, 10254 (2001); A. R. W. Mckellar, J. Chem. Phys. **127**, 044315 (2007).

[49] A. J. Legget, Rev. Mod. Phys. **71** S318 (1999).

[50] P. Kleban, Phys. Lett., **49A** , 19 (1974).

[51] Y. S. Jain, Ind. J. Phys. **79**, 1009 (2005); the factor $|\sin(\mathbf{k}.\mathbf{r}/2|$ in equation 5 for ψ^+ in this paper should be read as $\sin|(\mathbf{k}.\mathbf{r}/2)|$ and $E_g(T)/Nk_BT$ in equation 25 should be read as $E_g(T)/Nk_BT$.

[52] Y. S. Jain, arXiv:cond-mat/0603784 (2006).

[53] Y. S. Jain, arXiv:cond-mat/0611298 (2006).

[54] Y.S. Jain, arXiv:cond-mat.matrl.sci:0807.0732v2.

Chapter 3

Spectroscopic Property of LHe-4

ABSTRACT: Conventional Microscopic theory of LHe-4 believes that He I and He II differ only by the presence of $p = 0$ *condensate in He II. The change in microwave absorption, Raman scattering and NIS spectra with the onset of* λ *transition have never been associated with the change in atomic arrangement. Jain's theory finds that the roton is nothing but the excitation of a single particle trapped in a spherical cavity, clubbed weakly with the phonons of He II. Using Jain's theory, we can successfully explain the appearance of the sharp roton lines when the* λ *transition is reached. We find that the appearance of a well defined band corresponding to what we call as roton transition is the signature of the change in atomic arrangement and hardening of the atomic arrangement. In addition, Jain's theory reveals clear reasons for the existence of the two roton bound state observed in Raman scattering.*

3.1 Introduction

The elementary excitation spectrum in liquid helium-4 (LHe-4) has been the topic of intense theoretical investigations following the pioneering work of Landau. In 1941, Landau [1] suggested that the properties of LHe-4 could be explained by considering the system as a background fluid plus a spectrum of weakly interacting elementary excitations above the ground state. He called these excitations *phonons* and *rotons*. Phonons and rotons were associated with the normal fluid while the background fluid was identified with the superfluid. Phonons were long wavelength density fluctuations with energy E and momentum p, travelling with the velocity of sound c, so that in the long wavelength limit,

$$E = cp \tag{3.1.1}$$

In this model, the excitation spectrum of the rotons was given by

$$E = \Delta + \frac{p^2}{2\mu} \tag{3.1.2}$$

Landau modified this concept in 1947, introducing a common dispersion curve for both kinds of collective excitations [2], the energy spectrum of the rotons being described by

$$E = \Delta + \frac{(p - p_o)^2}{2\mu} \tag{3.1.3}$$

with Δ=9.6 K, $p_o/\hbar$= 1.95 Å^{-1} and $\mu = 0.77m$, where m is the mass of a ^{4}He atom.

This modification improved the agreement with experimental data and was consistent with the continuous dispersion curve for excitations in a dilute Bose gas derived microscopically by Bogoliubov [3].

Using variational approach, Feynman [4] derived the first expression for the phonon–roton energy spectrum appropriate to LHe-4. He argued that the excited state of the liquid containing a single excitation should be of the form

$$\Psi = \sum_l f(r_l)\phi \tag{3.1.4}$$

where ϕ is the ground state wave funtion and $f(r_l)$ is a function of position. He derived a variational equation for Ψ. This yielded a minimum energy eigenvalue

$$E(Q) = \frac{\hbar^2 Q^2}{2mS(Q)} \qquad \text{where } Q = \frac{p}{\hbar} \tag{3.1.5}$$

for a function of the form $f(\mathbf{r}) = e^{(i\mathbf{q}.\mathbf{r})}$. Feynman's variational phonon–roton energy is found to be significantly higher than the observed $E(Q)$ curve.

Feynman and Cohen [5] introduced the concept of backflow and used it to derive a relation for $E(Q)$ which was in better agreement with the experimental data at SVP. Similar result was obtained by Pitaevskii [6] using quantum-liquid hydrodynamics. However, Padmore and Chester [7] pointed out that Feynman–Cohen spectrum did not describe the pressure dependence of the roton minimum. Feenberg [8], Jackson and Feenberg [9,10] and others [11–13] included the effects of phonon–phonon interactions more fully to obtain improved phonon energies and phonon lifetimes. Cohen and Feynman [14] also suggested in 1957 that the excitation spectrum could be directly determined by neutron inelastic scattering experiments.

The first observation of the excitations in LHe-4 was made in 1957 by Palevsky *et al* [15] using neutron inelastic scattering. They measured the dispersion curve in the immediate roton region. Yarnell

et al [16, 17] and Henshaw [18] extended the dispersion curve measurement to the wave vector range 0.5 $\text{Å}^{-1} \leq Q \leq 2.4\ \text{Å}^{-1}$. In 1961, Henshaw and Woods [19] presented a systematic study of $S(Q,\omega)$ in the region of a single sharp peak of $S(Q,\omega)$ and measured the energy cp as well as the intensity $Z(Q)$ in the sharp peak. These measurements clearly verified the existence of sharp, well defined excitations in superfluid ^{4}He at low temperatures having dispersion of the form suggested by Landau [2]. Since then many experimental neutron scattering studies were performed [20–24] to measure the detailed shape of the dispersion curve as a function of temperature and pressure and the parameters of neutron scattering peaks for different values of the wave vector Q.

The interpretation of the wealth of experimental data required the introduction of new features in the theory of excitations: the multiphonon excitations, the changes in the Landau parameters with temperature and pressure and the binding force between two rotons. A review of the work is given by Woods and Cowley [25], Woo [11], Campbell [26] and most recently by Glyde and Svensson [27].

3.2 Roton linewidth

In 1949, Landau and Khalatnikov [28] proposed a four-quasiparticle decay process to explain the lifetimes of roton excitation. According to this model, the roton excited by an incoming neutron, decays by combining with a thermally excited roton and then decays into two other quasiparticles. At low temperatures the number of thermally excited rotons rapidly decreases, resulting in a strong temperature dependence to the roton linewidth. Calculating the decay rate by emission of phonons, they obtained an expression for the roton

linewidth at low temperature:

$$\hbar\Gamma(Q) = \frac{\hbar^2 Q_0^4}{15\eta_r}\left(\frac{k_B T}{8\pi^3\mu}\right)^{1/2} e^{-\Delta/k_B T} \tag{3.2.1}$$

where $\hbar\Gamma(Q)$ is the roton linewidth, Q_0 is the position of roton minimum and η_r, the viscosity of the normal fluid. Bedell *et al* [29,30] carried out a comprehensive study of roton states, roton–roton interactions and two roton bound states. As in Landau–Khalatnikov theory [28], they considered rotons as quasiparticles. The interaction between two rotons is then described in terms of a pseudopotential $f(\mathbf{r})$ of the polarization potential form. Since the strength of this interaction has been shown [31] to be too strong to be described within the Born approximation (as used by Landau and Khalatnikov [28]) they evaluated the interaction using the Bethe–Salpeter equation. Among many other properties, they calculated the roton energy $\Delta(T)$ and inverse lifetime τ^{-1} due to the four phonon scattering process. As in Landau–Khalatnikov theory, the temperature dependence of $\Delta(T)$ and τ^{-1} comes mostly from $N_r(T)$, the number of thermal rotons available to take part in the scattering. They obtained the following expressions for the roton energy and the roton linewidth

$$\Delta = \Delta_0 - 24.72(1 + 0.0603\sqrt{T})\sqrt{T}e^{-\Delta/T} \tag{3.2.2}$$

and

$$\Gamma_Q(T) = 41.6(1 + 0.0603\sqrt{T})\sqrt{T}e^{-\Delta/T} \tag{3.2.3}$$

where both energy and temperature are expressed in Kelvin and Δ_0 is the zero-temperature roton energy. In 1959, Pitaevskii [32] investigated the singular points of the excitation spectrum of superfluid ^{4}He using quantum field theory method. He pointed out that in the regions of the dispersion curve where the group velocity $v_g = dw/dQ$ exceeded the sound velocity c, the excitations would

be unstable against decay into two or more phonons of lower energy. He also discussed instabilities which arise when $Q \gg Q_0$, *i.e.*, when the energies of single excitations became sufficiently large to excite roton pairs. This condition was also studied by Enz [33] and by Ruvalds and Zawadowski [34]. Both Pitaevskii and Enz suggested that the dispersion curve would terminate when single excitations become unstable against decay into two rotons. They predicted that in this range the single excitation energy $\hbar\omega(Q)$ would approach the instability threshold value 2Δ asymptotically as Q approaches Q_c, as shown in the equation

$$\hbar\omega(Q) = 2\Delta - \alpha e^{a/(Q_c - Q)} \tag{3.2.4}$$

where Q_c is the wave number at which the slope of the dispersion curve equals the sound velocity. While the parameters a and α were not determined by the theory, Q_c was predicted to have a value less than $2Q_0$, Q_0 being the wave number at the position of roton minimum. Pitaevskii further predicted that in the wave vector range where equation (3.2.4) holds, the intensity of the single excitation scattering would be proportional to

$$[2\Delta - \hbar\omega(Q)] \ln^2\{\alpha / [2\Delta - \hbar\omega(Q)]\} \tag{3.2.5}$$

3.2.1 Neutron scattering studies of roton linewidth

Though most of the detailed measurements of $S(Q, \omega)$ were carried out at low temperatures ($T \approx 1.3$ K or lower) and SVP, there were also numerous studies for other temperature and pressures. The first measurement at higher pressure was reported by Henshaw and Woods [35] and subsequently by Dietrich *et al* [22], Woods *et al* [36], Graf *et al* [37] and Svensson *et al* [38]. Most of these studies were confined to $T \leq 1.3$ K. Most of the early temperature dependence study [17, 18, 22, 39] of the one-phonon excitations were confined to

the roton region of the dispersion curve. Dietrich *et al* [22] presented a systematic study of the excitation spectrum in the vicinity of the roton minimum within the temperature range 1.3 K to T_λ, and for pressures up to the solidification pressure. The dispersion curve was traced out using single excitation peaks in $S(Q,\omega)$. They found that the peaks widened as the temperature approached T_λ, which was attributed to the roton–roton interactions. They also observed that the roton energy Δ and effective mass μ were both decreasing functions of temperature and pressure. The momentum at the minimum changed with the density ρ as

$$p_0 = 36.4\ \rho^{1/3}\mathrm{nm}^{-1} \tag{3.2.6}$$

Blagoveshchenkiĭ and Dokukin [40] reported the temperature dependence study of the lifetime and energy of the roton by the method of inelastic neutron scattering. Their results showed deviation from those of Dietrich *et al* [22], and the linewidth obtained by them was not described by the Landau–Khalatnikov theory. Later experiments by Graf *et al* [37] concentrated on the region near the maximum of the Landau curve, (known as the *maxon* region). They found that the energy of the peak increased with pressure, but the momentum value at the peak was not changed. At the highest pressures, they found that the peak energy exceeds the Pitaevskii decay threshold at 2Δ. The calculations of thermodynamic properties by Bendt *et al* [41] using the excitation energies obtained by Yarnell *et al* [17] (for $T \leq 1.8$ K) was in good agreement with the known experimental values, even though the results of neutron measurements closer to T_λ appeared to be inconsistent with the results of thermodynamic measurements. In particular, roton linewidths (inverse lifetimes) appeared to be considerably larger than those calculated using the Landau–Khalatnikov theory, with the parameters deter-

mined from viscosity measurements, and also the roton energies Δ were considerably lower than the values inferred from thermodynamic measurements (for example, see [42]). Furthermore, all the studies prior to 1978 seemed to indicate that nothing drastic happened to $S(Q,\omega)$ on passing through T_λ; rotons as well as other one-phonon excitations appeared to persist to temperatures well above T_λ. This was clearly unexpected, since the one-phonon excitations had originally been believed to be associated with the superfluid phase of LHe-4. Later measurements by Svensson *et al* [43] and Woods and Svensson [44] however, gave evidence for a qualitative change in $S(Q,\omega)$ on passing through T_λ. They suggested that the one-phonon excitations disappeared at T_λ and hence were really a signature of the superfluid phase. Woods and Svensson [44] further observed that for all $T \leq T_\lambda$, $S(Q,\omega)$ could be well described as the sum of a superfluid component with a weight $n_s = \rho_s/\rho$ (where ρ_s is the macroscopic superfluid density) and a normal fluid component with a weight $n_n = 1 - n_s$, namely

$$S(Q,\omega) = n_s S_s(Q,\omega) + n_n S_n(Q,\omega) \tag{3.2.7}$$

Here, $S_s(Q,\omega)$ consists of a one-phonon peak (with a temperature dependent width) plus a broad multiphonon component at higher ω, while the $S_n(Q,\omega)$ consists of only the single broad peak characteristic of non-superfluid ^{4}He. While the one-phonon peak in $S_s(Q,\omega)$ can be described by the form suggested by Miller *et al* [45] at very low temperatures ($T \leq 1$ K), at higher temperatures this peak exhibits substantial broadening.

Woods and Svensson [44] found that the Lorentzian line shape

$$Z(Q,\omega) = \frac{Z(Q)}{\pi} \frac{\Gamma(Q,T)}{\Gamma^2(Q,T) + [\omega - \omega(Q)]^2} \tag{3.2.8}$$

gave a very good description of their results with the half-width

$\Gamma(Q,T)$ taken to be the value for rotons given by the Landau–Khalatnikov theory.

Using the neutron spin-echo technique, Mezei [23] then obtained very accurate roton linewidths and energy shifts at low temperatures ($T \leq 1.4$ K) where the Landau–Khalatnikov theory could be expected to give the correct temperature variation. Mezei's result indeed confirmed the variation expected on the basis of the Landau–Khalatnikov theory. As in the Landau–Khalatnikov theory, Bedell *et al* [29,30] evaluated Δ and Γ assuming a four-phonon decay process, and the temperature variation of Δ arose mainly from the changing number of the thermal rotons needed for the decay to occur. Other calculations of the temperature variation of Δ or Γ were carried out by Titulaer and Deutch [46] and Roberts and Donnelly [47]. At higher temperatures the Landau–Khalatnikov curves were found to be in excellent agreement with the Raman scattering results of Greytak and Yan [48] and the results of Woods and Svensson [44] but not with the results of Dietrich *et al* [22] or Tarvin and Passel [21].

Stirling and Glyde [49] reported high-precision neutron scattering measurements of the temperature dependence of the phonon and roton excitations in LHe-4 at SVP. They investigated in detail the behavior of the excitations at $Q = 0.4$ Å^{-1} (the phonon region) and $Q = 1.925$ Å^{-1} (at the roton minimum). They found that in the phonon region, the sharp peak in $S(Q,\omega)$ broadens with temperature but remains sharp and well defined in the normal phase up to $T \approx 3$ K. But at $Q = 1.925$ Å^{-1}, the sharp component of $S(Q,\omega)$ disappears at T_λ and the behavior of $S(Q,\omega)$ is much different above and below T_λ. Further, they found that the roton linewidth increases and the roton peak intensity drops rapidly with increasing temperature for $T \leq T_\lambda$. The increase in the linewidth is particularly rapid in the temperature range just below T_λ. They also observed that the

linewidth continues to increase as temperature is increased above T_λ. The roton linewidths agreed with the results of Woods and Svensson [44] at low temperatures but are larger than the value of Woods and Svensson at higher temperatures (*i.e.*, T near T_λ).

In 1994, Blagoveshchenskii *et al* [50] reported the results of study of high resolution measurements of inelastic neutron scattering from normal and superfluid ^{4}He. The roton linewidths obtained by them agreed satisfactorily at lower temperatures with the Landau–Khalatnikov theory, however, around the λ point, the Landau–Khalatnikov theory gives higher values than their results. Andersen *et al* [51] measured the roton line shape in superfluid ^{4}He down to $T = 0.8$ K using neutron backscattering technique, with energy resolution of less than 1 μeV. They found that the measured roton linewidths were in excellent agreement with the predictions of Bedell *et al* [29], but the temperature dependence of the roton energy showed clear deviation from the same prediction— the roton energy changed much more slowly with temperature than was expected from the theory of Bedell *et al* [29].

Using time-of-flight neutron inelastic scattering method, Gibbs *et al* [52] studied the collective excitations in normal and superfluid ^{4}He as a function of both temperature and pressure. They found that the roton linewidth increased with temperature at all pressures in agreement with the previous studies reported by Dietrich *et al* [22], Talbot *et al* [53] and Cowley and Woods [20]. They also found that the rate of increase of the roton linewidth ($d\Gamma/dT$) increased with pressure corresponding to a decrease in roton lifetime. However, on the roton branch beyond the roton minimum, (*i.e*, $Q = 1.93$ Å^{-1}), the dynamic structure factor $S(Q,\omega)$ is not a single Lorentzian (for example, see [54]), but is made of two components. The sharp roton peak is sitting on the slope of a broad

background, which is attributed to multiparticle excitations. This renders the extraction of the single excitation energy difficult, and high instrument resolution is required for accurate determination of the peak position. Pistolesi [55, 56] solved this problem by employing a more sophisticated analytical form of the roton spectral function. Glyde *et al* [57] were able to extract the single excitation energies with high precision by using a high-resolution time-of-flight spectrometer. However, the data of Pistolesi [55, 56] were available for the wave vector $Q \geq 2.3$ Å^{-1}, while the data of Glyde *et al* [57] have rather low Q resolution. Keller *et al* [58] measured both the energies and linewidths of the roton branch in the range 1.93 Å$^{-1} < Q < 2.6$ Å^{-1} at $T = 0.98$ K. The observed roton energies were significantly smaller than those reported by earlier neutron scattering experiments. While broadening of the roton linewidth was measured for the first time around $Q \simeq 2.2$ Å^{-1}, their data was in clear disagreement with the earlier experiments.

3.2.2 Raman scattering studies of roton linewidth

Raman scattering of light from LHe-4 was first studied by Greytak and Yan [59] in 1969, following the suggestion of Halley [60]. They measured the spectrum, intensity and polarization of light scattered from rotons and higher energy quasiparticle excitations in the temperature range 1.16 K–2.14 K. At low temperatures, they observed a sharp asymmetric peak with a maximum corresponding to an energy shift of 18.5 ± 0.5 K, above which there was a much smaller subsidiary maximum at an energy shift of 35.3 ± 1.0 K and a long high frequency tail. They also found that the intensity of the sharp peak decreases rapidly as the temperature is increased. To explain the observed spectrum, several authors [34, 61–63] tried to develop a theory. The asymmetric peak was explained to be due to a second

order Raman scattering process in which the scattered photon loses energy to create two rotons. The spectrum thus reflected the joint density of states of two rotons, and was influenced by the roton–roton interactions. A model for the joint density of states was proposed in which interaction between rotons was taken to be attractive, leading to the formation of a bound state [62–65].

Greytak *et al* [64] then carried out the study of the detailed shape of the sharp peak at 1.2 K using interferometric techniques. They found that the two-roton peak occured at an energy shift which was less than twice the energy of a single roton at the same temperature. They interpreted the result as a direct evidence for the existence of a two-roton bound state. They further calculated that the binding enery for the roton pair was 0.37 ± 0.10 K. However, several neutron workers [25,37,66] raised questions regarding the existence of the two-roton bound states: they considered that the result of Greytak *et al* [64] was inconclusive. In an attempt to prove the existence of a two-roton bound state, Ohbayashi and Ikushima [67] studied the Raman spectrum at 1.51 K. The spectrum they observed showed fine structures indicating the existence of the two-roton bound state and the coupling between elementary excitations in superfluid ^{4}He. The binding energy of the roton pair was determined to be 0.5 ± 0.3 K. With improvement in interferometric techniques, Murray *et al* [65] made a high resolution study of the two-roton Raman scattering at 0.6 K and SVP. Their results proved conclusively that roton–roton interactions are necessary to explain the observed spectrum. The two-roton binding energy was estimated to be 0.22 ± 0.07 K. The intrinsic zero temperature linewidth of the roton pair was found to be 0.11 ± 0.01 K. Ohbayashi *et al* [68,69] reported measurement of Raman spectrum from superfluid ^{4}He up to the melting pressure. They measured the temperature dependence of the two-roton Raman spectrum of superfluid ^{4}He at different pressures, from the low-

est temperature of 0.75 K to temperatures above the λ point. They found that the temperature dependence of both the spectral shape and intensity of the two-roton peak was simulated well by a model, where the temperature effect is simply broadening of the spectrum with small variation of the roton minimum energy. They concluded that the Raman spectrum of superfluid ^{4}He does not change qualitatively at elevated temperatures, even above the λ point. Recently, Shay *et al* [70] studied the properties of bound roton pairs in superfluid ^{4}He as a function of pressure. They found that the spectra were well described by a model of interacting rotons [34, 62, 63].

3.3 Spectroscopic Studies and Jain's theory

Jain analyzed the elementary excitation spectrum of LHe-4 using MO theory [71]. Clubbing Feynman's result with MO theory, he obtained

$$E(Q) = E(Q)_{mo} = \frac{\hbar^2 Q^2}{4mS(Q)} \tag{3.3.1}$$

where $E(Q)_{mo}$ represents MO value. He compared eqn (3.3.1) with $E(Q)_{exp}$ of He II and identified important aspects of an effective $S(Q)$ to be used in eqn (3.3.1). He also analyzed the basic factors responsible for the experimentally observed anomalous nature of small Q of phonons of He II. Using the experimental data compiled by Donnelly and Barenghi [72], and $S(Q) = S(Q)_{exp}$ in eqn (3.3.1), he obtained

$$E(Q)_{mo} = \frac{\hbar^2 Q^2}{4mS(Q)_{exp}} \tag{3.3.2}$$

He observed that $S(0) = 0$, in place of $S(0) = 0.051$ adopted in [72]. Price [73] also made the theoretical inference that $S(0)$ should be zero for a quantum fluid at zero temperature. The importance and validity of the inference of [73] had been emphasized by Lamacraft [74]. Jain further argued that since the structural configuration of quan-

tum fluid at $T \leq T_\lambda$ does not differ from that at $T = 0$ [75], $S(0)$ should be zero at all T below the λ point and this is corroborated by the experimental fact that $E(Q)$ of He II hardly depends on T. Correcting $S(Q)_{exp}$ taken from [72], for $S(0)(\doteq 0.051)$, he shifted the zero level of $S(Q)$ to 0.051 and defined $S(Q)^* = S(Q)_{exp} - S(0)$ as the effective $S(Q)$ that should be used in eqn (3.3.1), to find

$$E(Q)^*_{mo} = \frac{\hbar^2 Q^2}{4m[S(Q)_{exp} - S(0)]} \tag{3.3.3}$$

as a more appropriate relation to determine $E(Q)$ of an SIB. He noted that the maximum difference in $E(Q)^*mo$ and $E(Q)_{exp}$ was $\approx$ 1.8 at 1.1 Å^{-1}, which is about 13% of $E(Q)_{exp} \approx 13.8$ which compares with the fractional deviation of the recommended values of $E(Q)_{exp}$ and $S(Q)_{exp}$ [72] from their adopted database, since, as reported in [72], these deviations are as large as 3% for $E(Q)_{exp}$ and 10% for $S(Q)_{exp}$. To this effect, he also determined $S(Q)' = \hbar^2 Q^2 / 4mE(Q)_{exp}$ which when used in eqn (3.3.1), reproduced $E(Q)_{exp}$. Furthermore, analyzing the phonon group velocity v_g and phase velocity v_p, he concluded that the excitations of an SIB like LHe-4 are nothing but the motions of a single particle whose mass changes with Q as $m^* \approx 2m[S(Q)_{exp} - S(Q = 0)]$ which can be known as effective mass. Elementary excitation in MO theory is based on different footings [76]. In the superfluid state the closed pack arrangement of the wavepackets gives an excitation spectrum that is similar to the elastic wave in mono-atomic 1-D chain in crystalline solid. The only difference is the interatomic separation which is constant for solid due to its strong attractive inter-molecular forces whereas in liquid helium, where intermolecular forces are relatively weak, it varies with Q. This also explains why longitudinal mode is the lone possible mode of excitation in the system. Though the excitation spectrum of MO theory seems to be different, it reduces to familiar functional

form in the low Q range. Thus the excitation energy can be expressed as

$$E(Q)_{ph} = \hbar\omega_r(Q) = \hbar\sqrt{\frac{4C(Q)}{m}}|\sin(Qd(Q)/2)| \tag{3.3.4}$$

where $C(Q)$ is the force constant and $d(Q)$ is the interparticle separation. Both these quantities depend on excitation wave vector.

In a recent study [77], these energy relation is used to calculate the excitation energy for different Q values. It was found that the theoretically estimated values closely match with the experimental values obtained from neutron scattering experiments. This study further shows that this energy relation, *i.e*, eqn (3.3.4), can properly explain the anomalous dispersion observed in LHe-4.

3.4 Our analysis of Roton linewidth

3.4.1 Calculation of collision linewidth

In order to estimate the roton linewidth, we consider the line broadening due to collision. This kind of line broadening is caused by the sudden change of atomic radiation by collision [78]. This type of line broadening is dominant in high temperature arcs and plasma. In a gas, it is due to the collision of an atom with other atoms, ions, free electrons, or the walls of the container. In a solid it is due to the interaction of the atom with the lattice [79]. The application of this formalism to LHe-4 is justified by the fact that according to Jain's theory, the atoms in superfluid ^{4}He have solid-like arrangement. The formula for collision linewidth is given by [78, 79]

$$\Delta\nu_c = \frac{1}{\pi\tau_c} \tag{3.4.1}$$

where τ_c, the time interval between successive collisions is given by

$$\tau_c = \frac{(mk_BT)^{1/2}}{16\pi^{1/2}pa^2} \tag{3.4.2}$$

with m being the mass of the atom or molecule, p the pressure and a, the hard core radius of the atom or molecule.

We noted that the behavior of ^{4}He atoms in its superfluid phase is much similar to the atoms in a solid, rather than its random motion in a gaseous system. Hence in our calculation, we replace the hardcore radius by the interparticle separation of ^{4}He atoms.

To calculate the roton linewidth at SVP, we used the data for saturated vapor pressure at different temperatures tabulated by Donelly and Barenghi [72]. Further, to calculate the values of a at different temperatures, we used the density of LHe-4 at different temperatures, given by them. Our calculated values are presented in Table 3.1. We plot our results in Fig 3.5. Our results shows that the collision linewidth rapidly reduces to zero once the λ points is reached. Since our results closely match with the experimental results, they support Jain's theory which states that the superfluid phase is a collisionless and ordered state.

3.4.2 Results and discussion

It is well known that spectroscopic observations such as absorption and scattering of electromagnetic radiations render very reliable information about the arrangement of constituents of a many body systems such as polyatomic molecules, solids, *etc.* where the constituents occupy well defined positions in space and the systems assume structures of well defined molecular or crystalline symmetries. Any change in symmetry and structure of these systems is obviously reflected in their absorption and scattering spectra for which these

tools are widely used to investigate the different types of phase transitions, in particular, the structural phase transitions.

However, constituents (atoms or molecules) of many body systems such as liquids do not make a well defined structure; they keep moving with random velocities for which they never have well defined positions. Instead, they have mutual collisions for which the positions and shapes of absorption and scattering lines/bands of electromagnetic radiations are observed to be extremely broad and these tools seem to have limited scope for investigating the physics of a liquid. As indicated by Jain's theory supported by several experimental observations, He II is an exception in this regard, since its constituents define a kind of close packed arrangement of their representative wave packets (CPA-WP) where ^{4}He atoms cease to have their relative motions; they remain free to move coherently with the same velocity in the order of their locations. This differs significantly from He I where atoms (like in any other liquid) move randomly with different velocities causing them to have mutual collisions which forbid them to have well defined positions with respect to any chosen origin of a frame of reference. Naturally, the onset of λ transition brings a change in the arrangement of ^{4}He atoms when LHe-4 has a transition from He I to He II. Fortunately, this is reflected by the change in the position and shape of microwave absorption [80, 81] line and Raman scattering spectra [69], depicted in Figures 3.1, 3.2 and 3.6 respectively. As shown in Fig. 3.3, line shapes of neutron inelastic scattering (NIS) from LHe-4 revealing the details of quasiparticle excitations are also observed to differ significantly in respect of their width when it has the λ transition. Unfortunately conventional microscopic theory (CMT) of LHe-4 concludes that different number of ^{4}He atoms in He I as well as in He II have random motions with different momenta; they have mutual collisions in both phases, forbidding He I and He II to have different atomic arrange-

ments. The two phases are believed to differ only by the presence of $p = 0$ condensate in He II. Naturally, the change in microwave absorption, Raman scattering, and NIS spectra with the onset of λ transition have never been associated with change in atomic arrangement. Correlation with the existence of $p = 0$ condensate can not be justified since its existence is not only questioned theoretically by Jain but no experiment has ever provided unequivocal proof of its existence. In fact the physical reality of the change of particle arrangement with λ transition has been totally ignored. The account of the T dependence of the linewidth of roton transtion in NIS provided by Khalatnikov and Landau [28] or that of two roton transition observed in Raman scattering reported in [64] seem to stand valid because they basically talk about the change in linewidth with T basically for He II. The questions, why quasi-particle excitations do not show up with well defined line shapes and why do they have as much width as their energy in He I in contrast to He II, have not been addressed satisfactorily even qualitatively. In this respect, based on Jain's theory we find the following.

(i) Like any other liquids, the motions of ^{4}He atoms in He I can be seen as the motions of single particles and many atomic units such as dimmer, trimer, *etc.*, even though they may not be forming bound units like molecules having two, three, ... atoms. The momentum Q of the motion of such units is obviously shared by all of its atoms (say s) for which their energy varies inversely as their masses sm or more accurately, as $1/sm^*$, where m^* can be identified as the effective mass of an atom which differs from the real mass m of the atoms because all these units move through an interacting environment; we can expect $m^* \geq m$ as well as $m^* < m$. It is obvious that the energy of the motions of these sets $E(Q) = \hbar^2 Q^2/2(sm^*)$. This clearly

shows that the quasiparticle excitation of a given Q can have wide range of energy depending on the value of s and (sm^*). In addition since all these units keep on colliding with each other, the width of each of quasi-particle motion of momentum Q is controlled by the time of such collisions which complicates the process responsible for the width of such transtions. As such the broadening of the width of a quasiparticle excitation of momentum Q has large contributions from collisions due to the fact that Q can be shared between two or more than two atoms, and from the impact of interacting surroundings through which atoms have their movements.

(ii) In He II, each atom finds a nearly identical surrounding and it represents a kind of particle trapped in a spherical cavity. Hence, in principle, it is expected to have discrete energy levels in addition to collective motions which are rightly identified as the phonons of a single atomic chain for the fact that the arrangement of the atoms does not differ from the arrangement of atoms in a solid with one atom per unit cell. For such a solid, we expect three phonon branches: one branch of longitudinal accoustic phonon and two branches of transverse accoustic phonon. However, since He II is a liquid where each atom experiences vanishingly small shear force, it is neither expected to exhibit transverse acoustic phonons nor it is found to show such phonon branches through any experiment. As observed through NIS experiments, He II is expected to show only longitudinal phonon branch. Since CPA-WP of ^{4}He atoms in He II does not allow atoms to have mutual collisions and each atom sees identical surroundings, the excitations are rightly identified to have phonon-like waves of collective motion till the excitation wave length $\Lambda/2 = \pi/Q$ is larger than d, since the energy $E(Q)$ and momentum Q of such excitations are shared by many particles

(at least more than one). For $\Lambda/2 < d$ (*i.e.* $Q > 2\pi/d$), $E(Q)$ and Q of the excitations are carried only by a single particle for which corresponding motion of the excitations is identified as a single particle motion rather than the collective motions of two or more than two particles. This too agrees with experiments; naturally, excitations of $Q > 2\pi/d$ are expected to follow a dispersion of single particle motion, *i.e.*, $E(Q) = \hbar^2 Q^2/2m^*$ and this too is supported by experiments.

(iii) In what follows from Jain's theory, He II is a highly isotropic fluid where each atom has two motions; the q-motion (expected to have discrete energy) in the first excited level corresponds to what we call as roton and K-motion render what we call as phonons collective motions. However, the phonon type dispersion is not expected to last much beyond $Q > 2\pi/d$ as discussed above in **(ii)**, such motions represent a single particle motion. As such the excitations of He II (phonons, rotons or single particle motions) are expected to have well defined positions and shapes because the particles cease to have mutual collisions and they all have identical environment for which their width is expected to be orders of magnitude smaller than that in He I. Since He II represents a highly uniform homogeneous phase where each atom is a part of the entire liquid, it has a long distance position correlation and large scale energy correlation as concluded in [82]. Consequently, each quasi-particle excitation can propagate long distance without scattering and stays for a much longer period in comparison with He I. This explains why these excitations have sharper line shapes.

(iv) It is not difficult to identify that the G-state of LHe-4 which represents an isotropic system of spherically symmetric ^{4}He atoms has center of symmetry. Naturally different quasi-particle ex-

citations either have even or odd parity. In such situations, motions active in the absorption spectrum of electromagnetic radiations are expected to be forbidden in Raman scattering and *vice versa.* In this context, we find that single quantum excitation of a roton mode which is observed in microwave absorption is not seen in Raman scattering, while two roton excitation observed in Raman scattering is not reported to have been observed in microwave absorption spectrum, and guided by this observation, two-roton excitation may not be observed in absorption of electromagnetic radiations. It would be interesting to see whether this prediction is testified or not.

(v) Two roton mode excitation observed in Raman scattering is identified to represent a state of two rotons for the reason that energy of such an excitation is found to be less than two times the energy of a single roton. However, since the correct nature of motion that represents a roton has so far not been correctly understood, the conventional account can not be expected to represent the real basis for the said binding of two rotons. On the other hand Jain's theory finds that the roton is nothing but the excitation of a single particle trapped in a spherical cavity of size d clubbed weakly with the phonons of He II. In other words, a roton is a single particle excitation (related to the q motion) effected by the collective motions (or dynamics of phonon-clad particle) which obviously has an effective mass (m^*) that differs from the real mass of a ^{4}He atom; in general we expect $m^* > m$ since each particle in He II has a kind of binding with the entire system through what is known as *collective binding*, as concluded by Jain's theory. It is natural that two roton excitation, basically, means excitation of two particles in different cavities of neighbouring atoms with equal and opposite momenta (**Q**, -**Q**). This correlation among the

two particles each of which has a binding with the rest of the $N-1$ particles (N being the total number of particles in the system) in the system clearly reveals that such excited particles too have mutual binding. Evidently, Jain's theory reveals clear reasons for the binding of two roton excitation.

(vi) Conventional account of two roton excitation in Raman scattering selectively attributes that such rotons have equal and opposite **Q** because change in momentum in a Raman process has infinitely low value while a single roton has very large momentum $Q_{rot} \approx 2\pi/d$ which obviously demands that two rotons should correspond to **Q** and -**Q**, for want of momentum conservation. However, if we see the phenomenon in terms of Jains theory which finds that ^{4}He atoms in He II define a CPA-WP (a solid-like arrangement) we find that the recoil of the system during a single or two roton excitation does not represent the recoil of a single atom or two, it rather represents the recoil of the entire system which naturally corresponds to infinitely small energy. Evidently, while we have no doubt that two roton excitation observed in Raman scattering has to have net momentum to be nearly zero and for this reason the two rotons should be of momenta **Q** and -**Q**, it does not mean that the momentum conservation would be violated in an otherwise situation. This is corroborated by the fact that single roton excitation is seen experimentally in micro-wave absorption which is analyzed in detail in Chapter 6 (published in Current Science **101**, 769 (2011)) for the value of electric dipole moment of a ^{4}He atom. Here we also note that the said microwave absorption by rotons clearly means that the roton excitation has a change of electric dipole moment when the system goes from the ground state to its excited state. The roton motion has odd parity. Naturally two roton state corresponds to even par-

ity and it is expected to appear in Raman scattering spectrum as really observed experimentally.

(vii) It is well known that a structural phase transtion in solid leading to a change in the positions of its constituents is characterised by softening of the motions which leads at least one phonon to have nearly zero frequency around the transition temperature. This is a well known phenomenon of soft mode and is commonly observed in most cases of structural phase transition in solids. It is attributed to the singularity in the dielectric constant of the solid at the transition point. The softening of the mode means softening of lattice for the displacement atoms in a particular direction or orientation of molecular units for their rotation. However, the λ transition of LHe-4 is a different kind of transtion where ^{4}He atoms having nearly full freedom to move randomly from one place to another in He I get trapped in cavities formed by nearest neighbouring atoms in He II. This represents a kind of hardening of the atomic arrangement which should obviously be characterised by a change in the dynamics of system. In this context, following Jain's theory, we really find that the appearance of a well defined band corresponding to what we call as roton transtion is the signature of the change in atomic arrangement and hardening of the atomic arrangement.

(viii) In what follows from Jain's theory, quasiparticles excitations move freely from one point to another, keeping highly ordered atomic arrangement in the background. We note that this simple fact can easily be used to understand periodic change (decrease and increase) in the position and width of excitation lineshape observed in NIS in the range of higher Q values (as shown in Fig. 3.4) where dispersion of the excitation is repre-

sented closely by free particle motion. In this context we note that a freely moving quasi particle is influenced by atoms located nearly at points separated by equal distance d for their weak but real interaction. Guided by similar situation in the case of electron motion in periodic positions of ions in solid (which are explained by Kronig Penney model [83]), one can easily understand the periodic change in position and width of the allowed energy of the quasi-particle motion. A quantitative account of the observation would be taken separately in the future course of this study.

(ix) Experimental study of $E(Q)$ through NIS also finds that single excitation spectrum of LHe-4 with a kind of phonon-like collective motion terminates at higher Q. This observation is more important for our understanding in case of He II in comparison to He I, since a highly regular and ordered arrangement concluded for He II, in principle, is expected to sustain phonon-like collective motion at higher Q as observed in crystals. In He I the phonon-like motion is expected only at low Q as observed for other liquids. In the framework of Jain's theory we find that energy and momentum of the excitations at higher $Q > 2\pi/d$ is naturally shared by a single atom when the excitation wave length $\Lambda/2 < d$ (in fact more particularly when $\Lambda/2 < \sigma$ for which any tool of excitation can clearly target a single particle). Naturally for the fact that atoms in He II are not bound strongly as they are in crystals, phonon-like excitations with $Q > 2\pi/\sigma$ would cease to exist in He II. Guided by this observation we find that phonon-like motions for $Q > 2.6$ Å^{-1} should represent the free particle motions with $E(Q) = \hbar^2 Q^2/2m^*$, which closely agrees with experiments. This motion may, however, take place by way of transferring the energy/momentum successively to the next atom on the path.

Table 3.1: Calculation of roton linewidth as a function of temperature at SVP. Roton linewidth is calculated using the formula taken from Ref. [78, 79]

Temperature (K)	Roton linewidth (μeV)
0.6500	0.0043
0.7000	0.0110
0.7500	0.0251
0.8000	0.0520
0.8500	0.0997
0.9000	0.1789
0.9500	0.3037
1.0000	0.4916
1.0500	0.7633
1.1000	1.1438
1.1500	1.6615
1.2000	2.3481
1.2500	3.2370
1.3000	4.3694
1.3500	5.7813
1.4000	7.5167
1.4500	9.6230
1.5000	12.1443
1.5500	15.1278
1.6000	18.6134
1.6500	22.6500
1.7000	27.2785
1.7500	32.5528
1.8000	38.4800
1.8500	45.2211
1.9000	52.5412
1.9500	60.7095
2.0000	69.6705
2.0500	79.4021
2.1000	89.8665
2.1500	101.0786
2.2000	112.9770
2.2500	125.8133
2.3000	139.5704

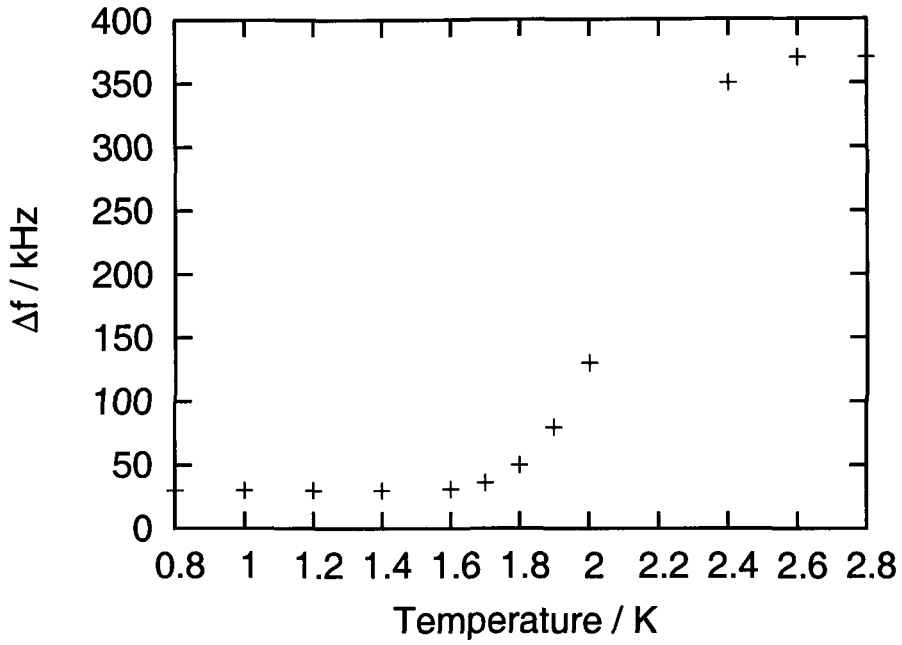

Figure 3.1: Temperature dependence of the resonance absorption frequency. Data points are taken from Ref. [80]

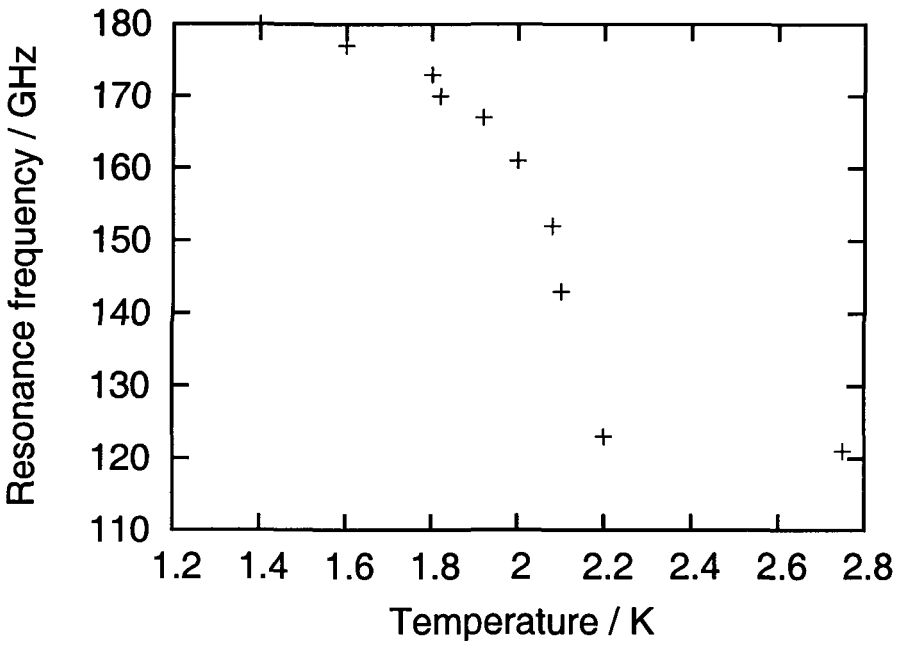

Figure 3.2: Temperature dependence of the width of the narrow resonance absorption line. Data points are taken from Ref. [81]

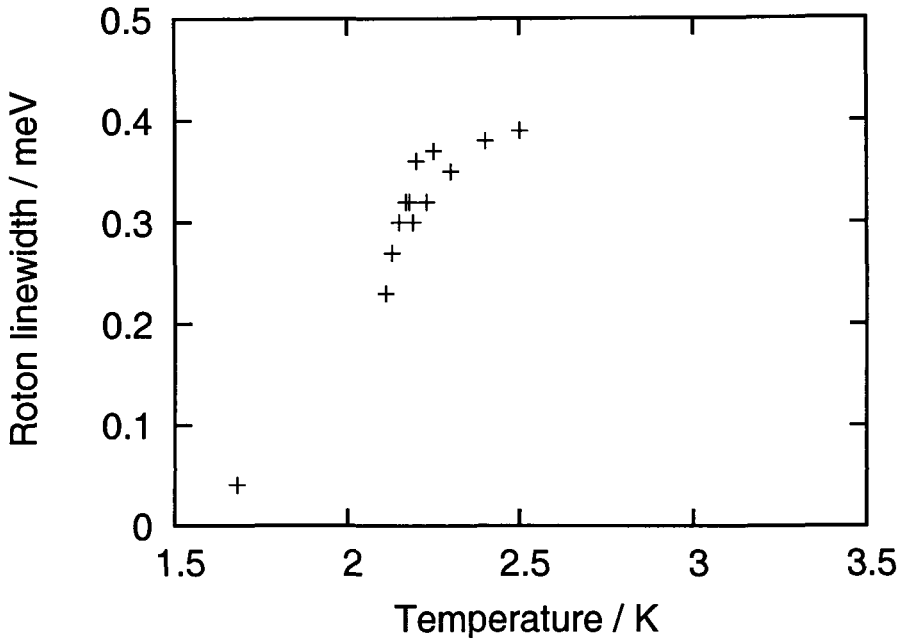

Figure 3.3: Roton linewidths *vrs* Temperature at Pressure= 1 atmosphere. Data points are taken from Ref. [22]

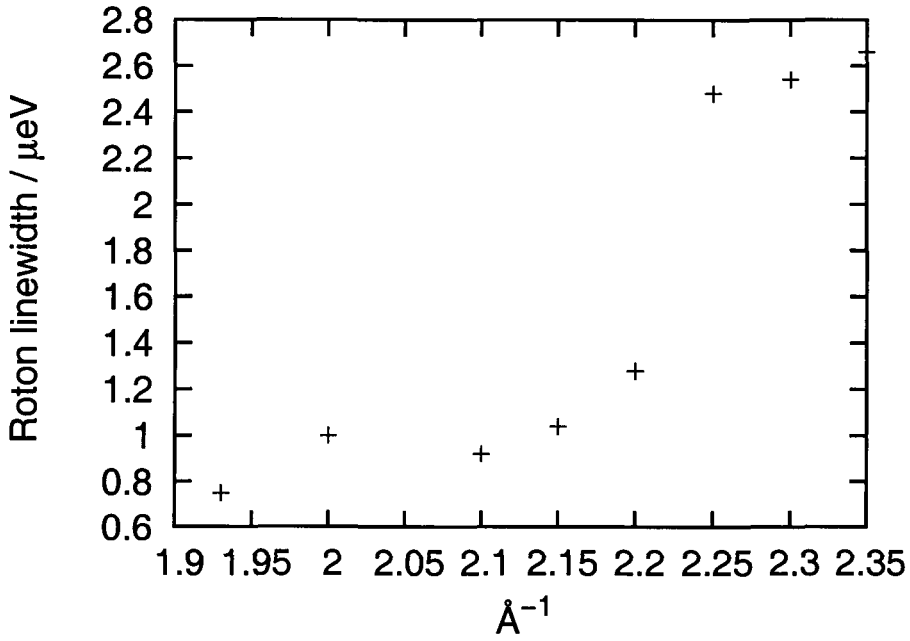

Figure 3.4: Roton linewidths *vrs* wavenumber at T=0.98 K. Data points are taken from Ref. [58]

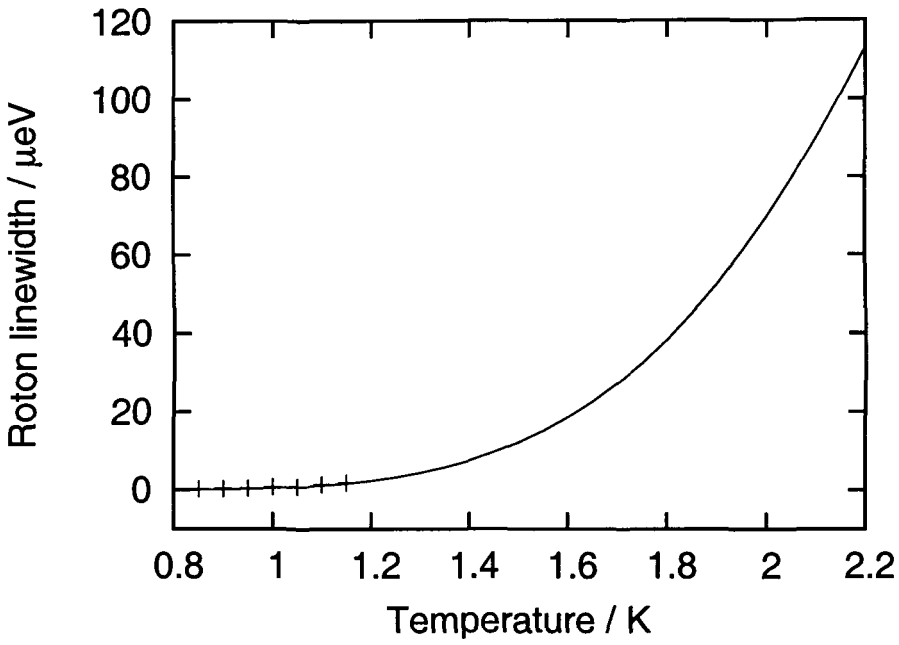

Figure 3.5: Temperature dependence of the roton linewidth, calculated using collision line broadening formula taken from Ref. [78, 79]. The solid line represents calculated values, while crosses are experimental points. Data points are taken from Ref. [84]

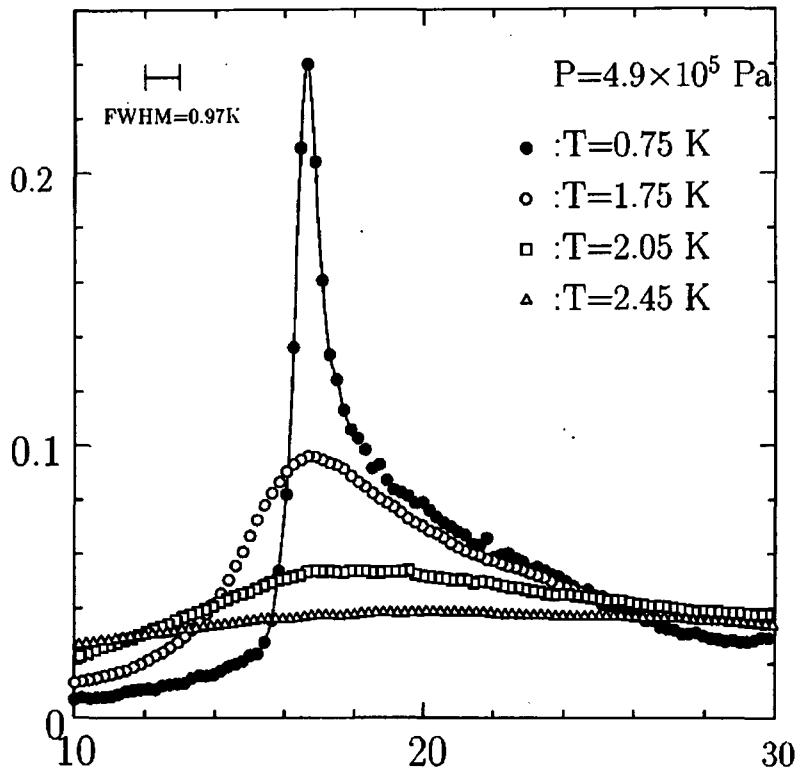

Figure 3.6: Temperature dependence of the Raman spectrum of superfluid ^{4}He measured at the pressure of 4.9 $\times 10^5$Pa. Source Ref. [69]

Bibliography

[1] L. D. Landau, J. Phys. (Moscow) **5**, 71 (1941).

[2] L. D. Landau, J. Phys. (Moscow) **11**, 91 (1947).

[3] N. N. Bogoliubov, J. Phys. (Moscow) **11**, 23 (1947).

[4] R. P. Feynman, Phys. Rev. **94**, 262 (1954).

[5] R. P. Feynman and M. Cohen, Phys. Rev. **102**, 1189 (1956).

[6] L. P. Pitaevskii, Sov. Phys. JETP **9**, 830 (1959).

[7] T. C. Padmore and G. V. Chester, Phys. Rev. A **9**, 1725 (1974).

[8] E. Feenberg, *Theory of Quantum Fluids*, Academic Press, New York, (1969).

[9] H. W. Jackson and E. Feenberg, Ann. Phys. NY **15**, 266 (1961).

[10] H. W. Jackson and E. Feenberg, Rev. Mod. Phys. **34**, 686 (1962).

[11] C. W. Woo in *The Physics of Liquid and Solid Helium*, (K. H. Bennemann and J. B. Ketterson, eds.), Part I, Wiley, New York, (1976).

[12] A. Bhattacharyya and C. W. Woo, Phys. Rev. Lett. **28**, 1320 (1972).

[13] A. Bhattacharyya and C. W. Woo, Phys. Rev. A **7**, 204 (1973).

[14] M. Cohen and R. P. Feynman, Phys. Rev. **107**, 13 (1957).

[15] H. Palevsky, K. Otnes, K. E. Larsson, R. Pauli and R. Stedman, Phys. Rev. **108**, 1346 (1957).

[16] J. L. Yarnell, G. P. Arnold, P. J. Bendt, and E. C. Kerr Phys. Rev. Lett. **1**, 9 (1958).

[17] J. L. Yarnell, G. P. Arnold, P. J. Bendt, and E. C. Kerr Phys. Rev. **113**, 1379 (1959).

[18] D. G. Henshaw, Phys. Rev. Lett. **1**, 127 (1958).

[19] D. G. Henshaw and A. D. B. Woods, Phys. Rev. **121**, 1266 (1961).

[20] R. A. Cowley and A. D. B. Woods, Can. J. Phys. **49**, 177 (1971).

[21] J. A. Tarvin and L. Passell, Phys. Rev. B **19**, 1458 (1979).

[22] O. W. Dietrich, E. H. Graf, C. H. Huang and L. Passell, Phys. Rev. A **5**, 1377 (1972).

[23] F. Mezei, Phys. Rev. Lett. **44**, 1601 (1980).

[24] A. D. B. Woods, E. C. Svensson and P. Martel, Phys. Lett. **57A**, 439 (1976).

[25] A. D. B. Woods and R. A. Cowley, Rep. Prog. Phys. **36**, 1135 (1973).

[26] C. E. Campbell, in *Progress in Liquid Physics*, (C. A. Croxton, ed.) Wiley, New York, (1978).

[27] H. R. Glyde and E. C. Svensson in *Methods of Experimental Physics*, (D. L. Price and K. Skold, eds.), Vol. 23, Part B, Academic Press, New York (1987).

[28] L. D. Landau and I. M. Khalatnikov, Zh. Eksp. Teor. Fiz. **19**, 637 (1949).

[29] K. Bedell, D. Pines and A. Zawadowski, Phys. Rev. B **29**, 102 (1984).

[30] K. Bedell, D. Pines, and I. Fomin, J. Low Temp. Phys. **48**, 417 (1982).

[31] J. Yau and M. J. Stephen, Phys. Rev. Lett. **27**, 482 (1971).

[32] L. P. Pitaevskii, Sov. Phys. JETP **36**, 830 (1959).

[33] C. P. Enz, Phys. Rev. A **6**, 1605 (1972).

[34] J. Ruvalds and A. Zawadowski, Phys. Rev. Lett. **25**, 333 (1970).

[35] D. G. Henshaw and A. D. B. Woods in *Proc. 7th Int. Conf. Low Temp. Phys.*, (G. M. Graham and A. C. Hollis Hallet, eds.), University of Toronto Press, Toronto, (1961).

[36] A. D. B. Woods, E. C. Svensson and P. Martel, Phys. Lett. **43A**, 223 (1973).

[37] E. H. Graf, V. J. Minkiewicz, H. B. Møller and L. Passell, Phys. Rev. A **10**, 1748 (1974).

[38] E. C. Svensson, P. Martel and A. D. B. Woods, Phys. Lett. **55A**, 151 (1975).

[39] K. E. Larsson and K. Otnes, Ark. Fys. **15**, 49 (1959).

[40] N. M. Blagoveshchenskiĭ and E. B. Dokukin, JETP Lett. **28**, 363 (1978).

[41] P. J. Bendt, R. D. Cowan and J. L. Yarnell, Phys. Rev. **113**, 1386 (1959).

[42] J. S . Brooks and R. J. Donnelly, J. Phys. Chem. Ref. Data **6**, 51 (1977).

[43] E. C. Svensson, R. Scherm and A. D. B. Woods, J. Phys. Colloq. **39(C6)**, 211 (1978).

[44] A. D. B. Woods and E. C. Svensson, Phys. Rev. Lett. **41**, 974 (1978).

[45] A. Miller, D. Pines and P. Nozieres, Phys. Rev. **127**, 1452 (1962).

[46] U. M. Titulaer and J. M. Deutch, Phys. Rev. A **10**, 1345 (1974).

[47] P. H. Roberts and R. J. Donnelly, J. Low Temp. Phys. **15**, 1 (1974).

[48] T. J. Greytak and J. Yan, in *Proc. 12th Int. Conf. Low Temp. Phys.*, (E. Kanda, ed.), p.89, Academic Press, Kyoto, (1971).

[49] W. G. Stirling and H. R. Glyde, Phys. Rev. B **41**, 4224 (1990)

[50] N. M. Blagoveshchenskii, I. V. Bogoyavlenskii, L. V. Karnatsevich, Zh. A. Kozlov, V. G. Kolobrodov, V. B. Priezzhev, A. V. Puchkov, A. N. Skomorokhov and V. S. Yarunin, Phys. Rev. B **50**, 16550 (1994).

[51] K. H. Andersen, J. Bossy, J. C. Cook, O. G. Randl and J. L. Ragazzoni, Phys. Rev. Lett. **77**, 4043 (1996).

[52] M. R. Gibbs, K. H. Andersen, W. G. Stirling and H. Schober, J. Phys. Condens. Matt. **11**, 603 (1999).

[53] E. F. Talbot, H. R. Glyde, W. G. Stirling and E. C. Svensson, Phys. Rev. B **38**, 11229 (1988).

[54] B. Fak and J. Bossy, J. Low Temp. Phys. **112**, 1 (1998).

[55] F. Pistolesi, Phys. Rev. Lett. **81**, 397 (1998).

[56] F. Pistolesi, J. Low Temp. Phys. **113**, 597 (1998).

[57] H. R. Glyde, M. R. Gibbs, W. G. Stirling and M. A. Adams, Europhys. Lett. **43**, 422 (1998).

[58] T. Keller, K. Habicht, R. Golub and F. Mezei, Europhys. Lett. **67**, 773 (2004).

[59] T. J. Greytak and J. Yan, Phys. Rev. Lett. **22**, 987 (1969).

[60] J. W. Halley, Phys. Rev. **181**, 338 (1969).

[61] M. J. Stephen, Phys. Rev. **187**, 279 (1969).

[62] F. Iwamoto, Prog. Theor. Phys. **44**, 1121 (1970).

[63] A. Zawadowski, J. Ruvalds and J. Solana, Phys. Rev. A **5**, 399 (1972).

[64] T. J. Greytak, R. Woerner, J. Yan, and R. Benjamin, Phys. Rev. Lett. **25**, 1547 (1970).

[65] C. A. Murray, R. L. Woerner and T.J. Greytak, J. Phys. C: Solid State Phys. **8** L90 (1975).

[66] R. A. Cowley, J. Phys. C : Solid State Phys. **5**, L287, (1972).

[67] K. Ohbayashi and A. Ikushima, J. Phys. C: Solid State Phys. **7**, L206 (1974).

[68] M. Udagawa, H. Nakamura, M. Murakami and K. Ohbayashi, Phys. Rev. B **34**, 1563 (1986).

[69] K. Ohbayashi, M. Udagawa and N. Ogita, Phys. Rev. B **58**, 3351 (1998).

[70] M. Shay, O. Pelleg, E. Polturak and S. G. Lipson, Phys. Rev. B **75**, 054516-1 (2007).

[71] Y. S. Jain, arXiv : cond-mat/06094181v1.

[72] R. J. Donnelly and C. F. Barenghi, J. Phys. Chem. Ref. Data **27**, 1217 (1998);

[73] P. J. Price, Phys. Rev. **94**, 257 (1954).

[74] A. Lamacraft, arxiv.org/Cond-mat/0510111.

[75] Y. S. Jain, Am. J. Cond. Mat. Phys **2**, 32 (2012).

[76] Y. S. Jain, J. Sci. Expl. **16**, 77 (2002).

[77] S. Chutia, Ph.D Thesis, Physics Department, North Eastern Hill University, Shillong (2007).

[78] B. B. Laud in *Lasers and Non-Linear Optics*, New Age International Publishers, New Delhi, 2007.

[79] O. Svelto in *Principles of Lasers*, 4th ed., Springer, (1998).

[80] A. Rybalko, S. Rubets, E. Rudavskii, V. Tikhiy, S. Tarapov, R. Golovashchenko, and V. Derkach, Phys. Rev. B **76**, 140503 (2007).

[81] A. S. Rybalko, S. P. Rubets, E. Ya. Rudavskii, V. A. Tikhiy , Yu. M. Poluectov, R. V. Golovachenko, V. N. Derkach, S. I. Tarapov, and O. V. Usatenko, Low Temp. Phys. **35**, 837 (2009).

[82] Y. S. Jain, arxiv:cond-mat/1008.0240v2

[83] C. Kittel, *Introduction to Solid State Physics*, 7th ed., Wiley, (1995).

[84] C. R. Anderson, K. H. Andersen, J. Bossy, W. G. Stirling, R. M. Dimeo, P. E. Sokol, J. C. Cook and D. W. Brown, Phys. Rev. B **59**, 13588 (1999).

Chapter 4

Logarithmic Singularity of Specific heat

ABSTRACT : The logarithmic singularity of heat capacity at constant pressure C_p is studied at different pressures using Macro-orbital theory. Our results agree closely with experiments and provide the explanation of the logarithmic singularity of C_p at different pressures. However, as shown by other studies reporting carefully measured C_p of liquid helium-4 around T_λ for $|t| = |(T_\lambda - T)/T_\lambda|$ ranging from 10^{-1} to 10^{-9}, in and out of the earth's gravitational field and in finite size samples, weak effects arising from the earth's gravity and small size round it off and C_p assumes asymptotic nature near $t \sim 0$.

4.1 Introduction

One of the most remarkable properties of liquid helium-4 (LHe-4) is the discontinuity in its specific heat at the λ transition. Dana and Kamerlingh Onnes [1] found in 1923 that the specific heat of LHe-4 has a sharp maximum around 2 K. However, in the publication of their experimental results in 1926, they decided to leave out these data points, because they feared that this anomaly might have been caused by experimental problems. Keesom and Clusius [2] measured the specific heat of LHe-4 again in 1932. They observed a jump in the specific heat in the vicinity of 2.17 K, which they attributed to a phase transition. As the shape of the specific heat *versus* temperature curve resembles the shape of the Greek letter λ, the transition is called λ transition, as suggested by Ehrenfest [3].

A series of more accurate measurements [4–10] later revealed that the discontinuity of the specific heat of LHe-4 is logarithmic in nature. The data of the earlier measurements [4–6] could be fitted to the empirical relation

$$C_p = -A \ln |T - T_\lambda| + B \tag{4.1.1}$$

where the constants A and B have the values $A = 3.00$ J g^{-1} K^{-1} for both $T > T_\lambda$ and $T < T_\lambda$ and $B = -0.65$ J g^{-1} K^{-1} for $T > T_\lambda$ and $B = 4.55$ J g^{-1} K^{-1} for $T < T_\lambda$ [11, 12]. However, later measurements [7–10] revealed deviation from the above empirical relation (4.1.1). This set of data are not consistent with equal amplitudes of the logarithmic term, specifically when $T_\lambda - T \geq 10^{-3}$ K, and rather demands that [7, 12]

$$1.04 \leq \frac{A}{A'} \leq 1.06 \tag{4.1.2}$$

where A' and A refer to $T < T_\lambda$ and $T > T_\lambda$ respectively.

Recently, Lipa *et al* [13, 14] measured C_p *in and out of the earth's gravitational field.* The effect of gravity was reduced by studying the C_p on STS-52 space craft, the space shuttle *Columbia.* The net dependence of C_p on $t = (T_\lambda - T)/T_\lambda$ is asymptotic but their analysis shows that once the observed C_p is corrected for the factors which round off its values near T_λ, the corrected C_p closely fits logarithmic variation. Similarly, Lipa *et al* [15–17] and Gasparini *et al* [18–20] carefully investigated the effects of finite size of the sample. Their results revealed that C_p variations are intrinsically logarithmic.

In addition to the logarithmic singularity of C_p, the λ transition of LHe-4 is characterized by logarithmic singularity of (i) the expansion coefficient α_p, (ii) the isothermal compressibility k_T and (iii) the pressure coefficient β [11, 12].

The early measurements of density of LHe-4 [21, 22] were repeated with improved accuracy by Atkins and Edwards [23], Kerr [24], Edwards [25] and Chase *et al* [26] for detailed analysis. These results are reviewed by Kerr and Taylor [27]. It is clear that α_p for its linear relations with C_p should have logarithmic singularity at the λ point. Similarly, the divergence of β investigated by Ahlers [9], Lounasmaa and Kaunisto [28], Lounasmaa [29] and Kiersted [30, 31] ought to be logarithmic. Also, the thermodynamic relations between various response functions, as discussed by Rice [32], Pippard [33, 34] and Buckingham and Fairbank [5], indicated that K_T is an asymptotically linear function of C_p and hence of α_p. Hence, K_T is naturally expected to show logarithmic singularity at the λ point.

4.2 Experimental Studies of C_p at different pressures

The superfluid transition of LHe-4 is one of the most important phenomenon in the study of scaling laws and universality of critical phenomena. Ahlers [9] reported the results of detailed measurements of C_p near the superfluid transition in LHe-4 at SVP. His analysis showed that certain simple interpretations of the results are not consistent with the original formulation of the scaling laws for critical phenomena. He extended [10] the heat capacity measurements to higher pressures in order to obtain further data for comparison with the scaling laws, and to test the principle of universality. From the measurements of the heat capacity at constant volume C_v and the pressure coefficients $(\partial P/\partial T)_v$ near the superfluid transition on six isochores, he determined the heat capacity at constant pressure C_p along six isobars. From these measurements he determined the values of the coefficients A, A', B and B' at different pressures. Okaji and Watanabe [35, 36] reported similar studies along six isobars. However, the coefficients determined by them did not agree with those of Ahlers for $P \geq 15$ bar.

However, even after seven decades of the liquefaction of ^{4}He, the exact nature and origin of the logarithmic singularity of C_p remained unknown. Recently, Jain [37] used unconventional approach to develop a microscopic theory of a system of interacting bosons such as LHe-4 based on Macro-orbital representation of a particle in a many body system and obtained a relation for the logarithmic singularity of C_p.

In this chapter, we study the logarithmic singularity of C_p at different pressures.

4.3 Logarithmic Singularity of C_p from Macro-orbital Theory

As discussed in Chapter 2, the λ transition is the manifestation of two seperate but simultaneous phenomena: (i) BEC of (-q, q) pairs at $K = 0$ state and (ii) ordering of particles in phase space. Macro-orbital theory predicts that an energy [37]

$$\triangle\epsilon = -Nk_BT_0\left[\ln 2\sin^2\left(\frac{2n\pi \pm \delta\phi_\lambda}{2}\right) - \ln 2\right] \tag{4.3.1}$$

must be associated with the ordering of particles in phase space. Macro-orbital theory identifies this energy as *the origin of logarithmic singularity of* C_p at the λ point. For a small range of $|t| < 0.1$ K, the theory gives the relation for C_p as

$$C_p = -A\ln|t| + B \tag{4.3.2}$$

where

$$A = \frac{N}{T_\lambda}k_BT_0 2\nu \tag{4.3.3}$$

and

$$B = \frac{N}{T_\lambda}k_BT_0\left[2\ln(\delta\phi_\lambda(0)) - \ln 4 + 2\nu\right] \tag{4.3.4}$$

To demonstrate that eqn (4.3.2) can correctly account for the logarithmic singularity of C_p, Jain [37] used the values T_0=1.49 K, ν=0.55 and $\delta_\lambda(0)=\pi$ to conclude that $A = 5.71$ for both $T < T_\lambda$ and $T > T_\lambda$. This value matches closely with (i) similar estimates based on Widom–Kadanoff scaling laws [34, 38–42] and (ii) $A = 5.1$ for $T < T_\lambda$ and 5.355 for $T > T_\lambda$ obtained from experimental values of C_p. Even though the close agreement between the experimental and the theoretical values of A shows the accuracy of eqn (4.3.2), the choice of the parameters render $B = -10.35$ which differs significantly from $B = -7.77$ for $T > T_\lambda$ and 15.52 for $T < T_\lambda$ estimated from the experimental value of C_p [12]. In a recent work, Chutia [43]

argued that the value of the constant $\delta\phi$ shoud be different above and below T_λ, resulting in different values of B above and below T_λ.

While many authors studied the logarithmic singularity of C_p, most of the authors reported studies of C_p at SVP, the pressure dependence of C_p is reported in [10,12,35,36].

4.3.1 Pressure Dependence of C_p

As can be seen from eqn (4.3.2), C_p depends on T_λ, T_0, $\delta\phi_\lambda(0)$ and ν. Dependence of any one of these quantities on pressure will lead to pressure dependence of C_p. We asssume that ν is the same on both sides of T_λ and remains unchanged irrespective of the variation in pressure, since changes in pressure is not expected to alter the symmetry of the order parameter, and we might expect the scaling parameters to be universal [10]. As pressure increases, density increases so that the volume per particle decreases. This leads to a variation in T_0 and T_λ with pressure. However, the effective mass of ^{4}He atoms also increases, hence the increase in pressure results in the reduction of T_0. While the decrease of T_λ with pressure is tabulated in [10], we determine the pressure variation of $\delta\phi_\lambda(0)$ logically.

4.3.2 Determination of the effective mass m^*

The idea of effective mass of ^{4}He atom in the superfluid phase was suggested by Feynman in 1953 [44], who stated that one should insert the effective mass slightly larger than the pure mass m of a pure atom in the expressions for the density matrix. Using the effective mass $m^* = 1.7m$, Isihara and Samulski [45] obtained good agreement of the sound branch of the excitation spectrum with the experimental data on the sound velocity. Using a self-consistent approach,

Rovenchak [46] obtained $m^* = 1.58m$. The effective mass of ^{4}He exceeds the bare mass because of the inertia of the liquid which has to make way for any atom to move [47]. In this analysis, we calculated the effective mass using the relation

$$T_\lambda = \frac{h^2}{8\pi m^* k_B}\left[\frac{1}{d^2} + \left(\frac{N}{2.61V}\right)^{2/3}\right] \tag{4.3.5}$$

where d is the interparticle separation. Using the experimental values of T_λ and molar volume of ^{4}He given by Ahlers at different pressures [10], we determined the value of m^* .

4.3.3 Determination of T_0

We determined T_0 from the equation

$$T_0 = \frac{h^2}{8\pi m^* k_B d^2} \tag{4.3.6}$$

The values of d and m^* at different pressures calculated in section 4.3.2 are used to calculate T_0 at different pressures.

4.3.4 Determination of $\delta\phi_\lambda(0)$

Above the λ transition temperature, the particles are randomly moving and they are not ordered in phase space. As a result of this random motion, the phase shift $\delta\phi_\lambda(0)$ is higher in the normal fluid state than in the superfluid state. For temperatures $T \leq T_\lambda$, however, the particles are all closely packed and are ordered in phase space. There is little room for the particles to change their ϕ positions so that they are largely locked with $\triangle\phi = 2n\pi$ which indicates that $\delta\phi_\lambda(0)$ on the $T \geq T_\lambda$ side should be slightly lower than π, while that on the $T \leq T_\lambda$ side should be fairly small. Also we note that $\delta\phi_\lambda(0)$ should, in principle, be lower than π because the shift in ϕ-positions of all particles

in the process of their oder–disorder arrangement in ϕ-space need not be equal to π. As the pressure increases, the randomness or disorder in the system also increases (increase in pressure results in increase in entropy of compression [48]). Hence $\delta\phi_\lambda(0)$ also increases with pressure.

Guided by these points we chose the parameters as shown in Table 4.1. We plot our calculated values of C_p in Figures (4.1–4.7) along with the experimental values [10] for comparison. We present our calculated values of C_p at different pressures in Tables (4.3–4.9). Further, since A depends on ν and our choice of its equal value for both sides of T_λ renders $A = A'$ whose experimental values have small difference [10, 12]. Evidently, if ν is assumed to have slightly different values on the two sides of T_λ for the same reason, the difference in A and A' can be easily explained. Evidently, Macro-orbital theory can account for the observed pressure dependence of logarithmic singularity of C_p in all its details.

4.4 Discussion

Several experimental studies of specific heat of LHe-4, investigated out of earth's gravity [13,14] and confined to different geometries [15–19], have been performed near the λ point. These studies aimed at verifying several predictions of renormalization group theory. Similarly, extensive investigations of the C_p of liquid $He^3 - He^4$ mixtures near their λ points have been reported by Gasparini *et al* [49, 50]. These studies revealed that the gravity of the earth and the effects of finite size of the sample round off the C_p of LHe-4 at the λ point and the position of its maximum is shifted to a temperature below T_λ by a small amount. In the absence of these effects, however, the divergence of C_p is logarithmic, as concluded by Jain's theory

(MO theory) [37]. In this context, we may mention that Jain's theory [37] does not incorporate weak effects arising from the gravity of the earth, the finite size of the sample, *etc* while concluding equation (4.3.2). Since such effects would always be present, the experimental C_p would always be rounded for one reason or the other as one tries to reach closer and closer to T_λ.

Fliessbach [51] proposed a semi-phenomenological microscopic model of λ transition of He II, known as *almost ideal Bose gas model* (AIBG). He intuitively modifies the wave function $\Psi_{IBG}=\sum\prod_k[\phi_k]^{n_k}$ representing a state of ideal Bose gas(IBG) with $\phi_k = \exp(i\mathbf{k}.\mathbf{r_j})$ replaced by $\phi_k = \sin(qx_j + \theta_j)$ and introduces the concept of localized phase ordering by physical boundary conditions at the walls of macroscopic volume V. While there is considerable resemblance of Fliessbach's single particle function $\phi_k = \sin(qx_j + \theta_j)$ with Jain's macro-orbital $\phi_{mo} = \sin(\mathbf{q}.\mathbf{r})\exp(\mathbf{K}.\mathbf{R})$ function which identifies each atom like a particle of quantum size $\lambda/2 = \pi/q$ moving freely with momentum $\mathbf{K}$, there is a significant difference in the allowed values of q permitted by Fliessbach's theory [51] ($viz., q \geq \pi/L$, with L being the size of macroscopic volume V) and Jain's theory [37] ($viz., q \geq \pi/d$, with $d = (N/V)^{1/3}$). It is interesting to note that Fliessbach finds that the energy, responsible for the logarithmic singularity of the specific heat of LHe-4 at the λ point, is related to phase ordering and it depends on t as $t\ln|t|$ which agrees with Jain's result forming the basis of equation (4.3.2) used in the present analysis, of course with a different multiplication factor to $t\ln|t|$. Since Fliessbach did not use his relation to show the nature of agreement of his theoretical results with experiments, no comparative analysis of his results with our results is possible. However, since Fliessbach's model also uses phase ordering (although introduced intuitively) to explain the logarithmic nature of the specific heat singularity, it may be argued that the phase ordering of particles, as concluded by Jain's

theory, has strong foundation and the fact that this ordering is an important characteristic of superfluid phases of LHe-4 type systems, cannot be ignored.

While our results show good agreements with the experimental results of [10] for pressures $P \leq 15$ bar, deviations appear at higher pressures. This may result from the contributions of terms which are not considered in Jain's theory. Ahlers [10] analyzed his experimental results using power law [52]

$$C_p = (A/\alpha)[|\epsilon|^{-\alpha} - 1] + B \text{ if } \alpha \neq 0 \tag{4.4.1}$$

or

$$C_p = -A_0 \ln|\epsilon| + B_0 \text{ if } \alpha = 0 \tag{4.4.2}$$

for He I and the equivalent expression with primed coefficients for He II. In this case, ϵ is given by $\epsilon = [T - T_\lambda(P)]/T_\lambda(P)$. The scaling prediction [39–41] requires that $\alpha = \alpha'$ and $A = A'$ if $\alpha = \alpha' = 0$. For pressures lying in the range of 1.6 bar $\leq P \leq 15$ bar, he found that $\alpha = \alpha' = 0$ within errors, in agreement with the scaling. At pressures greater than 15 bar, he found within errors that $\alpha > \alpha' = 0$. His analysis showed that $A_0/A_0' > 1$ at all pressures, in contradiction to scaling and the assumption $\alpha = \alpha' = 0$. He concluded that agreement between his data and existing theoretical predictions could be obtained only if singular higher–order contributions to C_p were allowed and if C_p was finite at T_λ. Even with these corrections, the ratio A/A' depends on the pressure, which contradicts existing theory. According to Jain's theory, the coefficient A is the same for both sides of T_λ. This agrees with the prediction of the scaling laws. However, according to experimental results $A_0/A_0' > 1$ at all pressures. This may be the reason of deviation of our results from experimental results.

4.5 Conclusion

It is evident that C_p of LHe-4, when observed in the absence of the effects of the earth's gravity or of finite size of the sample, exhibits logarithmic singularity at T_λ and this agrees closely with Jain's theory [37]. According to Jain's theory, logarithmic singularity of C_p is a consequence of order-disorder of particles in phase space forced by the wave nature of particles or quantum correlation between a pair of bosons. We find that Jain's theory is capable of explaining the difference in C_p at $T < T_\lambda$ and $T > T_\lambda$ for the same value of $|T_\lambda - T|$. Jain's theory attributes the change in C_p with pressure to the change in T_0, T_λ and $\delta(\phi)$ with pressure. T_0 and T_λ both decreases with increase in pressure, the increase of $\delta(\phi)$ with pressure are taken to be different on the two sides of the T_λ. The close agreement between experimental results and our results, calculated using Jain's theory confirms the accuracy of Jain's relation (4.3.2) beyond doubt. Until Jain developed his theory, there was no microscopic theory trying to explain the pressure dependence of C_p of LHe-4. While scaling laws provided relations between exponents of various divergent quantities which are in good agreement with experiments and with numerical studies, they are not microscopic theory of LHe-4. However, the relations satisfied by the coefficients A and B in Jain's microscopic theory is similar to that of scaling laws. This confirms that Jain's theory has firm foundations to be proper microscopic theory of LHe-4.

Table 4.1: Calculated values of T_0 and m^* at different pressures. Molar volume and T_λ values at different pressures are taken from Ref. [10]

Pressure (bar)	Molar volume ($cm^3 \cdot mol^{-1}$)	d (10^{-8} cm)	T_λ (K)	m^* (10^{-24}) g	T_o (K)
SVP	27.38	3.569	2.172	6.984	1.4219
1.646	26.81	3.544	2.157	7.132	1.4121
7.382	25.31	3.477	2.095	7.629	1.3714
15.031	23.95	3.413	1.998	8.300	1.3079
18.18	23.51	3.393	1.954	8.592	1.2797
22.53	22.97	3.366	1.889	9.027	1.2365
25.86	22.60	3.348	1.836	9.389	1.2019

Table 4.2: Parameters for Calculating C_p at different pressures

Pressure (bar)	T_λ (K)	T_0 (K)	ν	ϕ_1	ϕ_2
SVP	2.172	1.422	0.470	0.087	0.750
1.646	2.157	1.412	0.470	0.099	0.800
7.328	2.095	1.371	0.470	0.140	0.830
15.031	1.998	1.308	0.470	0.260	0.900
18.180	1.954	1.279	0.470	0.280	0.930
22.533	1.8898	1.236	0.470	0.330	0.940
25.868	1.836	1.202	0.470	0.340	0.970

Table 4.3: Calculated and Experimental values of C_p at SVP. Experimental points are taken from Ref. [9].

$10^4(T_\lambda - T)$ (K)	C_p(Cal) (J mol^{-1} K^{-1})	C_p(Expt) (J mol^{-1} K^{-1})
-60.480	23.203	23.770
- 53.390	23.841	24.440
-46.310	24.569	25.200
-39.490	25.384	26.040
-30.800	26.656	27.330
-27.530	27.230	27.930
-24.140	27.902	28.640
-20.690	28.691	29.460
-17.240	29.625	30.430
-13.780	30.771	31.630
-10.250	32.285	33.220
-6.855	34.343	35.410
-4.383	36.632	37.780
-2.660	39.187	40.430
-0.895	44.760	46.140
1.215	66.647	65.370
2.885	62.222	61.050
4.482	59.968	58.980
6.244	58.272	57.030
8.881	56.469	55.220
10.080	55.821	54.600
12.220	54.836	53.580
14.820	53.849	52.600
17.210	53.084	51.840
19.570	52.427	51.120
21.270	52.000	50.650
24.600	51.256	49.880
26.270	50.920	49.610
27.920	50.609	49.230
30.330	50.185	48.860
34.780	49.484	48.060
38.170	49.009	47.600
41.550	48.574	47.070
46.490	48.000	46.520
48.270	47.807	46.270
55.200	47.121	45.540
58.260	46.845	45.300
61.990	46.527	44.920
74.950	45.556	43.890
91.590	44.530	42.760
100.000	44.081	42.300
108.400	43.668	41.760
141.900	42.290	39.760
158.900	41.711	39.480
168.100	41.423	39.170
240.300	39.595	36.970
277.300	38.862	35.890
320.200	38.126	34.940
357.200	37.567	34.040

Table 4.4: Calculated and Experimental values of C_p of LHe-4 at 1.65 bar. Experimental points are taken from Ref. [10]

$10^3(T - T_\lambda)$ (K)	C_p(Cal) (J mol^{-1} K^{-1})	C_p(Expt) (J mol^{-1} K^{-1})
-22.6200	38.4683	37.0200
-21.0100	38.8462	37.5000
-19.4400	39.2436	37.9200
-17.8900	39.6688	38.3800
-16.3100	40.1420	38.9300
-14.7100	40.6703	39.4900
-13.1300	41.2518	40.1100
-11.5600	41.9035	40.8500
-9.9840	42.6535	41.6900
-8.3910	43.5430	42.5900
-6.8140	44.6083	43.6900
-5.7130	45.5102	44.5800
-4.4470	46.7921	45.9700
-3.8090	47.5846	46.6700
-2.5440	49.6501	48.7700
-1.7740	51.4949	50.6000
-1.0790	54.0392	53.1600
-0.9788	54.5379	53.5400
-0.8788	55.0894	54.0800
-0.7797	55.7017	54.9400
-0.6786	56.4124	55.3200
-0.5823	57.1956	56.1500
-0.3968	59.1583	58.2100
-0.2097	62.4219	61.3300
-0.1433	64.3702	63.7200
-0.0829	67.1709	65.8700
-0.0491	69.8513	69.1100
-0.0337	71.7772	70.4100
0.4843	35.3885	36.2500
0.5703	34.5521	35.3700
0.7775	32.9661	33.6200
0.9224	32.0916	32.8400
1.1200	31.0983	31.7200
1.4230	29.8730	30.4300
2.0370	28.0374	28.5300
5.0420	23.3995	23.7400
7.9590	21.0634	21.3700
9.4080	20.2075	20.5500
11.0400	19.3889	19.7400
12.4500	18.7739	19.1400
16.7300	17.2618	17.7700

Table 4.5: Calculated and Experimental values of C_p of LHe-4 at 7.33 bar. Experimental points are taken from Ref. [10]

$10^3(T - T_\lambda)$ (K)	C_p(Cal) (J mol^{-1} K^{-1})	C_p(Expt) (J mol^{-1} K^{-1})
-9.6090	38.9241	38.4200
-9.2550	39.1162	38.5900
-8.5560	39.5180	39.0900
-7.6070	40.1196	39.6400
-6.9430	40.5869	40.0800
-6.3170	41.0704	40.5700
-5.6820	41.6125	41.0500
-5.3540	41.9167	41.3900
-4.7320	42.5487	41.9400
-4.1250	43.2511	42.5900
-3.8160	43.6495	42.9900
-3.5140	44.0714	43.3200
-3.2100	44.5344	43.8300
-2.9130	45.0312	44.3200
-2.6100	45.5932	44.8000
-2.3160	46.2047	45.4000
-2.0230	46.8968	46.0300
-1.7330	47.6685	46.7900
-1.4460	48.6150	47.6300
-1.1570	49.7559	48.7000
-0.8716	51.2052	50.0200
-0.6505	52.7024	51.5700
-0.5922	53.1828	51.7900
-0.5631	53.4407	52.2500
-0.4794	54.2641	53.0100
-0.3961	55.2407	53.7500
-0.3143	56.4244	54.9100
-0.3117	56.4669	55.0700
-0.3024	56.6219	55.2500
-0.2147	58.3744	56.8200
-0.1307	60.9141	59.2200
0.0957	43.1326	40.7000
0.1271	41.6806	39.0800
0.2146	39.0004	36.7300
0.3537	36.4436	34.1400
0.5401	34.2776	31.9500
0.7208	32.8009	30.4300
0.8941	31.6984	29.3600
1.1350	30.4777	28.1900
1.4460	29.2385	26.8800
1.7530	28.2534	26.0100
2.0570	27.4351	25.1800
2.3650	26.7211	24.5000
2.6720	26.0966	23.8600

Table 4.6: Calculated and Experimental values of C_p at 15.03 bar. Experimental points are taken from Ref. [10]

$10^3(T - T_\lambda)$ (K)	C_p(Cal) (J mol^{-1} K^{-1})	C_p(Expt) (J mol^{-1} K^{-1})
-4.1320	36.2603	39.2200
-3.8600	36.6087	39.5600
-3.5920	36.9767	39.8500
-3.3230	37.3753	40.2300
-3.0580	37.8005	40.5700
-2.7870	38.2753	40.8400
-2.4200	38.9978	41.6500
-2.1600	39.5794	42.0600
-1.1850	42.6514	44.8200
-1.0610	43.2169	45.2700
-0.9263	43.9117	45.9300
-0.7962	44.6861	46.5500
-0.6636	45.6182	47.4100
-0.5402	46.6710	48.3600
-0.4209	47.9478	49.3300
-0.3159	49.4162	50.7600
-0.3106	49.5028	50.8000
-0.2360	50.9083	52.1900
-0.2007	51.7373	52.7100
-0.1667	52.6871	53.8300
-0.0976	55.4262	56.2500
-0.0871	56.0086	56.3400
-0.0343	60.7771	60.6600
0.0442	45.9611	40.3100
0.1231	40.7201	35.4200
0.1573	39.4656	34.3400
0.3095	36.0025	30.9800
0.3170	35.8800	30.9500
0.4764	33.7956	29.0300
0.6299	32.3665	27.6600
0.7871	31.2264	26.5400
1.0020	29.9912	25.2700
1.2720	28.7704	24.1000
1.5410	27.7888	23.2200
1.9450	26.5974	22.0900
2.4870	25.3396	20.9300
3.0280	24.3325	19.9500

Table 4.7: Calculated and Experimental values of C_p at 18.18 bar. Experimental points are taken from Ref. [10]

$10^3(T - T_\lambda)$ (K)	C_p(Cal) (J mol^{-1} K^{-1})	C_p(Expt) (J mol^{-1} K^{-1})
-4.1870	35.2665	37.8600
-3.7160	35.8770	38.3800
-2.7850	37.3525	39.6000
-2.3780	38.1608	40.3200
-2.1320	38.7194	40.7900
-1.9680	39.1289	41.1000
-1.7380	39.7648	41.8600
-1.3800	40.9448	42.6600
-1.1450	41.8999	43.4000
-1.0530	42.3284	43.7500
-0.9173	43.0342	44.2600
-0.7371	44.1532	45.4300
-0.6009	45.1983	46.2000
-0.5084	46.0536	46.9100
-0.4545	46.6269	47.3700
-0.3945	47.3512	48.0500
-0.2828	49.0543	49.2400
-0.1998	50.8317	51.0700
-0.1520	52.2306	51.9700
-0.1350	52.8374	52.5400
-0.1262	53.1823	53.0100
-0.0697	56.2195	55.4700
0.0341	46.8104	40.3500
0.0500	44.8524	38.7000
0.0981	41.4043	35.2800
0.1202	40.3649	34.3900
0.1682	38.6459	32.1400
0.1979	37.8140	31.7500
0.2776	36.0826	30.2000
0.3104	35.5112	29.4100
0.5671	32.4279	26.5900
0.7000	31.3508	25.5500
0.8341	30.4541	24.6600
1.0330	29.3599	23.6500
1.5520	27.2773	21.7000
1.8250	26.4483	20.9100
2.0960	25.7399	20.2800
2.5040	24.8300	19.5300
3.0420	23.8343	18.6400
3.5700	23.0155	17.8900
4.3970	21.9495	16.9900
5.5610	20.7480	15.9700
6.7930	19.7142	15.1300
8.0920	18.8289	14.4100
11.7100	16.9382	12.9700
18.0800	14.7160	11.3100
25.2600	13.0051	10.2700
33.1700	11.6113	9.3850

Table 4.8: Calculated and Experimental values of C_p at 22.53 bar. Experimental points are taken from Ref. [10]

$10^3(T - T_\lambda)$ (K)	C_p(Cal) (J mol^{-1} K^{-1})	C_p(Expt) (J mol^{-1} K^{-1})
-4.3270	33.1378	36.1600
-4.0710	33.4498	36.4200
-3.8490	33.7367	36.5800
-3.6170	34.0548	36.9600
-3.3890	34.3899	37.2200
-3.1730	34.7284	37.5400
-2.9940	35.0219	37.7400
-2.7230	35.5073	38.0800
-2.5050	35.9342	38.4200
-2.2750	36.4270	38.7100
-1.9350	37.2552	39.4600
-1.7230	37.8489	39.8000
-1.5120	38.5172	40.3900
-1.2990	39.2941	41.0300
-1.0900	40.1915	41.6800
-0.9261	41.0252	42.2800
-0.8601	41.4035	42.8200
-0.7952	41.8049	43.0500
-0.7315	42.2321	43.4500
-0.6687	42.6913	43.7400
-0.5421	43.7651	44.4200
-0.4811	44.3759	45.0000
-0.4207	45.0623	45.5200
-0.3607	45.8495	46.0300
-0.3012	46.7718	46.7600
-0.2467	47.7930	47.7900
-0.2432	47.8662	47.6300
-0.1875	49.1969	48.5800
-0.0769	53.7569	52.3800
-0.0259	59.3247	56.6300
0.0286	47.4224	39.6100
0.0287	47.4046	39.3900
0.0817	42.0522	34.0900
0.0891	41.6086	33.6400
0.1590	38.6455	30.8400
0.3143	35.1591	27.3100
0.5733	32.0839	27.3100
0.8267	30.2112	24.4700
1.0690	28.8961	22.7400
1.3090	27.8599	21.5800
1.6700	26.6138	19.5600
2.1740	25.2644	18.3800

Table 4.9: Calculated and Experimental values of C_p at 25.86 bar. Experimental points are taken from Ref. [10]

$10^3(T - T_\lambda)$ (K)	C_p(Cal) (J mol^{-1} K^{-1})	C_p(Expt) (J mol^{-1} K^{-1})
-21.7400	24.7329	29.0900
-20.6900	24.9862	29.3800
-19.5600	25.2735	29.7500
-18.5000	25.5586	29.9600
-17.3800	25.8781	30.2000
-16.3400	26.1938	30.5100
-15.3100	26.5269	30.8700
-14.2300	26.9012	31.1400
-12.1500	27.7097	31.8300
-11.0700	28.1859	32.2400
-10.0300	28.6908	32.7300
-9.0240	29.2314	33.1100
-8.0260	29.8311	33.6100
-7.0340	30.5060	34.1200
-6.0640	31.2652	34.7200
-5.1040	32.1470	35.3300
-4.3060	33.0168	36.1300
-3.9090	33.5117	36.3600
-2.9930	34.8777	37.4900
-1.8620	37.3060	39.3100
-1.5680	38.1852	40.0000
-0.8173	41.5187	42.8000
-0.6754	42.4944	43.3900
-0.5544	43.5044	44.4500
-0.4083	45.0694	45.4000
-0.3998	45.1770	45.7900
-0.2344	47.9087	47.8700
-0.1957	48.8319	48.8900
-0.1523	50.1147	49.9900
-0.1002	52.2568	51.6800
-0.0727	53.8982	52.6400
-0.0386	57.1372	55.4500
0.0185	49.1632	39.3900
0.1181	39.6790	31.0500
0.3644	33.9145	25.5800
0.5019	32.2766	24.0600
0.9740	28.8845	20.8800
1.9060	25.4497	17.8000
2.2620	24.5736	17.0600
3.3370	22.5843	15.3800
4.0620	21.5784	14.5700
5.2330	20.2824	13.5600
6.9040	18.8647	12.5000
7.8810	18.1875	12.0200
12.1500	15.9728	10.4800
17.1500	14.2094	9.3940
22.6000	12.7976	8.5740

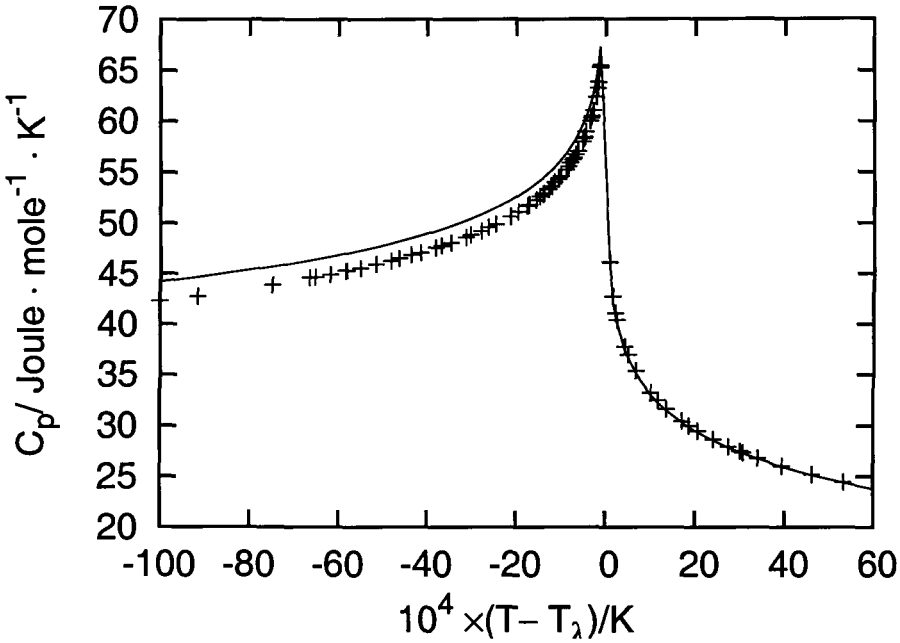

Figure 4.1: C_p *vrs* Temperature at SVP. Solid line represents our calculated values, crossses are experimental points [9].

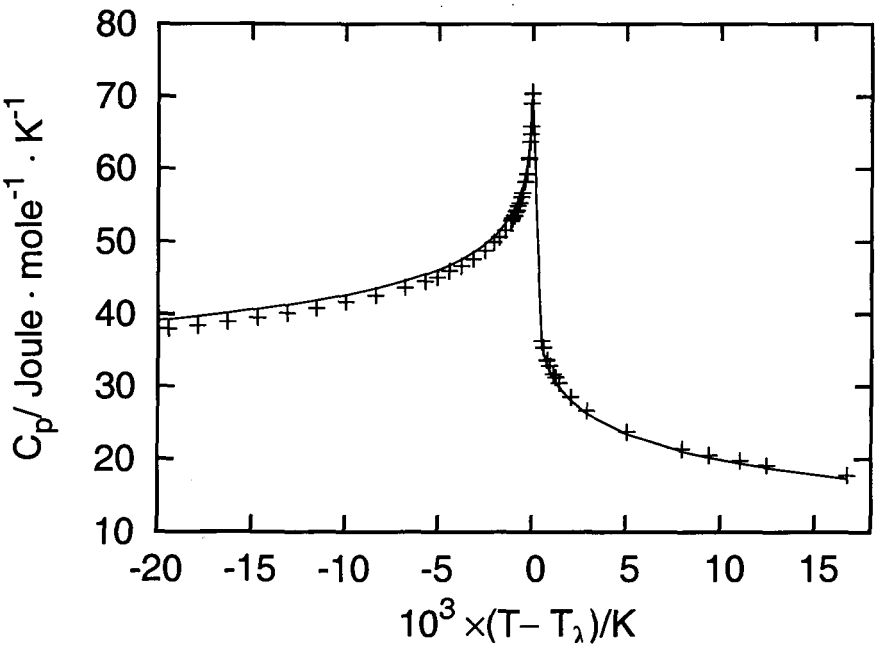

Figure 4.2: C_p *vrs* Temperature at 1.65 bar. Solid line represents our calculated values, crosses are experimental points [10].

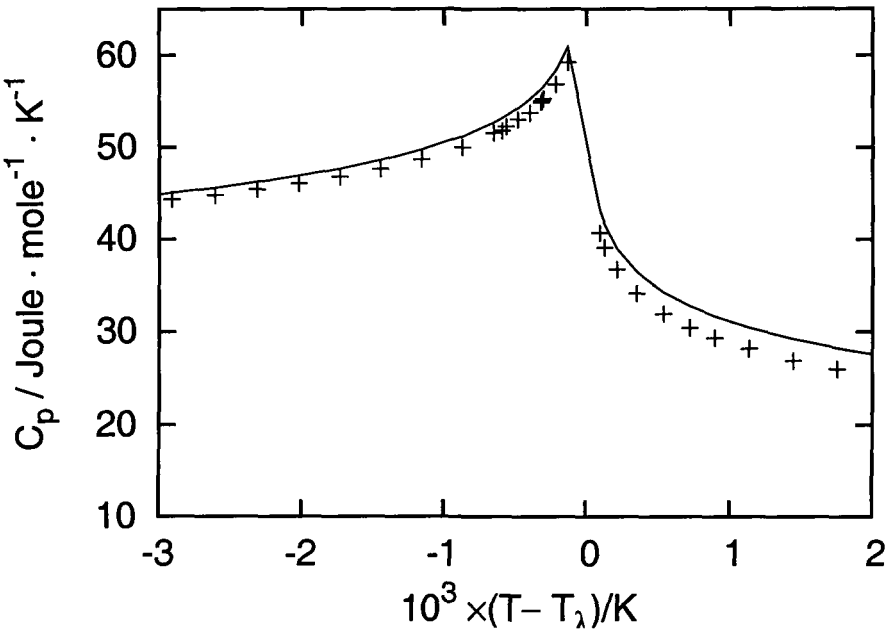

Figure 4.3: C_p *vrs* Temperature at 7.33 bar. Solid line represents our calculated values, crosses are experimental points [10].

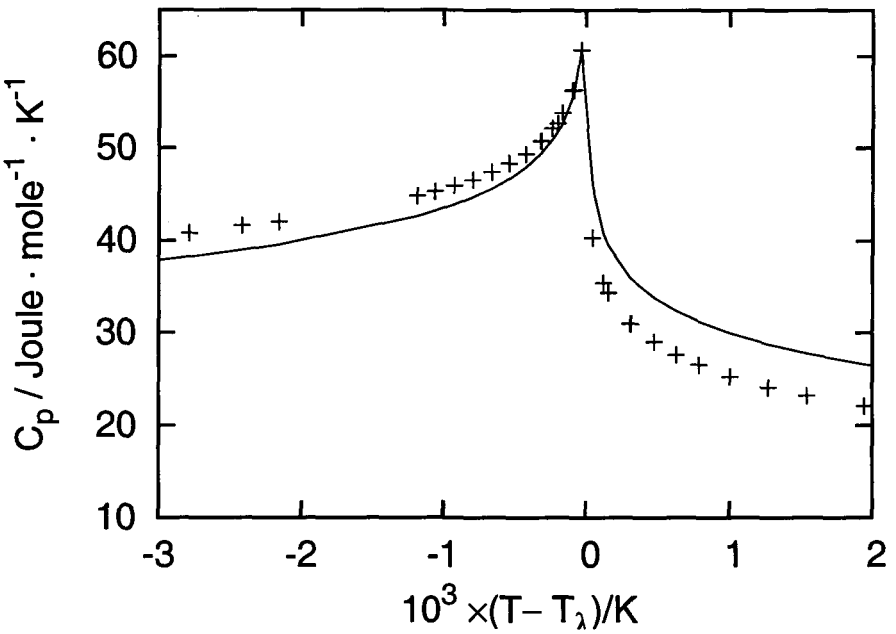

Figure 4.4: C_p *vrs* Temperature at 15.03 bar. Solid line represents our calculated values, crosses are experimental points [10].

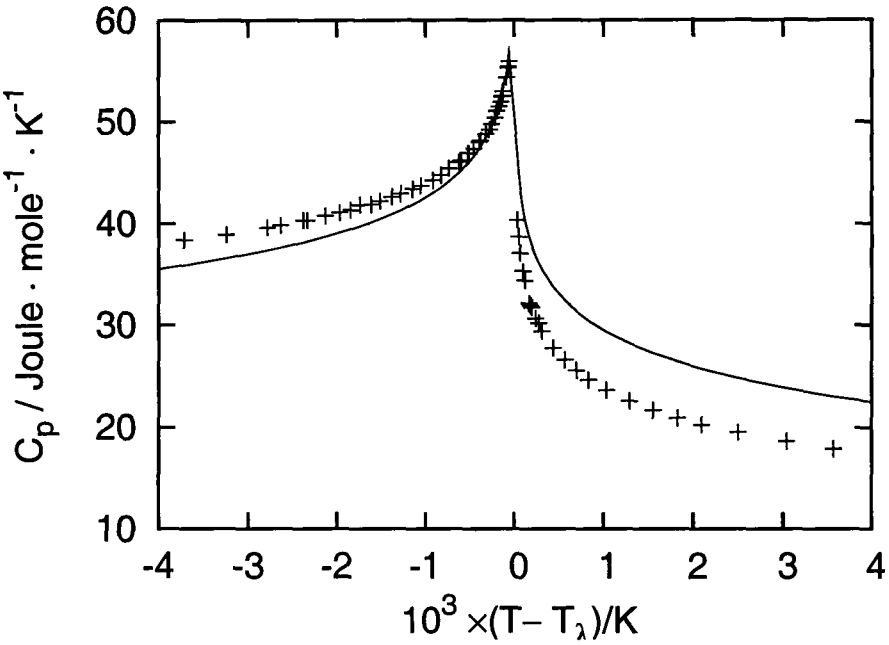

Figure 4.5: C_p *vrs* Temperature at 18.18 bar. Solid line represents our calculated values, crosses are experimental points [10].

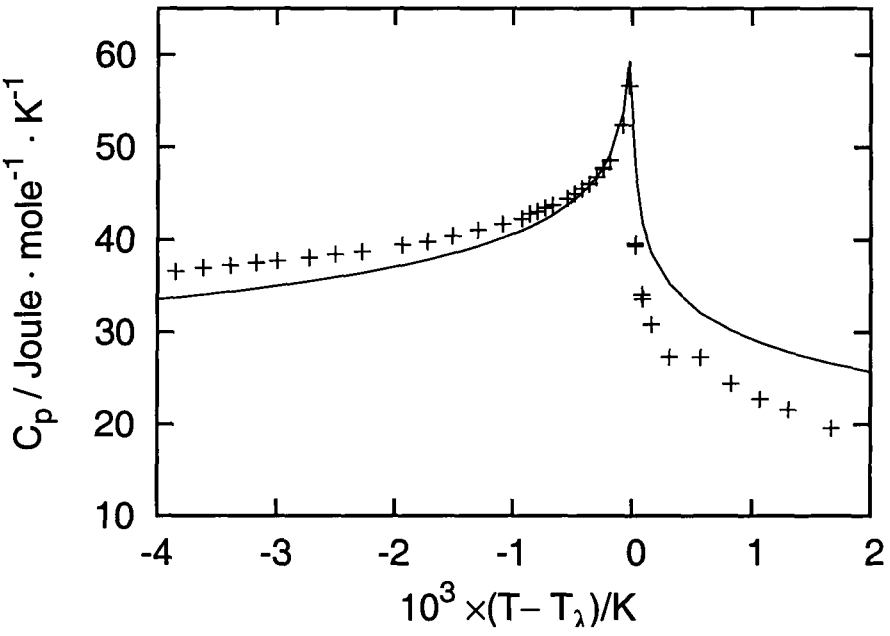

Figure 4.6: C_p *vrs* Temperature at 22.53 bar. Solid line represents our calculated values, crosses are experimental points [10].

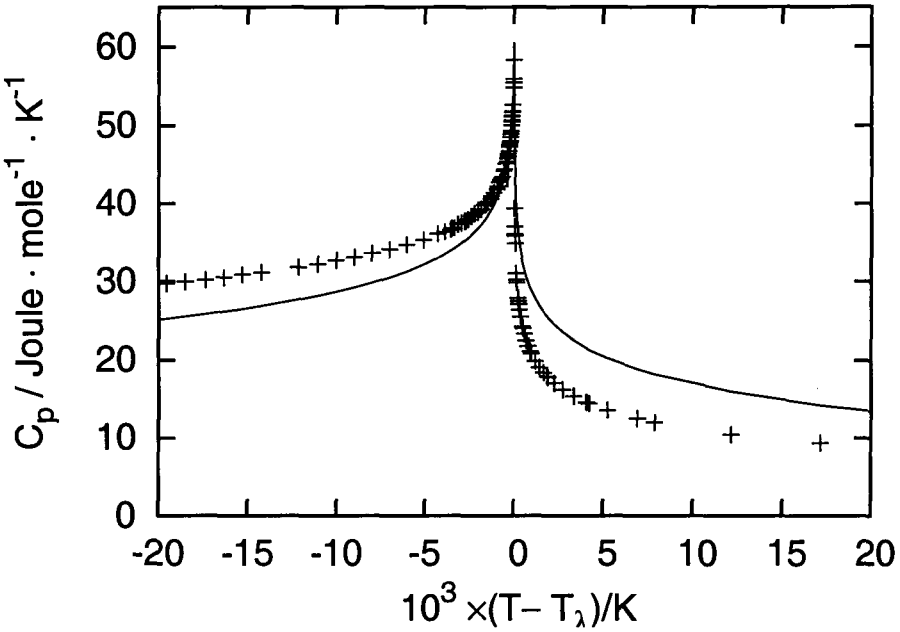

Figure 4.7: C_p *vrs* Temperature at 25.86 bar. Solid line represents our calculated values, crosses are experimental points [10].

Bibliography

[1] L. I. Dana, H. K. Onnes, Leiden Commun. **190b**, Proc. Roy. Acad. Sci. Amsterdam, **29**, 1061, 1926.

[2] W. H. Keesom, K. Clusius, Leiden Commun. **219e**, Proc. Roy. Acad. Sci. Amsterdam, **35**, 307, 1932.

[3] Z. M. Galasiewics, *Helium - 4*, Pergamon Press, Oxford, (1971).

[4] W. M. Fairbank, M. J. Buckingham and C. F. Kellers in *Low Temperature Physics and Chemistry*, (J. R. Killinger ed.), University of Wisconsin Press, Madison, Wisconsin, (1958).

[5] M. J. Buckingham and W. M. Fairbank in *Progress in Low Temperature Physics*, (C. J. Gorter ed.) Vol. III, North Holland, Amsterdam, (1961).

[6] W. M. Fairbank and C. F. Kellers in *Critical Phenomena, Proceedings of a Conference*, (M. S. Green and J. V. Sengers eds.), Natl. Bur. Std. Misc. Pub., U.S. GPO, Washington D.C., No. 273, (1966),

[7] G. Ahlers, Phys. Rev. Lett. **23**, 464 (1969).

[8] F. Gasparini and M. R. Moldover, Phys. Rev. Lett. **23**, 749 (1969).

[9] G. Ahlers, Phys. Rev. A **3**, 696 (1971).

[10] G. Ahlers, Phys. Rev. A **8**, 530 (1973).

[11] J. W. Wilks, *The Properties of Liquid and Solid Helium*, Clarendon Press, Oxford, (1967).

[12] G. Ahlers in *The Physics of Liquid and Solid Helium*, (K. H. Benneman and J. B. Ketterson eds.) Wiley, New York, (1976).

[13] J. A. Lipa, D. R. Swanson, J. A. Nissen, T. C. P. Chui and U. E. Israelsson, Phys. Rev. Lett. **76**, 944 (1996).

[14] J. A. Lipa, J. A. Nissen, D. A. Stricker, D. R. Swanson and T. C. P. Chui, Phys. Rev. B **68**, 174518-1 (2003).

[15] J. A. Lipa and T. C. P. Chui, Phys. Rev. Lett. **51**, 2291 (1983).

[16] M. Coleman and J. A. Lipa, Phys. Rev. Lett. **74**, 286 (1995).

[17] J. A. Lipa, D. R. Swanson, J. A. Nissen, Z. K. Geng, P. R. Williamson, D. A. Stricker, T. C. P. Chui, U. E. Israelsson and M. Larson, Phys. Rev. Lett. **84**, 4894 (2000).

[18] T. Chen and F. M. Gasparini, Phys. Rev. Lett. **40**, 331 (1978).

[19] S. Mehta and F. M. Gasparini, Phys. Rev. Lett. **78**, 2596 (1997).

[20] S. Mehta, M. O. Kimball and F. M. Gasparini, J. Low. Temp. Phys. **113**, 435 (1998).

[21] H. K. Onnes and J. D. A. Boks, Leiden Comm. **170b**, (1924).

[22] E. Mathias, C. A. Crommelin, H. K. Onnes and J. C. Swallow, Leiden Comm. **172**, (1925).

[23] K. R. Atkins and M. H. Edwards, Phys. Rev. **97**, 1429 (1955).

[24] E. C. Kerr, J. Chem. Phys. **26**, 511 (1957).

[25] M. H. Edwards, Can. J. Phys. **36**, 884 (1958).

[26] C. E. Chase, E. Maxwell and W. E. Millett, Physica **27**, 1129 (1961).

[27] E. C. Kerr and R. D. Taylor, Ann. Phys. **26**, 292 (1964).

[28] O. V. Lounasmaa and L. Kaunisto, Ann. Acad. Sci. Fenn. Sev. A **VI**, 59 (1960).

[29] O. V. Lounasmaa, Phys. Rev. **130**, 847 (1963).

[30] H. A. Kiersted, Phys. Rev. **138**, A1594 (1965).

[31] H. A. Kiersted, Phys. Rev. **153**, 258 (1967).

[32] O. K. Rice, J.Chem. Phys. **22**, 1535 (1954).

[33] A. B. Pippard, Phil. Mag. **1**, 473 (1956).

[34] A. B. Pippard in *The Elements of Classical Thermodynamics*, Cambridge University Press, (1957).

[35] M. Okaji and T. Watanabe, J. Low Temp. Phys. **32**, 555 (1978).

[36] M. Okaji and T. Watanabe, J. Low Temp. Phys. **49**, 435 (1982).

[37] Y. S. Jain, Am. J. Cond. Mat. Phys **2**, 32 (2012); J. Sci. Expl. **16**, 77 (2002).

[38] M. E. Fisher, Rep. Prog. Phys. **30**, 615 (1967).

[39] B. Widom, J. Chem. Phys. **43**, 3892 (1965).

[40] B. Widom, J. Chem. Phys. **43**, 3898(1965).

[41] L. P. Kadanoff, Physics **2**, 263 (1966).

[42] L. P. Kadanoff, W. Götze, D. Hamblen, R. Hecht, E. A. S. Lewis, V. V. Palciauskas, M. Rayl, J. Swift, D. Aspnes, and J. Kane, Rev. Mod. Phys. **39**, 395 (1967).

[43] S. Chutia, Ph.D Thesis, Physics Department, North Eastern Hill University, Shillong (2007).

[44] R. P. Feynman, Phys. Rev. **91**, 1291 (1953).

[45] A. Isihara and T. Samulski, Phys. Rev. B **16**, 1969 (1977).

[46] A. A. Rovenchak, Low Temp. Phys. **29**, 105 (2003).

[47] M. Haque, arXiv:cond-mat/0302076v1.

[48] D. L. Elwell and H. Meyer, Phys. Rev. **164**, 245 (1967).

[49] F. M. Gasparini and M. R. Moldover, Phys. Rev. B **12**, 93 (1975).

[50] F. M. Gasparini and A. A. Gaeta, Phys. Rev. B **17**, 1466 (1978).

[51] T. Fliessbach, arXiv:cond-mat/0203353v1.

[52] M. E. Fisher, J. Math. Phys. **5**, 944 (1964); Phys. Rev. **136**, A1599 (1964).

Chapter 5

A study of Liquid Helium Mixtures

ABSTRACT : The phase diagram of liquid helium mixture is analyzed using Macro-orbital theory. We can successfully account for the phase separation curve, which starts from $x \geq 0.0647$. *We can also successfully account for the end of the* λ *line at the tricritical point. Our analysis suggested that* ^3He *atoms form pairs in the mixture and behave like bosons. We also estimated the shift of* λ *point of the mixture with the increase in* ^3He *concentration. Our result agrees closely with experimental results.*

5.1 Introduction

Helium has two stable isotopes : ^{4}He and ^{3}He. While ^{4}He is a boson with nuclear spin $I = 0$, ^{3}He is a fermion with nuclear spin $I = 1/2$. Both the isotopes have very weak Van der Waals bonding and large zero point energies. The interplay of the weak binding force and the large zero point energy causes the two isotopes to remain liquid under saturated vapor pressure even for $T \rightarrow 0$. In addition, this is also responsible for the fact that the two isotopes have the lowest boiling temperatures and critical points known for any substance in nature.

While ^{4}He shows a sharp maximum in the temperature *vrs* density graph at 2.17 K [1, 2], the density of ^{3}He does not have a maximum and is much smaller than that of ^{4}He [3]. When Keesom and Clusius [4] observed a pronounced maximum in the specific heat of LHe-4 at about 2.17 K they attributed the unusual behavior to a phase transition, and the transition is referred to as λ transition. Since the phase transiton at the λ point was associated with the bosonic nature of ^{4}He, similar transition in LHe-3 was considered to be unlikely for a long time. In fact, the absence of a superfluid phase of ^{3}He was taken as confirmation of the interpretation that the λ transition is a Bose–Einstein Condensation [5]. This viewpoint remained unchanged until the publication of the revolutionary BCS theory [6] by Bardeen, Cooper and Schrieffer in 1957 that describes the superconductivity of metals on a microscopic basis. After many unsuccessful attempts, superfluid phases of ^{3}He were discovered in nuclear magnetic resonance measurements by Osheroff, Richardson and Lee [7] in 1972. Unlike ^{4}He which has only one superfluid phase, ^{3}He has three different superfluid phases, depending on temperature, pressure and magnetic field, but the superfluid transition in ^{3}He takes place at much lower temperatures, namely, in the millikelvin

range. While the latent heat of vaporization L of ^{4}He has a minimum at the λ point [8], the latent heat of ^{3}He is much smaller and there is no corresponding minimum around 2 K.

Since the amount of ^{3}He present in well helium or atmospheric helium is only about $10^{-5}\%$ and $1.4\times10^{-4}\%$ respectively, as shown by Aldrich and Nier [9], it was very difficult to obtain sufficient amount of ^{3}He for use in experiments. Thermal diffusion was initially used to prepare helium mixtures containing about 1% of ^{3}He. Later, in the U.S, pure ^{3}He was produced by nuclear processes (*cf.* Chapter 1). Even before any ^{3}He was prepared, several authors [10] had pointed out that it would be very important to study the behaviour of ^{3}He in LHe-4 in order to verify the interpretation of the λ point by London [5] as Bose–Einstein degeneracy.

The addition of small amounts of LHe-3 to LHe-4 produce dilute solutions having unique properties which found important applications in the fields of both pure science and technology [11,12]. Mixtures of LHe-3 and LHe-4 are widely used in dilution refrigerators to achieve cooling to temperatures in the millikelvin range [12,13]. Also, from theoretical viewpoint, they are excellent examples of interacting Bose and Fermi liquids in nature. A rich array of macroscopic properties can be observed as ^{3}He concentration is increased [14]. Among these, the natures of the λ transition and of the junction of λ and phase separation curves have been topics of long standing interest [15]. A review of work on the mixtures prior to 1964 is given by Taconis and Ouboter [16]. Later, Edwards and Pettersen [17] also gave a review of the empirical properties of liquid and solid $^3\mathrm{He}-^4\mathrm{He}$ mixtures (below ~ 0.5 K) and their phenomenological interpretation.

In this Chapter, we analyze the phase diagram of liquid helium mixture and the shift of λ point in the mixture as the concentration of ^{3}He increases.

5.2 The Phase Diagram

The phase diagrams of ^{4}He and ^{3}He are remarkably different from those of other known substances. The pressure–temperature phase diagram of ^{4}He (as shown in fig 5.1) has no triple point where gas, liquid and solid phase intersect [12]. It remains liquid at SVP even at $T = 0$ K as discussed in section 5.1. Solid ^{4}He can be produced only by applying pressures of at least 25 bar. Depending on temperature and pressure, three different crystalline structures are possible – hcp, bcc and fcc. LHe-4 has two phases : He I (normal fluid phase) and He II (superfluid phase). The transition from He I to He II depends on pressure — the transition temperature (λ temperature) decreases as pressure increases. At the melting curve, the λ transition takes place at $T = 1.9$ K. At temperatures lower than $T \approx 0.8$ K, the solid phase has higher entropy than the liquid phase. This unusual behavior can be explained by the fact that in this temperature range, the entropy of solid and liquid ^{4}He is determined by thermal excitations. Since solid ^{4}He has higher phonon heat capacity than liquid ^{4}He, at low temperatures the entropy of solid ^{4}He is higher than that of liquid ^{4}He.

The phase diagram of ^{3}He is qualitatively similar to that of ^{4}He, but the bcc phase is much more extended than that in ^{4}He. At $T \to 0$ K, ^{3}He solidifies at pressures above 34 bar. ^{3}He exhibits transitions from a normal fluid to three different superfluid phases. However, the transitions take place between 1 mK and 3 mK, three orders of magnitude lower than that in ^{4}He. The melting curve of ^{3}He shows an anomaly at low temperatures, having a distinct minimum at about 320 mK. Below the minimum, the entropy of solid ^{3}He is larger than that of liquid ^{3}He. However, this unusual behavior is not due to the contribution from the phonon spectrum, but the essential contribution to the entropy comes from nuclear spins.

A cooling mechanism known as *Pomeranchuk Cooling*, which was commonly employed for cooling before the arrival of dilution refrigerator, was based on the fact that below 320 mK, the entropy of solid ^{3}He is larger than that of liquid ^{3}He. With this technique, temperatures down to about 1 mK can be obtained.

The phase diagram of liquid ^{3}He–^{4}He mixtures is shown in Fig 5.2. It is clear from the diagram that the phase diagram of liquid helium mixture is completely different from the phase diagram of pure ^{4}He. That is, the phase diagram of ^{4}He is remarkably altered when ^{3}He is added to LHe-4.

The phase diagram of liquid ^{3}He–^{4}He mixture has three distinct regions:

(i) the region containing normal liquid ^{3}He–^{4}He mixture,

(ii) the region containing superfluid mixture and

(iii) the miscibility gap region.

For pure ^{4}He, the λ transition occurs at 2.17 K (at SVP). The λ temperature of a liquid ^{3}He–^{4}He mixture decreases with increasing ^{3}He concentration (x). The monotonic decrease of the λ temperature continues with increasing x until the phase separation critical point is reached at $T = 0.87$ K and $x = 0.67$. The concentration x is expressed in terms of mole fraction, *i.e.*, $x = N_3/(N_3 + N_4)$, where N_3 and N_4 respectively represent the number of moles of ^{3}He and ^{4}He respectively. Griffths [18] who investigated the theoretical limiting behavior of certain thermodynamic quantities in the neighborhood of this intersection point, suggested the name *tricritical point.* The λ line intersects the phase separation line at the tricritical point. The phase separation is a first order transition [12], while the λ transition is a second order. Below 0.87 K, the mixture seperates into two

phases, a heavier phase rich in ^{4}He, and a lighter phase rich in ^{4}He. The two phases are separated by an interface with a small surface tension of about 0.02 dyne/cm at $T = 0$ [19], compared to 0.355 dyne/cm for the interface between pure LHe-4 and its vapor [20], or 0.155 dyne/cm for the free surface of pure LHe-3 [21].

The liquid phase separation in liquid ^{3}He–^{4}He mixture was discovered in 1956 by Walters and Fairbank [22] in an NMR experiment. Against the initial expectation that the λ line would continue until $x = 1$ [23], where the transtion temperature would be at absolute zero, they found that below 0.87 K, at sufficiently high x, the homogeneous liquid helium mixture becomes unstable and splits into two co-existing phases, each of which is homogeneous, but one of the phases having a higher concentration of ^{3}He than the other. Since ^{3}He is lighter than ^{4}He, the ^{3}He-rich phase floats on top of the ^{4}He-rich phase. So, as the temperature of the mixture was decreased, at first two phases would appear that would both be superfluid but with different ^{3}He concentrations, and when the temperature was further decreased the ^{3}He-rich phase would become normal fluid. This phase separation is a first order transition where abrupt changes in the entropy S and volume V take place. In 1967 Graf *et al* [24] investigated the behavior near the tricritical point and found that the critical point for the phase separation is on the λ line. The measurements of Walters and Fairbank [22] and subsequent data were consistent with the idea that the two phases became pure LHe-4 and pure LHe-3 respectively at $T = 0$. However, the phase separation is incomplete at small concentration, and there is a limiting solubility of ^{3}He in LHe-4 of about 6.48% at zero temperature and pressure as demonstrated in specifc heat measurements by Edwards *et al* [25,26]. The incomplete phase separation at 0 K is the working principle of the ^{3}He–^{4}He dilution refrigerator [27].

5.3 Analysis of Phase Diagram

5.3.1 Finite Solubility of ^{3}He in ^{4}He, for $x < 6.48\%$

Liquid helium mixtures is a fascinating binary fluid where phase transition and superfluid transition can be studied in a variety of situations [28]. While many workers [29–35] determined the limiting solubility of ^{3}He in LHe-4 and the phase separation line [36–41], there is no satisfactory explanation of the end of the λ line at the tricritical point. At SVP and 0 K the limiting solubility of ^{3}He in superfluid ^{4}He is $x = 6.48\%$ [12]. The finite solubility at 0 K is explained by considering the zero-point energy and the binding energy [12, 27]. A helium atom, either ^{3}He or ^{4}He, is attracted by Van der Waals forces to other helium atoms. Due to its smaller mass, a ^{3}He atom has a larger zero-point energy than a ^{4}He atom, so that LHe-3 is much less dense than LHe-4. Hence a ^{3}He atom is closer to ^{4}He atoms than it is to other ^{3}He atoms, and consequently, the binding energy of a ^{3}He–^{4}He bond is stronger than that of a ^{3}He–^{3}He bond. When $x < 6.48\%$, the amount of ^{3}He atoms present in the mixture is too small to make a significant contribution to the macroscopic property of the system. As one can see from the phase diagram, the superfluid transition takes place at a temperature slightly lower than the λ point of pure ^{4}He. In this concentration range, each of the ^{3}He atom is completely surrounded by ^{4}He atoms, so that there is no communication between any two ^{3}He atoms. In other words, a ^{3}He atom in the mixture has no interaction with another ^{3}He atom present in the mixture.

According to the conventional microscopic theory (CMT) of superfluid ^{4}He, different number of ^{4}He atoms have different momenta; about 10% of them having zero momentum ($k = 0$) constitute what is known as Bose–Einstein condensate (BEC) or $p = 0 (= k)$

condensate and the rest, having non-zero momenta, k_1, k_2, k_3, *etc.*, (expressed in wave number), constitute the non-condensate component. These particles have relative motions and interparticle collisions even at $T = 0$ K. The collisions are bound to keep changing the positions of the atoms, which may lead to non-uniform distribution of atoms in the mixture. Some region may have a higher ^{3}He concentration than the surrounding. This may result in the formation of *energy pockets* in the mixture. If the energy pocket is formed near the surface, then the ^{3}He atoms will move out of the superfluid and phase separation may begin even at this concentration. Thus, CMT fails to provide a clear picture of the mixture even at 0 K.

On the other hand, according to MO theory or Jain's theory, the ground-state of an SIB has the minimum possible energy and all the atoms in the superfluid state of an SIB have identically equal energy ($\varepsilon_o = h^2/8md^2$) and the corresponding momentum ($h/2d$). Further, all atoms in the superfluid state have a close packed arrangement of their representative wave packets and this arrangement allows particles to have collective motions, such as phonons, rotons, *etc.*, (representing the thermal excitations of the system), and to move coherently in the order of their locations. They do not have relative motion and hence there can be no interparticle collisions. There is no question of uneven distribution of ^{3}He atoms in the mixture, so that there is no question of the formation of energy pockets. At this concentration, therefore, phase separation cannot take place. Hence, one can immediately see that MO theory gives a better picture of the mixture when $x < 6.48\%$.

5.3.2 The origin of miscibility gap, for $x \approx 6.48\%$

When $x \approx 6.48\%$, however, the concentration becomes high enough to have a significant effect on the behavior of the system and the

phase separation line begins. At this point there are two possibilities:

1. the ^{3}He atoms are randomly moving in the solution, surrounded on all sides by the ^{4}He atoms and

2. the ^{3}He atoms form pairs to become bosons.

At this concentration, approximately there are 6 atoms of ^{3}He for every 94 atoms of ^{4}He in the mixture. According to MO theory, the ^{4}He atoms in the superfluid state are in close packed arrangement, having solid-like lattice structure with zero shear forces so that particles can move in the order of their locations. In principle, the close packed arrangement needs not necessarily extend over the entire sample size, but within at least, the order of the correlation length. When a ^{3}He atom is added to the superfluid ^{4}He, it must also follow the same orderly arrangement. One can consider that every ^{3}He atom is surrounded by 15 atoms of ^{4}He on the average. The volume of a cube containing one ^{3}He atom and the surrounding 15 atoms of ^{4}He is given approximately by $16a^3$, so that the length of the edge of the cube is $\sqrt[3]{16a^3} \approx 2.52a$. That is, the two ^{3}He atoms are separated by a distance $\approx 2.52a$, (where a is the interatomic separation), which gives fractional multiple of a.

On the other hand, if the two ^{3}He atoms form a pair in the solution, for each such pair, there are approximately 29 atoms of ^{4}He. In this case, the volume of a cube containing the ^{3}He pair and the surrounding 29 atoms of ^{4}He is given by $31a^3$, with the edge $\sqrt[3]{31a^3} \approx 3.14a$. That is, the separation between ^{3}He pair is $\approx 3.14a$, which is much closer to an integral multiple of a. This suggests that there are two ^{4}He atoms between any pair of ^{3}He atoms and for the uniformity of zero-point energy distribution, this arrangement with pairs of ^{3}He atoms is more favorable.

When the concentration is $x \approx 6.48\%$, the concentration of ^{3}He is such that there is a finite probability that one of such pairs is in contact with another ^{3}He pair, or even a single ^{3}He atom, which invites the Pauli Exclusion principle to play its role, so that one ^{3}He atom has to move to higher energy level. This leads to increase in energy of the mixture and phase separation begins at this point since the energy of the single-phase mixture is higher than the sum of the energies of the two individual phases. However, if the temperature of the mixture is higher than 0 K, the thermal energy of the mixture also increases and the increase in the energy of the system due to the formation of ^{3}He pair can be compensated for and the mixture can remain a single-phase, uniform solution.

Next, we consider an arbitrary point like "A" along the phase separation curve where the concentration is approximately $x = 0.25$. There are approximately 25 atoms of ^{3}He for every 75 atoms of ^{4}He in the mixture. Following the same reasoning as above, we can say that each atom of ^{3}He is surrounded by a group of 3 atoms of ^{4}He. The volume of a cube that contains one atom of ^{3}He and the surrounding 3 atoms of ^{4}He is given by $4a^3$, so that the edge of the cube is $\sqrt[3]{4a^3} \approx 1.6a$, a fractional multiple of a. However, if two atoms of ^{3}He form pair, then for each such pair, we can associate 6 atoms of ^{4}He. The volume of the cube containing 8 helium atoms (2 atoms of ^{3}He and 6 atoms of ^{4}He) is $8a^3$, with the edge $\sqrt[3]{8a^3} = 2a$, which is an integral multiple of a. At this concentration, once again, the pair formation is much more likely as we have seen at $x \approx 6.48\%$. At this point on the phase separation line, the amount of ^{3}He atoms present in the mixture is such that one ^{3}He pair is almost certain to be in touch with another pair, leading to increase in energy of the mixture, as disscussed above. Consequently, phase separation takes place unless the temperature of the mixture is higher than ≈ 0.51 K. The same argument applies to any other point along the

phase separation curve.

5.3.3 The end of the λ line at the tricritical point

In what follows from section 5.3.2 if the ^{3}He atoms form pairs, they become bosons. At $x \approx 6.48\%$, for each such pair, one ^{4}He atom can be associated, and the mixture behaves like a bosonic system, and superfluid transition takes place. Since the effective mass of the bosonic system has become much larger, the λ transition takes place at a lower temperature. The superfluid transition can take place as long as there are more ^{4}He atoms than the ^{3}He pairs. When the concentration reaches $x \approx 66\%$, the number of ^{3}He pair is equal to the number of ^{4}He atoms in the solution. Beyond this concentration, there are more ^{3}He pairs in the solution than that can be associated with ^{4}He and the mixture exhibits a fermionic behavior and there is no superfluid transition (except perhaps in the millikelvin region where the ^{3}He superfluid transition is observed). Further, at this concentration, unless the temperature of the mixture $T \geq 0.87$K the mixture separates into two phases, a heavier phase rich in ^{4}He, and a lighter phase rich in ^{3}He. The ^{3}He-rich phase, being less dense, floats on the ^{4}He-rich phase. This explains the end of the λ line at the tricritical point. Hence our qualitative analysis shows that MO theory gives a clear picture of the phase separation diagram and can correctly account for the end of the λ line at $x \approx 66\%$.

5.4 The depression of λ point

The addition of ^{3}He to LHe-4 lowers its λ temperature. The depression of the λ temperature with increasing ^{3}He concentration continues until the tricritical point is reached at $T = 0.87$ K and $x = 0.67$ (as discussed in section 5.2). The effect was first observed

by Abraham *et al* [42]. Since then several authors determined with various methods the shift of the λ point to lower temperature of the mixture. We may mention the onset of superfluidity (Abraham *et al* [42], Daunt and Heer [23]), second sound propagation (King and Fairbank [43], Fairbank and Elliot [44]), discontinuity in the slope of vapor pressure curve (Roberts and Sydoriak [45]), the peak in the specific heat (Dokoupil *et al* [46, 47], Ouboter *et al* [48]) and the discontinuity in the slope of the density curve (Kerr [49]). King and Fairbank [43] found that for $x < 4\%$, the λ temperature decreases linearly with x with a slope of 1.5 K/mol. From Leiden specific heat measurements [47], the slope was also found to be 1.5 K/mol.

The variation of the λ temperature with x of has been the subject of many theoretical investigations [50–54]. These theories have been summarized by Atkins [55]. Even though most of the authors gave roughly the correct behaviour of this quantity, none of them could satisfactorily predict the initial slope, $(\partial T_\lambda/\partial x)_{x=0})$, which is found to be 1.5 K/mol from the Leiden specific heat measurements [46]. The initial slope given by various authors varied from as low as 0.8 K/mol (given by Pomeranchuk) to 3.4 K/mol obtained by Stout. Heer and Daunt gave the initial slope 1.9 K/mol which is closest to the the experimental value. A review of the early theoretical work is given by Beenakker and Taconis [56].

5.4.1 Analysis of the depression of T_λ using MO theory

We analyze the depression of the T_λ of the mixture using thermodynamic approach. Following standard books on Statistical Mechanics [57, 58] the equation of state of an ideal bose gas is given by (*cf.* Chapter 2)

$$\frac{PV}{k_BT} = \sum_{\epsilon} \ln(1 - ze^{-\beta\epsilon}) \tag{5.4.1}$$

with

$$N = \sum_{\epsilon} \frac{1}{z^{-1}e^{\beta\epsilon} - 1} \tag{5.4.2}$$

The fugacity z and the chemical potential μ of an ideal Bose gas are related as

$$z = \exp(\mu/k_BT) \tag{5.4.3}$$

On simplification, one gets

$$\begin{aligned} \frac{P}{k_BT} &= -2\pi \left(\frac{2mk_BT}{h^3}\right)^{3/2} \int_0^{\infty} x^{1/2} \ln(1 - ze^{-x})\, dx \\ &= \frac{1}{\lambda_t^3} g_{5/2}(z) \end{aligned} \tag{5.4.4}$$

and

$$\begin{aligned} \frac{N - N_0}{V} &= -2\pi \left(\frac{2mk_BT}{h^3}\right)^{3/2} \int_0^{\infty} \frac{x^{1/2}}{z^{-1}e^{x} - 1}\, dx \\ &= \frac{1}{\lambda_t^3} g_{3/2}(z) \end{aligned} \tag{5.4.5}$$

where N_0 is the number of particles in the ground state ϵ_0, λ_t is the thermal de Broglie wavelength given by

$$\lambda_t = \frac{h}{(2\pi m k_BT)^{1/2}} \tag{5.4.6}$$

and $g_\nu(z)$ are Bose–Einstein functions defined as

$$\begin{aligned} g_\nu(z) &= \frac{1}{\Gamma(\nu)} \int_0^{\infty} \frac{x^{\nu-1}}{z^{-1}e^{x} - 1}\, dx \\ &= z + \frac{z^2}{2^\nu} + \frac{z^3}{3^\nu} + \cdots \end{aligned} \tag{5.4.7}$$

The chemical potential of an ideal bose gas must remain negative or

zero [58], *i.e.*, $\mu \leq 0$. The critical temperature T_0 for an ideal bose gas at which the chemical potential vanishes is given by

$$T_0 = \frac{3.31\hbar^2}{mk_B g^{2/3}} \left(\frac{N}{V}\right)^{2/3} \tag{5.4.8}$$

where g is the degeneracy of each single-particle momentum state, and $g = 1$ for spinless particle.

Also, Jain redefined the fugacity as

$$\begin{aligned} z^{'} &= z \exp(-\beta\varepsilon_0) \\ &= \exp[\beta(\mu - \varepsilon_0)] \\ &= \exp(\beta\mu^{'}) \end{aligned} \tag{5.4.9}$$

where

$$\mu^{'} = \mu - \varepsilon_0 \tag{5.4.10}$$

and following the procedure of standard BEC [57], MO theory gives

$$\frac{P}{k_B T} = -\frac{2\pi(8mk_B T)^{3/2}}{h^3} \int_0^\infty x^{1/2} \ln(1 - z^{'} e^{-x})\, dx = \frac{1}{\lambda^3} g_{5/2}(z^{'}) \tag{5.4.11}$$

and

$$\frac{N - N_0}{V} = \frac{2\pi(8mk_B T)^{3/2}}{h^3} \int_0^\infty \frac{x^{1/2}}{z^{'-1} \exp^x - 1}\, dx = \frac{1}{\lambda^3} g_{3/2}(z^{'}) \tag{5.4.12}$$

This reduces the problem of an SIB to that of non-interacting bosons but with a difference. In this formulation, m is replaced by $4m$ and z by $z^{'}$. Secondly, the theory of non-interacting bosons gives $z = 1$ (or $\mu = 0$) for $T \leq T_\lambda$ and $z < 1$ (or $\mu < 0$) for $T > T_\lambda$. However, MO theory fixes $z^{'} = 1$ (or $\mu^{'} = 0$, rendering $\mu = \varepsilon_0$ (eqn (5.4.10))) for $T \leq T_\lambda$ and $z^{'} < 1$ (or $\mu^{'} < 0$ which requires $\mu < \varepsilon_0$ for $T > T_\lambda$). In other words, we have $z^{'}$ and $\mu^{'}$ in place of z

or μ used in the theory of non-interacting bosons [57].

5.4.2 Calculation of Chemical Potential

We calculated the chemical potential of ^{4}He atoms in the mixture using the formula for non-interacting bosons [59]

$$\frac{\mu}{k_B} = T\left[\frac{\lambda_t^3}{v} - \frac{1}{2^{3/2}}\left(\frac{\lambda_t^3}{v}\right)^2 + \cdots\right] \tag{5.4.13}$$

where $v = V/N$.

This expression is valid for $T \geq T_c$ and can be used to calculate the chemical potential of an SIB, after replacing m in equation (5.4.6) by $4m$ as discussed in section 5.4.1. The calculated chemical potential at different concentrations are given in Tables 5.1 and 5.2.

5.4.3 Calculation of ε_0

In Jain's theory, the ground state energy of an SIB is given by

$$\varepsilon_0 = \frac{h^2}{8\pi m d^2} \tag{5.4.14}$$

(with $d = v^{1/3}$). The temperature equivalent of the ground state energy is

$$T_0 = \frac{h^2}{8\pi m k_B d^2} \tag{5.4.15}$$

The number density of ^{4}He in liquid helium mixture is given by

$$n = (1-x)\frac{N}{V} \tag{5.4.16}$$

where x is the concentration of ^{3}He in the mixture. The inter-particle separation d and n are related as

$$d = \left(\frac{1}{n}\right)^{1/3} \tag{5.4.17}$$

Using the molar volume of the mixture at a given concentration given by [60], we calculated the ground state energy ε. These values are presented in Table 5.3.

5.4.4 Determination of T_λ from μ

As discusssed in section 5.4.1, the effective chemical potential μ' of an SIB vanishes when $\mu = \varepsilon_0$. The graphs of chemical potential *vrs* Temperature at different ^{3}He concentrations are shown in figures (5.4– 5.11). It may be noted that the curves are extrapolated to zero chemical potential values, even though the approximation formula used in the calculations is valid only for $T \geq T_c$, to give the graph a better appearance. From the graph of μ *vrs* Temperature, we find the intersection of μ and the straight line $\varepsilon_0 = -T_0$. This intersection gives the value of T_λ at that concentration. The values of T_λ at different concentrations are given in Table 5.4

5.5 Discussion

Several authors studied the behaviour of liquid helium mixture, following two different lines of thought. De Boer and Gorter [61], Rice *et al* [62], Stout [63] and Koide and Usui [64] adopted the thermodynamical approach, based on the properties of superfluid ^{4}He, extended to mixtures by making an *ad hoc* assumption about the entropy of mixing, and incorporating the assumption of Taconis and Beenakker [65, 66] that ^{3}He forms an ideal mixture with the normal

component of the fluid. On the other hand, Harasima [67], Heer and Daunt [51, 68], Mikura [52] and Toda and Isihara [69] studied the influence of ^{3}He on the properties of superfluid ^{4}He starting from the theory of λ transition in LHe-4. They started with the interpretation of the λ point in LHe-4 as a consequence of the BEC, while Pomeranchuk [70] started from Landau's theory of elementary excitations. Heer and Daunt suggested that the behaviour of liquid helium mixtures could be described as an ideal mixture of a degenerate Bose–Einstein gas and a non-degenerate Fermi–Dirac gas, confined to a more or less constant volume by the cohesive forces between the atoms. An ideal gas mixture at constant total number density would have a Bose condensation temperature varying as $(1-x)^{2/3}$. This is qualitatively similar to the behavior of T_λ in the liquid. However, a constant volume mixture of ideal Bose and Fermi gases would remain mixed at $T = 0$ and so this model fails to explain the phase-separation observed in the real liquid. De Boer and Gorter [71] criticised this approach and instead, they assumed that that ^{3}He forms an ideal mixture with the normal fluid. Mikura [52] later made a refinement of the treatment by introducing a Bose–Einstein liquid model for superfluid ^{4}He. In this model superfluid ^{4}He is composed of Bose–Einstein particles in a smoothed potential well. Then ^{3}He is introduced in this system as an ideal Fermi–Dirac gas to get expressions for the free energy of the mixture. Bogoliubov [72] in 1947 and Yang and Lee [73] in 1957 calculated the properties of a gas of hard spheres that follow Bose statistics. Yang and Lee found that the hard-sphere Bose gas differed from an ideal Bose gas in the same way as LHe-4 did. While the hard-sphere Bose gas still exhibits Bose–Einstein condensation phenomenon, it also possses elementary excitations not like those of free particles but like those of quantized sound waves (phonons). This leads to a low temperature specific heat $C_V \sim T^3$ as in LHe-4, instead of

$C_V \sim T^{3/2}$ as in an ideal Bose gas. In addition, the hard-sphere Bose gas does not have a constant pressure as a function of volume for $T < T_c$. Taking the hard sphere diameter as a small parameter, Cohen and Van Leeuwen [74] gave a phase-separation for the density and diameter appropriate for a LHe-3 and LHe-4 mixture. They also predicted the finite solubility of ^{3}He in LHe-4 and the insolubility of ^{4}He in LHe-3 [75]. Following these early work, several authors made calculations considering more realistic interatomic potentials . Most of the authors [60,76–80] considered dilute solutions of ^{3}He in LHe-4. These first-principle calculations have been quite successful in explaining the values of the binding energy, effective mass and effective interaction which have been determined empirically using the phenomenological models.

Pomeranchuk [70] considered very dilute mixtures and made some calculations regarding the equations of motion. Following Landau's theory, the excitations in superfluid ^{4}He composed of phonons and rotons, ^{3}He behaves as an ideal gas that contributes only to the roton spectrum, with an effective mass m_3^*, which could be determined from experiment. Pomeranchuk's treatment was quite succesful in explaining the behaviour of second sound in the mixture.

The theoretical calculations differed markedly from one another in the high concentration range because of basically different assumptions regarding the free energy of LHe-4. While most of the authors gave roughly the correct behavior of λ transition in the mixture, none of them could correctly give the initial slope (see Table 5.5). Stout's value of 3.4 K/mol is followed closely by 3.2 K/mol Rice *et al.* While Mikura and de Boer and Gorter gave -2.7 K/mol, Harasima obtained -2.6 K/mol. A depression of -0.8 K/mol can be expected from Pomeranchuk's theory. Heer and Daunt gave the closest value of -1.9 K/mol against the experimentally derived value

of -1.5 K/mol obtained from specific heat measurement [47]. From our analysis, we obtained -1.99 K/mol as the initial slope.

According to MO theory, when the concentration of ^{3}He in the mixture is less than 0.0647 ($x < 0.0647$), the ^{3}He atoms are completely shielded from one another by the ^{4}He atoms, so that there is no interaction among the ^{3}He atoms. MO theory predicts that when $x \geq 0.0647$, ^{3}He atoms will form pair and become bosons. Each of such pairs can be associated with one ^{4}He. When $x > 0.67$, the number of ^{3}He pairs exceeds the number of ^{4}He atoms in the mixture. The system becomes fermionic in nature and no superfluid transition can take place (except possibly in the millikelvin range).

5.6 Conclusion

Our analysis of the phase diagram of LHe-3 and LHe-4 mixture shows that MO theory can successfully explain the phase separation in the mixture. Furthermore, our calculation of the decrease in λ point agrees closely with the experimental results. This proves that Jain's theory is the only microscopic theory to successfully explain the phase diagram and the depression of the λ point. In addition, our analysis reveals that in the liquid helium mixture, the ^{3}He atoms form pairs, instead of $p = 0$ condensate, so that all the atoms of the mixture are in the lowest energy state which is different from the $p = 0$ state.

Table 5.1: Calculated Values of chemical potential at different x

Temp. (K)	$x = 0.0$	$x = 0.1$	$x = 0.2$	$x = 0.3$
1.5000	-0.6572	-0.7639	-0.8986	-1.0670
1.5180	-0.6777	-0.7884	-0.9270	-1.0992
1.5240	-0.6846	-0.7967	-0.9365	-1.1100
1.5300	-0.6916	-0.8050	-0.9461	-1.1209
1.5420	-0.7058	-0.8218	-0.9654	-1.1428
1.5600	-0.7275	-0.8474	-0.9948	-1.1760
1.5840	-0.7573	-0.8822	-1.0345	-1.2208
1.6020	-0.7801	-0.9088	-1.0648	-1.2548
1.6200	-0.8035	-0.9359	-1.0955	-1.2893
1.6320	-0.8193	-0.9542	-1.1161	-1.3124
1.6380	-0.8273	-0.9634	-1.1265	-1.3241
1.6440	-0.8354	-0.9726	-1.1370	-1.3357
1.6620	-0.8598	-1.0006	-1.1686	-1.3710
1.6680	-0.8680	-1.0101	-1.1792	-1.3828
1.6800	-0.8846	-1.0291	-1.2005	-1.4066
1.7040	-0.9184	-1.0676	-1.2437	-1.4547
1.7220	-0.9443	-1.0969	-1.2765	-1.4911
1.7400	-0.9705	-1.1266	-1.3096	-1.5278
1.7460	-0.9793	-1.1366	-1.3207	-1.5401
1.7520	-0.9882	-1.1466	-1.3319	-1.5525
1.7640	-1.0061	-1.1668	-1.3543	-1.5773
1.7820	-1.0333	-1.1973	-1.3883	-1.6149
1.8000	-1.0608	-1.2282	-1.4226	-1.6527
1.8240	-1.0981	-1.2700	-1.4688	-1.7036
1.8420	-1.1265	-1.3017	-1.5038	-1.7422
1.8480	-1.1361	-1.3123	-1.5156	-1.7551
1.8540	-1.1456	-1.3230	-1.5274	-1.7681
1.8600	-1.1553	-1.3337	-1.5392	-1.7811
1.8780	-1.1844	-1.3661	-1.5749	-1.8202
1.9020	-1.2237	-1.4098	-1.6229	-1.8729
1.9440	-1.2941	-1.4876	-1.7083	-1.9664
1.9800	-1.3557	-1.5556	-1.7828	-2.0477
2.0040	-1.3976	-1.6016	-1.8330	-2.1025
2.0340	-1.4506	-1.6598	-1.8966	-2.1718
2.0400	-1.4613	-1.6716	-1.9094	-2.1857
2.0460	-1.4721	-1.6834	-1.9223	-2.1997
2.0820	-1.5372	-1.7547	-1.9999	-2.2841
2.1240	-1.6148	-1.8393	-2.0919	-2.3839
2.1600	-1.6824	-1.9131	-2.1718	-2.4705
2.1780	-1.7167	-1.9503	-2.2122	-2.5142
2.1960	-1.7512	-1.9878	-2.2528	-2.5582
2.2030	-1.8185	-1.9888	-2.2571	-2.5703
2.2370	-1.8840	-2.0298	-2.3341	-2.6218
2.3000	-2.0083	-2.1764	-2.4794	-2.7304
2.3650	-2.1404	-2.3056	-2.5720	-2.8156
2.4000	2.2132	-2.3936	-2.6541	-2.8874

Table 5.2: Calculated Values of chemical potential at different x

Temp. (K)	$x = 0.4$	$x = 0.5$	$x = 0.6$	$x = 0.66$
0.5260	-0.6842	-0.2934	-0.1882	-0.1857
0.5620	-0.4623	-0.2480	-0.1948	-0.2108
0.6040	-0.3460	-0.2265	-0.2156	-0.2493
0.6400	-0.2953	-0.2250	-0.2420	-0.2887
0.6820	-0.2667	-0.2369	-0.2809	-0.3411
0.7240	-0.2589	-0.2598	-0.3268	-0.3995
0.7600	-0.2640	-0.2865	-0.3712	-0.4538
0.8020	-0.2802	-0.3244	-0.4279	-0.5215
0.8560	-0.3138	-0.3821	-0.5079	-0.6149
0.8620	-0.3182	-0.3890	-0.5172	-0.6257
0.8680	-0.3229	-0.3961	-0.5266	-0.6366
0.8740	-0.3276	-0.4033	-0.5361	-0.6475
0.8800	-0.3325	-0.4106	-0.5457	-0.6585
0.9220	-0.3702	-0.4642	-0.6151	-0.7378
0.9640	-0.4133	-0.5223	-0.6883	-0.8206
0.9700	-0.4199	-0.5309	-0.6990	-0.8327
0.9760	-0.4266	-0.5396	-0.7098	-0.8448
0.9820	-0.4333	-0.5484	-0.7207	-0.8570
0.9880	-0.4402	-0.5572	-0.7317	-0.8693
1.0120	-0.4685	-0.5935	-0.7761	-0.9191
1.0540	-0.5214	-0.6597	-0.8565	-1.0087
1.0960	-0.5781	-0.7292	-0.9398	-1.1011
1.1320	-0.6296	-0.7914	-1.0136	-1.1825
1.1560	-0.6654	-0.8341	-1.0639	-1.2379
1.1620	-0.6744	-0.8449	-1.0766	-1.2519
1.1680	-0.6836	-0.8557	-1.0894	-1.2659
1.1740	-0.6928	-0.8667	-1.1022	-1.2800
1.1800	-0.7021	-0.8777	-1.1150	-1.2941
1.2040	-0.7399	-0.9222	-1.1671	-1.3511
1.2340	-0.7884	-0.9791	-1.2332	-1.4235
1.2640	-0.8385	-1.0373	-1.3006	-1.4971
1.2940	-0.8899	-1.0968	-1.3693	-1.5719
1.3240	-0.9426	-1.1575	-1.4391	-1.6478
1.3360	-0.9641	-1.1822	-1.4673	-1.6785
1.3420	-0.9749	-1.1946	-1.4815	-1.6939
1.3480	-0.9858	-1.2070	-1.4957	-1.7094
1.3540	-0.9967	-1.2195	-1.5100	-1.7249
1.3720	-1.0297	-1.2572	-1.5531	-1.7716
1.3900	-1.0632	-1.2954	-1.5966	-1.8187
1.4140	-1.1085	-1.3469	-1.6552	-1.8822
1.4380	-1.1546	-1.3991	-1.7145	-1.9463
1.4740	-1.2250	-1.4787	-1.8046	-2.0436
1.4920	-1.2608	-1.5190	-1.8502	-2.0928
1.5160	-1.3092	-1.5734	-1.9116	-2.1589
1.5520	-1.3830	-1.6562	-2.0048	-2.2593
1.5700	-1.4204	-1.6982	-2.0519	-2.3099
1.5940	-1.4709	-1.7546	-2.1153	-2.3780
1.6300	-1.5479	-1.8404	-2.2114	-2.4812
1.6720	-1.6394	-1.9422	-2.3251	-2.6032
1.6960	-1.6925	-2.0011	-2.3909	-2.6737

Table 5.3: Calculated values of T_0 at different x. Volume of mixtures at different x are taken from Ref [60]

x	Mix. Vol. cu.cm	d $\times 10^{-8}$ cm	T_o K
0.00	27.52	3.575	1.496
0.10	28.28	3.737	1.364
0.20	29.07	3.922	1.238
0.30	29.86	4.137	1.112
0.40	30.69	4.396	0.985
0.50	31.55	4.714	0.857
0.60	32.98	5.154	0.717
0.66	33.61	5.475	0.635

Table 5.4: Transition temperature of Liquid helium mixtures at different concentrations. Experimental value of T_λ are taken from Ref [45]

x	T_0 K	T_λ(Cal) K	T_λ (Expt.) K
0.000	1.496	2.056	2.173
0.100	1.364	1.876	2.028
0.200	1.238	1.702	1.873
0.300	1.112	1.524	1.704
0.400	0.985	1.350	1.514
0.500	0.857	1.168	1.297
0.600	0.717	0.980	1.055
0.660	0.635	0.880	0.904

Table 5.5: Theoretical initial slope of the curve of T_λ *vrs* x. Source [56]

Author	$\frac{\partial T_\lambda}{\partial x}$ (in K/mol
Stout	- 3 .4
De Boer and Gorter	- 2.7
Rice	3.2
Heer and Daunt	- 1 .9
Harasima	- 2 .6
Mikura	-2.7
Pomeranchuk	- 0 .8
†This work	-1.99

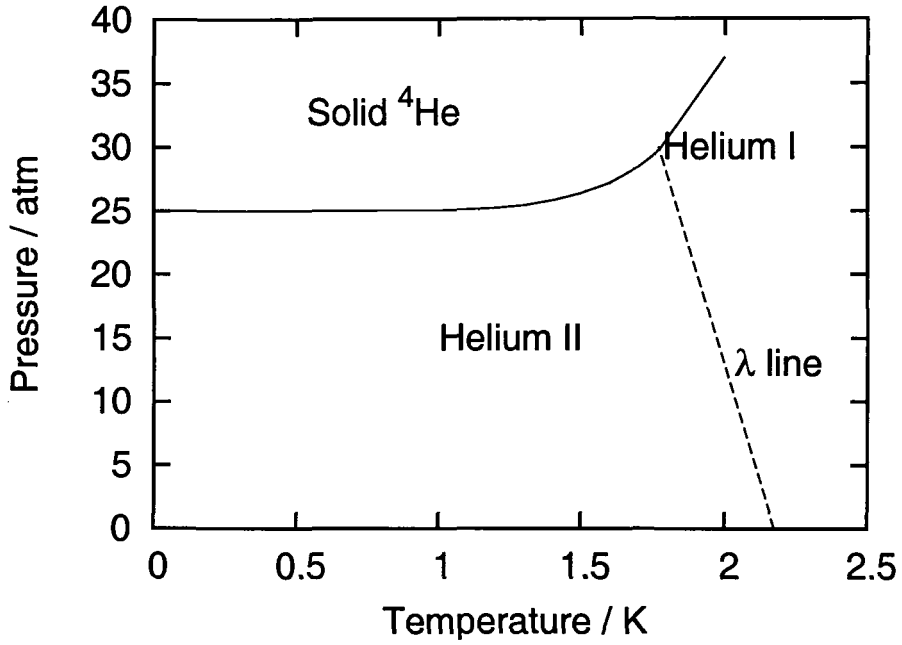

Figure 5.1: Phase diagram of ^{4}He. Source: Ref [80].

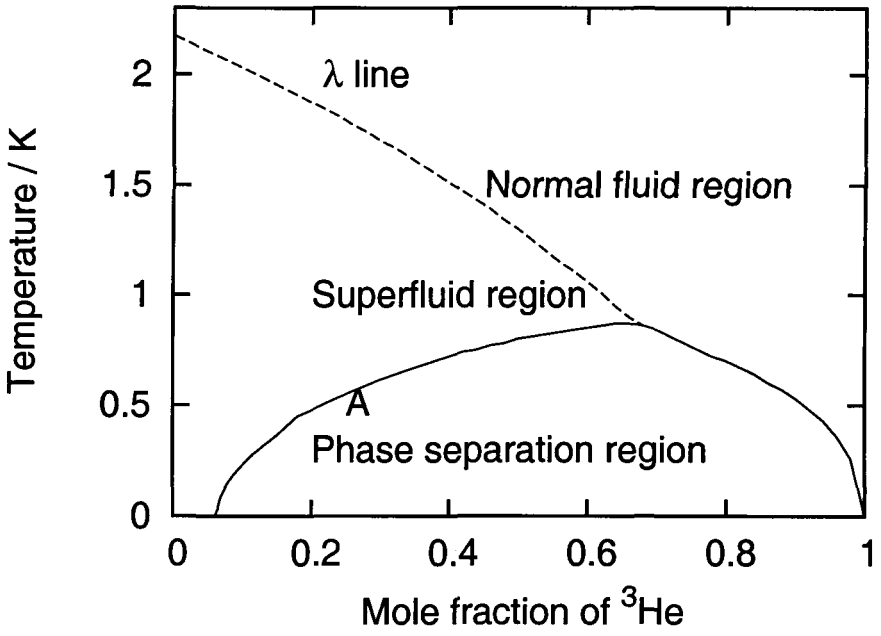

Figure 5.2: Phase diagram of liquid ^{3}He – ^{4}He mixture. Data taken from Refs. [29, 45].

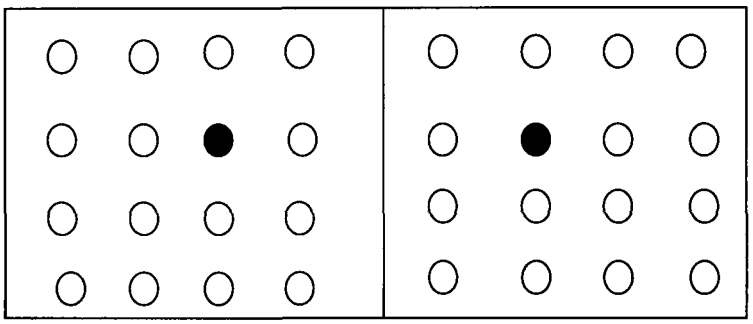

(A)

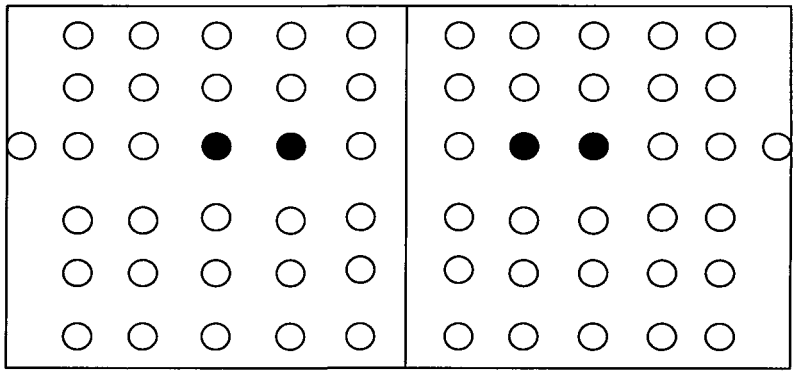

(B)

Figure 5.3: Schematic of ^{3}He pair formation in the mixture. The dark circles are ^{3}He atoms while the surrounding open circles represent ^{4}He atoms in the mixture (Not to scale). In Fig.(A), the ^{3}He atoms are isolated in the mixture. In Fig.(B), ^{3}He atoms form bound pairs in the mixture.

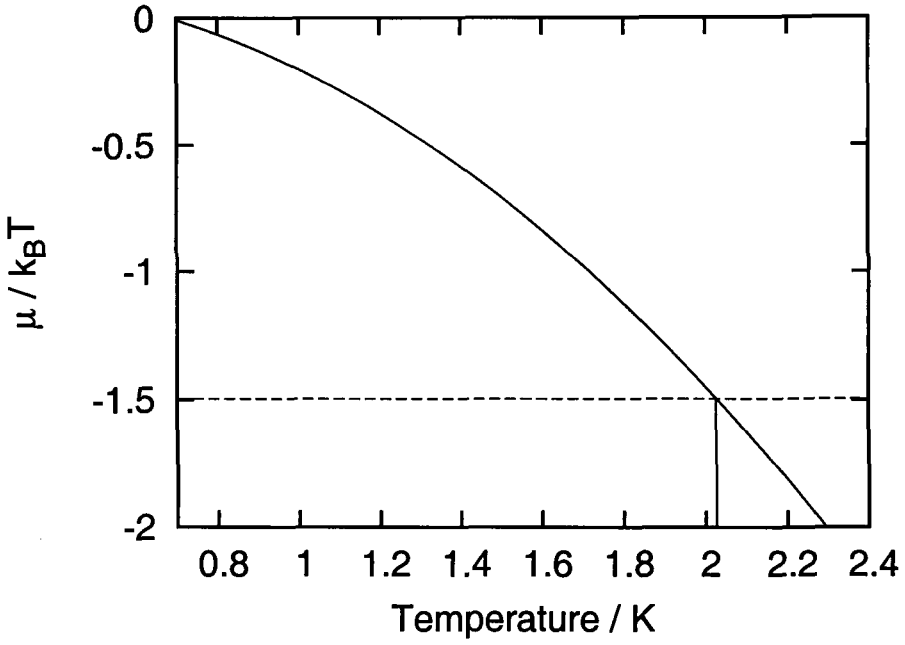

Figure 5.4: Chemical potential *vrs* Temperature for pure ^{4}He. The horizontal line is drawn at $\mu/k_BT = -1.496$, corresponding to the value of T_0 for pure ^{4}He. The chemical potential curve intersects the horizontal line at T_λ.

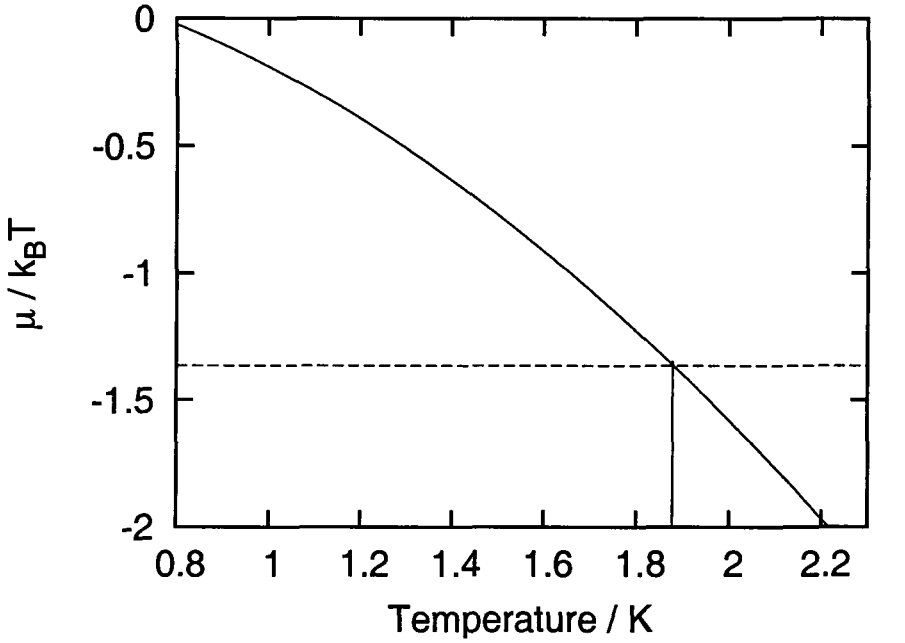

Figure 5.5: Chemical potential *vrs* Temperature at $x = 0.1$. The horizontal line is drawn at $\mu/k_BT = -1.364$. The chemical potential curve intersects the horizontal line at T_λ

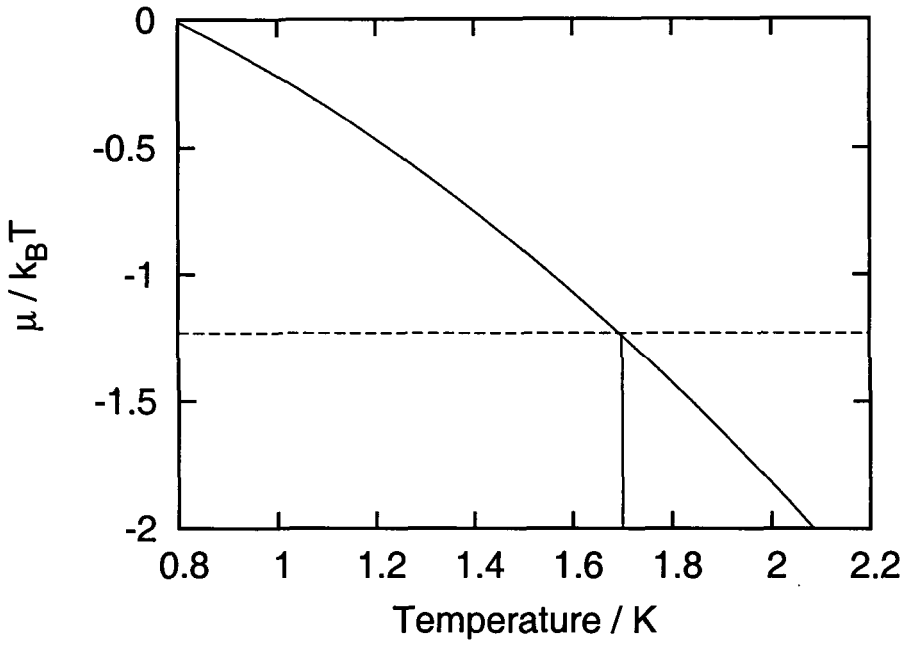

Figure 5.6: Chemical potential *vrs* Temperature at $x = 0.2$. The horizontal line is drawn at $\mu/k_BT = -1.238$. The chemical potential curve intersects the horizontal line at T_λ.

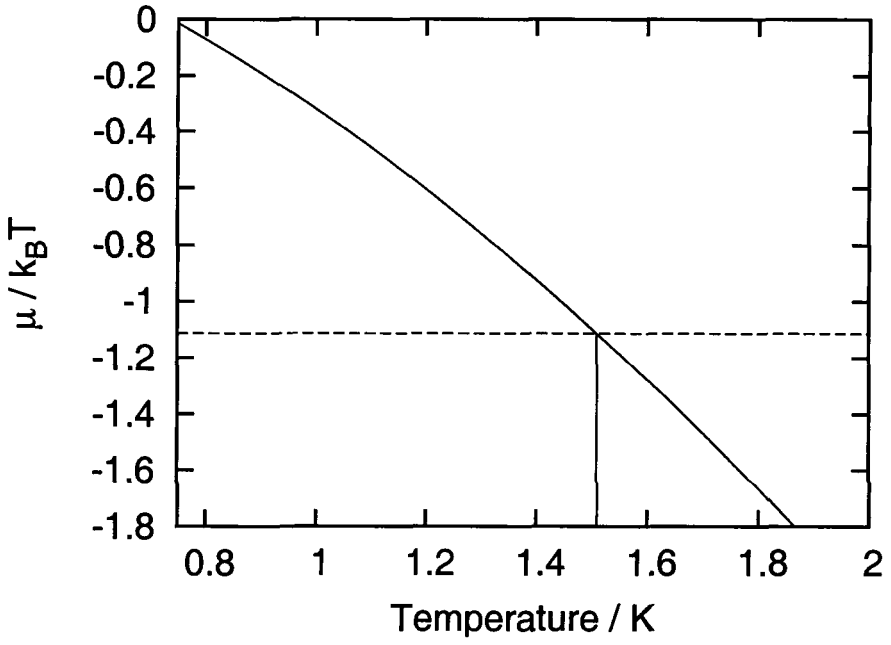

Figure 5.7: Chemical potential *vrs* Temperature at $x = 0.3$. The horizontal line is drawn at $\mu/k_BT = -1.112$.

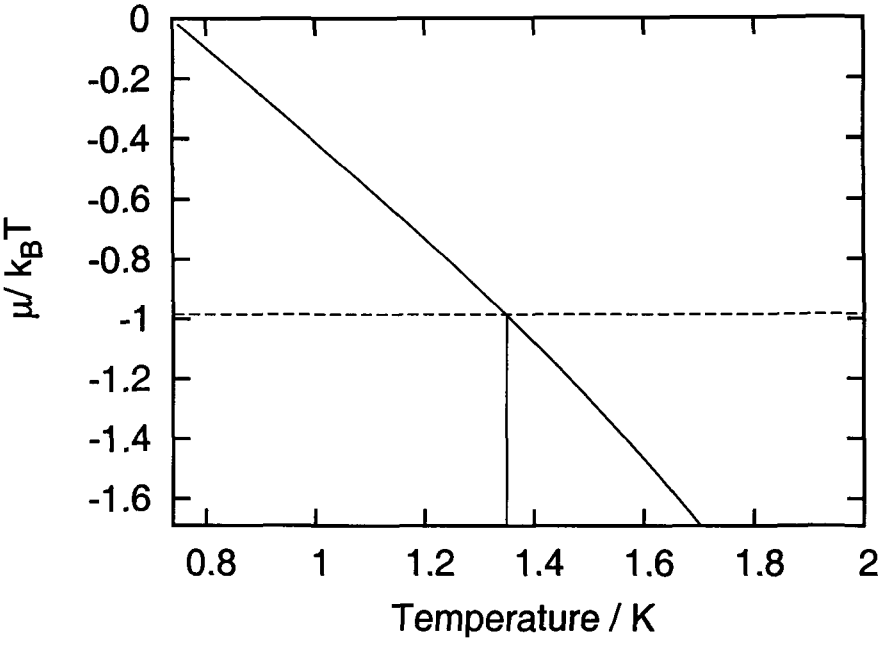

Figure 5.8: Chemical potential *vrs* Temperature at $x = 0.4$. The horizontal line is drawn at $\mu/k_BT = -0.985$.

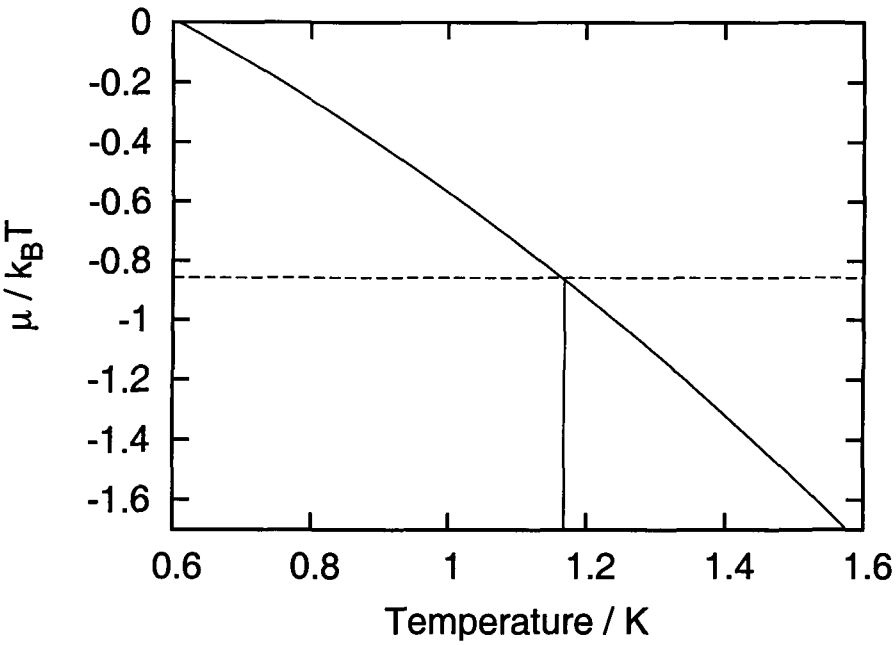

Figure 5.9: Chemical potential *vrs* Temperature at $x = 0.5$. The horizontal line is drawn at $\mu/k_BT = -0.857$.

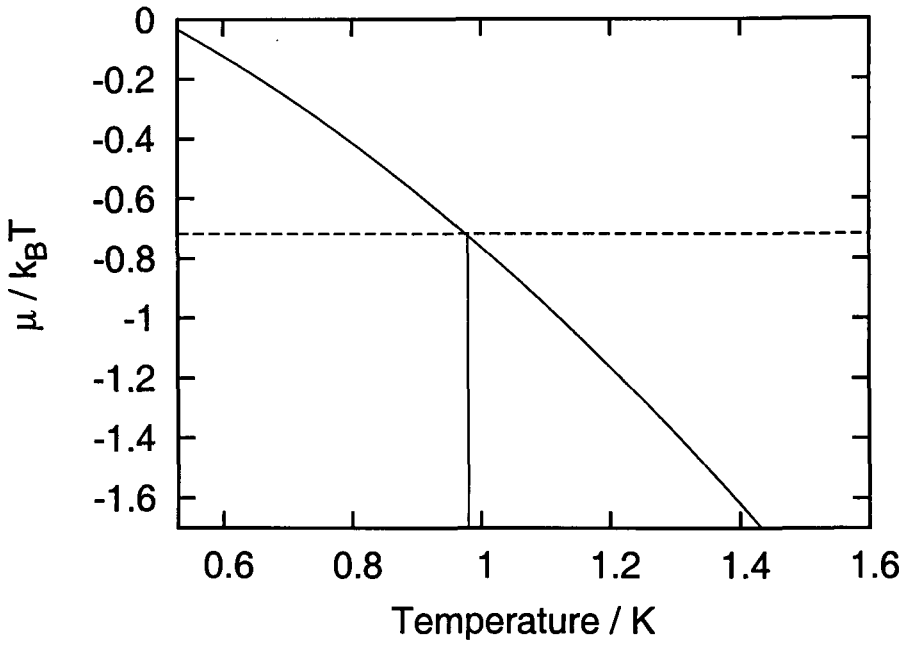

Figure 5.10: Chemical potential *vrs* Temperature at $x = 0.6$. The horizontal line is drawn at $\mu/k_BT = -0.717$.

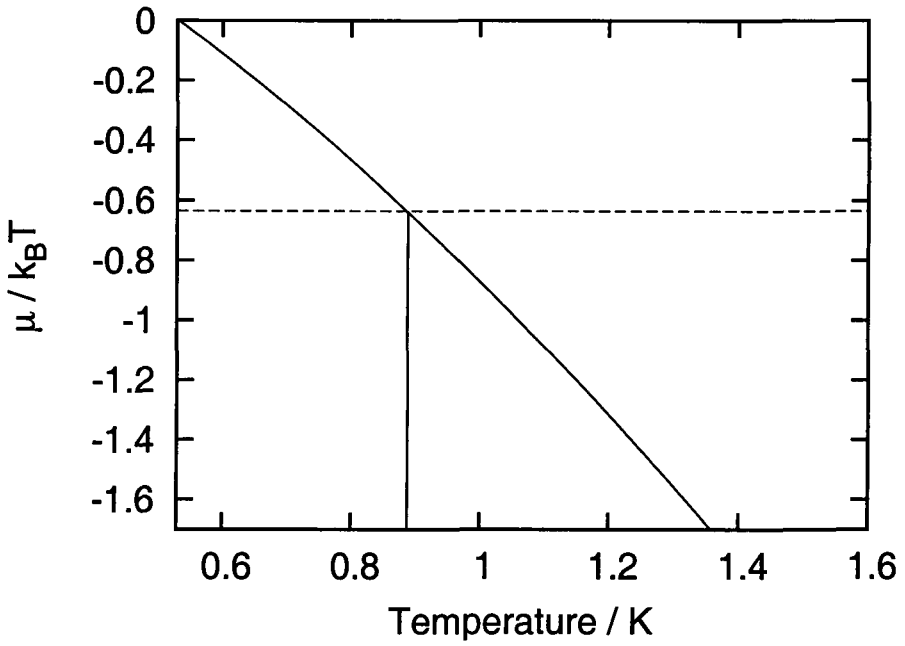

Figure 5.11: Chemical potential *vrs* Temperature at $x = 0.66$. The horizontal line is drawn at $\mu/k_BT = -0.635$.

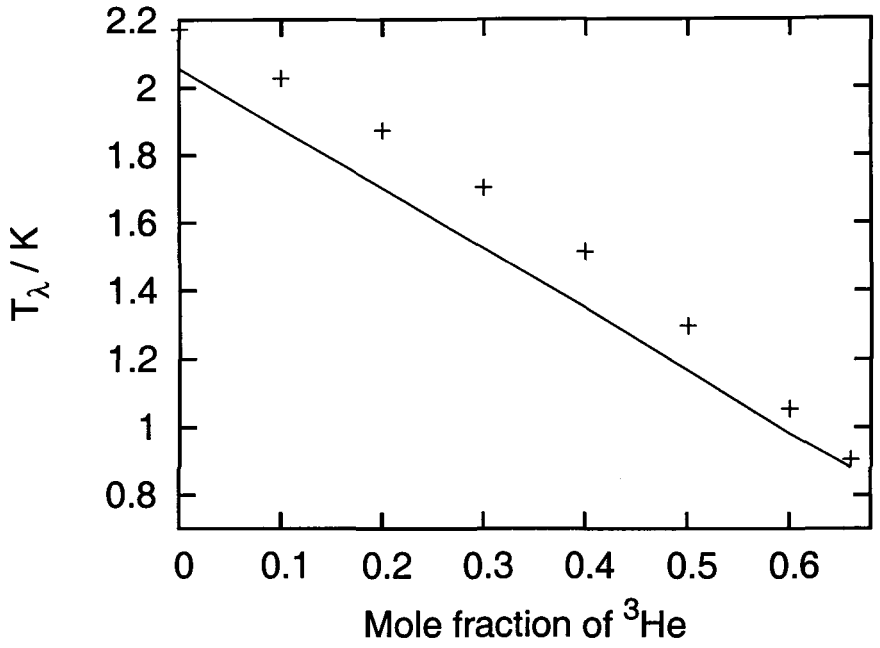

Figure 5.12: T_λ *vrs* Mole fraction of ^{3}He. The continuous line represents our calculated values while the crosses are experimental points [45]. The initial slope of our calculated values is found to be -1.99 (*cf.* Table 5.5).

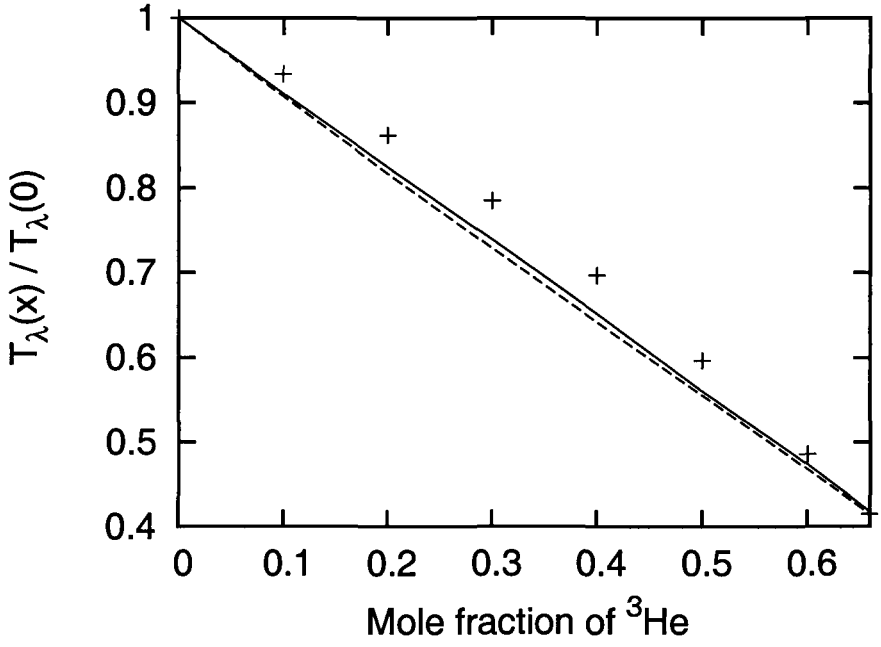

Figure 5.13: Ratios of T_λ at different concentrations. The continuous line represents our calculated points, the dotted line represents the points calculated using the formula given by Daunt and Heer [23], and the crosses are experimental points. The eperimental points are taken from Ref [45].

Bibliography

[1] H. K. Onnes, Leiden Comm. **119**; Proc. Roy. Acad. Sci. Amsterdam, **13**, 1093 (1911).

[2] H. K. Onnes and J. D. A. Boks, Leiden Comm. **170b**, 18 (1924).

[3] E. R. Grilly, E. F. Hammel and S. G. Sydoriak, Phys. Rev. **75**, 1103 (1949).

[4] W. H. Keesom and K. Clusius, Leiden Comm. **219e**; Proc. Roy. Acad. Sci. Amsterdam **35**, 307 (1932).

[5] F. London, Nature **141**, 643 (1938).

[6] J. Bardeen, L. N. Cooper, and J. R. Schrieffer, Phys. Rev. **106**, 162 (1957).

[7] D. D. Osheroff, R. C. Richardson and D. M. Lee, Phys. Rev. Lett. **28**, 885 (1972).

[8] L. I. Dana and H. K. Onnes, Leiden Commun. **190b** ; Proc. Roy. Acad. Sci. Amsterdam **29**, 1061 (1926).

[9] L. T. Aldrich and A. O. Nier, Phys. Rev. **70**, 983 (1946); Phys. Rev. **74**, 1590 (1950).

[10] J. Franck, Phys. Rev. **70**, 561 (1946).

[11] J. C. Wheatley, Am. J. Phys. **36**, 181 (1968).

[12] C. Enns and S. Hunklinger *Low Temperature Physics*, Springer Verlag, Berlin , (2005).

[13] G. Chaudhry and J. G. Brisson, J. Low Temp. Phys. **155**, 235 (2009).

[14] S. O. Diallo, J. V. Pearce, R. T. Azuah, F. Albergamo and H. R. Glyde, Phys. Rev. B **74**, 144503 (2006).

[15] T. A. Alvesalo, P. M. Berglund, S. T. Islander, G. R. Pickett and W. Zimmermann, Jr., Phys. Rev. A **4**, 2354 (1971).

[16] K. W. Taconis and R. de Bruyn Ouboter in *Progress in Low Temperature Physics*, (C. J. Gorter ed.) Vol. IV, North Holland, Amsterdam, (1964).

[17] D. O. Edwards and M. S. Pettersen, J. Low Temp. Phys. **87**, 473 (1992).

[18] R. B. Griffiths, Phys. Rev. Lett. **24**, 715 (1970).

[19] H. M. Guo, D. O. Edwards, R. E. Sarwinski and J. T. Tough, Phys. Rev. Lett. **27**, 1259 (1971).

[20] M. Iino, M. Suzuki, A. J. Ikushima, J. Low Temp. Phys. **61**, 155 (1985).

[21] M. Suzuki, Y. Okuda, A. J. Ikushima and M. Iino, Europhys. Lett. **5**, 333 (1988).

[22] G. K. Walters and W. M. Fairbank, Phys. Rev. **103**, 262 (1956).

[23] J. G. Daunt and C. V. Heer, Phys. Rev. **79**, 46 (1950).

[24] E. H. Graf, D. M. Lee and J. D. Reppy, Phys. Rev. Lett. **19**, 417 (1967).

[25] D. O. Edwards, D. F. Brewer, P. Seligman, M. Skertic and M. Yaqub, Phys. Rev. Lett. **15**, 773 (1965).

[26] D. O. Edwards and J. G. Daunt, Phys. Rev. **124**, 640 (1961).

[27] T. Guénault, Basic Superuids, Taylor and Francis, London, (2003).

[28] L. Pricaupenko and J. Treiner, Phys. Rev. Lett. **74**, 430 (1995).

[29] D.O.Edwards, E. M. Ifft, R. E. Sarwinski, Phys. Rev. **177**, 380 (1969);

[30] E. M. Ifft, D. O. Edwards, R. E. Sarwinski and M. M. Skertic, Phys. Rev. Lett. **19**, 831 (1967).

[31] B. M. Abraham, O. G .Brandt, Y. Eckstein and J. Munarin and G. Baym, Phys. Rev. **188**, 309 (1969).

[32] O. E. Vilches and J. C. Wheatley, Phys. Lett. **24A**, 440 (1967).

[33] R. I. Schermer, L. Passol and D. C. Rorer, Phys. Rev. **173**, 277 (1968).

[34] G. E. Watson, J. R. Reppy and R. C. Richardson, Phys. Rev. **188**, 384 (1969).

[35] S. Yorozu, M. Hiroi, H. Fukuyama, H. Akimoto, H. Ishimoto and S. Ogawa, Phys. Rev. B **45**, 12942 (1992).

[36] G. Goellner, R. Behringer and H. Meyer, J. Low Temp. Phys. **13**, 113 (1973).

[37] X. Qin, C. Howald and H. Meyer, J. Low Temp. Phys. **87**, 731 (1992).

[38] H. A. Kierstead, J. Low Temp. Phys. **24**, 497 (1976); J. Low Temp. Phys. **35**, 25 (1979).

[39] D. B. Roe, G. Rupperiner and H. Meyer, J. Low Temp. Phys. **27**, 747 (1977).

[40] G. Ahlers and D. S. Greywall, Phys. Rev. Lett. **29**, 849 (1972).

[41] E. H. Graf, D. M . Lee and J. D. Reppy, Phys. Rev. Lett. **19**, 417 (1967).

[42] B. M. Abraham, B. Weinstock and D. W. Osborne, Phys. Rev. **76**, 864 (1949).

[43] J. C. King and H. A. Fairbank, Bull. Am. Phys. Soc.(3) **28**, 65 (1953).

[44] S. D. Elliott and H. A. Fairbank in *Low Temperature Physics and Chemistry*, (J.R.Dillinger ed.) University of Wisconsin Press, Madison, Wisconsin (1958).

[45] S. G. Sydoriak and T. R. Roberts, Phys. Rev. **118**, 901 (1960).

[46] Z. Dokoupil, G. V. Soest, D. H. N. Wansink and D. G. Kapadnis, Physica **20**, 1181 (1954);

[47] Z. Dokoupil, D. G. Kapadnis, K. Sreeramamurty and K. W. Taconis, Physica **25**, 1369 (1959).

[48] R. de Bruyn Ouboter, K. W. Taconis, C. Le Pair and J. J. M. Beenakker, Physica **26**, 853 (1960).

[49] E. C. Kerr in *Low Temperature Physics and Chemistry*, (J.R.Dillinger ed.) University of Wisconsin Press, Madison, Wisconsin (1958).

[50] J. de Boer and C. J. Gorter, Physica **16**, 225 (1950).

[51] C. V. Heer and J. G. Daunt, Phys. Rev. **81**, 447 (1951).

[52] Z. Mikura, Prog. Theor. Phys. **11**, 25 (1954); Prog. Theor. Phys. **11**, 207 (1954); Prog. Theor. Phys. **11**, 244 (1954) and Prog. Theor. Phys. **11**, 503 (1954).

[53] O. K. Rice, Phys. Rev. **79**, 1024 (1950).

[54] I. Pomeranchuk, J. Exp. Theor. Phys. USSR, **20**, 1919 (1950).

[55] K. R. Atkins, in *Liquid Helium*, Cambridge University Press, London, (1959).

[56] J. J. M. Beenakker and K. W. Taconis in *Progress in Low Temperature Physics* Vol. I, (C. J. Gorter, ed.) North Holland, Amsterdam, (1955).

[57] R. K. Pathria, *Statistical Mechanics*, Pergamon Press, Oxford, (1976).

[58] A. L. Fetter and J. R. Walecka, *Quantum Theory of Many Particle Systems*, Dover Publications, (2003).

[59] J . Honerkamp *Statistical Physics, An Advanced Approach with Applications*, Second Edition, Springer–Verlag, New York, (2002).

[60] J. W. Wilks, *The Properties of Liquid and Solid Helium*, Clarendon Press, Oxford, (1967).

[61] J. de Boer and C. J. Gorter, Phys. Rev. **77**, 569 (1950); Physica **16**, 225, (1950).

[62] O. K. Rice, Phys. Rev. **76**, 1701 (1949); Phys. Rev. **77**, 142 (1950);

O. K. Rice and O. G. Engel, Phys. Rev. **78** 183 (1950); O. G. Engel and O. K. Rice, Phys. Rev. **77**, 55 (1950).

[63] J. W. Stout, Phys. Rev. **76**, 864 (1949).

[64] S. Koide and T. Usui, Prog. Theor. Phys. **6**, 622 (1951).

[65] K. W. Taconis, J. J. M. Beenakker, L. T. Aldrich and A. O. C. Nier, Physica **15**, 733 (1949).

[66] K. W. Taconis, J. J. Benakker, L. T. Aldrich and A. O. Nier, Phys. Rev. **75**, 1966 (1949).

[67] A. Harasima, J. Phys. Soc. Japan **11**, 25 (1954).

[68] J. G. Daunt, T. P. Seng and C. V. Heer, Phys. Rev. **86**, 911 (1952).

[69] M. Toda and A. Isihara, Prog. Theor. Phys. **6**, 480 (1951).

[70] I. Pomeranchuk, J. Exp. Theor. Phys. USSR **19**, 42 (1949).

[71] J. de Boer and C. J. Gorter, Physica **18**, 565 (1952); Leiden Comm. Suppl. **104e**.

[72] N. Bogoliubov, J. Phys. (Moscow) **2**, 23 (1947).

[73] T. D. Lee and C. N. Yang, Phys. Rev. **105**, 1119 (1957) ; Phys. Rev. **112**, 1419 (1958).

[74] E. G. D. Cohen and J. M. J. van Leeuwen, Physica **26**, 1171 (1960).

[75] J. M. J. van Leeuwen and E. G. D. Cohen, Physica **27**, 1157 (1961).

[76] J. C. Owen, Phys. Rev. Lett. **47**, 586 (1981).

[77] M. Saarela in *Recent Progress in Many Body Theory*, (A. Avishai, ed.) Plenum, New York, (1990).

[78] A. Fabrocini, S. Fantoni, S. Rosati and A. Polls, Phys. Rev. B **33**, 6057 (1986).

[79] W. Hsu, D. Pines and C. H. Aldrich, Phys. Rev. B **32**, 7179 (1985).

[80] C. A. Swenson, Phys. Rev. **79**, 626 (1950).

Chapter 6

Electrical Properties of Liquid Helium-4

ABSTRACT *: Experimentally observed micro-wave absorption in superfluid helium-4 in the presence of external electric field showing Stark Effect at the roton frequency has been critically analyzed. While our conventional microscopic understanding of the superfluid state of a system of interacting bosons (SIB) such as liquid helium-4 fails to explain the results, Macro-orbital theory gives their good account. Further, our analysis reveals that the observation of Stark Effect provides another firm foundation for the validity of Macro-orbital theory.*

6.1 Introduction

Even though liquid helium-4 (LHe-4) has been the subject of extensive research [1–5] for the last so many years for its unique behavior, such as superfluidity and the related properties which arise when the quantum nature of atoms dominates its behavior at macroscopic scale at low temperatures, the electrical properties of LHe-4 in the superfluid state, which are of significant interest, have been insufficiently investigated. Since helium atom is a spherically symmetric system, it possess no permanent dipole moment [4]. This may be the reason for the modest interest in the electrical properties of LHe-4. However, recent investigations revealed new and unexpected results.

A number of experimental studies of LHe-4 performed over the last fifteen years concluded its several interesting new aspects such as loss of viscosity for the rotation of the molecules embedded in microscopic clusters and droplets [6–9], absorption of microwaves at roton frequency in the presence and absence of external electric field [10–18], *etc.*, and all these seem to challenge the conventional microscopic understanding of an SIB [3, 19], based on the presumed existence of $p = 0$ condensate [4] which has been considered to be the origin of:
(a) superfluidity and the related properties of its low temperature phase (He II) for the last eight decades and
(b) the origin of superfluidity in trapped dilute Bose gases [1] for the last fifteen years.

However, Jain [20] pointed out that *the law of nature, which demands the ground state* (G-state) *of a physical system to have minimum energy, forbids the existence* $p = 0$ *condensate in the superfluid phase of an SIB.* This conclusion is found to have unequivocal ex-

perimental support [21,22] from the physical reality of the existence of electron bubble in LHe-4 [23] and the experimentally observed spectroscopy of embedded molecules [6–9].

In this Chapter we analyze the Stark effect of roton transition in superfluid ^{4}He observed in its microwave absorption by Rybalko and coworkers [10–18] to identify another experimental support for this conclusion.

6.2 Experimental Observations

In 2004, Rybalko [10] reported the results of the first experiments intended to search for and study the electric response induced by second sound waves in superfluid ^{4}He. He discovered that a standing half-wave of a wave of second sound in He II induces a potential difference. In this experiments, standing waves of first and second sounds were excited in a resonator filled with LHe-4 . When a second sound wave was excited, oscillations of the potential difference ΔU were observed, so that

$$\Delta T/\Delta U \cong \frac{2e}{k_B} \approx 2.3 \times 10^4 \text{ K/V}, \tag{6.2.1}$$

where e is the charge of the electron and ΔT is the temperature difference produced by the second sound between the plates of the capacitor. This ratio does not depend on temperature and is a constant. The effect was observed only below the superfluid transition temperature (λ transition) and was not observed with excitation of first sound, even for oscillations with large amplitude. He supposed that the effect observed in these experiments was due to the bulk polarization of He II and its appearance was due to the relative motion of the normal and superfluid components that occurs in the propagation of second sound. A reverse effect (*i.e*, generation of second

sound wave by an ac electric field) was also observed.

To confirm that the effect observed in Ref [10] was entirely due to the relative motion of the normal and superfluid components and not to temperature oscillations (which is a characteristic feature of second sound), subsequent experiment [11] was performed in which torsion oscillator method was used to generate relative motion of the superfluid and normal components without changing the temperature nor the normal and superfluid densities, thereby avoiding the problems associated with the thermal method of exciting the relative motion. In this experiment it was found that the rotational oscillations of the vessel containing He II produced an observable alternating potential difference between the walls of the vessel and the axial electrode. The potential difference was found to be proportional to the square of the lineal velocity of the walls of the oscillator. The effect was observed for bulk helium in the cylinder as well as for a saturated and an unsaturated film covering the walls of the oscillator. As observed in Ref [10], the potential difference was observed only below the λ transition. These experiments established that the excitation of macroscopic fluxes in He II by two different methods is accompanied by the appearance of electric displacement in the volume of the helium-filled cell.

The experimental result was clearly unexpected, since LHe-4 consists of electrically neutral and spherically symmetrical atoms.

The same group went on to investigate the interaction of microwaves with superfluid flow in He II. They observed [12–14] resonance absorption and emission of microwave radiation in superfluid ^{4}He at a frequency f corresponding to the roton minimum of the energy spectrum, $\varepsilon = \Delta/\hbar$. For $\Delta = 8.65$ K which corresponds to a temperature of the order of 1.4 K, $f = \omega/2\pi \approx 180.3$ GHz. The resonance frequency was found to decrease with the increase

in temperature, and its temperature dependence agrees well with the temperature dependence of the roton gap obtained from neutron experiments [24, 25]. This observation led them to conclude that the observed resonance line was due to the creation of a roton. In these experiments, they observed a very narrow line of absorption and radiation of electromagnetic waves at the roton frequency, in contradiction to the results of experiments on inelastic neutron scattering [24,26] and Raman scattering of light [27,28] in LHe-4, where only wide roton lines were found. Also, at this frequency the photon momentum $p_{pt} = 3.8 \times 10^3$ cm^{-1} is several orders of magnitude smaller than that of the roton, $p_r = 1.9 \times 10^8$ cm^{-1}, the question of how the law of conservation momentum is obeyed in this process poses difficulty. To address this apparent violation of the law of conservation of momentum, further experiments [15–18] were carried out and the results carefully compared with neutron scattering experiments. Based on their experimental results, they suggested that one should write the conservation laws taking into consideration a possible transmission of energy and momentum to a superfluid subsystem, so that

$$\begin{aligned} p_{pt} &= p_r + p_s \qquad \text{and} \\ \epsilon_{pt} &= \Delta + \epsilon_s \end{aligned} \tag{6.2.2}$$

where $\epsilon_{pt} = \hbar\omega$ and p_{pt} are the energy and momentum of photon; Δ and p_r are the energy and momentum of roton and ϵ_s, p_s are energy and momentum transferred to superfluid component of the fluid respectively. They estimated from their results that $\epsilon_{pt} \approx \Delta, p_s \approx -p_r$ and $\epsilon_s \approx 0$. They pointed out that this condition can be satisfied in He II by assuming that a superfluid flow $j_s = \rho_s v_s$ appears, where ρ_s and v_s are the density of the superfluid component and the superfluid velocity. Then the total momentum transferred of the superfluid component is given by $p_s = j_s V$, where V is the volume of liquid.

Since V and the mass M of liquid are macroscopic quantities, it is evident that the kinetic energy of the superfluid flow $E = p_s^2/2M$ is very small, and a superfluid flow can take up a finite momentum, practically without taking an energy from photon or roton. This mechanism is analogous to the Mössbauer Effect, where a photon transfers momentum but not energy to the crystal as a whole.

In another fine experiment [18], where they investigated the interaction between electromagnetic microwaves and superfluid ^{4}He in a stationary electric field, they found that the narrow resonance absorption line at the roton frequency is split in the electric field into two symmetric lines. In addition, the splitting magnitude increases almost linearly with the electric field, indicating the presence of linear Stark Effect. They concluded that the results of their investigations suggests orientational polarization.

In order to estimate the magnitude of polarization, they noted that the electric field dependence of the resonance frequency allowing for the splitting Δf can be approximated by the linear dependence

$$f = f_o + kE_{dc}, \tag{6.2.3}$$

where $f_o = 1.803 \times 10^{11}$ Hz and $k = 42.65$ Hz $\cdot$ cm/kV. Then, the additional energy of the system with the electric dipole moment $\mathbf{P}$ in the electric field $\mathbf{E}$ is given by

$$W = -(\mathbf{P}.\mathbf{E}) \tag{6.2.4}$$

Expressing the energy W in terms of splitting as

$$W = h\Delta f \tag{6.2.5}$$

They estimated that the dipole moment of the system in the electric

field is

$$P = \frac{h\Delta f}{E} \cong 3 \times 10^{-34}\ \mathrm{C \cdot m} \tag{6.2.6}$$

However, they were not able to specify the quantum system to which this dipole moment belongs.

Since a dipole moment is usually associated with polarizability of atoms, they estimated that the atoms have induced dipole moment

$$\mathbf{p}_{ind} = \alpha \mathbf{E} \tag{6.2.7}$$

where α is the atomic polarizability.

Taking $\alpha = 0.1232\ \mathrm{cm^3/mol} = 2.1 \times 10^{-41}\ \mathrm{A \cdot m^2 \cdot s/V}$ for helium at $T = 1.5\ \mathrm{K}$, they found that the potential energy of such induced dipole in the homogeneous field $E = 4 \times 10^5\ \mathrm{V/m}$ is given by

$$W = \frac{\alpha E^2}{2} = 1.6 \times 10^{-30} \mathrm{W \cdot s} \tag{6.2.8}$$

Further, their estimated shift of the spectral line frequency, given by $\delta f = W/h = 2.55$ kHz was almost two orders of magnitude smaller than the actual shift observed in the experiment (340 kHz). Hence, the induced polarization observed in the experiment (the formation of an induced dipole in the system) is inadequate to explain the effect observed.

The electric field E in eqn (6.2.7) stands for the local electric field at the site of the atom, $E = E_{dc}$ is valid only for an isolated atom. In LHe-4 the atoms experience an additional internal field E_{in} excited by the surrounding dipoles. They noted that E_{in} is much larger than the applied field.

In order to verify their estimated value of the dipole moment, they calculated the same quantity using other experimental data. Using Clausius–Mossotti equations and the data in [29, 30], they

found that $P = 10^{-33}\,\mathrm{C}\cdot\mathrm{m}$, which is quite close to the value estimated by them. Again, using the data in [10] they found that $P = 3 \times 10^{-34}\,\mathrm{C}\cdot\mathrm{m}$, which practically coincides with their result.

6.3 Theoretical Studies

The new extraordinary effects observed in He II aroused great interest and a number of theoretical studies aiming to explain its mechanism have been undertaken. Kosevich [31, 32] was the first theoretician who tried to explain these new experimental results. His initiative led to the publication of several theoretical works [31–45].

Kosevich proposed a phenomenological model to explain the electric activity in He II. He sugggested that the superfluid state is an ordered state of isotropic quadrupole moment of the atoms in the superfluid state, which shows no electric activity in an equilibrium liquid but can manifest electrical properties in the presence of a non-uniform superfluid flow. He however, did not propose any microscopic model of such ordering, and this approach left open the question of the physical nature of the observed effects.

Melnikovsky [33] suggested the possibility of inertial polarization of helium atoms as a result of accelaration, which is analogous to Stewart–Tolman effect in metals [46]. He derived general expressions for the gravitational or inertial polarizability vector, from which one can obtain an expression for the ratio $\Delta T/\Delta U$:

$$\frac{\Delta T}{\Delta U} = \frac{12e}{(\epsilon - 1)mC(T)} = \frac{2e}{k_B}\frac{6}{(\epsilon - 1)f(T)} \tag{6.3.1}$$

Here $C(T)$ stands for the specific heat capacity per unit mass in the approximation $C_p(T) \cong C_v(T) \cong C(T)$, and ϵ represents the dielectric permittivity of LHe-4, and $f(T)$ is a dimensionless

quantity. Using the data of [47,48] on the heat capacity of He II, it is found that the the calculated value of ΔU is two to three orders of magnitude smaller than the value observed in the experiment. Also, it is strongly temperature dependent, in contradiction to the experimental observation.

Natsik [34, 35] suggested that the electric displacement appeared on account of the same inertial effect as proposed by Melnikovsky [33] but under the influence of a centrifugal force arising in the field of a non-uniform azimuthal rotational velocity of the superfluid component around the axis of a quantum vortex in He II. Using the standard results of the hydrodynamics of a superfluid [49], he obtained the expression for the spontaneous electric polarization of a quantum vortex. He estimated [34] that the maximum electric field close to the vortex line is approximately 300 V/cm. However, for a macroscopic potential difference to appear across the electrodes in the experiments [10, 11], special conditions must be imposed on the concentration and vortex configuration; these conditions were not specified by Natsik. Further, in [11] it was found that the electric polarization in bulk He II fell off sharply at normal component velocities above the threshold of vortex creation.

Pashitskii and Ryabchenko [36] then showed that the ratio of the amplitude ΔU of the electric displacement in a second sound wave to the amplitude ΔT of the temperature oscillations in the wave is proportional to the entropy of He II. From their analysis, they noted that the amplitude ratio of the temperature and potential oscillations in the second sound wave obtained by Rybalko [10] can be used to determine the entropy of He II. For He II, they obtained the equation

$$\frac{1}{2}\left(\frac{1}{\rho}\nabla p - \frac{s}{m}\nabla T\right) = -\frac{2e}{m}\nabla\varphi \qquad (6.3.2)$$

where ρ is the density of He II, p, T and φ are respectively the pressure, temperature and electric potential, m is the mass of a ^{4}He atom, and s is the entropy per atom (with $s = mS/\rho$, where S is the entropy per unit volume). Comparing eqn (6.3.2) with eqn (6.2.1), they concluded that the entropy s of He II contains an additional contribution which is independent of temperature T, $s \approx 2k_B$, which was identified with s_s, the entropy per atom of the superfluid component. The appearance of electrical activity upon excitation of induced oscillations of the normal component velocity [11] was explained qualitatively by introducing a correction to the chemical potential which was quadratic in the velocity difference of the superfluid and normal components of He II.

Equation (6.3.2) was derived using Landau's two-fluid hydrodynamics. Loktev and Tomchenko [37] pointed out that the result $s_s \approx 2k_B$ contradicts the two-fluid hydrodynamics, which is derived on the assumption that $s_s = 0$. Moreover, they noted that the two different ways in which eqn (6.3.2) was derived, were both debatable. In fact, there was quantitative disagreement between the theoretical values and experimental results. The theoretical value of ΔU was found to be three to four orders of magnitude smaller than the observed value.

Loktev and Tomchenko [37] then showed using the standard principles of quantum mechanics that because of interatomic interactions with nearest neighbors, a fluctuating dipole moment with average modulus $\bar{d} \simeq 2e\delta$ where $\delta = 2.6 \times 10^{-4}$ Å, is induced in each He II atom. The experimental value of $\Delta U \approx k_B \Delta T/2e$ could be explained assuming that vortex rings in He II possess a dipole moment $d_{vr} \sim 10\bar{d}$, and the polarization of He II is due to the pressence of directed flux rings in a standing second sound half-wave. Considering the boundary conditions, they argued that the potential difference

ΔU depends on the dimensions of the resonator. Since such dependence was not observed in [10], they suggested that the effect observed in the experiment could be due to not volume but instead, the surface properties of He II or to the electrical properties of the materials used to measure ΔU.

Gutliansky [40] proposed a phenomenological model based on the existence of an adsorption potential well. Using many assumptions, he derived the expression for ΔU. This model could explain the experimental observation that an electric voltage is generated in the experiment with second sound and that the ratio $\Delta T/\Delta U$ is independent of temperature [10]. Also, it could explain the dependence of the observed voltage on the square of the velocity of the wall of the vessel [11]. However, Tomchenko [41] argued that only several layers of helium atoms are strongly polarized, and the electric signal from them may be too weak (which was not calculated in [40]) to account for the observed effect.

Shevchenko and Rukin [42] then attempted to explain the observed effect [10, 11] by using a model based on electron–hole gas in which the pair size is much smaller than the distance between pairs. Using the ground state wave function of electon–hole gas proposed by Keldysh [50], they performed microscopic calculation of the polarization of quantum vortices, in the presence and absence of a magnetic field. They found that in the presence of a magnetic field, vortices acquire additional polarization which results in the appearance of a quantized charge in a vortex core. They showed that the van der Waals interactions of a superfluid system with a solid surface gives rise to polarization near the surface. However, this approach was criticised by Tomchenko [41] who insisted that the approach could be used, at the most, only qualitatively because a ^{4}He atom possesses a more complicated structure compared with an electron–hole pair,

and the mass of the atomic nucleus is much larger than the electron mass.

In another work, Tomchenko [39] proposed a mechanism called *tidal mechanism.* According to this model, even though the free atoms of ^{4}He do not create electric field far from themselves as they have zero charge and zero dipole and multipole moments, a ^{4}He atom, surrounded on all sides by other atoms, can acquire a dipole moment by tidal mechanism, by which a dipole moment is induced by the interaction with neighboring atoms. He showed that, in the presence of a temperature or density gradient in He II, the originally chaotically oriented dipole moments of the atoms become partially ordered, leading to volume polarization of He II. This mechanism predicts a weak electric signal which is one to three orders of magnitude lower than the observed signal and a strong dependence of the signal on the size of a resonator and the temperature is indicated, which was not detected in the experiment.

Mineev [43] developed a theory of thermo-electric phenomena in superfluid ^{4}He based on the idea of atomic electron shell deformation. According to this model, the deformation of the shell is caused by forces acting on the electron shell of a given atom from the side of the surrounding atoms. He argued that second sound waves in superfluid ^{4}He generated polarization of the liquid induced by the relative accelerated motion of the superfluid and the normal component. He obtained

$$\frac{\Delta T}{\Delta U} \approx 0.55 \times 10^4 \text{ K/V} \tag{6.3.3}$$

which is about four times smaller than the experimental value.

Pashitskii and Gurin [44] then tried to explain the observed electric activity of superfluid ^{4}He [10] using a phenomenological mechanism of inertial polarization of atoms in a dielectric, in analogy with

Stewart–Tolman effect [46]. They pointed out that even though the same approach had been followed by Melnikovsky [33], he had made several unjustified assumptions in calculating He II polarization in a standing second sound wave and the corresponding potential difference ΔU. To refine Melnikovsky's work, they argued that a local linear relation between the electric induction $\mathbf{D}(t)$ and the electric field $\mathbf{E}(t)$ holds, *i.e.*,

$$\mathbf{D}(t) = \epsilon \mathbf{E}(t) \tag{6.3.4}$$

where ϵ represents the static dielectric constant of LHe-4. In addition, the polarization and the electric field are related as

$$\mathbf{P}(t) = \kappa \mathbf{E}(t) \tag{6.3.5}$$

where κ is the macroscopic polarizability of ^{4}He. Using several phenomenological assumptions, they showed that both the electric activity of He II in the second sound wave and the absence of an electric signal in the first sound wave could be explained in accordance with the experimental data [10, 11].

While the work in Refs. [43, 44] seem to agree closely with the experimental observation, Tomchenko [45] in a recent paper disagreed with the method of derivation of electric field in the two works. He showed that eqns (6.3.4) and (6.3.5) which were used to determine the electric field in Ref. [44], are valid only in the case where a dielectric is polarized by an external field, while there was no external field present in the experiment. He also pointed out that the authors of [43, 44] considered polarization is related to a motion. This has no meaning since spontaneous polarization is caused by processes in a fluid and is not connected with an external field. He also insisted that the electric field $\mathbf{E}$ was determined inaccurately in Refs. [43, 44]

Tomchenko [45] then attempted to explain the electric activity following the idea of one-directional polarization of ^{4}He atoms located at the electrode surface, first proposed by Gutlyanskii [40]. He presented a model that he called *approximate model.* He calculated the electric signal U arising at the electrode in the presence of a standing half-wave of first or second sound in He II. While the properties of the signal for second sound correspond to the experiment regarding the amplitude (approximately) and its independence on the resonator size and the temperature, he pointed out that the properties of He II near the metal surface are not clear and could be described only approximately. His predictions regarding the wave of first sound are yet to be observed experimentally. He also predicts the formula for the dependence of the signal on the coordinate Z along a resonator and the strong growth of the signal for a ^{3}He–^{4}He mixture. In addition, his model predicts dependence of the signal on the nature of electrode used to detect the signal.

Thus, one can easily see that in the theoretical models under discussion, a number of difficulties and contradictions arise in explaining the experimental results of [10] and [11].

6.4 Our analysis of Experimental Results

In what follows from Section 6.2, we observe that [12–17]

1. Microwave absorption in LHe-4 is observed as a sharp peak at the frequency corresponding to the energy of a roton minimum, - a well known quantum quasi-particle excitation, which increases smoothly from the value ≈ 5.2 K ($\cong 125$ GHz) at $T = T_\lambda$ to the value ≈ 8.65 K ($\cong 180.3$ GHz) at T=1.4 K with its width decreasing from ≈ 400 kHz at 2.2 K to ≈ 40 kHz at 1.6 K.

2. Under the effect of external electric field E_{ex}, the said peak is found to split into two Stark components separated by

$$\Delta f = pE_{ex}/h \tag{6.4.1}$$

showing linear dependence on E_{ex} with $p \approx 2.8 \times 10^{-34}$ C·m being the experimental value of electric dipole moment, presumably, of ^{4}He atom and h, the Planck constant.

3. The fact that p in the relation (6.4.1) remains constant for the entire range of external electric field $E_{ex} = 0$ to 4×10^5 V/m, implies that: (i) E_{ex} has insignificant effect in inducing p in spherically symmetric ^{4}He atom, (ii) it is the internal electric field E_{in} seen by a ^{4}He atom at its sight in superfluid ^{4}He which induces p and (iii) the strength of E_{in} is much larger than the maximum, $E_{ex} \approx 4 \times 10^5$ V/m, used in the experiment.

4. Using the equation

$$p = \alpha E_{in} \tag{6.4.2}$$

where α is the atomic polarizability of helium gas, with the value $\alpha = 0.1232$ cm^3/mol $= 2.1 \times 10^{-41}$ C·m^2/V, we find

$$E_{in} \approx 1.3 \times 10^7 \text{ V/m} \tag{6.4.3}$$

We note that the question about the origin of such a strong E_{in} at the site of each ^{4}He atom finds no answer from our conventional microscopic understanding of a SIB [1,3,4,20] like LHe-4. In what follows, even in the superfluid state of LHe-4, different number of ^{4}He have different momenta; about $\approx$ 10% having zero momentum ($k = 0$) constitute what is known as Bose Einstein condensate (BEC) or $p(= \hbar k) = 0$ condensate and the rest, having non-zero momenta, k_1, k_2, k_3, *etc.* (expressed in wave number), constitute the non-condensate component. These particles, obviously, have rela-

tive motions and inter-particle collisions. The situation is depicted in Fig. 6.1(A) and (B) for its better perception. It is natural that the said collisions are bound to keep changing the position(s) of atoms and the direction(s) of their dipoles and no atom in such a state of the system can be expected to experience an electric field at its site.

In variance with our conventional understanding, a microscopic theory of a SIB like LHe-4 recently developed by Jain [5] not only ensures that the G-state has minimum possible energy but also concludes that all the N atoms in the superfluid state of an SIB have identically equal energy ($\varepsilon_0 = h^2/8md^2$) and corresponding momentum ($h/2d$). The situation is depicted in Fig. 6.1(C) and (D) to distinguish it from that concluded by conventional theory [3, 20]. We note that all atoms in this picture also constitute a *close packed* arrangement of their representative wave packets and this arrangement assumes desired stability against its thermal motions and small energy perturbations such as its flow with a velocity below certain critical value because they acquire a kind of collective binding for which the entire system behaves like a single macroscopic molecule. This arrangement allows particles to have collective motions, such as phonons, rotons, *etc.* (representing the thermal excitations of the system), and to move coherently in order of their locations; they, obviously, do not have relative motions and collisions. Naturally, if ^{4}He atoms happen to have any electric dipole moment (possibly for the deformation of their electron density due to their mutual closeness), this arrangement of localized particles can allow their dipoles to align in a single direction, particularly, when they are subjected to a E_{ex} of even of 0^+ (slightly above zero stength). Unidirectional alignment of dipoles may also be possible in the absence of any E_{ex}, may be in the entire sample or over the scales of domains of the size of coherence length which is estimated to be of the order of 100 Å [51]. The collective binding of atoms with their close packed

arrangement can be expected to provide stability to such alignments of dipoles against the thermal motions of the system. The fact that the thermal motions representing a kind of a gas of non-interacting quasi-particles, representing what Landau identified as normal fluid component [52], move in the back-ground of the close packed arrangement of ^{4}He atoms (free to move coherently in order of their locations), representing the superfluid component, can also be expected to help the stability of the dipole alignment.

Here it is interesting to note that: (i) Rybalko *et al* [12], on the basis of their experimental observations, believe that the relative motion of the normal and superfluid components is a result of internal electromagnetic forces related to the *macroscopic quantum ordering* the system, and (ii) Examining the possible reasons of the effect, Tomchenko [39] concludes that all atoms in He II, acquiring small fluctuating dipole and multipole moments (oriented chaotically on the average) become partially *ordered* in the presence of a temperature or density gradient leading to volume polarization of He II. In other words, the origin of the effect is believed to have strong relation with ordering of atoms in terms of their positions and the direction of dipoles. Since the desired order is an obvious conclusion of our non-conventional theory [5] (not of conventional theory based on the presumed existence of $p = 0$ condensate) [1, 3, 4, 20] which clearly excludes the possibility of the existence of $p = 0$ condensate, the details of the experimentally observed absorption not only support Jain's theory [5] but also refutes the existence of $p = 0$ condensate in superfluid ^{4}He.

In what follows, one can use Feynman's relation [53]

$$E_{in} = \frac{p}{\epsilon_0}\frac{0.3812}{d^3} \tag{6.4.4}$$

developed for the electric field at the site of a dipole in an orderly simple cubic arrangement of a very large number of dipoles oriented in a single direction. In (6.4.4) $\epsilon_0 = 8.854 \times 10^{-12}$ F/m represents the dielectric permitivity of vacuum and d is identically equal to inter-dipole (atomic) distance which has a value of 3.57×10^{-10} m for superfluid ^{4}He. Using these values with $p = 2.8 \times 10^{-34}$ C$\cdot$m, we have $E_{in} = 2.6 \times 10^5$ V/m which, however, is about two order of magnitude smaller than $E_{in} \approx 10^7$ V/m (from (6.4.3)) needed for producing $p = 10^{-34}$ C$\cdot$m. It appears that this discrepancy may arise from the following possibilities:

(i) Feynman's relation (6.4.4) assumes an arrangement of classically fixed dipoles with SC structure while each dipole in superfluid ^{4}He has position uncertainty of the order of d itself and $1/d^3$ in (6.4.4) needs to be replaced by $< 1/r^3 >$ (quantum mechanical average of $1/r^3$ where r is the possible distance between two dipoles). However, this replacement may increase E_{in} by 10^2 which is possible only if the relative distance r is shorter than d by factor of $\approx \sqrt[3]{100} \approx 4.65$ with an extreme assumption that dipoles have nearly 100% probability to have $d/4.6$ distance. Due to the hard core nature of the particles, no two ^{4}He atoms can have a distance shorter than 2.6 Å which represents approximately the hard core diameter of an atom. This implies that the maximum possible increase can be by a factor of about $[3.57/2.6]^3 \approx 2.5$, which means that the said replacement is not expected to provide the desired change.

(ii) Particles in the experimental resonant absorption cell interact more strongly with metallic surface in comparison with their inter-atomic interaction and for this reason, atoms in contact with the surface get strongly polarised even in the absence of the applied electric field and it is this polarization which creates an additional

electric field near the walls of cell. However, this implies that absorption of microwave photons takes place in atoms located near the walls of the cell and interestingly this is consistent with the reasons for the conservation of momentum as discussed in [12]; it may be mentioned here that the roton mode of motion of superfluid ^{4}He has momentum $Q \approx 1.93$ Å^{-1} while the microwave photon nearly has zero momentum. We note that the Raman scattering, observed at twice the energy of roton, is believed to create two rotons of equal and opposite Q for the reasons of momentum conservation in the process [12]. As suggested rightly, the process of single photon absorption will not conserve Q unless the process occurs near the walls of the cell which takes away the recoil momentum [12].

(iii) The roton represents a collective excitation of about 100 atoms having dipole moment oriented orderly in one direction with total dipole moment equal to 2.8×10^{-34} C $\cdot$ m for which the per particle dipole moment gets reduced to 2.8×10^{-36} C $\cdot$ m and the neccessary E_{in} to the order of 10^5 V/m.

6.5 Conclusions

Analyzing the experimental observation of Stark effect of the roton transition in He II, we draw the following conclusions:

1. The observation does not support the random distribution of particles in normal space with random values of momenta (including about 10% ^{4}He atoms with $p = 0$ which constitute $p = 0$ condensate) leading to their relative motions and mutual collisions revealed by conventional microscopic theory of a system like LHe-4 [3, 19].

2. Alternatively, the observation supports an orderly arrangement of particles in normal space which is made possible by the fact that each particle manifesting itself as a wave packet occupies maximum possible space when it falls to its lowest possible energy and in this process all particles in the superfluid state constitute a close packed arrangement of their wave packets as concluded by [5] and supported by [20]. This arrangement provides clear possibility for the electric dipoles of ^{4}He atoms to have their orientation along a single direction may be in the entire sample or in a domain of the size of coherence length which is found to be of the order of 100 Å, which means a cluster of a minimum of about 2–3 thousand atoms.

This helps in identifying a few possible situations [(i)–(iii), as listed above] which could provide a viable explanation of the observation of the effect. It is hoped that a future course of study of these possibilities supported by desired theoretical analysis would identify the most viable situation responsible for the observation.

In what follows, one should not be surprised by either of these conclusions because the momentum distribution of particles over the single particle states of different momenta in the G-state of LHe-4 type system, as concluded by conventional theory [3, 19], does not agree [20] with the fact that the G-state of a physical system has to have minimum possible energy. On the contrary, the close packed arrangement of the wave packets of ^{4}He atoms as concluded in [5] is found to have lowest possible energy. Thus the observation of Stark effect not only supports non-conventional theory of LHe-4 type systems but also refutes the existence of $p = 0$ condensate in superfluid ^{4}He.

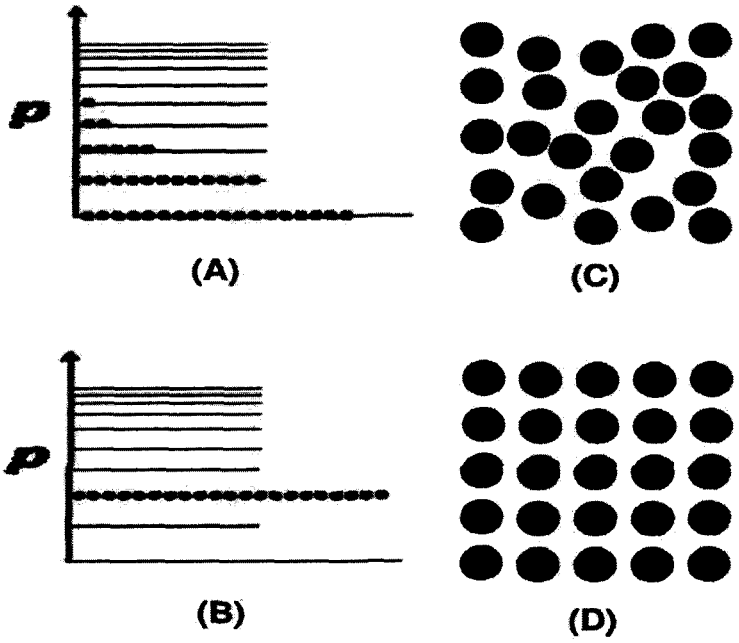

Figure 6.1: Schematic of momentum distribution of N bosons in their ground state in accordance with : (A) CMT based on Bogoliubov model [19] and (B) NCMT concluded in [5]; corresponding locations in normal space are depicted in (C) and (D), respectively.

Bibliography

[1] F. Dalfovo, S. Giorgini, L. P. Pitaevskii, and S. Stringari, Rev. Mod. Phys. **71**, 463 (1999); arxiv/Cond-mat/9806038.

[2] E. A. Pashitskii, S. V. Mashkevich, and S. I. Vil'chinskii, Phys. Rev. Lett. **89**, 075301 (2002).

[3] J. O. Anderson, Rev. Mod. Phys. **76**, 599 (2004).

[4] C. Enss and S. Hunklinger, *Low Temperature Physics*, Springer Verlag, Berlin, (2005).

[5] (a) Y. S. Jain, Ind. J. Phys. **79**, 1009 (2005); (b) Y. S. Jain, Am. J. Cond. Mat. Phys **2**, 32 (2012).

[6] J. P. Toennies and A. F. Vilesov, Ann. Rev. Phys. Chem. **49**, 1 (1998).

[7] S. Grebenev, J. P. Toennies and A. F. Vilesov, Science **279**, 2083 (1998).

[8] A. R. W. McKellar, J. Chem. Phys. **128**, 044308 (2008).

[9] S. Dey, J. P. Gewali, A. K. Jha, L. Chhangte and Y. S. Jain, Indian J. Physics **85**, 1309 (2011).

[10] A. S. Rybalko, Low Temp. Phys. **30**, 994 (2004).

[11] A. S. Rybalko and S. P. Rupets, Low Temp. Phys. **31**, 623 (2005).

[12] A. Rybalko, S. Rubets, E. Rudavskii, V. Tikhiy, S. Tarapov, R. Golovashchenko, and V. Derkach, Phys. Rev. B **76**, 140503 (2007).

[13] A. S. Rybalko, S.P. Rubets, E. Ya. Rudavskii, V. Tikhiy, R. V. Golovachenko, V. N. Derkach and S. I. Tarapov, Low Temp. Phys. **34**, 254 (2008).

[14] A. S. Rybalko, S.P. Rubets, E. Ya. Rudavskii, V. A. Tikhiy, R. V. Golovachenko, V. N. Derkach and S. I. Tarapov, Low Temp. Phys. **34**, 497 (2008).

[15] A. Rybalko, E. Rudavskii, S. Rubets, V. Tikhiy, V. Derkach and S. Tarapov, J. Low Temp. Phys. **148**, 527 (2007).

[16] A. S. Rybalko, S. P. Rubets, E. Ya. Rudavskii, V. A. Tikhiy, Yu. M. Poluectov, R. V. Golovachenko, V. N. Derkach, S. I. Tarapov, and O. V. Usatenko, Low Temp. Phys. **35**, 837 (2009).

[17] A. Rybalko, S. Rubets, E. Rudavskii, V. Tikhiy, Y. Poluectov, R. Golovashchenko, V. Derkach, S. Tarapov, and O. Usatenko, J. Low Temp. Phys. **158**, 244 (2010).

[18] A. S. Rybalko, S. P. Rubets, E. Ya. Rudavskii, V. A. Tikhiy, R. Golovachenko, V. N. Derkach and S. I. Tarapov, arXiv: 0807.4810v1.

[19] N. N. Bogoliubov, J. Phys, USSR **11**, 23 (1947).

[20] Y. S. Jain, arxiv:1008.0240v2

[21] Y. S. Jain, arxiv:1011.1552v1.

[22] Y. S. Jain, arXiv:1011.3190v1.

[23] H. Marris and S. Balibar, Physics Today **53**, 29 (2000).

[24] D. G. Henshow and A. D. B. Woods, Phys. Rev. **121**, 1266 (1961).

[25] W. G. Stirling and H. R. Glyde, Phys. Rev. B **41**, 4224 (1990).

[26] G. Zsigmond, F. Mezei and M. T. F. Telling, Physica B **338**, 43 (2007).

[27] T. J. Greytak and J. Yan, Phys. Rev. Lett. **22**, 987 (1969).

[28] T. J. Greytak, R. Woerner, J. Yan and R. Benjamin, Phys. Rev. Lett. **25**, 1547 (1970).

[29] W. Kempinski, T. Zuk, J. Stankovski and S. Sitarz, Fiz. Nizk. Temp. **14**, 451 (1988).

[30] J. Stankovski, S. Sitarz, Z. Trybula, W. Kempinski, and T. Zuk, Acta Phys. Polonica, A**70**, 291, (1986).

[31] A. M. Kosevich, Low Temp. Phys. **31**, 37 (2005).

[32] A. M. Kosevich, Low Temp. Phys. **31**, 839 (2005).

[33] L. A. Melnikovsky, J. Low Temp. Phys. **148**, 559 (2007).

[34] V. D. Natsik, Low Temp. Phys. **31**, 915 (2005).

[35] V. D. Natsik, Low Temp. Phys. **33**, 999 (2007).

[36] E. A. Pashitsky and S. M. Ryabchenko, Low Temp. Phys. **33**, 8 (2007).

[37] V. M. Loktev and M. D. Tomchenko, Low Temp. Phys. **34**, 262 (2008).

[38] V. M. Loktev and M. D. Tomchenko, arXiv: 0903.2153v3.

[39] M. D. Tomchenko, J. Low Temp. Phys. **158**, 854 (2010).

[40] E. D. Gutliansky, Low Temp. Phys. **35**, 748 (2009).

[41] M. D. Tomchenko, Phys. Rev. B **83**, 094512 (2011).

[42] S. I. Shevchenko and A . S. Rukin, Low Temp. Phys. **36**, 596 (2010).

[43] V. P. Mineev, J. Low Temp. Phys. **162**, 686 (2011).

[44] E. A. Pashitskii and A. A. Gurin, JETP **111**, 975 (2010).

[45] M. D. Tomchenko, Phys. Rev. B **83**, 094512 (2011).

[46] R. C. Tolman and T. D. Stewart, Phys. Rev. **8**, 97 (1916).

[47] M. J. Bukingham and W. M. Fairbank, Prog. Low Temp. Phys. **3**, 80 (1961).

[48] B. N. Esel'son, V. N. Grigor'ev, V. G. Ivantsov, V. A. Koval, E. Ya. Rudavskii and I.A. Serbin in *Solutions of* ^{3}He$-^4$He *Quantum Liquids*, Nauka, Moscow, (1973).

[49] E. M. Lifshitz and L. P. Pitaevski, *Physical Kinetics*, Pergamon Press, Oxford, (1981).

[50] L. V. Keldysh in *Problems of Theoretical Physics*, Nauka, Moscow (1972).

[51] S. Chutia, Ph.D Thesis, Department of Physics, North-Eastern Hill University, Shillong-793022, India (2008).

[52] L. D. Landau, J. Phys. (USSR) 11, 91 (1947); Reprinted in Z. M. Galasiewics, *Helium 4*, Pergamon, Oxford (1971).

[53] R. P. Feynman in *The Feynman Lectures on Physics*, Vol. 2, Addison - Wesley, (1970).

Chapter 7

Summary and Conclusion

7.1 Summary and Conclusion

LHe-4 has continued to fascinate physicists for its superfluid behavior. LHe-4 exhibits a liquid to liquid phase transition (from its normal phase He I to superfluid phase He II) at $T = 2.17$ K. He II possesses several unusual and fascinating properties such as zero resistance to linear flow, zero entropy, very high thermal conductivity, thermomechanical and mechano-caloric effects, *etc.* To explain these properties, London [1] suggested in 1938 that superfluidity is related to the occurrence of an ordered state in momentum space ($p = 0$ state), as would be expected for a Bose–Einstein condensate. Since then, numerous efforts have been made to understand LHe-4 but the microscopic origin of its unique properties has not been clearly understood.

Microscopic approaches based on pseudo-potential [2] and variational principles [3] have been used to develop theories of the system. But none of these attempts was able to conclude the desired theory even though several research articles have been published. Microscopic theories based on varying assumptions such as the existence of $p = 0$ condensate [4], (q, -q) pair formation [5], pair condensation [6] and many particle condensation [7] have been tried, but

none of these theories could fully explain the experimental properties of the liquid to an acceptable degree of accuracy. Also, several authors tried to calculate the amount of $p = 0$ condensate and the excitation spectrum using variational principles, but with contradicting results. While some of the theories give 50% condensate [8,9], others yield as low as 10% [10, 11]. Theories that use variational method such as Green's function or Monte Carlo also yield varying$(0 - 13\%)$ amount of $p = 0$ condensate [12]. On the other hand, experimentalists are not able to prove conclusively the existence of $p = 0$ condensate in LHe-4 [13]. In fact, many authors [13–16] doubted the existence of $p = 0$ condensate.

Since the conventional theories are based on the existence of $p = 0$ condensate, it is not surprising that those theories fail to give a complete description of the system. The weaknesses of these theories are discussed by Woods and Cowley [14], Rickayzen [17], Kleban [18] *etc.* Most recently, discussing the shortcomings of the conventional theories, Ettouhami [19] even questioned the validity of Bogoliubov theory [4] of weakly interacting bosons which is used as the starting point of the field theoretical approach, combined with the assumption of the existence of $p = 0$ condensate. As such, Landau's two fluid phenomenological theory [20, 21], supplemented by the idea of quantized circulation presented by Onsager [22] and Feynman [23] remained the only way to understand the properties of LHe-4.

As such the need for a proper microscopic theory had been felt for a long time [14, 17]. Recently, Jain developed a microscopic theory of a system of interacting bosons which is well equipped to explain the properties of LHe-4. This theory vindicates (i) Landau's two fluid phenomenology [20] (ii) London's idea of macroscopic wave function of the S-state [1] (iii) the observation of Bogoliubov [4] that superfluidity is the manifestation of an inter-particle interaction and

(iv) Ginzburg –Landau ψ-theory [24], *etc.* Within experimental errors, Jain's theory explains different properties of LHe-4. Consequently, it could be regarded as the answer to the long awaited theory of LHe-4.

The salient features of Jain's theory can be summarized as follows:

1. It is a theory which deals with the dynamics of particles in an interacting system like LHe-4 and is based on the wave mechanics of two hard core particles.

2. No presumption of $p = 0$ condensate.

3. The basic unit of the system is a pair of hard core (HP) particles.

4. Each particle is a member of the pair of particles moving with equal and opposite momenta $(q, -q)$ about their center of mass (CM) which itself moves with momentum K in the laboratory frame.

5. Each particle can be represented by a kind of pair waveform proposed to be known as *macro-orbital.*

6. While the q-motion defines its quantum size ($\lambda/2 = \pi/q$), the K-motion defines its motion as a free particle of mass $4m$.

7. The onset of superfluid transition represents the BEC of these particles in a state of $K = 0$ and $q = q_0 = \pi/d$ and the system transforms from its disordered state in the phase space to an ordered state.

8. There exists an energy gap between the superfluid and normal fluid state and the origin of different properties (including superfluidity and related aspects) of the system lies with this energy gap.

9. It provides a basis for the validity of ψ-theory.

10. This theory vindicates Landau's two fluid phemenology and London's idea of macroscopic wave function of the superfluid state of LHe-4.

11. It can successfully explain the experimental results pertaining to the velocity of third sound in thin films of He II.

12. It reveals the origin of phase coherence of particles and quantized vortices observed in He II

13. The excitation spectrum obtained from this theory agrees quantitatively with experimental ones.

Using this theory we have studied certain physical properties of superfluid ^{4}He and mixture of LHe-3 and LHe-4. In this context, we have studied the roton linewidth in LHe-4, logarithmic divergence of the heat capacity at different pressures, the phase diagram of liquid helium mixture as well as the reduction of λ temperature of the mixture and finally, the electric activity of superfluid ^{4}He. The close agreement between experiments and our results reveals the accuracy and the potential of Jain's theory in explaining the behavior of LHe-4 type different systems of interacting bosons.

We have qualitatively analyzed the roton linewidth using Jain's theory (*cf. Chapter 3*). We have calculated the roton linewidth at SVP using collisional line broadening mechanism. This collisional line broadening formalism is applicable to gaseous as well as solid systems [25]. Macro-orbital theory predicts that LHe-4 system is more close to a solid structure than to a gaseous system. Our results at SVP closely agrees with the experimental values. In addition, we find that the appearance of a well defined band corresponding to what we call as roton transition is the signature of the change in atomic arrangement and hardening of the atomic arrangement.

Jain's theory also reveals clear reasons for the existence of the two roton bound state observed in Raman scattering.

Macro-orbital theory estimates the energy associated with the λ transition and concludes that this energy is responsible for the logarithmic singularitiy of the specific heat at constant pressure (C_p) at T_λ. We have used this energy to calculate the numerical values of C_p at different pressures and compared our results with experimental values (*cf.* Chapter 4). Close agreement of our calculated values with the experimental values establishes the accuracy of the relations of Jain's theory.

We have analyzed the phase diagram of liquid helium mixtures. While conventional theory fails to give a clear picture of the phase separation, Jain's theory gives a satisfactory explanation by assuming ^{3}He pair formation. Further, our estimate of the initial slope of the λ line agrees closely with the experimental value. Using the expressions for chemical potential given by Macro-orbital theory, we have estimated the reduction of the λ point in the mixture as a function of ^{3}He concentration (*cf.* Chapter 5). Our result closely agrees with experimental values.

In Chapter 6 of this thesis, we have presented a critical study of electric activity of He II, observed in a series of recent experiments. These experiments revealed that a ^{4}He atom in LHe-4 possesses dipole moment $p \approx 10^{-34}$ C $\cdot$ m. This observation is contrary to the earlier belief that LHe-4 does not possess any internal electric field or dipole moment because of the spherical symmetry of helium atom. Our investigation reveals that due to a solid-like arrangement of LHe-4 atoms in the system, such an internal electric field is possible.

The estimated results of various physical properties of LHe-4 that are presented in Chapters 3, 4, 5 and 6 closely agree with ex-

periments and thus establish that Macro-orbital theory succesfully explains these properties of the system. In addition, the theory can be used to study entropy, thermal conductivity, specific heat, pressure dependent dispersion relation, static structure factor $S(Q)$ and dynamic form factor $S(Q,\omega)$ at a quantitative level. Formalism of this theory can be extended to differents systems like ^{3}He, superconductor, 2-D bosonic system, *etc.* Our group plans to investigate these aspects and hope to open new frontier for future studies.

Bibliography

[1] F. London, Nature **141**, 644 (1938).

[2] K. Bedell, D. Pines and A. Zawadowski, Phys. Rev. B **29**, 102 (1984).

[3] R. P. Feynman, Phys. Rev. **94**, 262 (1954).

[4] N. N. Bogoliubov, J. Phys, USSR **11**, 23 (1947).

[5] J. G. Valatin and D. Butler, Nuovo Cimento **10**, 37 (1958).

[6] M. Girardeau and R. Arnowitt, Phys. Rev. **113**, 755 (1959).

[7] M. Luban, Phys. Rev. **128**, 965 (1962).

[8] W. E. Parry and D. Ter Haar, Ann. Phys.(N Y) **19**, 496 (1962).

[9] E. Ostgaard, J. Low Temp. Phys. **4**, 239 (1971).

[10] D. Schiff and L. Verlet, Phys. Rev. **160**, 208 (1967).

[11] W. P. Francis, G.V. Chester and L. Reatto, Phys. Rev. A **1**, 86 (1970).

[12] S. Moroni, G. Senatore and S. Fatoni, Phys. Rev. B **55**, 1040 (1997).

[13] A. J. Leggett, Rev. Mod. Phys. **71**, S318 (1999).

[14] A. D. B. Woods and R. A. Cowley, Rep. Prog. Phys. **36**, 1135 (1973).

[15] H. W. Jackson, Phys. Rev. A **10**, 278 (1974).

[16] P. E. Sokol, in *Bose–Einstein Condensation*, (A. Griffin, D.W. Snoke and S. Stringari, ed.), Cambridge University Press, Cambridge (1995).

[17] C. Rickayzen in *The Helium Liquids*, (J. G. M. Armitage and I. E. Ferquhar, eds.), Academic Press, London (1975).

[18] P. Kleban, Phys. Lett. **49A**, 19 (1974).

[19] A. M. Ettouhami, arXiv.org, 0703498 (2007).

[20] L. D. Landau, J. Phys. (USSR) **5**, 71 (1941).

[21] L. D. Landau, J. Phys. (USSR) **11**, 91 (1947).

[22] L. Onsager, Nuovo Cim. **6** (Supplement-2), 249 (1949).

[23] R. P. Feynman in *Prog. Low Temp. Phys.* , Vol. I, (C. J. Gorter, ed.), North Holland, Amsterdam (1955).

[24] V. L. Ginzburg and L. D. Landau, Zh. Eksperim. i. Teor. Fiz., **20**, 1064 (1950).

[25] B. B. Laud, *Lasers and Non-Linear Optics*, New Age International Publishers, New Delhi (2007).

LIST OF PUBLICATIONS

In Conference:

L. Chhangte, S. Chutia and Y.S. Jain, *Logarithmic Singularity of C_p of LHe-4*, National Conference on Condensed Matter Physics, Physics Dept., NEHU, Shillong, 2010.

In Journals:

1. L. Chhangte, S. Chutia, S. Dey and Y. S. Jain, Current Science **101**, 769 (2011).
2. L. Chhangte, S. Dey, J. P. Gewali, A. K. Jha and Y. S. Jain, Ind. J. Phys. **85**, 1309 (2011).

PARTICULARS OF THE CANDIDATE

Name	:	Lalmuanawma Chhangte
Degree	:	Ph. D
Department	:	Department of Physics, NEHU.
Title of the Dissertation	:	Spectroscopic, Electrical and Thermal Properties of Certain Condensed Systems.
Date of Admission	:	11.12.2007.
Approval of the Proposal	:	01.05.2008.
Registration No. and Date	:	1277 of 01.05.2008.
Name of Original Supervisor	:	Prof. Y.S. Jain (Retd.) (Joint Supervisor)
Date of Change of Supervisor	:	03.05.2011
Name of New Supervisor	:	Prof. S. Kumar
Extension (If any)	:	None

Head,
Department of Physics
North-Eastern Hill University,
Shillong, India